Bridging the gaps between cell stress, mitochondrial dysfunction and lipid metabolism in ALS cellular pathophysiology

Chiara Rossi

Universitat de Lleida

TESI DOCTORAL

Bridging the gaps between cell stress, mitochondrial dysfunction and lipid metabolism in ALS cellular pathophysiology

Chiara Rossi

Memòria presentada per optar al grau de Doctor per la Universitat de Lleida
Programa de Doctorat en Salut

Director/a
Manel Portero Otín
Reinald Pamplona Gras

Tutor/a

Manel Portero Otín

2022

TESI DOCTORAL

Bridging the gaps between cell stress, mitochondrial dysfunction and lipid metabolism in ALS cellular pathophysiology

Chiara Rossi

Memòria presentada per optar al grau de Doctor per la Universitat de Lleida
Programa de Doctorat en Salut

Director/a
Manel Portero Otín
Reinald Pamplona Gras

Tutor/a

Manel Portero Otín

2022

ABSTRACT·RESUMEN·RESUM

ABSTRACT

Amyotrophic lateral sclerosis (ALS) is a neurodegenerative disorder affecting primarily the motor system, but also including well documented extra-motor manifestations. It is characterized by the loss of upper and lower motor neurons (MNs) in the motor cortex, in addition to a progressive muscle waste and weakness starting from the brain stem nuclei and the anterior horn of the spinal cord. ALS frequently shows a focal onset that evolves with the spreading of the illness to several body regions, where failure of respiratory muscles generally limits survival to 2-5 years after disease onset. In up to 50% of cases, extra-motor manifestations are observed, including changes in behavior, executive dysfunction, and language problems. In 10% of cases ALS is hereditary with an autosomal dominant inheritance pattern (familial ALS, fALS). The remaining 90% have no ALS family history and are classified as sporadic ALS (sALS). So far, more than 20 genes have been associated with ALS, being the hexanucleotide repeat expansion in the C9orf72 gene the most common genetic cause. One of the better-established hallmarks of ALS is the presence of protein aggregates in the cytosol of MNs. Their main component is the ribonucleoprotein TDP-43, which appears to be delocalized, hyperphosphorylated and fragmented in the cytoplasm. Various cellular stressors, such as oxidative, proteasomal, endoplasmic reticulum (ER), osmotic and mitochondrial stresses could contribute to TDP-43 deregulation. Nevertheless, TDP-43 dysfunction is only a component a vaster physiopathological scenario in which a diffuse imbalance of proteostastis interacts with a variety of dysfunctions involving mitochondria and lipid metabolism in a tethering network.

This thesis focuses on highlighting the connection among three aspects of ALS cellular physiopathology, such as cell stress, mitochondrial impairment, and lipid metabolism. Briefly, the results obtained depicted a scenario in which other nuclear proteins (p-ERK, p-Jun and REST) besides TDP-43 can be delocalized as a consequence of cellular stress and interact with mitochondria, as demonstrated by their presence in subcellular fractions of a murine model for TDP-43^{Q331K} genotype. Also, TDP-43 mislocalization is related to changes in REST regulated genes. Finally, response of different TDP-43 genetic backgrounds to metabolic stress is heterogeneous with regard to mitochondrial health preservation, while LDs accumulation seems to be a common trait in different cellular models upon stress induction. Interestingly, this was not the case for astrocytes, in which the stressors we tested seemed to interfere with lipid droplets (LDs) formation. Altogether, these results can open up new perspectives for a finest characterization of ALS physiopathology, both in relation with cellular stress and specificity of stress-responses on the basis of TDP-43 genetic background.

RESUMEN

La esclerosis lateral amiotrófica (ELA) es un trastorno neurodegenerativo relacionado con el envejecimiento. Se caracteriza por la pérdida de neuronas motoras superiores o inferiores en la corteza motora y desgaste muscular progresivo. La ELA suele mostrar un inicio focal propagándose a varias regiones del cuerpo; una falla de los músculos respiratorios limita la supervivencia de 2 a 5 años después del inicio de la enfermedad. Las manifestaciones extra-motoras incluyen cambios en el comportamiento, disfunción ejecutiva y problemas de lenguaje. En el 10% de los casos, la ELA es hereditaria con patrón de herencia autosómico dominante (ELA familiar, fALS). El restante 90% se clasifica como ELA esporádica (sALS). Las causas de la ELA son heterogéneas y poco comprendidas. Una de las características mejor establecidas de la ELA es la presencia de agregados proteicos en el citosol de las neuronas motoras. Uno de sus componentes es TDP-43, una ribonucleoproteína deslocalizada, hiperfosforilada y fragmentada en el citoplasma celular. Otras proteínas, como ERK, JUN y REST, muestran reordenamientos similares en otras enfermedades neurodegenerativas.

Con respecto a TDP-43, no están bien determinadas las causas moleculares de su desregulación, pero diferentes estreses celulares, como el oxidativo, proteasómico, de retículo endoplásmico (RE), osmótico y mitocondrial, podrían contribuir a ello. Sin embargo, la disfunción de TDP-43 solo es un componente de un escenario fisiopatológico más amplio en el que un desequilibrio difuso de la proteostasis interactúa con una variedad de disfunciones mitocondriales y el metabolismo de lípidos.

Esta tesis pretende aclarar la conexión entre estrés celular, la disfunción mitocondrial y el metabolismo de los lípidos en la ELA. Los resultados muestran como otras proteínas nucleares (p-ERK, p-Jun y REST), además de TDP-43, se deslocalizan debido al estrés celular e interactúan con las mitocondrias, como demostrado por microscopia confocal y su presencia en fracciones subcelulares de un modelo murino para el genotipo TDP-43^{Q331K}. Además, la deslocalización de TDP-43 se relaciona con cambios en genes regulados por REST. Finalmente, las respuestas de diferentes backgrounds genéticos de TDP-43 al estrés metabólico son heterogéneas con respecto a la preservación de la salud mitocondrial, mientras que la acumulación de gotas lipídicas parece ser un rasgo común en diferentes modelos celulares ante varios tipos de estrés. Curiosamente, este no fue el caso de los astrocitos, en los que los factores de estrés testados parecen interferir con la formación de gotas lipídicas. Estos resultados pueden abrir nuevas perspectivas para una mejor caracterización de la fisiopatología de la ELA en relación con el estrés celular y las respuestas específicas al estrés basadas en diferentes mutantes de TDP-43.

RESUM

L'esclerosi lateral amiotròfica (ELA) és principalment un trastorn neurodegeneratiu que afecta el sistema motor. Es caracteritza per la pèrdua de neurones motores superiors i inferiors de l'escorça motora i desgast muscular progressiu. L'ELA mostra sovint un inici focal que evoluciona amb la propagació de la malaltia, amb una falla dels músculs respiratoris que limita la supervivència de 2 a 5 anys. Sovint, s'observen manifestacions extra motores, amb canvis en el comportament, disfunció executiva i problemes de llenguatge. En un 10% de casos, l'ELA és hereditària amb un patró d'herència autosòmic dominant (ELA familiar). El 90% restant no mostra antecedents familiars i es classifica com a ELA esporàdica. Les causes de l'ELA són heterogènies i parcialment compreses.

L'ELA es caracteritza per la presència d'agregats de proteïnes al citosol de les neurones motores. Un component d'aquests és TDP-43, una ribonucleoproteïna deslocalitzada, hiperfosforilada i fragmentada al citoplasma cel·lular. Altres proteïnes, com ara ERK, JUN i REST, mostren reordenaments similars en altres malalties neurodegeneratives. En el cas de TDP-43, avui dia no s'ha aconseguit un coneixement complet dels mecanismes moleculars de la seva desregulació, però diferents factors d'estrès cel·lular, com l'estrès oxidatiu, proteasòmic, de reticle endoplàsmic (RE), osmòtic i mitocondrial, hi podrien contribuir. La disfunció de TDP-43 és un component d'un escenari fisiopatològic més ampli en què un desequilibri difús de la proteòstasi interactua amb disfuncions dels mitocondris i del metabolisme de lípids.

Aquesta tesi analitza la connexió entre l'estrès cel·lular, la disfunció mitocondrial i el metabolisme dels lípids en la ELA. Els resultats mostren com altres proteïnes nuclears (p-ERK, p-Jun i REST), a més de TDP-43, es deslocalitzen a causa de l'estrès cel·lular interactuant amb els mitocondris, com demostrat per microscòpia confocal i la seva presència en fraccions subcel·lulars d'un model murí del genotip TDP-43^{Q331K}. A més, la deslocalització de TDP-43 es relaciona amb canvis en gens regulats per REST. Finalment, les respostes de diferents mutants de TDP-43 a l'estrès metabòlic són heterogènies pel que fa a la preservació de la salut mitocondrial, mentre que l'acumulació de gotes lipídiques sembla un tret comú en diferents models cel·lulars davant de diversos tipus d'estrès. Curiosament, aquest no va ser el cas dels astròcits, en què els factors d'estrès testats semblen interferir amb la formació de gotes lipídiques. Aquests resultats poden obrir contribuir a una caracterització millor de la fisiopatologia de l'ELA en relació amb l'estrès cel·lular i les respostes específiques a l'estrès de diferents mutants de TDP-43.

ACKNOWLEDGEMENTS

To my beloved and forever missed parents

I have no idea on how to start writing this, but for sure I will always remember this moment. The truth is that I am here alone, crying in front of a screen (not so cool) at the end of this hard but enriching experience that is writing a PhD thesis. I would keep it simple.

Many, infinite, thanks to my parents who I like to think can still see and guide me through life from a place of joy and peace. This work is my little gift for them, as a sign of gratitude for all the efforts they made for me.

Thanks to my brother Emilio for supporting me through this journey and encouraging me to never give up in every aspect of life.

Thanks to Carlos for always being my perfect companion in life. For standing by my side with respect and love. Especially, for making me smile every single day. Also, for lending me his old desktop to write this thesis on Sundays, with the greatest understatement for my strategical disappearances during family lunches.

Thanks to my Spanish family for their presence and support; to Rosa, Antonia, Rosemary, Javi and little Alyson to share with me so many cheerful moments.

A special thanks to Elena for starting this adventure with me; for all the experiences we lived together in Lleida, for all her precious advice and unconditional presence during these years.

Thanks from the bottom of my heart to Manel and Reinald for guiding me at their best during the writing of this work. It would have been really impossible for me without their help and support.

Thank you so much to all my lab mates for making a great team; a special thanks to Pascual for being always supportive, available and willing to help. Also, to Omar, whose PhD thesis has been inspirational to me, and to Reyna for her great support in spite of distance, for being always wise and positive; definitely one of the sweetest people I have met.

Science is magic that works

INDEX

INDEX

LIST OF FIGURES

LIST OF TABLES

ABBREVIATIONS

ABBREVIATIONS

ABBREVIATION	MEANING
8-OHdG	8-dihydro-2' -deoxyguanosine
AA	arachidonic acid
AAA	ATPase associated with diverse cellular activities
AC	Acylcarnitine
ACAT	Acyl-CoA:cholesterol acyltransferase
Acsl	Acyl-CoA synthetase long-chain
AGPS	Alkylglycerone phosphate synthase
ALS	Amyotrophic lateral sclerosis
ALS/PDC	Amyotrophic lateral sclerosis/parkinsonism dementia complex
ANLS	Astrocyte-neuron lactate shuttle
AP-1	Activator protein 1
AR	Adrenergic receptor
ASK1	Apoptosis signal- regulated kinase 1
ATGL	Adipose triglyceride lipase
ATM	Phospho-ataxia-telangiectasia mutated
ATP	Adenosine triphosphate
BACs	Bacterial artificial chromosomes
BBB	Blood-brain barrier
BHK	Baby hamster kidney
BMAA	β-N-methylamino-l-alanine
BSA	Bovine serum albumine
BSA FAF	Fatty acid free bovine serum albumine
CARM-1	Coactivator-associated arginine methyltransferase
CCNF	Cyclin F
Cdk6	Cyclin-dependent kinase 6
CEs	Cholesteryl esters
CHCHD10	Coiled-helix coiled-helix domains containing protein 10
CIDE	Cell death-inducing DFF45-like effector
cKO	Conditional KO
c-Myc	Transcriptional regulator Myc-like
CNS	Central Nervous System
COX-2	Cyclooxygenase-2
CPT1	Carnitine palmitoyltransferase 1
CREB	Response element-binding protein
CSF	Cerebrospinal fluid
DAGs	Diacylglycerols
DDR	DNA damage response
DGATs	Diacylglycerol transferases
DGAT-1	Diacylglycerol acyltransferase-1
dHMN-V	Distal hereditary motor neuropathy type V
DLK	Leucine zipper kinase
DPR	Dipeptide repeat protein
DRG	Large dorsal root ganglion
eIF2α	Phosphorylation of eukaryotic initiation factor-2α
ER	Endoplasmic reticulum
ERAD	ER-associated degradation
ERMES	ER-mitochondria encounter structures
ERKs	Extracellular signal-regulated kinases
ES	Embryonic stem cell medium

ABBREVIATION	MEANING
ETC	Electron transport chain
F16BP	Fructose 1, 6-bisphosphate
F6P	Fructose 6- phosphate
fALS	Familial ALS
FAs	Fatty acids
FFAs	Free fatty acids
FTD	Frontotemporal dementia
FTLD	Frontotemporal lobar degeneration
FUS	Fused in sarcoma
G3P	Glyceraldehyde 3- phosphate
G6P	Glucose 6-phosphate
G6PDH	Glucose 6-phosphate dehydrogenase
GAD	Glutamate decarboxylase
GD	Gaucher disease
GEF	Guanine exchange factor
Gln	Glutamine
GOF	Gain-of- function
GPCR	G-protein coupled receptors
GS	Glutamine synthetase
GSH	Glutathione
GSL	Glycosphingolipids
H_2O_2	Hydrogen peroxide
hALS	Hereditary ALS
HBSS	Hank's Balanced Salt Solution
HGK	Kinase-like/germinal center kinase-like kinase
HIPK2	Homeodomain-interacting protein kinase 2
hiPCS	Human induced pluripotent stem cells
HK	Hexokinase
hnARN	Heterogeneous nuclear RNA
hnRNP	Heterogeneous nuclear ribonucleoprotein
HSF	heat shock factor
hSOD1-G93A	Human superoxide dismutase 1 with the G93A mutation
Hsp	Heat shock proteins
hVAPB	Human VAMP-associated protein B
Iba-1	Ionized calcium-binding adapter molecule 1
IBM	Inclusion body myositis
IF	Immunofluorescence
iPSC	Induced pluripotent stem cell
IRE1	Inositol-requiring enzyme1
JNKs	c-Jun N-terminal kinases
KBs	Ketone bodies
KRB	Krebs-Ringer Buffer
LCD	C-terminal low complexity glycine-rich domain
LD	Luminal domain
LDs	Lipid droplets
LIG3	DNA ligase 3
LMNs	Lower motor neurons
LOF	Loss- of- function
LPS	Lipopolysaccharides
MADD	MAP kinase activating death domain
MAMs	Mitochondria-associated ER membranes

ABBREVIATION	MEANING
MAPK	Mitogen-activated protein kinase
MDA	Malone dialdehyde
MDPs	Mitochondrial derived peptides
MEFs	Mouse embryonic fibroblasts
MEKK1–4	MEK kinase 1, 2, 3, and 4
miRNAs	MicroRNAs
MN	Motor neuron
MNP	Motor neuron progenitor
MND	Motor neuron disease
MNK	MAPK interacting kinase
MNs	Motor neurons
MPC	Mitochondrial pyruvate carrier
MSC	Mesenchymal stomal/stem cells
MSK	Mitogen and stress-activated protein kinase
mtDNA	Mitochondrial DNA
NADH	Nicotinamide adenine dinucleotide
NAFLD	Non-alcoholic fatty liver disease
NAO	Nonyl acridine orange
NES	Nuclear export signal
NF-kB	Nuclear factor-kappa B
NFTs	Neurofibrillary tangles
Ngb	Neuroglobin
NGS	Normal goat serum
NLS	Nuclear localization signal
NMD	Nonsense-mediated decay
NOX	NADPH oxidase
NOX2	NADPH oxidase 2
OGDH	Oxoglutarate dehydrogenase
OS	Oxidative stress
OsmS	Osmotic stress
OXPHOS	Oxidative phosphorylation
P2X7	Purinoceptor 7
PAG	Phosphate activated glutaminase
PDH	Pyruvate dehydrogenase
PDI	Protein disulfide-isomerase
PDIs	Protein disulfide isomerases
PEP	Phosphoenolpyruvate
PERK	PKR-like ER kinase
PFA	Paraformaldehyde
PFK	Phosphofructokinase
PI	Propidium Iodide
PLIN-2	Perilipin 2
PPP	Pentose phosphate shunt pathway
PQC	Protein quality control
pre-miRNAs	Precursor miRNAs
P/S	Penicillin-Streptomycin
PTPs	Tein tyrosine phosphatases
PUFAs	Polyunsaturated fatty acids
R5P	Ribose 5-phosphate
RBPs	RNA-binding proteins
RF	Retention factor

ABBREVIATION	MEANING
RMRM2	Recognition motif 2
RNP	Ribonucleoprotein
ROS	Reactive oxygen species
ROS/RNS	Reactive oxygen and nitrogen species
RRM1	Recognition motif 1
RS	Reactive species
RTK	Receptor tyrosine kinase
RTKs	Receptor tyrosine kinases
sALS	Sporadic ALS
SCAF1	Supercomplex assembly factor I
SCs	Respiratory supercomplexes
SGs	Stress Granules
SH3BP5/SAB	SH3-domain binding protein 5
SIRT3	Sirtuin-3
SN	Substantia nigra
SOD1	Superoxide dismutase 1
SOD1(WT)	Wild-type SOD1
SODs	Superoxide dismutases
SOS	Son of sevenless
SV40	Simian vacuolating virus 40
TAGs	Triacylglycerides
TAGs	Triacylglycerols
TAO1	Thousand-and-one amino acid 1
TCA	Tricarboxylic acid
TDP-43	TAR DNA-binding protein 43
TFEB	Transcription factor EB
Thp	Thapsigargin
TIA-1	T-cell restricted intracellular antigen-1
TLRs	Toll-like receptors
TMAO	Trimethylamine N-oxide
TLC	Thin-layer chromatography
TNPO	Transportin
TRAF2	Receptor-associated protein 2
UMNs	Upper motor neurons
TRAF2	receptor-associated protein 2
UPR	Unfolded protein response
UPS	Ubiquitin-proteasome system
VCP	Valosin-containing protein
WT	Wild type
XBP-1	X-box binding protein 1

INTRODUCTION

1. INTRODUCTION

1.1 ALS: Amyotrophic lateral sclerosis

1.1.1. An overview

ALS is a fatal motor neuron disorder characterized by the progressive loss of the upper and lower motor neurons (LMNs) at the corticospinal or bulbar level. The word amyotrophic arises from Greek, with "a" meaning no or negative, “myo” meaning muscle, and “trophic” meaning nourishment. Thus, amyotrophic stands for "no muscle nourishment ". Lateral refers to the column of the spinal cord where some of the affected motor neurons are located, and sclerosis outlines the hardening of the lateral white matter funiculus in spinal cord as a consequence of motor neuron degeneration and death (Wijesekera & Leigh, 2009). ALS was first described in 1824 by Scottish anatomist Charles Bell (Rowland, 2001). Studies conducted between 1865 to 1869 by Jean-Martin Charcot and his colleague Joffroy related lesions within the lateral column in the spinal cord with chronic progressive paralysis and contractures (no atrophy of muscles), while lesions of the anterior horn of the spinal cord were associated with paralysis without contractures (with atrophy of muscles). These findings contributed to the hypothesis that the motor component of the spinal cord consisted of a bipartisan system, and that the location of the lesion results in a diversified clinical presentation. The term “amyotrophic lateral sclerosis” first appeared in 1874, in a collection of his work titled “Oeuvres Completes”. Nevertheless, ALS is still known as Charcot’s disease in many parts of the world (D. R. Kumar et al., 2011); the disease became popular in the United States when baseball player Lou Gehrig was diagnosed in 1939, being known there as Lou Gehrig’s disease.

ALS slowly takes away the ability to walk, eat, or breathe from patients. This devastating adult-onset neurodegenerative disease leads to the loss of motor neurons, the extended nerve cells in the brain, UMNs, and spinal cord, LMNs, which innervate the muscles (Keon et al., 2021). These motor neurons (MNs) are essential for the conveying between the brain and the muscles and transmit vital instructions for mobility. When these nerve cells are defective or impaired, they gradually stop interfacing with the muscles, and the brain shows inability to control and initiate voluntary movements such as walking, chewing, or talking. This brings to progressive weakness, muscle twitches, and atrophy of voluntary

skeletal muscles. The final stages of the disease lead to fatal paralysis and death caused by respiratory failure (Keon et al., 2021).

The worldwide incidence of ALS fluctuates from 0.6 to 3.8 cases per 100,000 people per year, whereas the prevalence is approximately 4.1 to 8.4 per 100,000. In addition, cases of ALS are projected to globally increase from 222,801 in 2015 to 376,674 in 2040, with an upsurge of 69%. This phenomenon is linked to population aging, especially among developing countries (Barbalho et al., 2021). Incidence of ALS appears to be lower in Asian countries compared with Europe and North America. Demographic factors could explain this trend. ALS is primarily a middle and old-age disease and the density of the population at risk differs in countries. Despite that, it is contentious that the prevalence of known ALS genes in Asian countries is low. Besides geographic differences, many studies examining the change of ALS incidence over the years point up the gradually increasing incidence of the disease. Contrastingly, registry centers in Europe can index around 60-100 new cases per year due to the rarity of the disease (Barbalho et al., 2021). Larger sample sizes are needed to elucidate other aspects of the disease epidemiology, such as explaining the aging-related changes or the reasons why the incidence starts to decline from the age of 75 years. Likewise, working with many patients from different regions could be extremely useful to find out the environmental risk factors correlated with ALS and to analyze genetic differences (Aktekin & Uysal, 2020).

According to recent studies, the mean age of ALS onset is between 51 and 66 years. Europeans usually show a later ALS onset in comparison with Chinese, Cuban or Uruguayan patients (Longinetti & Fang, 2019). Chinese ALS patients show a median age of ALS onset at 51 years, whereas German patients develop the first symptoms of the disease around 10 years later. In addition, the mean age at ALS is 4-9 years younger in Cuba and Uruguay compared with Ireland (Longinetti & Fang, 2019; Mehta et al., 2018). However, the tardier ALS onset in Europe could be partly attributable to the use of population-based studies, which tend to include patients showing a greater spectrum of disease features than clinical-based studies. Differences in age at ALS onset can also be related to the form of the condition, familial or sporadic. In fact, patients suffering from familial ALS show an earlier age of onset when compared with patients with sporadic beginning. This could be due to a closer surveillance of the symptoms in patients with familiarity for ALS, leading to an earlier diagnosis of the disease but also to a Mendelian gene variant (Longinetti & Fang, 2019; Mehta et al., 2018). All in all, these data suggest the fact that age and aging are relevant in ALS pathophysiology, similarly to other neurodegenerative diseases.

1.1.2. Clinical features

As shown above, the hallmark of ALS is progressive muscle weakness, along with muscle atrophy and rigidity, fasciculations, muscle cramps and slowness of movements. Muscle weakness usually appears in a focal pattern and progressively spreads to adjacent body regions (Masrori & van Damme, 2020). This manifestation resumes the spreading of disease pathology within the motor system, characterized by neuroanatomic propagation within the spinal cord segments and the motor cortex. ALS usually presents with *unilateral distal muscle weakness* and atrophy in upper or lower limb muscles (spinal ALS) or in bulbar muscles (bulbar ALS). Upper limb onset is most commonly in the dominant hand, with thenar muscles showing a greater affection than hypothenar muscles (split-hand syndrome). An early involvement of the first interosseous muscle and finger extensors is also typical of the upper limb onset. In the lower limb the anterior tibial muscle is typically affected earlier than the gastrocnemius muscle, followed by the hamstrings and the quadriceps muscles. Dysarthria or dysphagia is the first symptom of bulbar ALS onset (Masrori & van Damme, 2020). Dysphonia reduced mouth closure or chewing difficulty is less common. In later stages of the disease, axial muscle weakness, head drop, and postural problems are commonly observed but they are rarely found to be the presenting symptoms. In about one-third of patients, bouts of uncontrolled laughing or crying, known as pseudobulbar affect, can be detected. A combination of signs of UMNs and LMNs involvement is frequently found in patients with classic ALS. Signs of LMNs involvement include muscle weakness, atrophy, fasciculations and reduced muscle tone. Signs of UMNs involvement to look for include hyperreflexia, increased muscle tone and slowness of tongue movement (Masrori & van Damme, 2020). Those facts support the hypothesis that many ALS patients may have both UMNs and LMNs involvement, suggesting that the disease spreads amongst different cells.

Approximately 50% ALS patients die within 30 months of disease onset, with respiratory insufficiency being the main cause of death. Only 10% of patients may survive for more than a decade (Ingre et al., 2015). The typical time to diagnosis for ALS is 10-16 months from symptom onset. Several points of delay in the diagnosis course have been identified, including specialist referrals and misdiagnoses mainly due to the heterogeneity of symptoms in the onset, often resulting in unnecessary procedures and surgeries (Richards et al., 2020). For this reason, biomarkers in ALS have been the subject of intense research over the past 20 years. Sensitive and specific biomarkers have the potential to speed up early detection of the disease and improve patient outcomes. They

are also fundamental for the design of clinical trials and the development of novel therapeutics (Verber et al., 2019).

1.1.3. Risk factors for ALS

As mentioned in the previous section, the incidence of ALS is largely uniform across the world, but it has shown a significant increase during the last decades (Ingre et al., 2015).The most relevant risk factors for ALS are age, with the disease being more common between the ages of 40 and the mid 60-s, masculine sex, and heredity. Approximately 10% of ALS cases show a familiar history of the disease, which can be inherited either as an autosomal dominant or recessive trait. This version of the illness is known as familial ALS (fALS) (H. X. Deng et al., 2011). Sporadic ALS (sALS) accounts for the remaining 90% of cases (Rotunno & Bosco, 2013). Despite the complexity of the illness, several risk factors are found to be possibly related with an increasing risk of developing ALS and its rate of progression. Investigation on ALS risk factors could also open new scenarios to better understand pathological mechanisms and heterogeneity of the disease.

1.1.3.1. Environmental risk factors

It has been reported that workers with apparently different exposures could be at risk of developing ALS, such as athletes, carpenters, cockpit workers, construction workers, electrical workers, farm workers and hairdressers (Ingre et al., 2015). However, an exposure to lead for professional reasons for 20 or more years prior to diagnosis was associated with ALS (A. S. Andrew et al., 2021). Also, hobbies involving this metal, such as casting lead bullets or making stained glass with lead joints shows a strong association with ALS with an approximately three-fold increased risk adjusted for age, gender, family history and smoking status (A. S. Andrew et al., 2021). Other metals with a potential link to ALS onset are manganese, aluminum, cadmium, cobalt, copper, zinc, vanadium and uranium, all of them found at significantly higher concentrations in ALS cerebrospinal fluid (CSF) compared to control CSF (Roos et al., 2013). Higher concentrations of these metals were also found in ALS CSF than in ALS plasma, indicating mechanisms of accumulation, such as inward directed transport. These findings could indicate that metals displaying neurotoxic effects are involved in the pathogenesis of ALS (Roos et al., 2013). Moreover, a role of military service in ALS has been hypothesized, considering the deep exposure of military personnel to a range of harmful factors, such as physical and psychological

traumas, chemicals, and transmissible agents (e.g., viruses). However, it is too premature to establish a firm causal relationship (Beard & Kamel, 2015).

Toxic habits of life such as cigarette smoking have also been associated with a higher risk of ALS. The risk increases significantly with the years smoked and the number of cigarettes smoked per day, while it decreases in the never smokers (H. Wang et al., 2011). Smoke can directly cause neuronal impairment from nitric oxide, traces of pesticides derived from tobacco cultivation or oxidative stress (H. Wang et al., 2011).

Investigators have also focused on several preventive factors for ALS. Among these, a higher consumption of fruits and vegetables was related to a decrease in ALS risk. On the other hand, the dose-response relationship between the intake of beta-carotene, vitamin C and vitamin E was found to be not statistically significant (Okamoto et al., 2009). Other aspects of nutrition that have been considered are coffee and tea consumption. However, a recent study has denied the hypothesis that coffee or tea consumption is associated with the ALS progression rate, contrasting with previous findings about their potential protective effect (Cucovici et al., 2021). In the absence of a cure or treatment, affected individuals may make use of popular nutritional supplements such as Ω-3 as a form of "self-medication". However, recent findings from independent laboratories indicate that such an approach could be harmful (Boumil et al., 2017). On the other hand, it has been suggested that a critical balance of Ω-6 and Ω-3 may temporarily preserve motor neuron function during the terminal stages of ALS, which could provide a substantial improvement in quality of life for affected individuals and their caregivers (Boumil et al., 2017).

Also, it is worth mentioning that the relationship between environmental toxins and neurological disease has been of interest since residents of Minamata Bay, Japan, were sickened by chronic dietary exposure to methyl-mercury-laden fish (Cox et al., 2016). Similarly, many Chamorro villagers on the Pacific island of Guam suffer from Alzheimer's disease (AD) and an unusual paralytic illness called Guamanian amyotrophic lateral sclerosis/parkinsonism dementia complex (ALS/PDC), and in some villages one-quarter of the adults perished from the disease (Cox et al., 2016) Like Alzheimer's, the causal factors of Guamanian ALS/PDC are poorly understood. In replicated experiments, it has been found that chronic dietary exposure to a cyanobacterial toxin present in the traditional Chamorro diet, β-*N*-methylamino-l-alanine (BMAA), triggers the formation of both neurofibrillary tangles (NFTs) and β-amyloid deposits similar in structure and density to those found in brain tissues of Chamorros who died with ALS/PDC(Cox et al., 2016).Vervets (*Chlorocebus sabaeus*) fed for 140 days with BMAA-dosed fruit developed

NFT and sparse β-amyloid deposits in the brain., while co-administration of the dietary amino acid l-serine with l-BMAA significantly reduced the density of NFT. These findings indicate that while chronic exposure to the environmental toxin BMAA can trigger neurodegeneration in vulnerable individuals, increasing the amount of l-serine in the diet can reduce the risk (Cox et al., 2016).

A 2021 study focused on the effect of pesticides applied to crops in the USA and ALS risk, concluding that pesticides with the largest positive statistically significant associations in both the discovery and the validation studies and evidence of neurotoxicity in the literature were the herbicides 2,4-D and glyphosate, and the insecticides carbaryl and chlorpyrifos (A. Andrew et al., 2021).

A further field of investigation is the study of the relationship between physical activity and ALS. Results are quite divergent, with Visser et al. (Visser et al., 2018)suggesting that physical exercise could increase the risk of developing ALS, while Gallo et al. (Gallo et al., 2016)draw the conclusion that high levels of physical activity could diminish the probability of suffering from the illness. Fang et al. (Fang et al., 2016)meanwhile suggest that the risk of ALS depends on the intensity of physical exercise, differentiating elite athletes from recreational athletes. Comparing these two groups, elite athletes could be exposed to a higher risk, while recreational athletes show an opposite trend (Visser et al., 2018)

Controversies in the conclusions of these studies show how hard it can be to study the factors influencing a rare disease such as ALS at a population level. Actually, it is remarkable how these investigations report association and cannot infer causality from the data that are presented. In conclusion, we still have no solid evidence that physical activity or any other environmental factor has an influence on ALS incidence (Hu & Np, 2020).

1.1.3.2. Genetic risk factors

ALS shows an important but varied genetic background. As previously mentioned, up to 10% of ALS patients have at least one affected family member and are defined as suffering from fALS; most of these cases are inherited in an autosomal dominant manner (Kirby et al., 2016). The remaining 90–95% of ALS cases has no relation to family history; these individuals show the so-called sALS (S. Chen et al., 2013).

In the past years, technological progress has allowed the application of the most advanced molecular genetic techniques to search for ALS-related genes in large sample sets (Boylan, 2015). These technical improvements in molecular genetics have been crucial for a better understanding of the genetic factors of fALS, showing that 40-55% of

cases are linked to variants in known ALS-linked genes (Zou et al., 2017). More than 50 causative genes have been identified for fALS, but pathogenic variants in SOD1, C9ORF72, FUS and TARDBP are the most frequently observed, with the remaining being less common. Genetic risk factors also contribute to sALS, even if they also can explain a small fraction of cases and the identification of genetic risk in sALS is still quite difficult to track down (Mejzini et al., 2019). Figure 1 displays the proportion of ALS cases linked to variants of the most common ALS-related genes in Europe and Asia.

Despite being relatively rare, there is a need for sequencing all ALS patients, no matter whether they are fALS or sALS. This is due to the fact that many novel therapeutic assays are addressed to gene therapy; therefore, an adequate knowledge of the genetic background is required (Heath et al., 2013).

Although much effort has been made to elucidate molecular determinants underlying the onset and progression of the disorder, the causes of ALS remain largely unknown, thus sequencing studies can be of great help. In 2017 a study was published, in which researchers deeply sequenced the whole transcriptome from spinal cord ventral horns of post-mortem ALS human donors affected by the sporadic form of the disease, which is less investigated than the inherited form of the disease (D'Erchia et al., 2017). They observed 1160 deregulated genes including 18 miRNAs and show that down regulated genes are mainly of neuronal derivation while up regulated genes have glial origin and tend to be involved in neuroinflammation or cell death. Remarkably, they found strong deregulation of SNAP25 and STX1B at both mRNA and protein levels suggesting impaired synaptic function through SNAP25 reduction as a possible cause of calcium elevation and glutamate excitotoxicity. They also note aberrant alternative splicing but not disrupted RNA editing (D'Erchia et al., 2017).

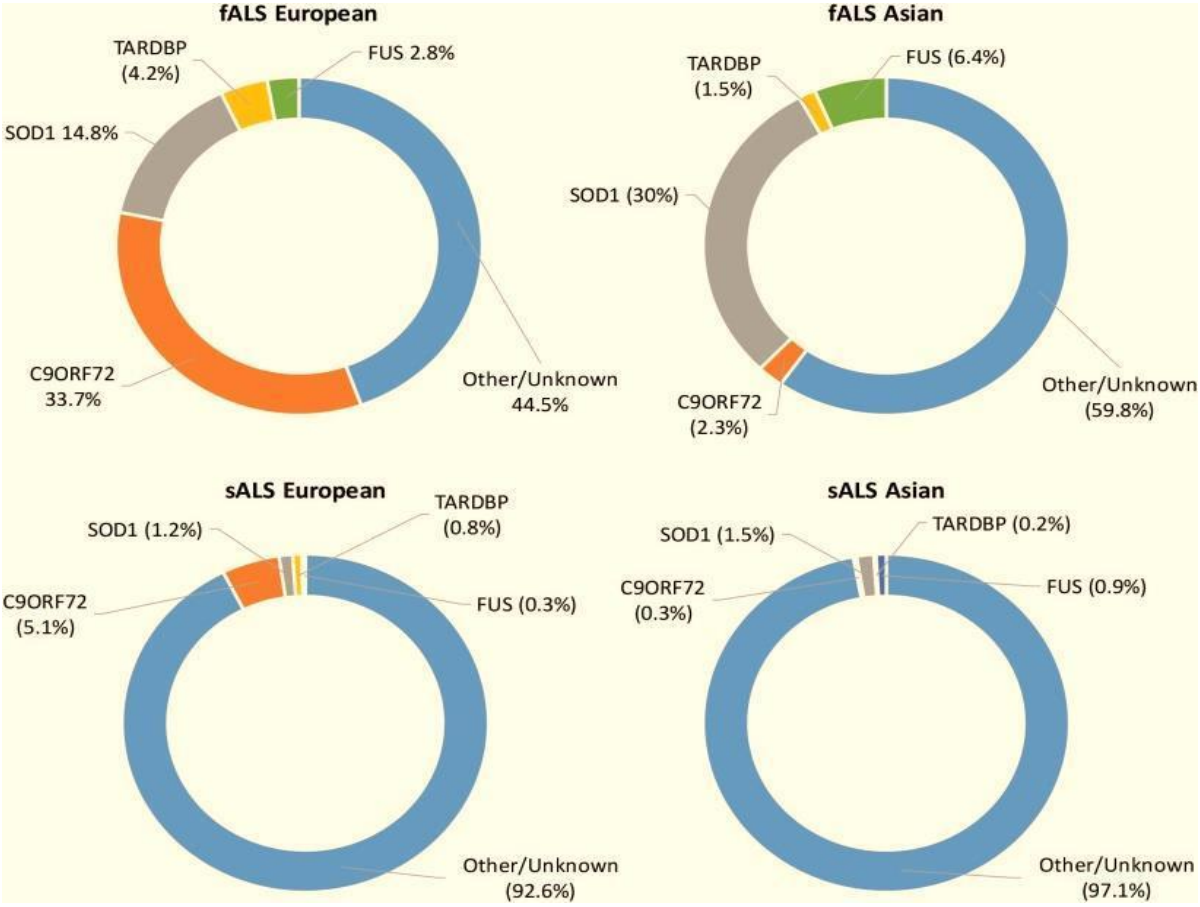

Figure 1. Proportion of ALS cases linked to the most ALS-related genes in Europe and Asia. (Adapted from Zou et al., 2017).

1.1.3.3. ALS and SOD1 mutations

It has been estimated that heritability in ALS is 40%-53% but only 5%-13% of patients show a family history for the disease. One of the most described causes of hereditary ALS (hALS) is a group of mutations in the five encoding exons encoding Superoxide-Dismutase 1 (CuZn-SOD; SOD1). The human SOD1 is located on chromosome 21q22.1 and it codes for the monomeric SOD1 protein, which is composed of 154 amino acids and has a molecular weight of 16 kDa. This protein is responsible for the conversion of superoxide radicals to hydrogen peroxide (H_2O_2) and its expression is ubiquitous (Müller et al., 2021)

The relationship between SOD1 and fALS was first identified in 1993 and, since this first report, mutations in SOD 1 gene have been found in 8%-23% of patients suffering from fALS but also in 1%-4% of individuals with sporadic or simplex ALS (Müller et al., 2021). Pathogenic potential has been well established only for some of SOD 1 punctual

mutations (Andersen, 2006). However, considering their extensive distribution along the gene, their effect is not negligible and involves several domains in SOD1 protein (Kirby et al., 2005).

Thanks to the discovery of SOD1 mutations involvement in ALS pathology, the first rodent models to study ALS were generated. Since SOD1 knockout mice appear to be healthy, it has been supposed that SOD1 causes disease via a toxic gain of function (Philips & Rothstein, 2015). On the other hand, these SOD1 null mice have enhanced sensitivity to stress and show muscle denervation at 18 months of age (Philips & Rothstein, 2015). This is the reason why a loss of function could also be involved in the pathology (Philips & Rothstein, 2015).

It has also been shown that human wild-type SOD1 (SOD1(WT)) overexpression accelerated disease in mice expressing human SOD1 mutants linked to ALS. However, there is a controversy whether the exacerbation mechanism occurs through coaggregation of human SOD1(WT) with SOD1 mutants, stabilization by SOD1(WT) of toxic soluble SOD1 species, or conversion of SOD1(WT) into toxic species through oxidative damage (Audet et al., 2010). To address whether the exacerbation of disease requires misfolding, modifications, and/or interaction of SOD1(WT) with pathogenic forms of SOD1 species, the effect of human SOD1(WT) overexpression in mice expressing the murine mutant Sod1(G86R) has been studied, concluding that SOD1(WT) overexpression did not affect the life span of Sod1(G86R) mice. The spinal cord extracts of these mice revealed a lack of heterodimerization or aggregation between human SOD1(WT) and mouse Sod1(G86R) proteins (Audet et al., 2010). Additionally, no evidence of conversion of SOD1(WT) into misfolded or abnormal SOD1 isoforms based was detected. Thus, it is thought that a direct interaction between wild type and mutant forms of SOD1 is required for exacerbation of ALS disease by SOD1 (WT) protein (Audet et al., 2010).

Up to now, more than 10 rodent models overexpressing mutant SOD1 have been generated, carrying missense mutant or truncated forms of SOD1 protein (Philips & Rothstein, 2015). These animals present some important features of the disease, such as early onset astrogliosis and microgliosis, glutamate-mediated excitotoxicity, aberrant neurofilament processing and lower metabolic support to motor neurons by glial cells. Furthermore, in the SOD1G85R dismutase inactive mutant, researchers clearly detected intraneuronal and glial SOD1 inclusions (Philips & Rothstein, 2015).

In a 2014 study, the SOD1(G93A) mouse model for ALS was used to detect, by means of conformational-specific anti-SOD1 antibodies, whether misfolded SOD1-mediated neurotoxicity extended to neuronal types other than MNs (Sábado et al., 2014) The researchers reported that large dorsal root ganglion (DRG) proprioceptive neurons accumulate misfolded SOD1 and suffer a degenerative process involving the inflammatory recruitment of macrophagic cells (Sábado et al., 2014) As large proprioceptive DRG neurons project monosynaptically to ventral horn MNs, they hypothesized that a prion-like mechanism may be responsible for the transsynaptic propagation of SOD1 misfolding from ventral horn MNs to DRG sensory neurons (Sábado et al., 2014).

In these murine models, various pathogenic mechanisms lead to a selective loss of spinal neurons with muscle wasting and atrophy that has paralysis and death as extreme consequence. Nevertheless, most of these mouse models don't show any kind of gross cortical motor neuronal degeneration, which is a central hallmark of human disease. This relevant difference may underline pathogenic deficiencies of the SOD1 murine model as a tool to investigate neuron disease (Philips & Rothstein, 2015).

1.1.3.4. ALS and C90RF72 mutations

It has been demonstrated that 5–50% of ALS patients show symptoms of frontotemporal dementia (FTD). FTD manifests as frontal and/ or temporal lobe atrophy with changes in personality and behavior as well as language dysfunction (Q. Yang et al., 2020a). ALS and FTD show clinical overlapping; moreover, ubiquitin-positive and tau-negative TDP-43 inclusion bodies are a hallmark in both diseases (Q. Yang et al., 2020a). An outstanding discovery connecting ALS and FTD was made in 2011, when the non-codifying GGGGCC hexanucleotide repeat of the *C9orf72* gene was considered as an important genetic cause for ALS/FTD. This mutation has been found in approximately 40% of familial ALS patients, 25% of familial FTD patients and 88% of familial ALS/FTD patients. Since ALS and FTD share significant clinical, genetic and histopathological features, they are seen as extremes of the same disease continuum (Q. Yang et al., 2020a).

C9ORF72 locus is located on the reverse strand of chromosome 9 (41 kb). It includes two non-coding exons (1a and 1b) and 10 coding exons (from 2 to 11) and produces three coding variants. Alternative splicing of these three RNA variants produces two different isoforms: the 222-amino acid (aa) isoform encoded by V1, and the 481-aa

isoform encoded by V2 and V3. This gene shows a peculiar form of translation known as no-ATG since it doesn't require an AUG starting codon (Zu et al., 2011).

The *C9ORF72* human gene is highly conserved in primates and across different species, suggesting that the protein(s) encoded by *C9ORF72* play primary biological roles (Smeyers et al., 2021). Indeed, the C9ORF72 complex has been implicated in many cellular processes, including vesicle trafficking, lysosome homeostasis, mTORC1 signaling, and autophagy. *C9orf72* deficiency in mice results in exaggerated inflammatory responses and human patients with *C9ORF72* mutations show neuroinflammation phenotype. Recent studies indicate that C9ORF72 regulates trafficking and lysosomal degradation of inflammatory mediators, including toll-like receptors (TLRs) and STING, to affect inflammatory outputs (Pang & Hu, 2021).

Neurologically healthy individuals show ≤11 hexanucleotide repeats in the *C9ORF72* gene. Even if a pathological repeat-length threshold has not been defined, most studies assume a cut-off of 30 repeats; although, much larger expansions from hundreds to thousands of repeats are frequently found in ALS/FTD patients (Balendra & Isaacs, 2018).

The repeat expansions could cause disease through a toxic gain-of- function (GOF) mechanism, involving RNA and protein toxicity by an aberrant accumulation of a dipeptide repeat protein (DPR). On the other hand, reduced levels of *C9ORF72* mRNA and protein have been detected in a vast range of patients' tissues and patient-derived cell lines. These findings may suggest that C9ORF72 implication in ALS/FTD pathology could also be related to a loss of function mechanism (LOF) by haploinsufficiency (Butti et al., 2021). While GOF pathogenic mechanisms are largely studied, LOF counterpart is still poor understood. The exact mechanism that leads GGGGCC to cause neurodegeneration is still unknown. To date we know that C9ORF72 protein functions in a complex with WDR1 and SMCR proteins function as a guanine exchange factor (GEF) for Rab8 and Rab9. It can also contribute to the regulation of the autophagic flux, the endosomal trafficking and the AMPA receptor levels (Butti et al., 2021).

Briefly summarizing, cytoplasmic insoluble aggregates of *C9ORF72*-derived proteins could negatively affect the nuclear importing of TDP-43, suggesting that aberrant aggregation and distribution of proteins may be a common factor in ALS pathology independently of the primary genetic cause of the disease (Khosravi et al., 2017).

1.1.3.5 ALS and FUS mutations

As previously stated, approximately 15% of ALS cases are familial, and mutations in the *fused in sarcoma* (FUS) gene contribute to a subset of fALS cases. FUS is a multifunctional protein participating in numerous RNA metabolism pathways.

Mutations in *FUS* have been demonstrated to cause aberrant splicing (Svetoni et al., 2016); however, the molecular mechanism by which cells handle defective mRNA has not been explored in ALS. It is also known that ALS-linked *FUS* mutations cause a liquid–liquid phase separation of FUS protein *in vitro*, inducing the formation of cytoplasmic granules and inclusions. However, it remains elusive what other proteins are sequestered into the inclusions and how such a process leads to neuronal dysfunction and degeneration (Kamelgarn et al., 2018).

Recently, a protocol has been developed to isolate the dynamic mutant FUS-positive cytoplasmic granules in order to characterize those (Kamelgarn et al., 2018). Proteomic identification of the protein composition and subsequent pathway analysis led investigators to hypothesize that mutant FUS can interfere with protein translation. It has been demonstrated that the ALS mutations in *FUS* indeed suppressed protein translation in N2a cells expressing mutant FUS and fibroblast cells derived from FUS ALS cases. In addition, the nonsense-mediated decay (NMD) pathway, which is closely related to protein translation, was altered by mutant FUS (Kamelgarn et al., 2018) NMD is a major mRNA surveillance system that is known to degrade defective mRNA and 3-20% of all mRNAs (Karam et al., 2013). NMD and protein translation are interrelated, as NMD utilizes the translocating ribosome as a proofreading mechanism for sensing defective mRNAs (Celik et al., 2017).

Specifically, NMD-promoting factors UPF1 and UPF3b increased, whereas a negative NMD regulator, UPF3a, decreased, leading to the disruption of NMD autoregulation and the hyperactivation of NMD. Alterations in NMD factors and elevated activity were also observed in the fibroblast cells of FUS ALS cases. These findings lead to the conclusion that mutant *FUS* suppresses protein biosynthesis and disrupts NMD regulation, both of which likely contribute to motor neuron death (Kaelan et al., 2018).

1.2. ALS physiopathology. TARDBP implication

ALS physiopathology is complex and partially understood. Cellular dysfunction not only affects motor neurons, but also non-neuronal cells of the nervous system (Neumann et al., 2006).

Protein cytoplasmic inclusions or aggregates in degenerating motor neurons and surrounding oligodendrocytes are a pathological main feature in ALS (Blokhuis et al., 2013). Inclusions are not exclusively found in the spinal cord but also in other brain regions such as the frontal and temporal cortices, hippocampus, and cerebellum. The most common aggregates found in ALS patients are ubiquitinated and they are classified as either Lewy body-like hyaline inclusions or skein-like inclusions (Blokhuis et al., 2013). Bunina bodies, which are small eosinophilic ubiquitin-negative inclusions and round hyaline inclusions without a halo, are another group of inclusions found in ALS patients. They consist of amorphous electron-dense material surrounded by tubular and vesicular structures. In addition, neurofilamentous inclusions have been found in the axon hillock in close contiguity to ubiquitinated inclusions (Blokhuis et al., 2013). These inclusions have been found not only in neuronal cells, but also in patients' spinal glial cells (Arai et al., 2006). It has been proposed that astrocytes can also incite protein aggregation in motor neurons by inhibiting their autophagic capacity and by secreting prion-like protein aggregates (Halpern et al., 2019) (Figure 2).

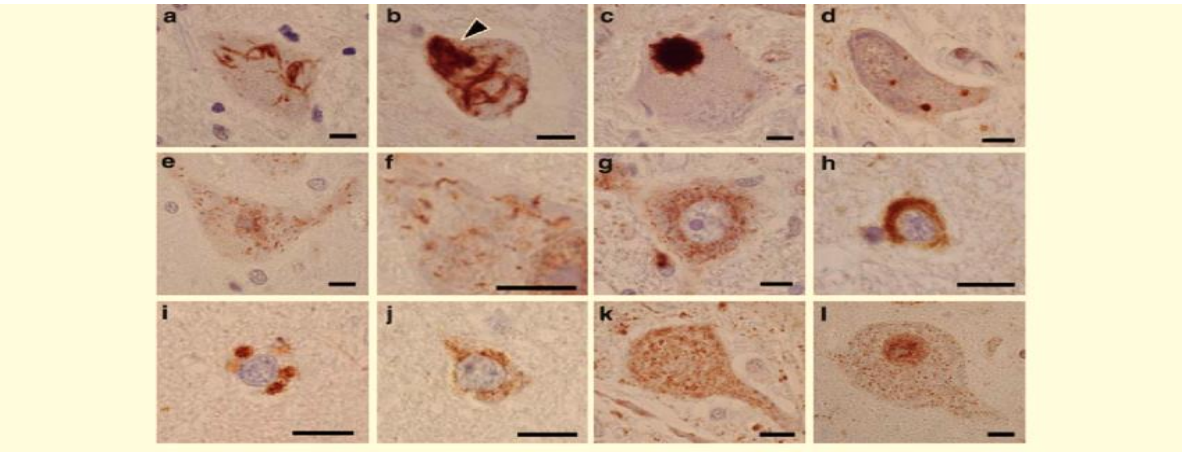

Figure 2. TDP-43 immunohistochemistry in the brain and spinal cord of ALS patients (a–j) and control subjects (k, l). a and b Skein-like inclusions in the anterior horn cells. Dense compacted area (arrowhead) is also evident (b). c Rounded, spicular inclusion in the anterior horn cell. d Dot-like inclusions in the anterior horn cell. e Minute thread-like structures scattered in the cytoplasm of the anterior horn cell. f Higher magnification view of the area in (e) showing straight or wavy, linear wisps. g Punctate granules in the spinal anterior horn. Note that nuclear TDP-43 immunoreactivity is absent. h Circular inclusion in the putamen. i and j Coarse or Wne granular cytoplasmic staining in the neostriatal small neurons. k and l Punctate granules in the spinal anterior horn (k) and motor cortex (l). Note that nuclear TDP-43 immunoreactivity is preserved (l) (bars 10 micrometers) (Adapted from Mori et al., 2008).

As previously mentioned, TDP-43 is one of the major components of protein inclusions in ALS patients motor neurons and in cortical neurons of FTD. Also, both SOD1 and FUS mutations have been related to juvenile-onset malignant ALS, even in absence of an apparent family history (Zou et al., 2015). The proteostasis network is particularly important in nondividing, long-lived cells, such as neurons, as its failure is implicated with the development of neurodegeneration.

ALS shares protein aggregation as a pathological mechanism with other neurodegenerative diseases like AD, Parkinson's disease (PD) and frontotemporal lobar degeneration (FTLD). These neurological disorders have shared risk factors such as aging, oxidative stress, environmental stress, and protein dysfunction, which can alter cellular proteostasis (Höhn et al., 2020).

The proteostasis network is particularly important in nondividing, long-lived cells, such as neurons, as its failure is implicated with the development of neurodegeneration. It encloses molecular chaperone proteins, degradation pathways (proteasomal and autophagic), and the protein trafficking (McAlary et al., 2020) Chaperones protect vulnerable proteins from misfolding and aggregation, potentially through the amyloid pathway. Proteins vulnerable to amyloid aggregation can form polymorphic assemblies through template-directed growth. Amyloid assemblies are thought to propagate from cell-to-cell through exocytosis in vesicles and exosomes, through membrane breakages and macropinocytosis (Figure 3) (McAlary et al., 2020).

Thus, the integrity of the proteostasis network is essential to cell viability and especially in nonproliferative cells, such as neurons, as its failure is associated with several neurodegenerative diseases. In addition, protein deposition diseases are also strongly associated with perturbations in mitochondrial function, ER, and UPS/autophagy degradation pathways (Höhn et al., 2020). However, whether some ALS-associated proteins such as TDP-43 or other are associated with mitochondrial demise, it is currently unknown.

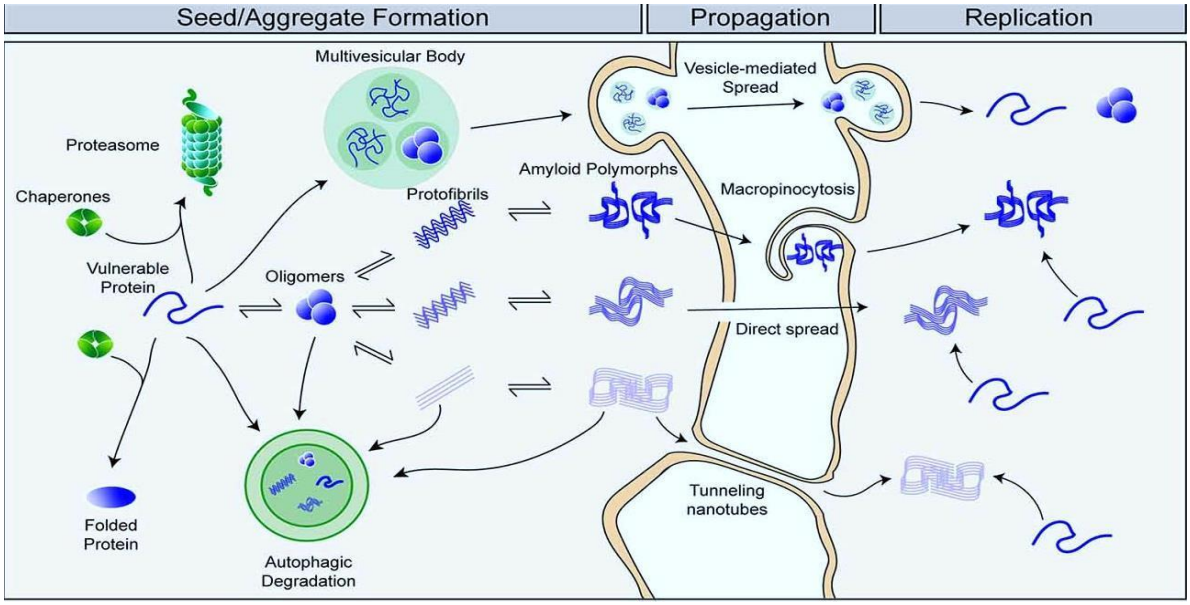

Figure 3. Relationship between proteostasis and prion-like protein propagation. Green objects represent the components of the proteostasis network such as chaperone proteins, degradation pathways (proteasomal and autophagic), and the trafficking of proteins. Chaperones prevent protein misfolding through the amyloid pathway, in blue. Amyloid assemblies may propagate from cell-to-cell through exocytosis in vesicles and exosomes, membrane breakages, or macropinocytosis (Adapted from McAlary et al., 2020).

1.2.1 An overview on structure and function of TDP-43

TDP-43 is a ubiquitous 414 amino acids protein encoded by the *TARDBP* gene and belonging to the heterogeneous nuclear ribonucleoprotein (hnRNP) family. The protein structure includes an N-terminal region, a nuclear localization signal (NLS), two RNA recognition motifs called RRM1 and RRM2, a nuclear export signal (NES), a C-terminal region enclosing a prion-like glutamine/asparagine-rich (Q/N) domain and a glycine-rich region (Figure 5) (de Boer et al., 2021). Its localization is mainly nuclear, but it can shuttle between the nucleus and the cytoplasm through a process mediated by active and passive transport. In the cytoplasm, TDP-43 acts as an important mediator in RNA metabolism, modulating RNA splicing, transcriptional repression, micro-RNAs synthesis and RNA trafficking between nuclear and cytoplasmic compartments (Lagier-Tourenne et al., 2010). TDP-43 has also previously been found in the mitochondrial compartment, where it interacts with the mitochondrial genome and participates in the respiratory chain pathways (de Boer et al., 2021).

The members of hnRNP protein family play an important role in RNA stability, trafficking, and splicing regulation as well as RNA processing (Geuens et al., 2016). In healthy cells, TDP-43 localization is mainly nuclear and acts in RNA regulation, such as transcriptional regulation, alternative splicing, and mRNA stabilization (Geuens et al.,

2016). Cleavage, hyperphosphorylation and ubiquitination of TDP-43 can be observed under pathological conditions leading to its cytoplasmic accumulation and aggregation. It has been also shown that TDP-43 undergoes a breakage to generate 25 and 35 kDa C-terminal fragments which contributes to toxicity (Igaz et al., 2009). Moreover, hyperphosphorylated TDP43, in the serine 403/404 and 409/410 residues (p-TDP-43), can also be found in the pathological inclusions (Jo et al., 2020a). The C-terminal domain encloses the majority of TDP-43 known mutations (Figure 4). The main effect of these mutations consists in the inhibition of TDP-43 with other proteins that belong to the hnRNP family, blocking the formation of a complex rich in heterogeneous nuclear RNA (hnARN) (Buratti, 2015).

One of the first described functions for TDP-43 was the modulation of HIV-1 virus through its binding capacity to the HIV-1 LTR, promoting the suppression of HIV-1 transcription and gene expression (Nehls et al., 2014). In the cytoplasmic compartment, TDP-43 plays an important role in *Nefl* and *HDAC6* mRNA stabilization and co-localizes with known mRNA transport proteins, such as Staufen 1, FMRP and SMN in dendrites and axons. Regarding mRNA translation it can associate with initiation/elongation factors and act as a repressor of *Rac1, Map, and GluA1* mRNA by recruitment of the FMRP-CYFIP translational inhibitor complex (Ederle & Dormann, 2017).

More recently, high levels of TDP-43 were detected in spermatocytes in the preleptotene and pachytene stages of meiosis and it was demonstrated that conditional KO (cKO) of the *TARDBP* gene in male germ cells of mice leads to reduced testis size, depletion of germ cells, vacuole formation within the seminiferous epithelium, and reduced sperm production (Campbell et al., 2021).

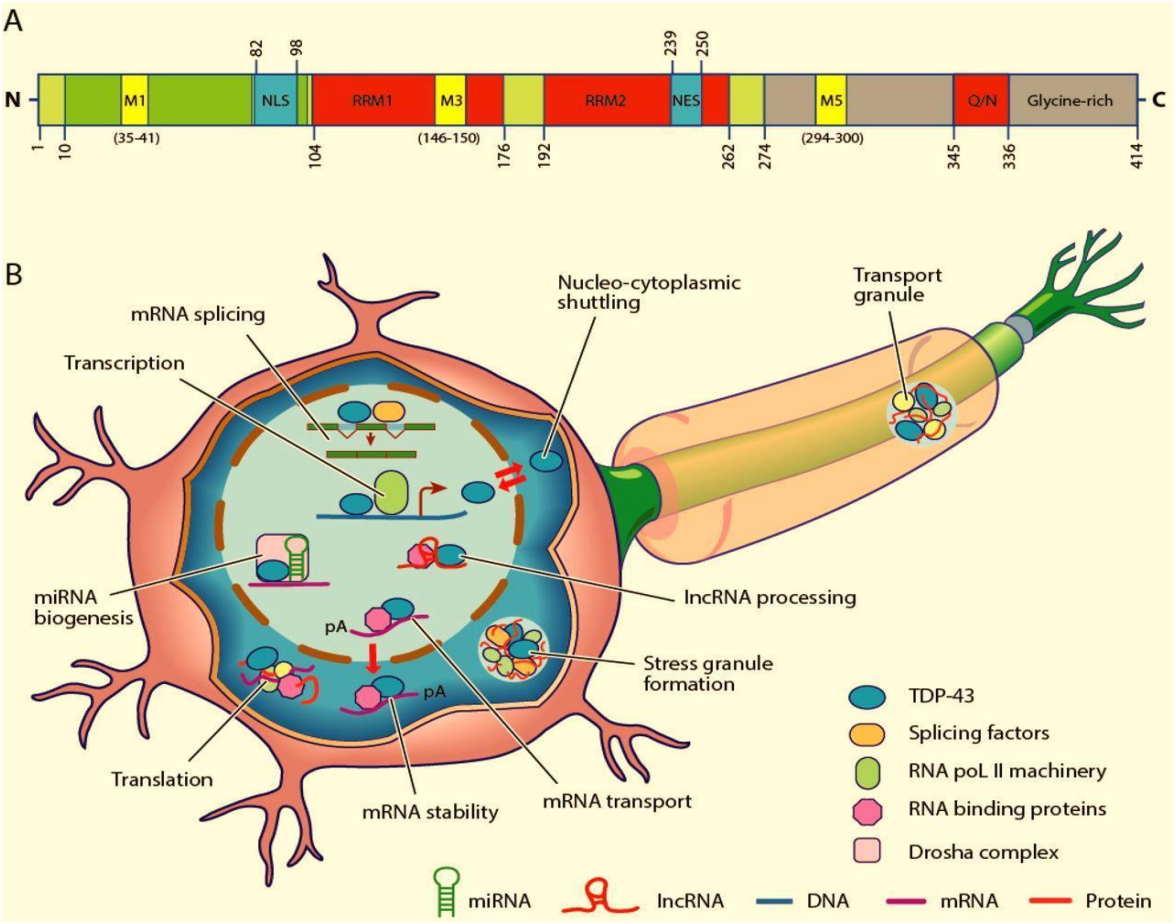

Figure 4. (A) Structure of TAR DNA-binding protein 43 (TDP-43). The TDP-43 protein contains 414 amino acids and shows an N-terminal region with a nuclear localization signal (NLS), two RNA recognition motifs (RRM1 and RRM2), NES and a C-terminal domain with a Q/N and glycine-rich regions. It also includes the mitochondrial localization motifs M1, M3 and M5. Pathogenic mutations are frequently located within the C-terminal region which has prion-like properties. The numbers represent amino acid lengths. (B) The TDP-43 protein is a critical mediator in RNA metabolism. In the nucleus, TDP-43 is important for transcription and splicing mRNA, as well as maintaining RNA stability and transport to the nucleus. In addition, TDP-43 regulates biogenesis of microRNA and processing of long non-coding RNA. Although predominantly located within the nucleus, TDP-43 shuttles between the nucleus and the cytoplasm, where it acts on mRNA stability, translation, formation of stress and ribonucleoprotein (RNP) transport granules (Adapted from de Boer et al., 2021).

An additional TDP-43 function was described in 2008, when it was found that removal of TDP-43 in human cells significantly increases cyclin-dependent kinase 6 (Cdk6) protein and transcript levels (Y. M. Ayala et al., 2008). The control of Cdk6 expression mediated by TDP-43 involves GT repeats in the target gene sequence and Cdk6 up-regulation in TDP-43-depleted cells is accompanied by an increase in phosphorylation of two of its major targets, the retinoblastoma protein pRb and pRb-related protein pRb2/p130 (Y. M. Ayala et al., 2008).

TDP-43 silencing also determines changes in the expression levels of several factors involved in cell proliferation (Y. M. Ayala et al., 2008).

TDP-43 has various roles in determining expression levels and splicing variants of several different protein-coding genes. Some of these genes codify for RNA-binding proteins, including TDP-43. Thus, TDP-43 can exert an autoregulation on its own levels through a negative feedback loop (Y. M. Ayala et al., 2011).

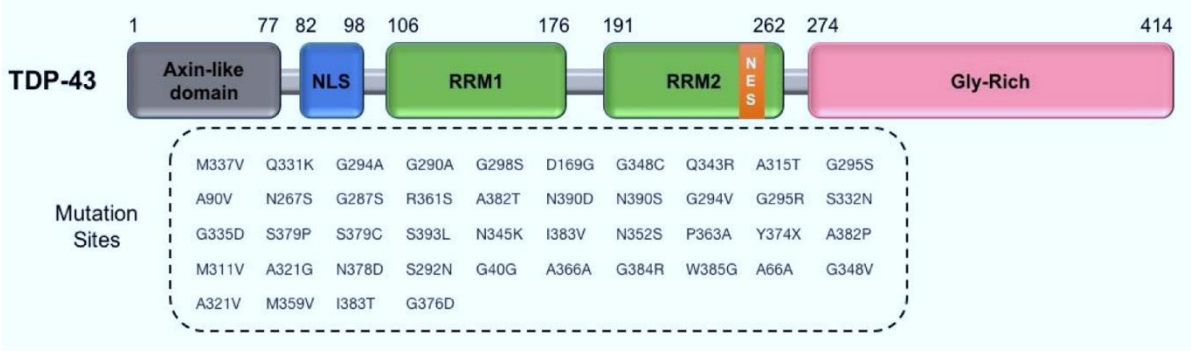

Figure 5. A scheme for TDP-43 domain structure (top) and TDP-43 variants frequently found in ALS patients (bottom). The majority of variants are missense variants located in the glycine-rich region, which interacts with other heterogeneous ribonucleoproteins (Adapted from Yousefian-Jazi et al., 2020).

In a recent study it has been demonstrated that de novo paraspeckle assembly in spinal neurons and glial cells is a hallmark of both sporadic and familial ALS in close association with TDP-43 pathology (Shelkovnikova et al., 2018). Depletion of TDP-43 results in accumulation of endogenous dsRNA and activation of type I interferon response which also stimulates paraspeckle formation (Shelkovnikova et al., 2018). In addition, TDP-43 contributes to the synthesis of a subset of precursor miRNAs (pre-miRNAs) by both interacting with the nuclear Drosha complex and binding directly to the relevant primary miRNAs (pri-miRNAs). In the cytoplasmic compartment, TDP-43 which interacts with the Dicer complex enhances the processing of some of these pre-miRNAs via binding to their terminal loops. Furthermore, involvement of TDP-43 in miRNA biogenesis appears to be indispensable for neuronal outgrowth (Kawahara & Mieda-Sato, 2012).

Related to RNA processing, TDP-43 also plays a role in the determination of cryptic and skiptic exons. Cryptic exons can be defined as splicing variants that may introduce frameshifts or stop codons, among in the resulting mRNA. In 2015, it was shown that TDP-43 is able to repress the splicing of nonconserved cryptic exons, to maintain intron integrity. These aberrant mRNA have been demonstrated in motor cortex and middle temporal gyrus of ALS and FTLD patients (Ling et al., 2015; Torres et al., 2018). In fact, in mouse embryonic stem cells depleted from TDP-43, these cryptic exons were spliced into mRNAs, disrupting their translation, and triggering non-sense mediated decay. In addition,

induced repression of cryptic exons appeared to prevent cell death in TDP-43-deficient cells. The finding that cryptic repression was impaired in ALS and FTD, suggest a relationship between this splicing defect and TDP-43 proteinopathy (J. P. Ling et al., 2015). In 2018, it was shown that TARDBP action on splicing is relevant in ATG4B autophagic function. Deregulation of TARDBP expression in human neural tissue and in HeLa cells, demonstrated that TARDBP is required for maintaining the expression of ATG4B (Torres et al., 2018).

Physiologically, TDP-43 shows high-level expression during embryonic development; the protein expression decreases during postnatal development. In mice where the TDP-43 gene (*Tardbp*) was disrupted using a gene trap that carries a β-galactosidase marker gene, heterozygous (*Tardbp/−*) mice are fertile and healthy, but no viable monozygotic null (*Tardbp−/−*) mice were obtained from the intercrosses of *Tardbp/−* mice. *Tardbp−/−* embryos die between 3.5 and 8.5 days of development (Sephton et al., 2010). Similarly, *Tardbp−/−* blastocysts grown in cell culture display abnormal expansion of their inner cell mass (Sephton et al., 2010).

Several studies on TDP-43 and its importance in ALS pathology, have found that TDP-43 can assemble into stress granules (SGs) in response to oxidative stress and to environmental insults. Stress granules are ribonucleoprotein complexes in which protein synthesis is temporarily blocked (Colombrita et al., 2009). A specific amino acid interval (216-315) in the C-terminal region and the RNA-recognition motif 1 domain are both implicated in TDP-43 participation in SGs as their deletion prevented the recruitment of TDP-43 into SGs (Colombrita et al., 2009). Thus, TDP-43 is a specific component of SGs, but it has been proved that it is not necessary for SG formation, and its gene silencing does not impair cell survival during stress (Colombrita et al., 2009). The analysis of spinal cord tissue from ALS patients showed that SG markers are not enclosed in TDP-43 pathological inclusions (Colombrita et al., 2009).

Interestingly, other cellular stresses, in addition to oxidative stress, have been described as possible triggers for the formation of TDP-43 enclosing SGs. Indeed, osmotic stress (Dewey et al., 2011a), mitochondrial stress (Chalupníková et al., 2008), endoplasmic reticulum stress (Goodier et al., 2007) and proteasome inhibition (Colombrita et al., 2009) have been all involved in SGs generation. Also, it has been hypothesized that SGs genesis could be involved in the origin of the irreversible TDP-43 aggregation in the cytoplasm (Bentmann et al., 2012). In general, several cellular stresses could determine proteostasis disruption and be associated with ALS aberrant

protein aggregates. Whether SGs formation is linked to changes in other pathogenic mechanisms, such as mitochondrial dysfunction, it is not well established.

Globally, post translational changes, fragmentation and cytoplasmic aggregation of TDP-43 are well established hallmarks of ALS and FTD pathology (Ferrari et al., 2011). Nonetheless, TDP-43 contribution to neurodegeneration is still very controversial. A recent study has aimed to dissect TDP-43 function at physiological levels (Ferrari et al., 2011). It was found that mutations enclosed in the C-terminal domain of the protein lead to a gain of splicing function, in which skipping of constitutive exons determines changes in gene expression. On the other hand, TDP-43 LOF mechanisms can also contribute to motor neuron loss through an altered modulation of alternative splicing (Fratta et al., 2018).Thus, these findings are compatible with the hypothesis that gain-of-function and loss-of-function mechanisms can both contribute to TDP-43 proteinopathies. In particular, TDP-43 cytoplasmic aggregation and nuclear depletion in post-mortem tissue supports a strong role of LOF at the late stage of the illness, while gain-of-function (GOF) mechanisms seem to be predominant at a early stage (Figure 6) (Fratta et al., 2018).

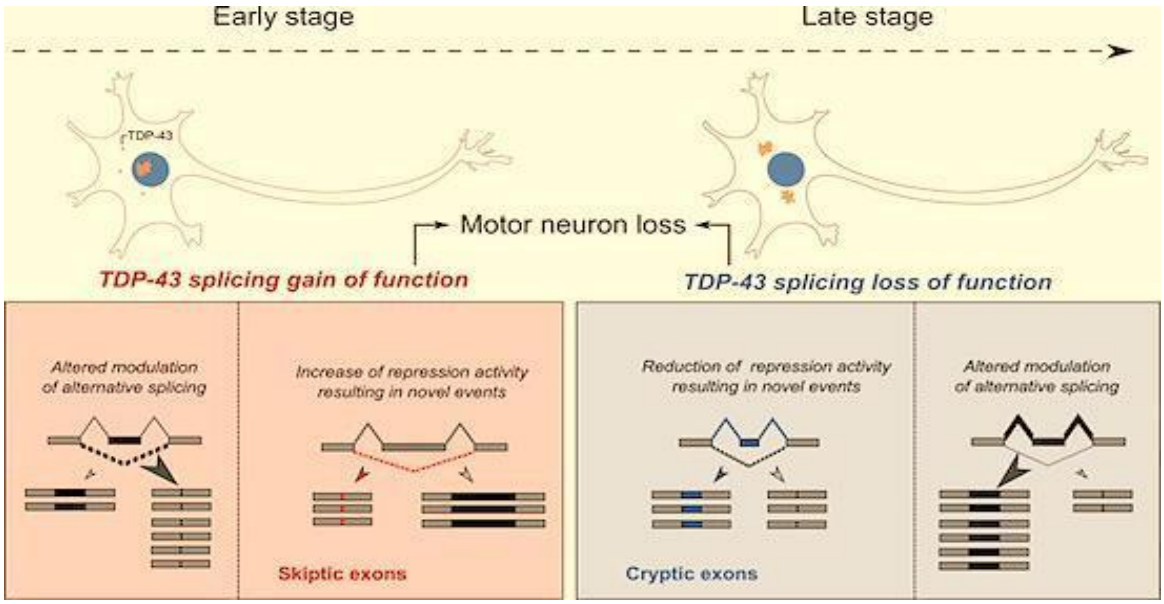

Figure 6. **Point mutations within the low complexity C-terminal domain of TDP-43 induce phenotypes resembling ALS in mice.** At the molecular level, these mutations induce a novel gain of splicing activity leading to skipping of certain constitutive exons, called “skiptic exons”. This phenomenon is predominant at an early stage of neurodegeneration, while at later stages TDP-43 splicing loss of function is evident. A shared consequence of both mechanisms is motor neuron loss (Adapted from Fratta et al., 2018).

With respect to protein aggregates toxicity, contrasting hypotheses have been proposed, with several authors suggesting a neuroprotective role for protein aggregation in neurodegeneration processes (Saad et al., 2017). Actually, these aggregates can frequently be found in motor neurons that survivor motor neurons. In this scenario, real responsible for toxicity could be found instead in small oligomeric misfolded proteins (Ciechanover & Kwon, 2015).

1.2.1.2 ALS and TARDBP mutations

Protein aggregation is determined by the aberrant folding of a protein that results in the formation of oligomers fibrils rich in beta sheet structure via polymerization (Q. Yang et al., 2020). Physiologically, proteins undergo folding through chaperones to reach a biologically stable conformation and their structure is stabilized by covalent and non-covalent interaction between the amino acid residues (Q. Yang et al., 2020). In a pathological context, structural destabilization determines the exposure of hydrophobic amino acids patches in the outer environment. The adhesive nature of these patches could result in self-association into oligomers and fibrils found in several neurodegenerative diseases (Yang et al., 2020).

TDP-43 protein was firstly identified as a main component of ubiquitin-positive protein inclusions in ALS patients motor neurons and in FTD patients' cortical neurons (Arai et al., 2006). It is currently known that the vast majority (97% approximately) of both familial and sporadic ALS cases are associated to the presence of cytoplasmic TP43-positive aggregates (Guo & Shorter, 2017), thus their finding in necropsy samples can be related to the disease.

It has been proved that the internalization of pre-formed TDP-43 aggregates in the human neuroblastoma N2a cells results in their ubiquitination and hyperphosphorylation (Cascella et al., 2019). In this system, aggregated TDP-43 appears to be responsible for the alteration of calcium homeostasis involving mitochondria and the increase in reactive oxygen species that, finally, leads to caspase activation (Cascella et al., 2019). Proteasomal inhibition and failure of macroautophagic systems showed that these features are both involved in TDP-43 accumulation, and they interact in neurodegenerative disorders involving TDP-43 proteostasis (Cascella et al., 2019) (Figure 7).

The discovery of TP43 as a main component of cytoplasmic inclusions, led to the investigation on TARDBP gene mutations in families with autosomal dominant forms of fALS and FTD (Chiò et al., 2011).

To date, 63 mutations in TARDBP gene have been identified as reported in ALSoD (https://alsod.ac.uk/output/gene.php/TARDBP#variants). Most of them are classified as missense mutations located in the glycine-rich C-terminal domain of the protein, which mediates protein-protein interactions (Berning & Walker, 2019).

Although TDP-43 dominant mutations are not very common, they have been linked to ALS. The screening of genomic DNA extracted from spinal cord specimens of sporadic ALS patients for mutations in the TARDBP gene has shown that the C-terminal Q331K mutation in the spinal cord tissue of patients is associated with accumulation of higher levels of DNA strand breaks (Cascella et al., 2019).Moreover, the same study has detected higher levels of the DNA double-strand break marker γH2AX in the spinal cord tissue of patients in comparison with age-matched controls, suggesting a role of the Q331K mutation in genome-damage accumulation (Cascella et al., 2019).

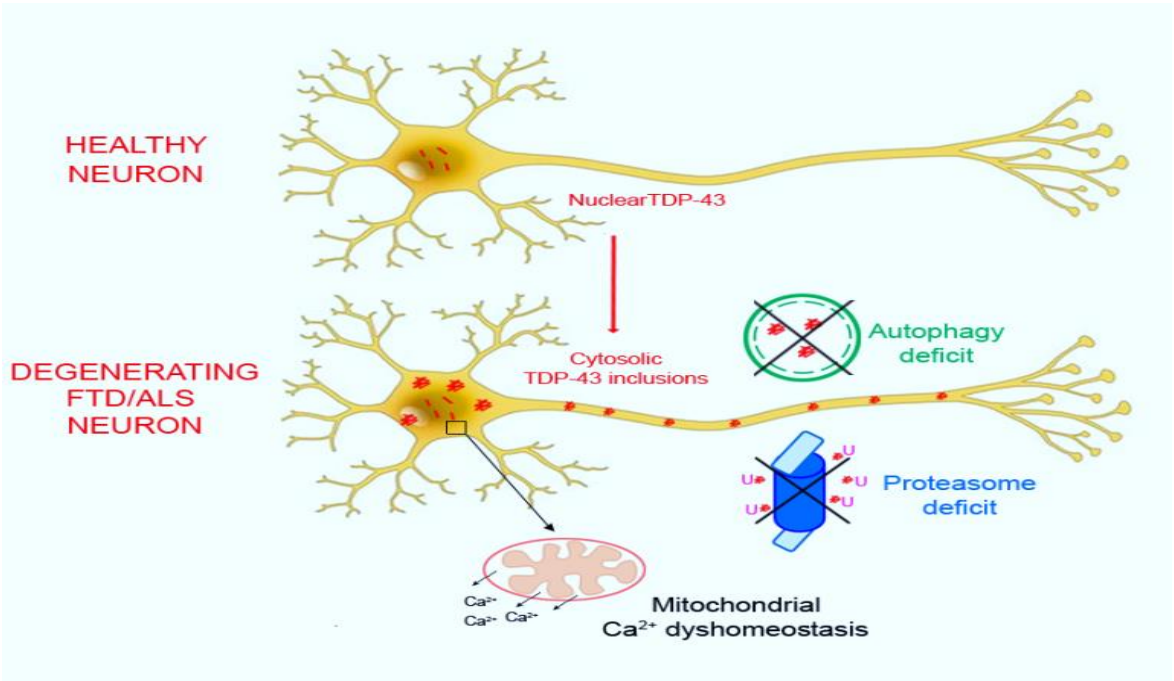

Figure 7. TPD43 expression under physiologic and pathologic conditions. In healthy neurons, TDP-43 is mainly nuclear, and it takes part in gene expression, a regulator of RNA splicing. TDP-43 can undergo a trafficking between the nucleus and the cytoplasm, where it can bind and stabilize the RNA. In degenerating FTD/ALS neurons, TDP-43 leaves the nucleus and accumulates in the cytoplasm where it appears to be ubiquitinated, hyperphosphorylated and cleaved in insoluble inclusions. TDP-43 cytoplasmic inclusions are responsible for mitochondrial calcium homeostasis alteration (Adapted from Berning & Walker, 2019).

In conditional SH-SY5Y lines ectopically expressing wild-type (WT) or Q331K-mutant TDP-43, increased cytosolic sequestration of the poly-ubiquitinated and aggregated form of mutant TDP-43 was reported, in correlation with increased genomic DNA strand breaks, activation of the DNA damage response factors phospho-ataxia-telangiectasia mutated (ATM), phospho-53BP1, γH2AX and neuronal apoptosis. Furthermore, the mutant cells showed elevated levels of reactive oxygen species, suggesting the mutation could have both dominant negative and loss-of-function effects (Cascella et al., 2019).

A knock-in mouse model bearing a Q331K mutation in the endogenous mouse gene has been recently described as the most physiological model described to date, showing features of both ALS and FTD such as weight gain, lack of classical TDP-43 pathology and elevated nuclear TDP-43 (Watkins et al., 2021). TDP-43^{Q331K} mice display cognitive dysfunction and a scarcity of parvalbumin interneurons. In this context, TDP-43 autoregulation is altered resulting in TDP-43 GOF, and altered splicing of MAPT, a crucial dementia gene (White et al., 2018).

A further TDP-43 mutation (M323K) falls within the protein C-terminal low complexity glycine-rich domain (LCD) where almost all known ALS-causing mutations are clustered specifically within a 20 amino acid region that influences TDP-43 alpha-helix structure which is important for liquid phase separation, aggregation and protein self-interaction (Fratta et al., 2018) In an in vitro turbidity assay it has been found that the M323K mutation decreases the propensity for phase separation compared to wild type, similarly to the human TDP-43 ALS-causing mutation Q331K (Fratta et al., 2018).

A third TDP-43 mutation of interest in this thesis, F210I, is located in the TDP-43 recognition motif 2 (RMRM2). Hence these two last two mutations, M323K and F210I, are also known as LCDmut and RMRM2mut, respectively (Figure 8).

The effects of these TDP-43 mutations on splicing function in an endogenous physiological context have been studied in a CFTR minigene assay in mouse embryonic fibroblasts (MEFs). Results show that RRM2mut causes a highly significant shift towards exon inclusion, similarly to the well-documented effect of TDP-43 knockdown, showing a dose-dependent LOF. Interestingly, the LCDmut has an opposite effect, increasing exon exclusion, thus suggesting a GOF (Fratta et al., 2018).

Both mutated MEFs lines didn’t show any alteration in TDP-43 protein levels, but through an electromobility shift assay it was compared the RNA binding capacity of WT,

RRM2mut and LCDmut recombinant TDP-43. RRM2mut showed a reduction in RNA binding, which remained unchanged for the LCDmut (Fratta et al., 2018).

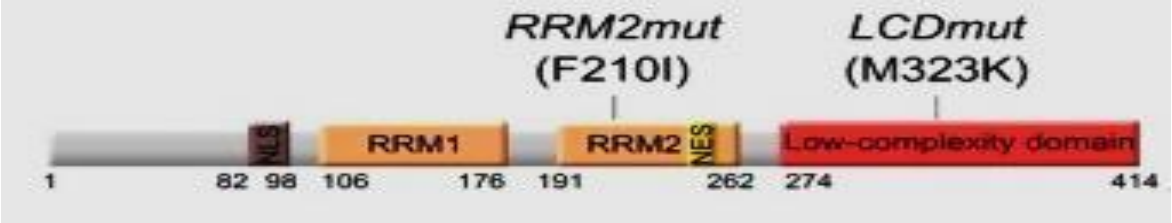

Figure 8. Diagram of TDP-43 illustrating the location of RRM2mut and LCDmut (Adapted from Fratta, et al., 2018).

Regarding the geographical distribution of ALS familial mutations, they show a uniform global distribution, with regional variability (Chiò et al., 2011) . A representative case for this phenomenon is that of A382T mutation of the TARDBP gene, which accounts for nearly one third of ALS cases in the Italian island Sardinia. This increase in A328T mutation frequency could be due to the fact that the Sardinian population has been genetically isolated, showing the so-called founder effect (Chiò et al., 2011).

Some people with ALS caused by *TARDBP* gene mutations also develop a condition called frontotemporal dementia (FTD), which is a progressive brain disorder that affects personality, behavior, and language (Borroni et al., 2010). It is unclear why some people with *TARDBP* gene mutations develop FTD and others do not. Individuals who develop both conditions are diagnosed as having ALS-FTD (Borroni et al., 2010)

Globally, more than 60 mutations in the *TARDBP* gene have been found to cause ALS. Most mutations change single amino acids in the TDP-43 protein. Most of these changes affect the region of the protein involved in mRNA processing, likely disrupting the production of other proteins(Hergesheimer et al., 2019). Changes to the TDP-43 protein cause the protein to misfold and form protein aggregates, which have been found in nerve motor neurons from people with ALS. It is still unclear whether TDP-43 protein aggregates cause the nerve cell death that leads to ALS or if they are a byproduct of a dying cell (Hergesheimer et al., 2019).

1.2.2. Toxicity mechanisms in ALS pathophysiology

As discussed above, aberrant intracellular or extracellular protein accumulation in the affected brain regions is a typical pathological feature of neurodegenerative diseases and it is thought to lead to neurotoxicity, neurodegeneration, and finally clinical manifestation

of the disease (Takalo et al., 2013). The intracellular inclusions detected in the brain of patients are often ubiquitin-positive and contain misfolded disease-specific proteins. This conformational change results in the exposure of the hydrophobic regions of the protein that are normally buried within the protein structure when it is in its natively folded conformation. The exposed hydrophobic structures promote oligomerization and aggregation of the protein (Takalo et al., 2013).

Healthy cells can efficiently utilize their protein quality control (PQC) system to manage the misfolded proteins and preserve the protein homeostasis. A series of molecular chaperones involved in the cellular PQC systems, such as heat shock proteins (Hsp), recognize misfolded proteins, promote their refolding, prevent their aggregation, and help to repair the damaged proteins (Hartl et al., 2011). The molecular chaperones may also interact with the ubiquitination machinery and target the misfolded proteins to degradation by the ubiquitin-proteasome system (UPS) (Ciechanover et al., 2000) or the autophagosome-lysosome pathway (ALP) (Kundu & Thompson, 2008). It has been suggested that deficiencies in PQC and clearance mechanisms is likely to cause the abnormal accumulation of proteins in neurodegenerative diseases (Takalo et al., 2013). In addition, the excessive accumulation of misfolded and aggregated proteins could determine the overwhelming of the PQC and clearance systems, which leads to further protein accumulation (Takalo et al., 2013). Different stress conditions can promote failure of the PQC system (Alberti & Hyman, 2021); a brief review of different kinds of cellular stresses follows, all of which have been frequently implicated in neurodegeneration.

1.2.2.1 Oxidative stress

Under normal conditions, mitochondria are the main source of reactive oxygen species (ROS) that physiologically take part in cellular signaling pathways and oxygen homeostasis maintenance (Roy et al., 2017).

As indicated in section 1.1.3, ALS pathological mechanisms are still unknown, but evidence indicates that ROS production associated with an inefficient antioxidant response is a crucial pathological feature in ALS (Cunha-Oliveira et al., 2020). Oxidative stress (OS) appears to be implicated in the loss of MNs and in mitochondrial dysfunction, all contributing to neurodegeneration in ALS(Cunha-Oliveira et al., 2020).

Several pathways involved in ROS-induced cell death have been proposed. ROS can directly act on proteins, lipids, and nucleic acids, causing injury and consequent cell death. Among these mechanisms, protein oxidation and nitrosylation can impair a variety

of enzymatic processes and growth factors leading to cellular dysfunction (Sola et al., 2007). In our laboratory, we have previously investigated on OS stress markers for ALS, focusing on the analysis of features of mitochondrial oxidative metabolism, as well as mitochondrial chain complex enzyme activities and protein expression, lipid profile, and protein oxidative stress markers, in the Cu, Zn superoxide dismutase with the G93A mutation (hSOD1-G93A) transgenic mice and N2A cells overexpressing hSOD1-G93A (Cacabelos et al., 2016).

Lipid peroxidation has been involved in cell death through effects on cellular phospholipids as major cell membrane components through activation of sphingomyelinase and release of ceramide species, which act as apoptosis activators (Auten et al., 2002). Also, nucleic acid oxidation plays a relevant role in physiologic and premature aging as well as DNA strand breaks, determining necrosis and/or maladaptive apoptosis (Auten et al., 2002). It is of note that vulnerable neurons in human ALS accumulate DNA damage and strongly activate and mobilize response effectors and DNA repair genes (B. W. Kim et al., 2020). This DNA damage response (DDR) in ALS motor neurons involves recruitment of c-Alb and BRCA1 to the nucleus *in vivo*, and repair of DNA double-strand breaks in human ALS MNs with SOD1 mutations in cell culture. The extent of these changes and the cellular ability to repair the subsequent damage establish whether the effects are adaptive or maladaptive (B. W. Kim et al., 2020).

Biochemical integrity of the brain cells can seriously be compromised upon excess ROS production and lack of proper antioxidant response (Salim, 2017). The brain shows a high oxygen consumption rate and a lipid-rich content; thus, it is extremely susceptible to oxidative stress. Consequently, oxidative stress-induced damage can negatively impact normal Central Nervous System (CNS) functions (Salim, 2017). In line with OS, neuroinflammation is a process characterized by the presence of reactive astrocytes and microglia, infiltration of peripheral immune cells and high levels of inflammatory mediators in nervous tissues. Microglia is the primary form of active immune defense in the CNS. When these cells lose their ability in neutralizing a toxic insult, they remain active in the recruitment of oligodendrocytes and astrocytes sustaining the inflammatory process (Obrador et al., 2020). OS in ALS patients and animal models causes an excessive proliferation of astrocytes surrounding the degenerating MNs. In addition, these proliferative astrocytes are positive for inflammatory markers such us cyclo-oxygenase-2 (Vargas & Johnson) and molecules that prevent the regeneration of injured axons (Radford et al., 2015). Interestingly, astrocytes derived from spinal cord tissue of

both sporadic and familial ALS patients are cytotoxic to cultured motor neurons (Haidet-Phillips et al., 2011). All in all, these findings support an active role for astrocytes in ALS pathogenesis. Indeed, astrocytes are the most abundant glial cell in the central nervous system and are involved in multiple processes including metabolic homeostasis, blood brain barrier regulation and neuronal crosstalk (J. A. Lee et al., 2021). They act as the main storage point of glycogen in the brain, and it is well established that astrocyte uptake of glutamate and release of lactate prevents neuronal excitability and supports neuronal metabolic function. However, the role of lipid metabolism in astrocytes in relation to neuronal support has been until recently, unclear (J. A. Lee et al., 2021). Lipids play a fundamental role in astrocyte function, including energy generation, membrane fluidity and cell to cell signaling. There is now emerging evidence that astrocyte storage of lipids in droplets has a crucial physiological and protective role in the central nervous system (J. A. Lee et al., 2021). This pathway links β-oxidation in astrocytes to inflammation, signaling, oxidative stress and mitochondrial energy generation in neurons. Disruption in lipid metabolism, structure and signaling in astrocytes can lead to pathogenic mechanisms associated with a range of neurological disorders (J. A. Lee et al., 2021).

Regarding oxidants in ALS patients, the expression levels of oxidative stress products such as 8-dihydro-2' -deoxyguanosine (8-OHdG) and malone dialdehyde (MDA) as well as antioxidant system products SOD-1 and GPX have been reported to be altered in body fluids in ALS patients in comparison with healthy individuals; thus, these changes have been proposed as a promising biomarker candidate for ALS (Hosaka et al., 2021). Also, it has been demonstrated that glutathione (GSH) levels in motor cortex samples from ALS patients are significantly lower in comparison with healthy control (Weiduschat et al., 2014). GSH is the most abundant non-protein thiol, and acts as a crucial antioxidant in neurons maintaining the redox homeostasis in the CNS (Aoyama, 2021). Interestingly, expression of the A315T mutant TDP-43 *in vitro* showed decreased GSH level and increased ROS productions as well as cell death; however, treatment with GSH monoethyl ester was able to prevent cell death and TDP-43 aggregation in motor neurons (T. Chen et al., 2018). Thus, restoration of GSH in neuronal cells could be an interesting strategy in the development of novel treatments for TDP-43 mediated ALS (Aoyama, 2021).

Several studies support the evidence of a close link between OS and protein aggregation processes, which are involved in the development of proteinopathies (Lévy et al., 2019). The intrinsic parameters of protein aggregation are still not completely

understood, but it is known that certain proteins have a stronger tendency to aggregate than others. A representative case is peptide poly(Q) tracts that can easily form high molecular weight aggregates in neurodegenerative disease (Lévy et al., 2019). Nevertheless, the aggregation of proteins lacking the obvious features which promote this phenomenon is more interesting. Thus, the exposure of yeast cells to oxidative stress agents such as hydrogen peroxide, arsenite or the amino acid analogue azatine-2-carboxylic acid, promotes the aggregation of similar proteins independently from the different mechanism of action of each of the stressors (Weids et al., 2016). It seems that proteins that aggregate under physiological conditions and stress share various features; however, stress induction may produce an alteration of the aggregation propensity of proteins making it easier. This suggests that the proteins in aggregates are intrinsically aggregation-prone, rather than being proteins which are affected in a stress-specific manner (Weids et al., 2016). In ALS pathology, OS can lead to the oxidation of TDP-43 cysteine residues with the subsequent establishment of disulphide bonds; these structural alterations trigger TDP-43 loss-of-function and accumulation in insoluble aggregates (Cohen et al., 2012) OS is also related to TDP-43 acetylation in correspondence with two lysine residues enclosed in the RNA binding domains; similarly to oxidation of cysteine residues, lysine acetylation decreases TDP-43 solubility and encourages both aggregation and loss-of function (Cohen et al., 2015)

TDP-43 susceptibility to OS has been studied in different cell lines, using treatments with several oxidant chemicals, such as paraquat or hydrogen peroxide. Indeed, OS induced by paraquat leads to the formation of cytosolic aggregates of TDP-43 in SHSY5Y cell line and induces cell death. DJ-1, a multifunctional redox-stress protein, showed protective capacity against cell death, acting as an inhibitor of TDP-43 aggregation (Lei et al., 2018).

Curiously, it has been proved that TDP-43 is not just a victim of OS in neurodegenerative processes, but it can be its causing agent. A recent study has underlined the capacity of aggregated TDP-43 to sequester a series of specific microRNAs (miRNAs) and proteins, inducing increased levels of other proteins which can functionally act against others (Zuo et al., 2021). Many of those are nuclear-genome-encoded mitochondrial proteins, thus their impairment causes a general mitochondrial imbalance that ultimately increases OS (Zuo et al., 2021)

Therefore, it is considered that the role of mitochondria in ROS production is an important contributor to ALS pathology. Several mitochondrial dysfunctions have been

reported in experimental models both *in vitro* and *in vivo*. Mitochondrial abnormalities have been found in spinal cords of animal disease models and ALS patients (Delic et al., 2018). Despite that, molecular mechanisms leading to mitochondrial dysfunction in sALS patients are still poorly understood (Delic et al., 2018). The activity of mitochondrial electron transport chain complex IV was studied in post-mortem grey and white matter of the cervical and lumbar spinal cords from male and female sALS patients and controls along with mitochondrial density and distribution in spinal cord motor neurons. Complex IV activity was significantly decreased only in gray matter in both cervical and lumbar spinal cords from ALS patients (Delic et al., 2018)This finding can depict an important role for mitochondrial defects in the spinal cord may as a contribution to ALS pathogenesis and should be taken in account in development of therapeutic strategies for this disease (Delic et al., 2018). Consistently, the widely studied SOD1 G93A mouse model of ALS also showed impaired activities of OXPHOS complexes I + III, II + III, IV(Jiang et al., 2015). The role of mitochondrial dysfunction in disease progression is confirmed by the fact that reduced respiration and ATP synthesis is previously manifested rather than behavioral negative changes, indicating a strong contribution of mitochondrial dysfunction in ALS progression(Jiang et al., 2015).

Moreover, superoxide dismutase (SOD1) mutants display a proportion of SOD1 misfolded protein onto the cytoplasmic side of mitochondria in spinal cord cells(Vande Velde et al., 2011). By generation of mice in which enhanced green fluorescent protein is selectively expressed in mitochondria of MNs, it has been demonstrated that axonal mitochondria of MNs are primary *in vivo* targets for misfolded SOD (Vande Velde et al., 2011). Mutant SOD1 is responsible for the alteration of axonal mitochondrial morphology and distribution. In particular, dismutase active SOD1 causes mitochondrial clustering at the proximal side of Schmidt-Letterman incisures within motor axons and dismutase inactive SOD1 produces aberrantly elongated axonal mitochondria. These alterations begin in a pre-symptomatic phase and increase in severity with disease progression (Vande Velde et al., 2011), in line with the findings above mentioned.

Finally, a recent investigation has proposed a novel mechanism by which TDP-43 cytosolic aggregates are able to enter the mitochondria and trigger the release of mitochondrial DNA (mtDNA) causing an inflammatory state in ALS. This event starts a cascade in which TDP-43 induces mtDNA accumulation and the activation of the cGAS/STING pathway, a component of the innate immune activation. The result is the establishment of a strong inflammatory response sustained by IFNβ, IL-6 and TNF with consequent loss of motor neurons (C. H. Yu et al., 2020a).

The free radical scavenger Edaravone (Radicava ®) is a proven neuroprotective drug for ALS patients (Ohta et al., 2020). It is administered via intravenous infusions. Although the exact mechanism of action of Edaravone in the treatment of ALS is unknown, its therapeutic effect may be due to its known antioxidant properties; in fact, oxidative stress is a part of the process that kills neurons in patients with ALS (Cruz, 2018).

1.2.2.2 Endoplasmic reticulum stress

The endoplasmic reticulum (ER) is the first subcellular compartment where secreted and membrane proteins are synthesized and folded. For this task, a large and efficient network of chaperones, foldases, and co-factors are expressed at the ER to promote folding and prevent protein misfolding. The ER also acts as a major intracellular calcium store and performs a crucial role in the synthesis of lipids (Matus et al., 2013). Several stress conditions can alter the function of this organelle and cause abnormal protein folding at the ER lumen, determining “ER stress” (Figure 9) (Hetz, 2012). ER stress leads to the activation of the unfolded protein response (UPR), an integrated signal transduction pathway that restores homeostasis by increasing the protein folding capacity and quality control mechanisms of the ER (Walter & Ron, 2011). However, chronic ER stress results in apoptosis of irreversibly damaged cells through diverse complementary mechanisms(Hetz, 2012). Although the molecular mechanisms underlying ER stress-induced apoptosis are not completely understood, increasing evidence suggests that ER and mitochondria cooperate to signal cell death (Malhotra & Kaufman, 2011). Mitochondria and ER form structural and functional networks (mitochondria-associated ER membranes [MAMs]), essential to maintain cellular homeostasis and determine cell fate under various pathophysiological conditions. Moreover, regulated Ca^{2+} transfer from the ER to the mitochondria is important in maintaining control of prosurvival/prodeath pathways (Malhotra & Kaufman, 2011).

Three proteins are activators of the UPR signal: inositol requiring enzyme 1α/β (IRE1) (Cox et al., 1993), PKR-like ER kinase (PERK) (Harding et al., 1999), and activating transcription factor 6α/β (ATF6)(Haze et al, 1999). They include three domains: an ER luminal domain (LD), a single pass membrane spanning domain, and a cytosolic domain. IRE1 activation leads to promiscuous endoribonuclease activity, which causes mRNA decay at the ER membrane, helping to reduce the protein load in a process called regulated IRE1 dependent decay (Hollien & Weissman, 2006). PERK kinase activation leads to phosphorylation of eukaryotic translation initiation factor-2α (eIF2α), which determines ribosome inhibition and transient attenuation of global cell translation (Harding

et al., 1999). This contributes to the reduction of the demands placed on the protein folding machinery (Adams et al., 2019). ATF6 is the third member of UPR signaling. It mediates a transcriptional response that promotes protein folding and ER-associated degradation pathways. However, ATF6 is very different from IRE1 and PERK in primary amino acid sequence, domain architecture, and role in the UPR. Following the accumulation of misfolded proteins, ATF6 migrates to the Golgi apparatus where it is cleaved by site-specific proteases S1P and S2P(Shen et al., 2002). This cleavage produces a cytosolic portion which migrates to the nucleus and mediates the activation of UPR targeted genes, such as chaperones, leading to alleviation of the initial insult.

A link between IRE-1 and TDP-43 has been recently described (de Mena et al., 2021).In fact, it has been demonstrated that forebrain neurons of rats conditionally expressing mutated TDP-43 M337V equally failed to produce evidence of UPR activation despite finding significant signs of Golgi fragmentation, a common hallmark of neurodegeneration, and ubiquitin aggregation, a sign of an overloaded ubiquitin-proteasome degradation system(Tong et al., 2012). Instead, the authors noticed that the levels of X-box binding protein 1 (XBP-1), although highly upregulated in reactive microglia, appeared significantly reduced in neurons when compared to controls. Notably, XBP-1 is a transcriptional activator for many of the UPR target genes. A hypothesis suggests that TDP-43 overexpression could cause XBP1 deficiency in neurons through an undefined mechanism(Tong et al., 2012). If so, the cell could not activate an IRE-1-mediated ER stress response to deal with TDP-43 toxicity, thereby contributing to the development of pathogenesis(Tong et al., 2012). However, since then, these results have not been replicated nor further evidence has been found supporting that theory.

In contrast, an independent analysis of Neuro2a cells transfected with both WT and mutant TDP-43 (Q331K or A315T) exhibited significantly increased levels of the ER markers XBP1 and ATF6 when compared to control cells(Walker et al., 2013). Despite differences in intensity, these data indicate that both WT and mutant TDP-43 can indeed activate the main UPR pathways. Then, it’s interesting to clarify why previous studies failed to detect the activation of UPR. This may be due, at least in part, to the different TDP-43 mutant species and/or experimental models used in each study. In this regard, Walker and colleagues proposed that the use of single-cell analysis, a more specialized methodology than the ones previously used, allows for a finer quantification of ER markers. In addition, analysis of ER activation at different time points post-transfection may also play a relevant role. For instance, analysis of samples between 18 and 24 h

post-transfection showed an increase of ATF6, XBP-1, and CHOP, however, induction of ER stress was highly variable or absent at later time points (Walker et al., 2013).

In a recent study, 44 target genes strongly influenced by XBP-1 and ATF6 were characterized and the expression of a subset of genes in the human post-mortem spinal cord from ALS cases and in the frontal and temporal cortex from FTLD and AD cases and controls was quantified (Montibeller & de Belleroche, 2018).

It was found that IRE1α-XBP1 and ATF6 pathways are strongly activated both in ALS and AD. In ALS, XBP1 and ATF6 activation was confirmed by a significant increase in the expression of both known and novel target genes involved in co-chaperone activity and ER-associated degradation (ERAD) such as DNAJB9, SEL1L and OS9 (Montibeller & de Belleroche, 2018). In AD cases, targets involved in protein folding were more prominent, such as CANX, PDIA3 and PDIA6. These results revealed that overlapping and disease-specific patterns of IRE1α-XBP1 and ATF6 target genes are both activated in AD and ALS, which may be relevant to the development of new therapies (Montibeller & de Belleroche, 2018). Other interesting findings which disclose the importance of ER stress in ALS pathology are the detection of increased levels of PERK, ATF6 and IRE1 in thoracic spinal cord samples of ALS patients (Tabas & Ron, 2011). A publication from our laboratory also claimed the involvement of ER stress in ALS pathology. Indeed, the ERK 1/2 pathway was analyzed in N2A cells treated with thapsigargin (Thp) in order to induce ER stress, observing that ER stress can activate ERK 1/2 response and promote the cytoplasmic accumulation of TDP-43 (V. Ayala et al., 2011).

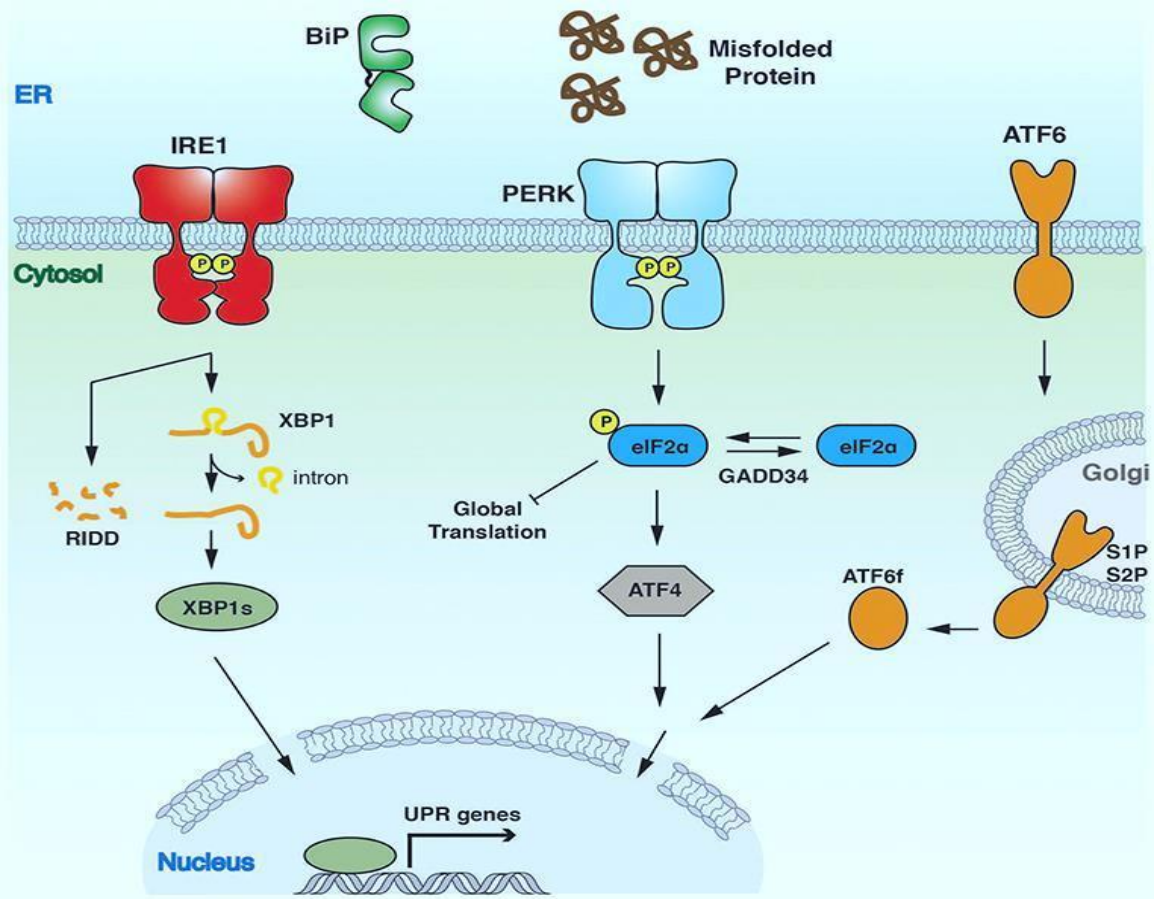

Figure 9. **Overview of the UPR as a consequence of ER stress and accumulation of misfolded proteins in the ER lumen.** The UPR instigates a transcriptional and translational response to ER stress. IRE1, PERK, and ATF6 are the main UPR activators. Each one of them gives rise to a separate branch of the response, all of which aim to palliate the burden of misfolded protein and to restore ER protein homeostasis (Adapted from Adams et al., 2019).

In summary, disturbance of ER proteostasis is a common feature of ALS. Protein disulfide isomerases (PDIs) are ER foldases identified as possible ALS biomarkers, as well as neuroprotective factors. Four ALS-linked mutations recently identified in two major PDI genes, PDIA1 and PDIA3/ERp57 have been recently characterized through phenotypic screening in zebrafish (Woehlbier et al., 2016) It has been found that the expression of these PDI variants induce disruption of MN connectivity. In addition, the expression of mutant PDIs impaired dendritic outgrowth in motor neuron (MN) cell culture models. Thus, ER proteostasis imbalance may act as a risk factor for ALS, driving initial stages of the disease (Woehlbier et al., 2016). Also, ERAD and the UPR are two key quality-control machineries in the cell that have been recently linked. ERAD is responsible

for the clearance of misfolded proteins in the ER for cytosolic proteasomal degradation. It has long been thought that ERAD is an integral part of UPR because expression of many ERAD genes is controlled by UPR; however, recent studies have suggested that ERAD has a direct role in controlling the protein turnover and abundance of IRE1, the most conserved UPR sensor. Recent advances in our understanding of IRE1 activation have led to the conclusion that UPR and ERAD engage in an intimate crosstalk to define folding capacity and maintain homeostasis in the ER (J. Hwang & Qi, 2018).

1.2.2.3 Osmotic stress

Osmotic shock or osmotic stress (OsmS) is a sudden change in the solute concentration around a cell, which determines a rapid change in the movement of water across the cell membrane. In presence of high concentrations of either salts, substrates or any solute in the supernatant, water is osmotically drawn out of the cells. Consequently, the transport of substrates and cofactors into the cell is arrested, thus causing a state of "shock"(Lang et al., 2005). On the other hand, when concentrations of solutes around a cell are low, water enters the cell in large amounts, causing it to swell and undergo apoptosis (Lang et al., 2005)

All organisms respond to osmotic stress with several mechanisms, through sensors and signal transduction pathways that can transmit to the cell information about osmolarity in its surroundings(Kültz & Burg, 1998). Because the plasma membrane is freely permeable to water, cells have evolved evolutionarily highly conserved mechanisms to handle changes in the osmolarity of their surrounding medium (Alvarez-Miranda et al., 2015). These mechanisms aim to activate survival responses under extreme conditions (Kültz, 2007). However, Osms in the cells and tissue may also plays a significant role in many human diseases (Ho, 2006). In eukaryotic cells, calcium is a main regulator of Osms; effectively, intracellular calcium levels increase in certain cells during hyper-osmotic stress response as an attempt to return to their initial volume (Erickson et al., 2001). Of note, calcium homeostasis is very relevant not only in mitochondrial function, but also for ER homeostasis and ALS pathophysiology (Grosskreutz et al., 2010).

Most land-living organisms regularly undergo dehydration. In nature, one common strategy to protect against this osmotic stress is to introduce small polar molecules with low vapor pressure, commonly called osmolytes. Two examples of naturally occurring small polar compounds are urea and trimethylamine N-oxide (TMAO), which are known to have counteracting effects on protein stability (Pham et al., 2018). The effects of urea and TMAO on lipid self-assembly at varying water contents have been investigated with a

special focus on dehydrated conditions (Pham et al., 2018). It has been shown that urea and TMAO have clearly different effects in dehydrated conditions due to differences in the molecular interactions between the solutes and the lipid headgroups. In fact, TMAO is expelled from lipid lamellar systems with low water contents with no effect on the lipid phase behavior. Urea, on the other hand, shows a slight affinity for the lipid headgroup layer, and it is present in the lipid lamellar system at all water contents. As a result, urea may exchange with water in dry conditions and thereby prevent dehydration-induced phase transitions (Pham et al., 2018). Osms may also change the expression and subcellular localization of some proteins, such as in Juvenile CLN3 (formerly known as juvenile neuronal ceroid lipofuscinosis), a fatal childhood neurodegenerative disorder caused by mutations in the *CLN3* gene. *CLN3* encodes a putative lysosomal transmembrane protein with unknown function. Cell culture studies using CLN3-overexpressing vectors and/or anti-CLN3 antibodies have also localized CLN3 in cellular structures other than lysosomes (Getty et al., 2013). Osmoregulation of the mouse *Cln3* mRNA level in kidney cells was recently reported. It has been reported that hyperosmolarity (800 moms), achieved by either NaCl/urea or sucrose, dramatically increased the mRNA and protein levels of CLN3 as determined by quantitative real-time PCR and Western blotting in a stably transfected baby hamster kidney (BHK) cell line that expresses a moderate level of myco-tagged human CLN3 under the control of the human ubiquitin C promoter (Getty et al., 2013).Under isotonic conditions (300 mOsm), human CLN3 was found in a punctate vesicular pattern surrounding the nucleus with prominent Golgi and lysosomal localizations. CLN3-positive early endosomes, late endosomes, and cholesterol/sphingolipid-enriched plasma membrane microdomain caveolae were also observed. Increasing the osmolarity of the culture medium to 800 mOsm extended CLN3 distribution away from the perinuclear region and enhanced the lysosomal localization of CLN3. These results reveal that CLN3 has multiple subcellular localizations within the cell, which, together with its expression, prominently change following osmotic stress (Getty et al., 2013).

Regarding the participation of osmotic stress in pathological processes, in 2011 it was published a study in which the authors proposed sorbitol as a novel physiological inductor of osmotic stress, that can induce TDP-43 migration to stress granules in Hek293T cells and primary cultured glia (Dewey et al., 2011b)

Moreover, a recent study has focused on the effect of osmotic stress on RNA-binding proteins (RBPs), which contribute to the pathogenesis of many neurodegenerative disorders (Harley & Patani, 2020). Particularly, in ALS, nuclear-to-cytoplasmic

mislocalization and accumulation of RBPs are a well-established pathological hallmark of the disease, but the spatiotemporal responses of RBPs to different extrinsic stressors in human neurons remain not fully understood (Harley & Patani, 2020). Healthy induced pluripotent stem cell (iPSC)-derived motor neurons were used to model how different types of cellular stress affect the nucleocytoplasmic localization of key ALS-linked RBPs. It has been found that osmotic stress is able to induce nuclear loss of TDP-43, SPFQ, FUS, hnRNPA1 and hnRNPK, with characteristic changes in nucleocytoplasmic localization in an RBP-dependent manner (Harley & Patani, 2020). As previously stated, in ALS/FTD, the nuclear protein TDP-43 is cleared from the nucleus and accumulates in the cytoplasm to form inclusion bodies (Neumann et al., 2006); however, the factors that drive TDP-43 mislocalization are not well known. The progressive accumulation of TDP-43 in stress granules (SGs) in the cytoplasm could contribute to the mislocalization of TDP-43 in ALS/FTD (Y.-B. Lee et al., 2021). To test this hypothesis, SG inducers arsenite (OS) and sorbitol (Osms) were applied to a neuronal cell line (SH-SY5Y) and TDP-43 distribution was monitored by immunofluorescence (Y.-B. Lee et al., 2021).

In unstressed SH-SY5Y cells, TDP-43 and T-cell restricted intracellular antigen-1 (TIA-1), a component of SGs shows a predominant nuclear localization; one-hour incubation with 500 gm. arsenite did not increase cytoplasmic TDP-43 levels compared with unstressed controls (Y.-B. Lee et al., 2021). While TIA-1-positive SGs were detected in most arsenite-stimulated cells, these were rarely positive for TDP-43. Conversely, osmotic stress induced by sorbitol treatment (600 mM) caused a dramatic shift of TDP-43 and TIA-1 from nucleus to the cytoplasm. These results support the hypothesis that osmotic stress is more effective in translocating TDP-43 to the cytoplasm than OS in this cell system (Hock et al., 2018; Y.-B. Lee et al., 2021)

Hypertonic stress also leads to cytoplasmic translocation and loss of function of neuronal FUS, independently from SGs formation (Hock et al., 2018). The mechanism that underlies this change in FUS protein localization involves an aberrant transportin (TNPO) -mediated nuclear import (Figure 10). Interestingly, astrocytes display resistance to FUS mislocalization under hypertonic stress and don’t show any pathological protein accumulation in FTD-FUS brains (Hock et al., 2018). All these data illustrate the complexity of response towards different cell stressors, which are not only protein and stress type dependent, but also cell dependent.

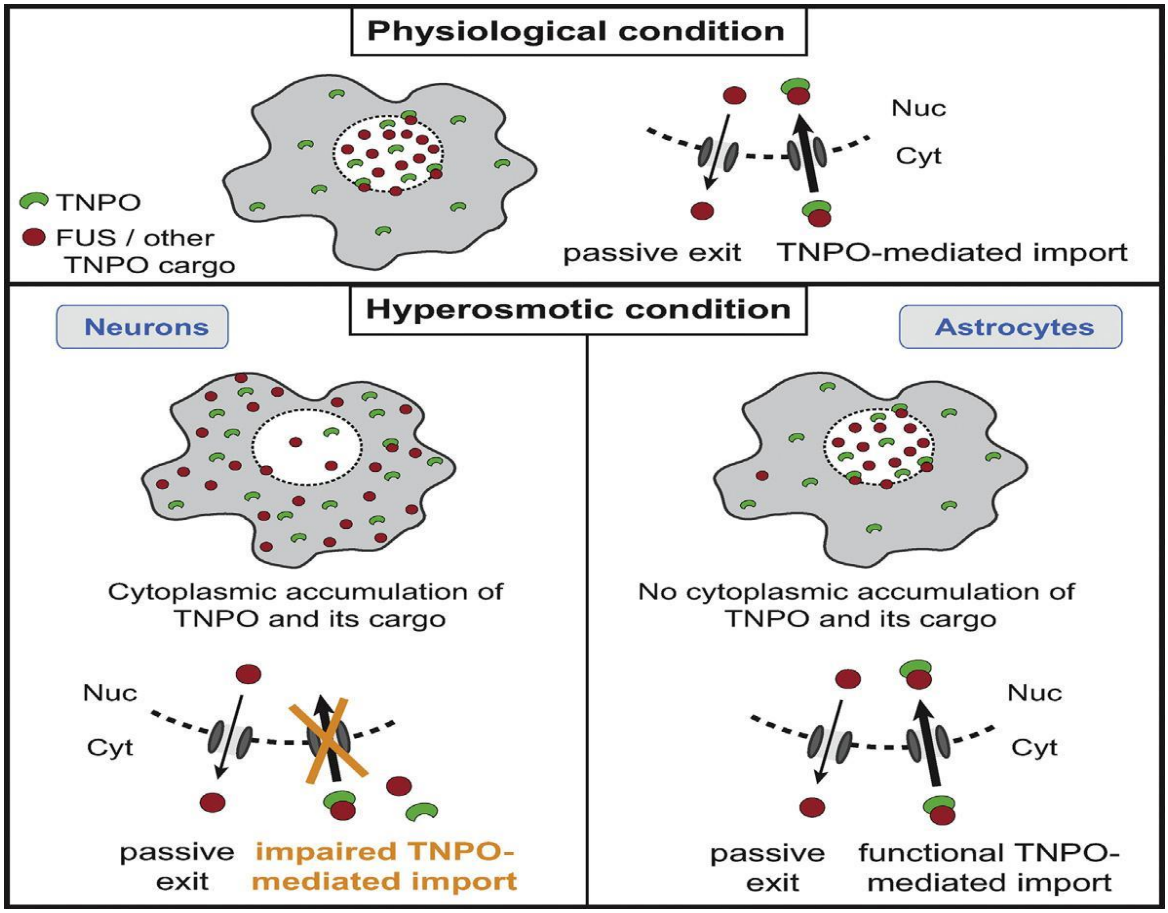

Figure 10. **FUS and TNPO migration patterns**. Under physiological conditions FUS or other transportin (TNPO) cargos migrate from the nucleus to the cytosol through passive diffusion and are returned to the nucleus with a TNPO-mediate import (upper panel). Under hyperosmotic conditions, neurons and astrocytes show a differential response to the stress (lower panel). In neurons, hypertonic stress promotes the cytoplasmic relocation of endogenous FUS, which leaves the nucleus, but it is no longer capable to re-enter this compartment due to an impaired TNPO-mediated import (lower panel, left) On the contrary, astrocytes show resistance to stress-induced FUS translocation. (Adapted from Hock et al., 2018).

In addition to that, it has been reported that the Golgi apparatus responds to osmotic stress. More than two decades ago, it was reported that in mammalian cells, hypertonic stress inhibits ER-to-Golgi transport (Docherty & Snider, 1991). Hypotonic stress determines tubulation of Golgi membranes, whereas hyperosmotic conditions induce its fragmentation and redistribution of the Golgi back to the ER (T. H. Lee & Linstedt, 1999). It remains not fully understood how these phenomena are generated; however, experimental evidence supports that the osmotic shock is perturbing the function of vesicle trafficking machineries, which results in Golgi fragmentation. For instance, hypo-osmotic shock leads to reduction in the number of export sites on the ER (T. H. Lee &

Linstedt, 1999). Consequently, there is less trafficking from the ER to the Golgi, a condition described by others to result in alterations of Golgi structure (Cutrona et al., 2013). Moreover, hypo-osmotic conditions seem to potentiate retrograde transport from the Golgi to the ER (T. H. Lee & Linstedt, 1999).

Interestingly, fragmentation of the Golgi apparatus is detected in ALS patients MNs and in animal/cellular disease models. The Golgi is a highly dynamic organelle that acts as a dispatching station for the vesicular transport of secretory/transmembrane proteins. It also mediates autophagy and maintains ER and axonal homeostasis. Both the trigger for Golgi fragmentation and the functional consequences of a fragmented Golgi apparatus in ALS remain unclear. However, recent evidence has highlighted defects in vesicular trafficking as a pathogenic mechanism in ALS. Fragmentation of the Golgi was first identified in ALS patient motor neurons 30 years ago (Mourelatos et al., 1993). In contrast to control patients, the Golgi in ALS patients was reduced and fragmented, appearing as disconnected punctate structures, similar to its morphology in cells treated with microtubule depolymerization agents (Mourelatos et al., 1996). Since then, other studies have confirmed Golgi fragmentation in 10–50% sporadic patients (Gonatas et al., 2006;van Dis et al., 2014) and up to 70% of familial ALS patient motor neurons, bearing SOD1, FUS or optineurin mutations (Fujita et al., 2008; Ito et al., 2011). Interestingly, Golgi fragmentation is more prominent in larger human motor neurons, such as those in the cerebral cortex (Fujita et al., 1999) and anterior horn (Fujita et al., 2000) , suggesting they are specifically vulnerable to disturbances in Golgi function.

Golgi fragmentation is also present in spinal anterior horn cells in sporadic ALS patients with cytoplasmic mislocalization of WT TDP-43, implying that a link exists between TDP-43 and Golgi pathologies (Fujita et al., 2008b). Similarly, Golgi fragmentation is present in transgenic rats expressing mutant TDP-43^{M337V} (Tong et al., 2012), in mutant SOD1^{G93A} transgenic mice and in neuronal cells expressing SOD1$^{G93A,\ G85R}$ mutants (Mourelatos et al., 1996; Stieber et al., 2004). Interestingly, Golgi fragmentation precedes SOD1 inclusion formation, neuromuscular denervation, and mitochondrial-mediated apoptosis in low-copy number SOD1^{G93A} transgenic mice, implying it is upstream in pathogenesis (van Dis et al., 2014). Similarly, ALS patients with optineurin mutations (<1% familial cases) demonstrate Golgi fragmentation in ~70% of anterior horn cells (Ito et al., 2011). Furthermore, Golgi fragmentation is present in cells expressing ALS-linked mutant FUS, optineurin and vesicle-associated membrane protein B (VAPB) (Teuling et al., 2007; Farg et al., 2013; Sundaramoorthy et al., 2015). However, despite being widely associated with ALS, the cellular events triggering Golgi fragmentation and the resulting consequences are not

established. Increasing evidence implicates inhibition of vesicular trafficking between the ER-Golgi in ALS, which may explain the previous observations of Golgi fragmentation.

Osmotic stress also influences lysosome biogenesis. Lysosomes play an important role as cellular degradation and signaling centers that coordinate metabolism in response to intracellular cues and extracellular signals. Lysosomal capacity is adapted to cellular needs by transcription factors, such as TFEB and TFE3, which activate the expression of lysosomal and autophagy genes (López-Hernández et al., 2020) Nuclear translocation and activation of TFEB are induced by a variety of conditions such as starvation, lysosome stress and lysosomal storage disorders. It has been recently described a pathway initiated at the plasma membrane that controls lysosome biogenesis via the endocytic regulation of intracellular ion homeostasis and serves to control intracellular ion homeostasis and thereby Ca2+/calcineurin-mediated activation of TFEB and downstream lysosome biogenesis in response to osmotic stress to promote the turnover of toxic proteins and cell survival (López-Hernández et al., 2020).

The CNS is particularly vulnerable to lysosome dysfunction, causing impairment of neuronal and glial function, which ultimately leads to neurodegeneration. For example, autophagosomes and lysosomes accumulate in Lewy Bodies, the intraneuronal inclusions that are characteristic of PD neuropathology (Mahul-Mellier et al., 2020; Shahmoradian et al., 2019). Lysosome dysfunction has been observed in the tissue of FTD and ALS patients. Neurons and microglia in the frontal cortex brain tissue of FTD patients have increased lipofuscin deposits, a diagnostic feature of many lysosomal storage disorders (LSDs)(Clayton et al., 2015; Ward et al., 2017). Lipofuscin is an auto-fluorescent aggregate composed of undegraded lipids, proteins, and metals, which is thought to develop from defective lysosome function over time(Moreno-García et al., 2018). These protein deposits co-localize with LAMP1 and LAMP2(Clayton et al., 2015), two well-characterized lysosome markers, suggesting that lipofuscin deposits may be derived from lysosomal compartments. Additionally, enlarged endosomes occur in primary fibroblasts and frontal cortical neurons of FTD (Urwin et al., 2010). Further, large autophagic vesicles containing CTSB activity accumulate in myoblasts from FTD patients (Tresse et al., 2010). A lipidomic analysis also found evidence that lysosomal degradation of triacylglycerides (TAGs) was impaired in human FTD brain tissue and a mouse model of FTD (Evers et al., 2017).

In ALS, motor neurons in the spinal cord have increased levels of glycosphingolipids (GSL), a characteristic feature of Gaucher disease (GD) (Dodge et al., 2015), and

inclusion bodies composed of autophagosomes and autolysosomes (Sasaki, 2011). Furthermore, LAMP1 positive vesicles are decreased in iPSC-derived motor neurons from ALS patients that carry the *C9orf72* mutation, suggesting a reduced number of functional lysosomes (Shi et al., 2018). Finally, post-mortem ALS brain tissue has a ~62% reduction in the nuclear localization of transcription factor EB (TFEB), a master transcriptional regulator of lysosomal genes, suggesting that the regulation of the lysosome-autophagy pathway is impaired (H. Wang et al., 2016). Together, these data strongly support the idea that lysosomal dysfunction is a critical pathogenic cause of FTD and ALS.

1.2.2.4 Proteasomal stress and proteostasis disturbance

Proteostasis can be defined as network of interconnected quality control processes maintaining the functional proteome (Balch et al., 2008; Hetz et al., 2015). Consequently, adaptive mechanisms in the cell induce the expression of chaperones, foldases, and protein degradation mechanisms under proteotoxic stress (Hetz et al., 2015). Several studies suggest that perturbation in the efficiency of the protein-folding machinery may be related with selective vulnerability of MNs in ALS (Ruegsegger & Saxena, 2016). In line with this notion, strategies to enhance the clearance of abnormal proteinaceous aggregates may be protective against MN degeneration, extending survival in pre-clinical models of the disease(Menzies et al., 2002; Vidal et al., 2014). However, the exact molecular mechanisms driving the misfolding and aggregation of ALS-linked proteins in most common sALS and its impact to MN homeostasis is still not completely understood. Recently, several genes associated with proteostasis control as risk factors to develop ALS have been identified and many functional studies are showing the benefits of targeting proteostasis to alleviate MN degeneration.

The degradation of the majority of intracellular proteins involves ubiquitin proteasome system (UPS), which label proteins for proteolysis with polyubiquitin chains and a variety of ubiquitin-activating (E1), ubiquitin-conjugating (E2), and ubiquitin-ligases (E3) enzymes to assure protein turnover in a tightly regulated spatio-temporal manner (Glickman & Ciechanover, 2002).

The accumulation of ubiquitin-positive inclusion bodies in sALS and fALS, in addition to several disease models, has been related with UPS dysfunction (Bendotti et al., 2012) The catalytic activity of the proteasome has been shown to be significantly reduced in sALS tissue (Kabashi et al., 2012), while cell culture studies have demonstrated that the ALS-linked mutant SOD1 is a substrate of the UPS, and it is selectively recognized by E3 ubiquitin-ligase like Dorfin (Medinas et al., 2017). Interestingly, mutant SOD1 accumulates

as polyubiquitinated high-molecular-weight species, suggesting the proteasome fails to handle the burden misfolded mutant SOD1 species (Niwa et al., 2002). Indeed, studies in mutant SOD1 transgenic mice indicated that the proteasome activity is already impaired as early as 45 days of age, significantly decreasing as the decreasing as the disease progresses (Kabashi et al., 2004a) .

In addition to the extensive reports in mutant SOD1 models, the discovery of ALS genes related to UPS suggest its dysfunction as part of the etiology of the disease (Kabashi et al., 2004b). Expression of RAN (Repeat-associated non-ATG translated) peptides of C9orf72 repeat expansion has been associated with proteasome impairment (Zhang et al., 2014). The ATPase valosin-containing protein (VCP)/p97 is a member of the AAA (ATPase associated with diverse cellular activities) family, which employs ATP hydrolysis to structurally remodel proteins. VCP/p97 has found to bind to ubiquitylated substrates or interact with ubiquitin conjugates through adaptor proteins to assist proteasomal degradation (Meyer & Weihl, 2014). Mutations in VCP/p97 have been found to determine autosomal dominant ALS (Meyer & Weihl, 2014). An ALS-associated VCP/p97 mutant shows disrupted interaction with proteasome impairing substrate presentation for proteolysis(Barthelme et al., 2015). Another ALS-linked gene associated with UPS encodes for ubiquilin-2, a ubiquitin-like protein involved in delivering cargo to proteasome (Ko et al., 2004). Of note, ubiquilin-2 mutations are also implicated in X-linked ALS and ALS/dementia(H. X. Deng et al., 2011). Mutations in ubiquilin-2 result in impairment of protein degradation associated with the accumulation of ubiquilin-2-positive skein-like inclusions (J. Deng et al., 2015). Transgenic mice overexpressing mutant ubiquilin-2 develop MN disease with muscle denervation and ubiquitylated TDP-43 inclusions accumulating in the cytoplasm (Le et al., 2016). Indeed, TDP-43 has been shown to be a substrate of the UPS, and the genetic ablation of proteasome components causes TDP-43 mislocalization and MN pathology (Scotter et al., 2014). Additionally, mutations in cyclin F (CCNF), a component of E3-ubiquitin ligase complex, have been observed both in sALS and fALS (Williams et al., 2016). Thus, expression of mutant CCNF leads to abnormal accumulation of ubiquitylated proteins including TDP-43 (Williams et al., 2016). Overall, although a reduced activity of the UPS has been shown to occur in ALS models and human tissue, no functional studies have tested the influence of these alterations to the progression of the disease.

1.2.2.5 Mitochondrial stress

Mitochondria are considered as the cellular powerhouses acting in bioenergetics and metabolism of amino acids and lipids, since they are the headquarter for fatty acid β-oxidation, Kreb's cycle and oxidative phosphorylation (OXPHOS) (Picard et al., 2016). Nevertheless, bioenergetics is not the only fundamental role of mitochondria in global cell biology. Mitochondria are also responsible for the regulation of calcium stores, lipogenesis and the production of steroid hormones (Picard et al., 2016). They can also determine cell fate via apoptotic cues. These organelles also play a crucial function in cellular redox homeostasis, as leakage of electrons through the electron transport chain generates ROS which, under controlled conditions, constitute valuable secondary messengers (Gruber et al., 2008) as discussed above.

Mitochondria communicate with the cellular environment through multiple molecules which nature of these is very broad and includes mitochondrial DNA (mtDNA) fragments, mitochondrial lipids (e.g.: cardiolipin), metabolites and small peptides (Hill et al., 2018). These communication mechanisms are not only directly related to mitochondrial dysfunction but used as information on nutrient fluxes or redox states. Mitochondrial derived peptides (MDPs), for example, are signaling peptides encoded by short open reading frames in the mitochondrial genome (Okada et al., 2017). They have an important role in many cellular pathways, promoting cellular viability and reducing apoptosis (Okada et al., 2017).

As depicted above, mitochondria are also an important source for ROS. ROS have long been known as being damaging and agents to the cell, resulting in OS. However, ROS also act as signaling molecules to maintain physiological functions. In this regard, it was found that superoxide anions and hydrogen peroxide can activate signaling pathways controlled by tyrosine phosphorylation such as NF-κB, PKC, MAPK or JNK (J. Zhang et al., 2016). Nevertheless, given that excessive ROS production can be damaging to the cell, mitochondrial ROS levels are well regulated by multiple systems to ensure their ability to participate in physiological cell signaling preserving cell homeostasis (Valera-Alberni & Canto, 2018).

Excessive ROS production or an ineffective antioxidant response result in OS (Sies & Cadenas, 1985) (Figure 11), promoting mitochondrial dysfunction and negatively affecting cell viability with damaging of nucleic acids, proteins, and lipids. Thus, ROS accumulation

can cause DNA base modification, DNA strand breaks, inter- and intrastrand crosslinks and DNA-protein crosslink affecting genomic structure and stability (Jena, 2012).

Eukaryotic cells can activate complex antioxidant strategies to protect against an uncontrolled increase in free radicals. These strategies include both enzymatic and non-enzymatic mechanisms. The enzymatic response is primarily mediated by superoxide dismutases (SOD), catalases, thioredoxin reductases or glutathione peroxidases (Espinosa-Diez et al., 2015). SOD enzymes catalyze the conversion of O_2^- to H_2O_2 and O_2, acting as the most powerful antioxidant agents in cells (Ighodaro & Akinloye, 2019). SOD enzymes exist in various forms which differ in their cellular localization and the metal cofactor they use for the catalytic activity (Fridavich, 2003). SOD1 is a soluble Cu/Zn enzyme that is mainly localized in the cytosol, but a small percentage (3% approximately) also can be found in the intermembrane space of mitochondria (Sturtz et al., 2001). In presence of increased levels of H_2O_2, SOD1 can translocate to the nucleus, where it binds to DNA promoters and activates the expression of oxidative resistance and repair genes(Tsang et al., 2014). MnSOD is an exclusively mitochondrial and operates as a primary defense against mitochondrial OS (Kranti et al., 2013). Many SOD isoforms are involved in diseases; this is the case of SOD1, which is mutated in ALS (Sau et al., 2007). In fact, neuronal cells which are no longer able to cope with mitochondrial damage and oxidative stress appear to undergo degeneration and this has been observed in SOD-1 linked genetic variants of ALS (Carrì et al., 2015). Whether this is due to loss of antioxidant activity is not clear.

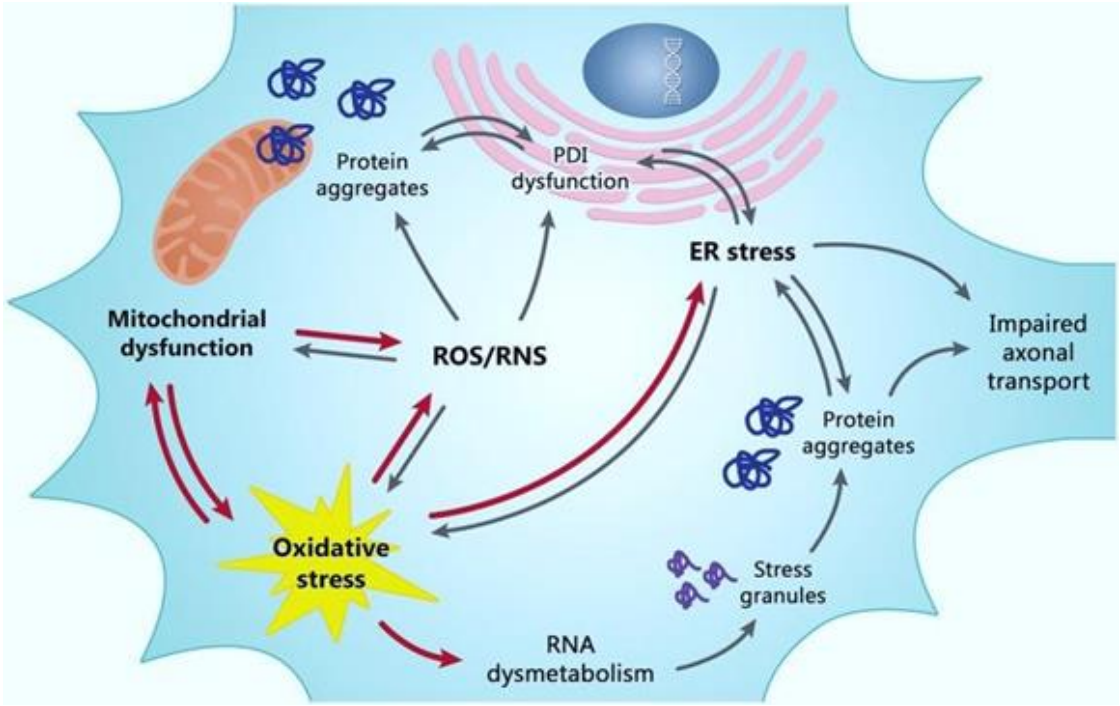

Figure 11. Mitochondrial dysfunction and OS are closely related and are the basis of the redox dysregulation in ALS. Increased production of reactive oxygen and nitrogen species (ROS/RNS) , the ER stress, transcriptional dysregulation and abnormal RNA processing are all consequences of mitochondrial dysfunction and OS contributing to death of motor neurons. These pathological events cause other correlated detrimental effects as the formation of misfolded protein leading to insoluble cytosolic and mitochondrial aggregates, impaired axonal transport and alteration of the enzymatic activity of protein disulfide-isomerase (PDI). Red arrows may be considered as primary causes, gray arrows as secondary causes/effects (Adapted from Carrì et al., 2015).

In addition to that, several studies have reported alteration of the respiratory complex activity in ALS post-mortem brain and spinal cord tissues, patients' lymphocytes and in the SOD1 murine mouse of ALS (Cozzolino & Carrì, 2012; Tan et al., 2014). Mitochondrial damage in ALS could occur subsequently to SOD1 aggregation (Ferri et al., 2006) and be a consequence of the interaction between misfolded SOD1 and other mitochondrial proteins (Carrì et al., 2015; Israelson et al., 2010). Mitochondrial dysfunction also may be a result of the expression of other ALS-related proteins which are directly implicated in the function of these organelles (Carrì et al., 2015). For instance, single missense mutations in valosin-containing protein (VCP) are found in about 2% of familial ALS cases and can be also linked to FTD. VPC, also known as p97, is a highly expressed member of the type II AAA+ (ATPase associated with multiple activities) ATPase family (Bartolome et al., 2013).

Neuronal mitochondrial abnormalities also have been detected in models of familial ALS associated with proteins that are apparently not related with these mitochondria. Mitochondrial dysfunction, together with OS and mitophagy activation has been reported in motor-neuron-like NSC34 cells, expressing mutant TDP-43 (Duan et al., 2010). Furthermore, mice expressing the wild-type form of human TDP-43 develop a pathology that resembles ALS with motor neurons showing cytoplasmic TDP-43 inclusions and mitochondrial aggregation (Y. F. Xu et al., 2010), that may be consequent to defective intracellular trafficking and determine a reduction of mitochondria at nerve terminals of neuromuscular junctions (Shan et al., 2010).

It is well established the importance of mitochondria for neuronal survival but the developmental timing and mechanistic importance of mitochondrial dysfunction in sALS neurons is not fully understood. A recent study employed human iPSCs and generated a developmental timeline by differentiating sALS iPSCs to neural progenitors and to motor neurons and comparing mitochondrial parameters fALS and control cells at each developmental stage (Singh et al., 2021). The authors report that sALS and fALS motor neurons have elevated reactive oxygen species levels, depolarized mitochondria, impaired oxidative phosphorylation, ATP loss and defective mitochondrial protein import compared with control motor neurons. This phenotype develops with differentiation into motor neurons, the affected cell type in ALS, and does not occur in the parental undifferentiated sALS cells or sALS neural progenitors (Singh et al., 2021). This work demonstrates a developmentally regulated unifying mitochondrial phenotype between patient derived sALS and fALS motor neurons. The occurrence of a unifying mitochondrial phenotype suggests that mitochondrial etiology known to SOD1-fALS may be applicable to sALS. Furthermore, in the light of these findings, disease-modifying treatments focused on rescue of mitochondrial function may benefit both sALS and fALS patients (Singh et al., 2021).

Accumulating evidence suggests that many amyloidogenic proteins, including motor neuron disease (MND)-associated RNA/DNA-binding TDP-43, are strongly linked to mitochondrial dysfunction (Kodavati et al., 2020). Animal models and patient studies have highlighted changes in mitochondrial structure, plasticity, replication/copy number, mitochondrial DNA instability, and altered membrane potential in several subsets of MNDs, and these observations are consistent with the evidence of increased excitotoxicity, induction of reactive oxygen species, and activation of intrinsic apoptotic pathway (Kodavati et al., 2020). Studies in MND rodent models also indicate that mitochondrial abnormalities begin prior to the clinical and pathological onset of the

disease, suggesting a causal role of mitochondrial dysfunction. It has been recently demonstrated the involvement of specific defects in DNA break-ligation mediated by DNA ligase 3 (LIG3) in FUS-associated ALS, raised a key question of its potential implication in mitochondrial DNA transactions because LIG3 is essential for both mitochondrial DNA replication and repair (Kodavati et al., 2020). This question, as well as how wild-type and mutant MND-associated factors affect mitochondria, remain to be elucidated. These new investigation focuses into the mechanistic role of mitochondrial dysfunction in MNDs are critical to identify therapeutic targets to alleviate mitochondrial toxicity and its consequences.

1.3 Beyond TARDBP. Stress response pathways involved in ALS pathology

1.3.1. MAPK signal pathways

Most ALS cases exhibit TDP-43 aggregation; this evidence suggests converged patho-physiological mechanisms. Indeed, the role of SGs in ALS pathogenesis points to the importance of cellular stress response pathways in this disease. Cellular stress response pathways have been widely implicated in neurodegeneration and aging (Taylor et al., 2016). In particular, the mitogen-activated protein kinase (MAPK) pathway may be involved in ALS etiology and progression (Sahana & Zhang, 2021).

MAPKs comprise a family of serine and threonine kinases that integrate extracellular and intracellular stimuli into cellular responses regulating differentiation, proliferation, cell death, survival and transformation (E. K. Kim & Choi, 2010). They are activated by a large number of stimuli, such as mitogens and stress. Extracellular stimuli activate surface receptors like G-protein coupled receptors (GPCR), receptor tyrosine kinase (RTK) or integrins; subsequently, adaptor proteins are recruited, such as son of sevenless (SOS), or small G-proteins such as Ras superfamily GTPases. These receptor complexes recruit and activate several downstream effectors, for example the MAPK members (E. K. Kim & Choi, 2010).

MAPK members can be classified into MAP4K, MAPK3, MAPK2 and MAPK. These proteins act in sequence: once activated, MAP4Ks phosphorylate and activate MAP3Ks, which subsequently phosphorylate and activate MAP2Ks, and then MAPKs. Activation of MAPK members is achieved by dual phosphorylation of threonine and tyrosine residues. Activated MAPKs further activate downstream targets, causing transcriptional, translational, or post-translational changes in cells (Cuevas et al., 2007).

Several MAPK members and four tiers of kinase activity are involved in signal integration, signal amplification, closed regulation, and spatial-temporal regulation (Wei & Liu, 2002). The MAPK pathway is evolutionarily conserved across species, suggesting its importance in cellular physiology. Three MAPK subgroups have been identified, namely extracellular signal-regulated kinases (ERKs), p38, and c-Jun N-terminal kinases (JNKs). ERKs are activated by mitogens and play roles in cell proliferation and differentiation, whereas JNKs and p38 are activated by internal or external stress and play roles in cell survival and death (Wei & Liu, 2002) (Figure 12). Here we will focus on ERK and JNK pathways.

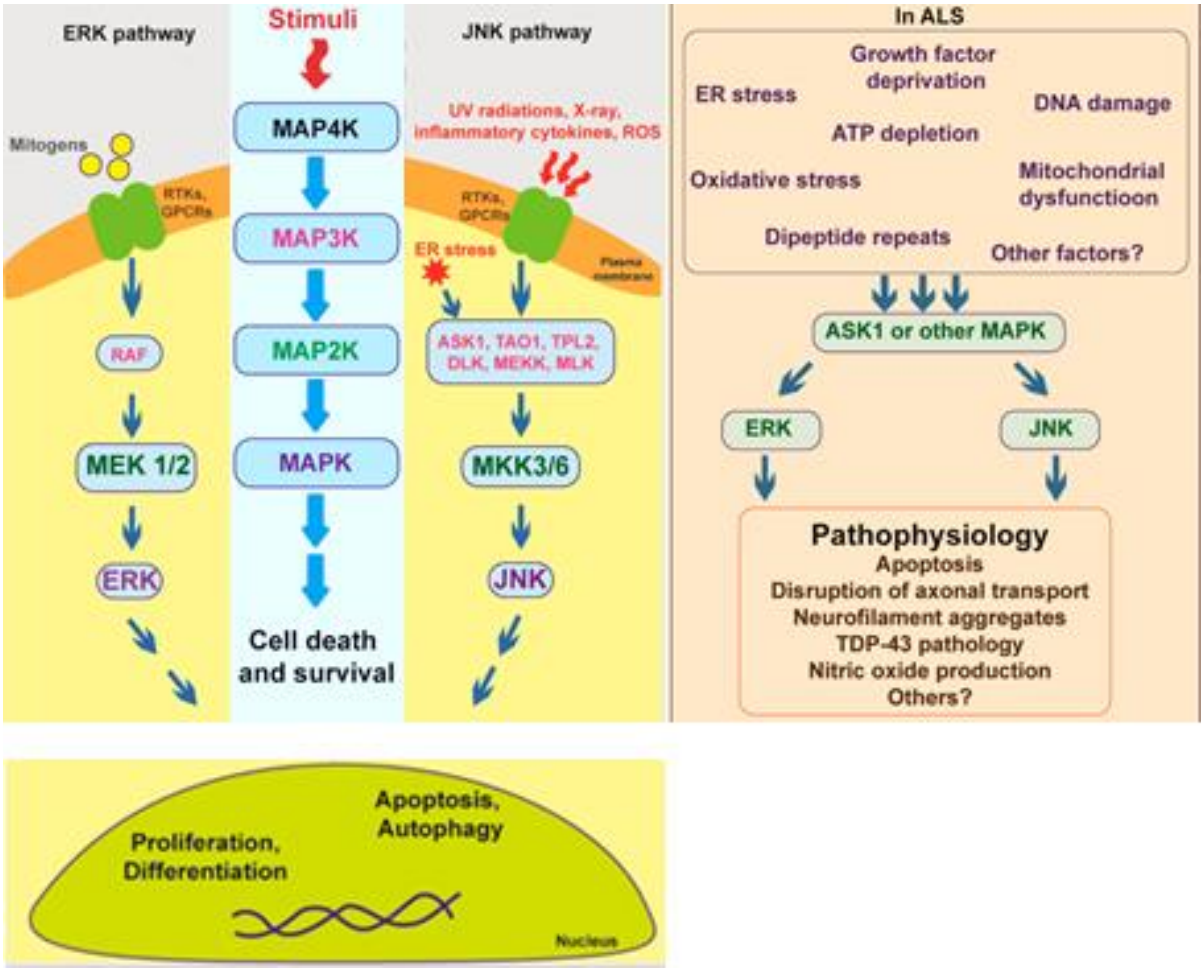

Figure 12. Schematic representation of mitogen-activated protein kinase (MAPK) pathway. Figure shows the interaction of multiple MAPK members under normal physiological conditions and in ALS pathogenesis (Adapted from Sahana & Zhang, 2021).

As discussed above, ERKs are activated mainly by growth factors, which bind to and activate cell surface receptors, such as RTKs and GPCR**.** Activated receptors are able to recruit scaffold and effector proteins (e.g., Ras), which further activate the MAP3K Raf. Activated Raf phosphorylates MAP2K members include MAP kinase ERK kinase 1 and 2

(MEK1/2), which activate ERKs (Figure 11). There are several ERKs, namely ERK 1, 2, 3, 4, 5, and 7. Activated ERK phosphorylates downstream targets, cytosolic or nuclear. The most common ERK targets are MAPK interacting kinase (MNK) 1 and 2, ribosomal S6 kinase 1–4 (RSK1–4), cAMP response element-binding protein (CREB), transcriptional regulator Myc-like (c-Mya), nuclear factor-kappa B (NF-kB), microtubule-associated protein (MAP), Tau, and mitogen and stress-activated protein kinase (MSK) 1 and 2. The ERK pathway is involved in the activation of pro-survival factors, resulting in cellular proliferation, migration, and differentiation (E. K. Kim & Choi, 2010). Abnormal phosphorylation or hyperactivation of ERK associates with ALS conditions. Motor neurons from transgenic mice and patient tissues show ERK activation.

Thus, previous data from our lab show that ER, proteasomal and OS inducers, such as epoxomicin, prevent ERK 1/2 localization to the nucleus, leading to the formation of cytosolic aggregates (V. Ayala et al., 2011) in N2a cells. These cells also show impaired nuclear import, loss of nuclear TDP-43, fragmentation, and subcellular localization of TDP-43 (V. Ayala et al., 2011). Conversely, inhibition of ERK 1/2 activity was able to cause TDP-43 defects in MNs but not in other cells. Furthermore, the cytosolic TDP-43 aggregates do not include cytotoxic granule-associated RNA binding protein 1 (TIA1), which is a stress granule marker, but co-localizes with abnormally phosphorylated ERK 1/2 (V. Ayala et al., 2011). These data suggest the possible role of stress-induced ERK activation in TDP-43 proteinopathy (Mitra & Hegde, 2019).

Of note, astrocytes and other glial cells may also display abnormal ERK activation, which induces neurotoxicity. A study claimed that loss of nuclear TDP-43 in microglia induces activation of ERK 1/2, which subsequently activates activator protein-1 (AP-1) complex inducing the expression of pro-inflammatory molecules such as cyclooxygenase-2 (COX-2) and prostaglandins E2 (PGE2) (Sahana & Zhang, 2021). On the other hand, this process was not detected in astrocytes, suggesting that microglia cause the initiation of a neurotoxic mechanism (Chung et al., 2005). In transgenic G93A mice, the astrocytes showed p-ERK accumulation at eight weeks, with p-ERK level increasing as the disease progressed. Hippocampal and cerebellum regions also display ERK staining in correlation with cognitive and motor impairment, both in ALS and FTLd patients (Ryu et al., 2019). This agrees with the role of ERK in memory formation and synaptic plasticity (Silingardi et al., 2011). Similarly, in G93A mutant mice, extracellular ATP depletion in astrocytes has been related with the activation of ERK 1/2 through purinoceptor 7 (P2X7). ERK activation is also dependent on NADPH oxidase 2 (NOX2) activation, which enhances ROS

generation in glial cells feeding a vicious cycle in which neurotoxicity appears to be mediated by glial cells (Apolloni et al., 2013).

1.3.1.3 JNK

JNKs are another group of MAPK members activated in response to stress stimuli. JNKs are activated by various types of stress signals, such as cytokines, UV radiation, DNA damage, and growth factor deprivation, via multiple receptors such as RTKs, GPCRs and TNF receptors (Zhou et al., 2015). Following their activation, these receptors recruit several scaffold proteins that activate MAP3K members, including MEK kinase 1, 2, 3, and 4 (MEKK1–4), dual leucine zipper kinase (DLK), thousand-and-one amino acid 1 (TAO1) and apoptosis signal- regulated kinase 1 (ASK1). Activate MAP3Ks phosphorylate MAP2K members, such as MEK 4 and 7, which further activate JNKs by phosphorylation of their tyrosine and threonine residues (Zhou et al., 2015). Active JNKs can act on both cytoplasmic and nuclear substrates. Their cytoplasmic substrates include glucocorticoid receptors, such as cytoskeletal proteins, tumor suppressor protein p53, MAP kinase activating death domain (MADD), Tau, and STAT, whereas their nuclear substrates include ATF2, heat shock factor (HSF)1, STAT3 and c-jun which is the best characterized (Plotnikov et al., 2011). Activated c-Jun can homodimerize or heterodimerize with c-Fos, forming the AP-1 transcription factor complex (Darling & Cook, 2014).

JNK is hyperactivated in several conditions related to ALS, such as in SOD1-ALS, in which accumulation of misfolded mutant SOD1 might activate ER stress pathways(Kikuchi et al., 2006)**.** As previously mentioned, misfolded proteins in the ER cause the UPR, which activates an ER transmembrane protein inositol-requiring enzyme1 (IRE1). Activated IRE1 binds to Derlin 1 on the surface of ER, recruiting TNF receptor-associated protein 2 (TRAF2) and ASK1, a MAP3K protein. Activated ASK1 inhibits the ERAD pathway, thus activating JNK (Nishitoh et al., 2002).

It has been found that homeodomain-interacting protein kinase 2 (HIPK2) is involved in ER-stress-mediated activation of IRE1 both in the G93A SOD1 and TDP-43 transgenic mouse models of ALS, as well as in sALS and C9orf72-related ALS patient postmortem tissues (S. Lee et al., 2016).Consistently with these findings, MAP4K4 activates c-Jun and causes apoptosis, while inhibition of MAP4K4 in mice and iPSC-derived MNs promotes survival (C. Wu et al., 2019).

JNKs activation has been observed through a further mechanism in FUS-ALS Drosophila model: loss of function of the protein kinase Hippo, one of the key signaling

components in a pathway that controls cell proliferation and apoptosis, rescues FUS-mediated toxicity, while overexpression of Hippo shows the opposite effect, increasing toxicity. Thus, Hippo activates JNKs in FUS-ALS (Gogia et al., 2020)

Therefore, the inhibition of the JNK pathway has displayed neuroprotective effects. Indeed, URMC-099, an inhibitor to hepatocyte progenitor kinase-like/germinal center kinase-like kinase (HGK), is able to rescue cyclopiazonic acid-induced cell death in human ALS motor neurons and also prevents microgliosis in mouse microglial cells (Bos et al., 2019) HGK is a MAP4K member that is upstream of JNK activation (Bos et al., 2019).

Despite evidence from different studies, other authors showed contrasting results for JNK activation in ALS; they suggested a complex role of the MAPK pathways in ALS. Actually, multiple MAPK members are involved, showing crosstalk, in the disease process. Thus, elucidating the role of MAPKs in pathology leads often to ambiguous results. MAPKs involved in stress response, such as p38 and JNK, show overlap in their functions and act on shared substrates (Sahana & Zhang, 2021). For instance, c-Jun can be activated by ERK, p38 and JNK. Also, several kinases in the MAP2K and MAP3K groups can activate p38 and JNK. The activation of a particular MAPK shows specificity, depending on the type of cell exposed to the stressor. This is proved in astrocytes and microglial cells, which have a different behavior and activate different stress responses (Sahana & Zhang, 2021) Also, two independent studies have reported selective activation of p38 but not JNK in the spinal MNs of SOD1 mutant mice (Veglianese et al., 2006; Holasek et al., 2005). Nevertheless, enriched AP1 was identified in MNs, while in SOD1 mutant-induced pluripotent stem cell (iPSC)-derived motor neurons, c-Jun levels were upregulated up to five-folds, in comparison to the control. These MNs also showed increased ERK and JNK activation. Contrastingly, FUS mutant iPSC-derived motor neurons showed p38 and ERK activation but not JNK (Bhinge et al., 2017)

Despite the differences in Jun and ERK activation, the increased Jun protein and mRNA localization into the nucleus in MNs compared to other neurons across various models of ALS, underlines the specific vulnerability of MNs to stress-induced neurodegeneration (Bhinge et al., 2017)

In another neuronal cell model, the localization of TDP-43 in SGs induced by the oxidative stressor paraquat was prevented by the inhibition of p38a and ERK, whereas inhibition of JNK did not prevent TDP-43 pathology (Meyerowitz et al., 2011) However,

under sodium arsenite stress conditions, JNK prevented the formation of SGs and localization of C-terminal fragments to SGs in these models (Meyerowitz et al., 2011)

In addition to these, few studies show opposing roles of JNK and p38 activation in ALS disease pathogenesis. A genetic screen in Drosophila identified that Wallenda (wnd), a fly homolog of the MAPK2 member DLK which is upstream to both p38 and JNK, rescued TDP-43 induced toxicity. In this TDP-43 fly model, JNK is cytoprotective, whereas p38 is cytotoxic. In fact, loss of function of p38 and gain of function of JNK increased lifespan of flies (Yoon et al., 2005). These results suggest the balance in p38 and JNK activation is a critical factor for the overall cellular response to a stress signal.

Interestingly, a JNK-mitochondrial SH3-domain binding protein 5 (SH3BP5/SAB)-ROS activation loop has been elucidated, which is required to sustain JNK activity. Importantly, the level of SAB expression in the outer membrane of mitochondria is a major determinant of the set-point for sustained JNK activation. SAB is a docking protein and substrate for JNK, leading to an intramitochondrial signal transduction pathway, which impairs electron transport and promotes ROS release to sustain the MAPK cascade (Win et al., 2018)

Recent studies have shown that mitochondrial JNK signaling is partly responsible for ischemic myocardial dysfunction; however, the underlying mechanism remains unclear. It has been reported that activation of mitochondrial JNK, rather than JNK localization on mitochondria, induces autophagy and apoptosis and aggravates myocardial ischemia/reperfusion injury (J. Xu et al., 2015). Myocardial ischemia/reperfusion induced a dominant increase of mitochondrial JNK phosphorylation, while JNK mitochondrial localization was reduced. In this study, treatment with Tat-Sab_{KIM1}, a retro-inverse peptide which blocks JNK interaction with mitochondria, decreased mitochondrial JNK activation without affecting JNK mitochondrial localization following reperfusion (Xu et al., 2015). Tat-Sab_{KIM1} treatment reduced Bcl2-regulated autophagy, cytochrome c-mediated apoptosis and myocardial infarct size. Notably, selective inhibition of mitochondrial JNK activation using Tat-Sab_{KIM1} produced a similar infarct size-reducing effect as inhibiting universal JNK activation with JNK inhibitor SP600125 (J. Xu et al., 2015). Moreover, insulin-treated animals exhibited significantly dampened mitochondrial JNK activation accompanied by reduced infarct size and diminished autophagy and apoptosis following reperfusion. Taken together, these findings demonstrate that mitochondrial JNK activation, rather than JNK mitochondrial localization, induces autophagy and apoptosis and exacerbates myocardial ischemia/reperfusion injury (J. Xu et al., 2015)

In conclusion, hyperphosphorylation or abnormal phosphorylation of MAPK members could be linked to several ALS-associated cell defects, such as OS, neuroinflammation, ER stress, protein aggregation and axonal transport impairment. Hence, several inhibitors to MAPK members have been tested in multiple ALS models, such as MAP4K inhibitor 29, SB203580 and semapimod. The first was tested in motor neurons (MNs) from human SOD1 and TDP-43 mutant iPSC and was able to increase MNs survival reducing thapsigargin/ tunicamycin induced toxicity (Wu et al., 2019). SB203580 and semapimod are both inhibitors of p38 which increased survival of the SODG93A mice and decreased axon degeneration pathology (Dewil et al., 2007)

1.3.2 REST

REST (also known as NRSF) is a gene silencing transcription fact which is widely expressed during embryogenesis and acts in end-stage neuronal differentiation (Chong et al., 1995; Schoenherr & Anderson, 1995). In pluripotent stem cells and neural progenitors, REST actively repress a vast number of coding and noncoding neuron-specific genes involved in synaptogenesis, axonal pathfinding, synaptic plasticity and structural remodeling (Ballas & Mandel, 2005; Ooi & Wood, 2007). In silico analysis identifies close to 2000 putative REST targets in the mammalian genome, including coding and noncoding genes (A. W. Bruce et al., 2004). In the final stages of neuronal differentiation, loss of REST is crucial for the acquisition of the neuronal phenotype (Ballas & Mandel, 2005).

It was initially thought that REST acted as a master regulator of neuronal genes involved in neurogenesis in undifferentiated neurons and stem cells. Recent findings claim that REST is expressed in differentiated neurons during the critical period, a time of heightened sensitivity to plasticity in brain development, where it plays a role in fine-tuning of genes important to synaptic plasticity (Rodenas-Ruano et al., 2012) and in normal aging, where it suppresses genes involved in neuronal death, providing neuroprotection (Lu et al., 2014).

Dysregulation of REST is implicated in several neurodegenerative disorders. REST is activated in selectively vulnerable mature hippocampal neurons in response to ischemic insults (Calderone et al., 2003; Formisano et al., 2007) and seizures (Garriga-Canut et al., 2006; McClelland et al., 2011). In Huntington's disease, REST aberrantly accumulates in the nuclei of vulnerable striatal neurons (Zuccato et al., 2003). In aging neurons, loss of REST is associated with the onset of AD in humans (Lu et al., 2014) (Figure 12).

Perturbation of REST expression during embryogenesis causes cellular apoptosis, aberrant differentiation, patterning, and lethality (Z. F. Chen et al., 1998). In differentiated neurons, REST is quiescent, but can be activated in response to neuronal insults (Calderone et al., 2003). Increased expression of REST in response to neuronal insults would be expected to repress not only postsynaptic receptors and transporters, but also presynaptic vesicle proteins such as synapsin I and the SNARE protein SNAP25 (Thiel et al., 2015). Thus, not only neurotransmission in adult neurons, but also stimulus-induced exocytosis in PC12 cells and pancreatic β-cells, rely on exceedingly low levels of REST expression (Thiel et al., 2015). In contrast, in aging neurons, low levels of REST are neuroprotective, and loss of REST is associated with AD (Lu et al., 2014)

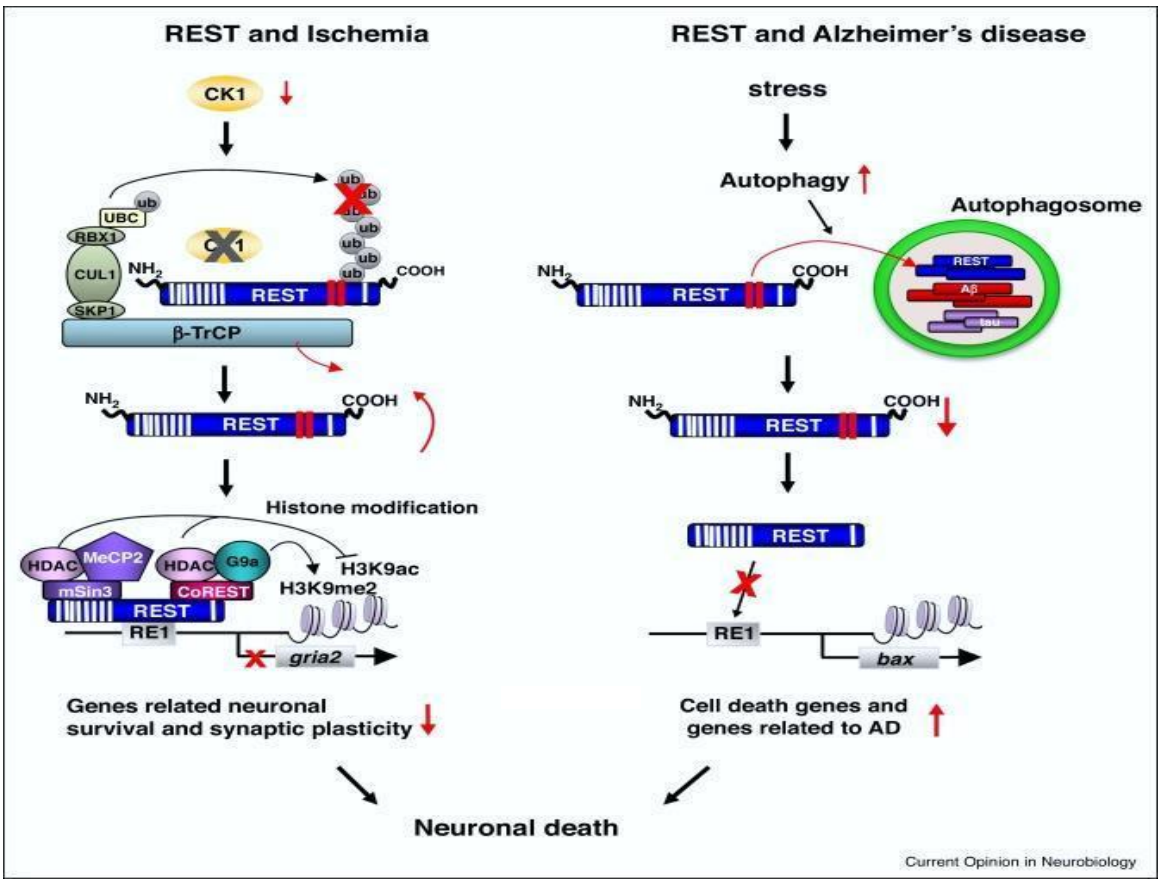

Figure 13. Regulation of REST in ischemia and AD. Left, global ischemia reduces abundance of CK1 and E3 ligase β-TrCP, resulting in an increase in REST in the hippocampal CA1. REST binds to the RE1 element within the promoter of target genes such as *gria2* and guides the assembly of mSin3A and CoREST, HDACs 1 and 2, G9a and MeCP2. The REST-corepressor complex enhances epigenetic remodeling of core histone proteins at the promoter of target genes and represses transcription of genes involved in synaptic plasticity and neuronal survival. Right, in AD brains OS activates autophagy and formation of autophagosomes. REST is enclosed in autophagosomes, together with misfolded proteins, such as Aβ and tau, which, in turn, reduces REST abundance in the nucleus. Loss of REST in the nucleus causes an increase in expression of genes involved in neuronal death and AD pathology (Adapted from J. Y. Hwang & Zukin, 2018).

CA3 that was lost in subjects with mild or severe cognitive impairment AD (Lu et al., 2014). ChIP-seq experiments in SH-SY5Y cells revealed occupancy of REST primarily at targets involved in neuronal death such as p38 MAPK, FAS, FADD, TRADD, BAX, BID, BBC3 (also known as PUMA), mitochondrial permeability transition pore proteins and cytochrome c and AD pathology (γ-secretase, presenilin 2, presenilin enhancer-2, and CDK5R1). In fact, aging mice with reduced REST exhibited enhanced vulnerability to oxidative stress (Lu et al., 2014). However, REST could also be involved in ALS pathology, according to recent findings.

For instance, an interesting link was found between Neuroglobin (Ngb), a REST/NRSF-regulated protein, and ALS progression (van Acker et al., 2019). Ngb is active in ROS detoxification and cytochrome c inhibition, which provides a beneficial outcome in pathologies such as AD and stroke. Considering that OS and cell death are typical hallmarks of late ALS stages, Ngb's involvement was explored along the disease progression. Results show that Ngb transcription was two-fold down-regulated in late-stage SODG93A mice (van Acker et al., 2019). In addition, accordingly to REST/NRSF transcription, Ngb expression is higher in spinal cords than in cortices. In order to look further into the link between Ngb and ALS, in the same study a double mutant Ngb-/-SODG93A mouse model was generated, which shows an earlier onset and severity of hind limb deficits (van Acker et al., 2019). Mitochondria derived from the model showed an altered mean volume, granularity and Ca2+-induced swelling in comparison with NgbWt/WtSODG93A mice. These results indicate Ngb to be involved in and affected by the SOD1G93A pathology, which could in part be attributed to its role in destabilizing events of mitochondrial swelling and phenotypes (van Acker et al., 2019)

REST also showed an important role in alpha-synuclein pathology, associated with dopaminergic neuronal loss in the substantia nigra (SN) of PD. Working across human and mouse models, mechanisms by which the accumulation of soluble α-synuclein oligomers leads to neurodegeneration in PD have been investigated (Ryan et al., 2021)

Biochemical analysis of the midbrain of synuclein overexpressing male and female transgenic mice generated using bacterial artificial chromosomes (BACs) revealed age and region-dependent mitochondrial dysfunction and accumulation of damaged proteins downstream of the REST. Moreover, vulnerable SN dopaminergic neurons displayed low REST levels compared to neighboring protected SN GABAergic neurons, which correlated with the accumulation of α-synuclein oligomers and disrupted mitochondrial morphology (Ryan et al., 2021). Consistent with a protective role, REST levels were reduced in patient

iPSC-derived dopaminergic neurons carrying the SNCA-Triplication mutation, which accumulated α-synuclein oligomers and mitochondrial damage, and displayed REST target gene dysregulation (Ryan et al., 2021). Furthermore, CRISPR-mediated REST knockout induced mitochondrial dysfunction and impaired mitophagy *in vitro*. Conversely, REST overexpression attenuated mitochondrial toxicity and mitochondrial morphology disruption through the transcription factor PGC-1. These findings show that increased levels of α-synuclein oligomers cause dopaminergic neuronal- specific dysfunction through mitochondrial toxicity, which can be attenuated by REST in an early model of PD (Ryan et al., 2021) and highlight REST as a mediator of dopaminergic vulnerability in PD. Whether REST plays a similar role in ALS pathology or is mislocalized to mitochondria is still unknown.

1.4 Mitochondria and energy metabolism in ALS

Basic physiological functions in CNS require significant amounts of energy (Ames, 2000) In fact, the adult human brain represents 2% of the total body weight but it consumes 20% of the body's energy. This energy is mainly used to generate action potentials and postsynaptic signaling (Attwell & Laughlin, 2001). Since energy storage in the brain is low, neurons require a significant amount of energy and need a constant availability of glucose from the blood (McKenna et al., 2012a). Consequently, such a high energy requirement is mostly met by oxidation of glucose via mitochondrial OXPHOS). Under normal physiological conditions, glucose is the main energy source in the brain. However, when glucose availability is low such as during excessive physical activity, development, or prolonged starvation, low glucose levels can be supplemented. Because entry of neuroactive compounds (e.g., glutamate, aspartate, glycine, D-serine) into the brain is highly restricted by the blood-brain barrier (BBB), these compounds must be synthesized from glucose within the brain (Mergenthaler et al., 2013)

Cellular energy is produced through glycolysis and oxidative metabolism via the tricarboxylic acid (TCA) cycle and the electron transport chain in the mitochondrion. Glycolysis converts glucose to pyruvate in the cytosol generating adenosine triphosphate (ATP) and nicotinamide adenine dinucleotide (NADH). Pyruvate can be then converted into lactate by lactate dehydrogenase or into alanine by alanine aminotransferase. However, pyruvate largely enters the mitochondria where it is converted to acetyl-CoA by pyruvate dehydrogenase (PDH). In astrocytes, pyruvate can be carboxylated by pyruvate carboxylase to generate the TCA cycle intermediate oxaloacetate (A. C. H. Yu et al., 1983). Within the TCA cycle a series of reactions oxidize acetyl-CoA and generate

reducing equivalents, which then transfer electrons to oxygen via the enzyme complexes of the electron transport chain, resulting in the final generation of ATP by ATP synthase, secondary to the maintenance of mitochondrial potential (Denel, 2012). The TCA cycle is important not only in producing reduction equivalents for ATP generation, but it is also crucial as a source of intermediates to synthesize lipids, neurotransmitters, and amino acids (McKenna et al., 2012).

Efficient exchange of energy substrates between the blood and the brain is sustained by the expression of distinct transporters, including GLUT1 for glucose, MCTs for monocarboxylates (such as lactate, pyruvate and ketone bodies) and FAT for fatty acids, at the level of the BBB (Pierre & Pellerin, 2005). As already mentioned, from these various molecules, glucose is the prime energetic substrate for the adult human brain. Its catabolism through primary (e.g., glycolysis and mitochondrial TCA) cycle) or secondary [e.g., pentose phosphate shunt pathway (PPP)] metabolic pathways not only generate ATP to fulfill the brain's energy demands, but also provides critical precursors for the synthesis of neurotransmitters, neuromodulators, and cellular components. In addition, glucose is important to sustain cellular antioxidant systems (Dienel & Rothman, 2020).

Nevertheless, under specific circumstances, brain cells can rely upon other substrates that are imported from the blood (e.g., ketones bodies during starvation and lactate during intense activity) or produced locally (e.g., lactate, glutamine). Out of these alternative substrates, lactate was identified as a key player mediating the metabolic interplay between astrocytes and neurons. Both these cell types can efficiently metabolize glucose and lactate, however, while astrocytes present a more pronounced glycolytic profile, neurons preferentially rely on oxidative metabolism *via* mitochondrial OXPHOS (Bélanger et al., 2011a). This notion was central to the formulation of the astrocyte-neuron lactate shuttle (ANLS) hypothesis (Pellerin & Magistretti, 1994), which was supported by studies suggesting incomplete glucose oxidation and/or increased lactate production following neuronal activity (Morita et al., 2019).

This model, which was first introduced in the early nineties (Pellerin & Magistretti, 1994) postulates that extracellular glutamate increase during intense neuronal activity leads to active astrocytic glutamate uptake, which in turn triggers Na^+/K^+ ATPase activation in astrocytes (to maintain Na^+/K^+ homeostasis) with an associated energy consumption and a drop in cellular ATP levels (Magistretti & Chatton, 2004). To counteract this effect, astrocytic glucose uptake and glycolysis is elevated, secondarily increasing lactate production and excretion, which will then be available as a fuel to neuronal cells (Pellerin

et al., 2007). However, this concept is not consensual, and evidence has been raised to dispute some of its premises (Dienel & Rothman, 2020). Interestingly, an alternative neuron-astrocyte lactate shuttle was also proposed (Dienel & Rothman, 2020).

Brain hypoperfusion is accompanied by reduced glucose and oxygen metabolic rates. This hypometabolism of glucose characterizes the normal aging process, with glucose metabolic rates decreasing by 26% from age 18 to 78 (Marcus et al., 2014), but is further accentuated in pathological conditions such as AD and PD (Marcus et al., 2014) In early AD, fluorodeoxyglucose-PET showed a characteristic reduction of total glucose metabolism in the parietotemporal association cortices, posterior cingulate cortex and the precuneus (Marcus et al., 2014). Interestingly, aerobic glycolysis, which corresponds to the fraction of glycolysis not coupled to oxidative phosphorylation and which was previously associated with biosynthetic and neuroprotective roles, was found to be reduced in brain regions with higher levels of Tau deposition (Vlassenko et al., 2018). Contrariwise, AD postmortem brain-derived data points to an overall upregulation of glycolytic enzymes, which was interpreted as a compensatory mechanism to mitochondrial dysfunction and to the reduced levels of glucose transporters that accompanies disease progression (Bell et al., 2020).

The majority of synapses in the CNS are glutamatergic (Danbolt, 2001; Rothstein et al., 1994). During neurotransmission, neurons release glutamate, into the synaptic cleft. Glutamate is then taken up by astrocytes via glutamate transporters (Martinez-Hernandez et al., 1977; Rothstein et al., 1994) and an astrocyte specific glutamine synthetase converts glutamate into glutamine (Martinez-Hernandez et al., 1977). Glutamine can be transferred to neurons and converted back to glutamate by phosphate activated glutaminase to complete the glutamate-glutamine cycle (Laake et al., 1999; Lazar & McIntyre, 2019). This cycle protects neurons from excitotoxicity (Tefera et al., 2021). In this sense, in sALS, excitotoxicity due to overactivation of glutamate receptors may mediate the motor neuron degeneration in the spinal cord (Corona et al., 2007).Glutamate’s toxicity is apparently due to calcium flooding the cell. Calcium is supposed to briefly enter the neuron with each signal and triggers the cell to fire off its own signals and adjust its own activities accordingly. But prolonged calcium inside the cell evidently can do damage and will even activate programmed cell death (Corona et al., 2007). Research in the early 1990s determined that ALS patients have raised levels of glutamate in the fluid bathing the brain and spinal cord. In fact, 40 percent of sporadic cases of ALS are characterized by this elevated glutamate in cerebrospinal fluid (CSF). Abundant evidence points to glutamate as a destructive factor in ALS (Cheah et al., 2010)

Consequently, one of the few approved drugs for the treatment of ALS is Riluzole, which acts by binding voltage-gated sodium channels, thereby preventing the propagation of action potentials and eventual axonal release of glutamate. In addition, Riluzole acts on astrocytes to increase uptake of glutamate (Lazar & McIntyre, 2019).This mechanism is protective against exotoxicity by over-stimulation of the glutamate receptors during glutamatergic neurotransmission (van den Bosch et al., 2006).

Glutamate is also a substrate for oxidative metabolism. In fact, seventy percent of glutamate in astrocytes is metabolized by the TCA cycle, while 30% is converted into glutamine (Schousboe et al., 1993) GABA released from the synaptic cleft during neurotransmission can be taken up by astrocytes and enter the astrocytic TCA cycle as succinate via GABA transaminase and succinate semialdehyde dehydrogenase. Succinate can be further metabolized in the TCA cycle to form α-ketoglutarate, glutamate and glutamine. Astrocytes release glutamine where it is taken up by neurons to synthesize glutamate or GABA. In GABAergic cells, glutamate produced via phosphate activated glutaminase is decarboxylated to GABA. This glutamate/GABA-glutamine cycle is important for the maintenance of the neurotransmitter pool in the CNS (Bak et al., 2006)

It has been widely demonstrated that alterations in any phase of these glucose metabolism pathways can cause reduced generation of ATP, with negative effects on cellular functions. In presence of ATP sub-optimal levels, other energy generating pathways can be activated and lead to an increased production of ROS followed by oxidative stress. Moreover, since glucose metabolism is linked with amino acid neurotransmitter metabolism, impaired glucose metabolism pathways determine glutamate excitotoxicity and neurodegeneration (Tefera et al., 2021)

Many authors have reported changes in glucose utilization in certain brain and spinal cord regions of ALS patients as well as animal models of the disease. MNs are highly energetic cells, and it has been suggested that altered energy metabolism is an event that precedes MN loss in ALS. Figure 14 shows a simplified scheme of CNS normal glucose metabolism in comparison with commonly observed defects in ALS (Tefera et al., 2021).

As previously stated, ALS-associated abnormalities can negatively affect different steps of the glucose metabolism; here we will especially focus on oxidative phosphorylation and mitochondrial dysfunctions. Mitochondria are the primary site of energy production in the cells, but they are also the most important source of ROS and OS. An uncontrolled production of ROS may be detrimental for lipids, proteins, nucleic acids and impair mitochondrial function (de Aguilar et al., 2005). Several studies have detected functional

and morphological impairment in mitochondria in the spinal cord and brain of ALS patients as well as in mouse models of the disease (Wong et al., 1995; Sasaki & Iwata, 1996; Jung et al., 2002). These abnormalities can play a role in reduced energy production and increased OS. In addition, OS-associated defects in the electron transport chain, reduced oxidative phosphorylation and ATP production have been found (Jung et al., 2002; Browne et al., 2006). Specifically, subunits of ATP synthase, the enzyme complex responsible for ATP production from ATP at the end of the mitochondrial phosphorylation, have lower expression levels in spinal cord (Dangond et al., 2004) and motor cortex of ALS patients (Lederer et al., 2007). This could cause a decrease in ATP generation. On the other hand, in MNs isolated from SOD1G93A mice, it was observed an increased expression of genes involved in the mitochondrial machinery, including ATP synthase (Ferraiuolo et al., 2007). These opposite findings may be explained by a compensatory activation of energy generating pathways in order to properly respond to increased energy demand. Ultimately, mitochondrial dysfunction can determine a depletion of cellular energy resulting in MN death (Cozzolino & Carrì, 2012).

The exact mechanisms underlying alterations in CNS glucose metabolism in ALS are still poorly understood. Nevertheless, protein aggregation and oxidative stress may strongly contribute to the observed abnormalities. With respect to protein aggregation, studies have found that mutant TDP-43 accumulates in the mitochondria of ALS patients determining impairments in complex I activity and causing alterations in cellular (Menzies et al., 2002). Also, experiments with Drosophila overexpressing mutant human FUS have found mitochondrial fragmentation in this model due to pathological aggregation of FUS (J. Deng et al., 2015). Mutant forms of TDP-43 as well as FUS have also been linked to impairment of mitochondrial-endoplasmic reticulum interaction with consequent disturbance of protein homeostasis and decreased ATP generation (J. Deng et al., 2015). As indicated above, SOD1 is another ALS-related protein whose mutant form was found accumulated in brain mitochondria causing defects in the electron transport chain, particularly involving complex I and IV (Vijayvergiya et al., 2005; Ferri et al., 2006). Altogether, these studies reach the conclusion that mitochondrial protein aggregation may alter mitochondrial, both functionally and structurally resulting in impaired glucose metabolism and synthesis of ATP.

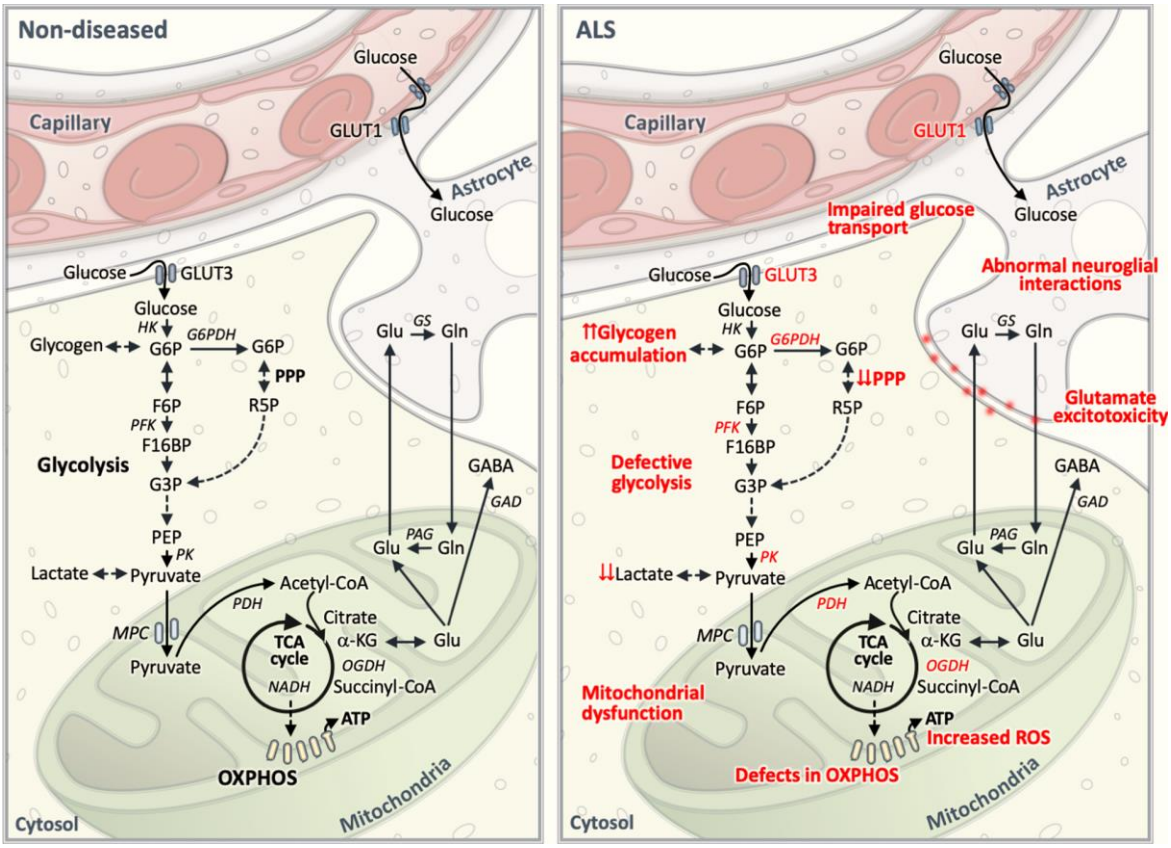

Figure 14. **A schematic diagram of normal CNS glucose metabolism, and frequently observed defects in ALS.** Glucose enters via GLUT3 transporter into neurons and via GLUT1 into astrocytes. Then, glucose is phosphorylated by hexokinase (HK) to glucose 6-phosphate (G6P). G6P can be converted by glucose 6-phosphate dehydrogenase (G6PDH) to 6-phosphogluconolactone to enter the PPP pathway, where it is converted to PPP intermediates, such as R5P (ribose 5-phosphate) which later can enter the glycolytic pathway via glyceraldehyde 3-phosphate (G3P) or provide nucleotide backbones. If G6P continues through glycolysis, it is converted into F6P (fructose 6 phosphate) and fructose 1,6-bisphosphate (F16BP) by phosphofructokinase (PFK). F16BP is further metabolized to G3P, phosphoenol pyruvate (PEP) and pyruvate. Pyruvate can be reduced to lactate by lactate dehydrogenase or enters mitochondria via mitochondrial pyruvate carrier (MPC) and gets converted into acetyl CoA by pyruvate dehydrogenase (PDH). Acetyl-CoA condenses with oxaloacetate to citrate and enters the TCA cycle. The TCA cycle generates various intermediates, from which glutamate is synthesized. In neurotransmission, glutamate is released from the presynaptic vesicles into the synapse where it is taken up by glutamate transporters in astrocytes and then converted into glutamine (Gln) by glutamine synthetase (GS). In GABAergic neurons, Glu is converted into GABA by glutamate decarboxylase (GAD) enzyme. The TCA cycle also generates reducing equivalents such as NADH and flavin adenine dinucleotide, which transfer electrons to oxygen via the electron transport chain, generating ATP. In ALS, numerous metabolic defects at various steps in the glucose metabolism pathway alter glucose metabolism and ATP generation. This include impairments in glucose transport and PPP, glycogen accumulation, reduced entry of pyruvate into the TCA cycle which downregulates PDH activity; reduced activities of oxoglutarate dehydrogenase (OGDH), mitochondrial dysfunction, reduced mitochondrial ATP production, increased ROS production, and impaired neuronal-glial interactions (Adapted from Tefera et al., 2021).

Defective glucose metabolism in the CNS may also arise from an increased OS, an imbalance between ROS and antioxidant defenses. OS has widely been involved in the onset and progression of ALS. Numerous studies have shown that OS is involved in the onset and progression of ALS (Barber et al., 2006) showing that oxidative damage to the enzymes involved in the glucose metabolism pathways as well as to mitochondrial DNA can impair energy production (Barber et al., 2006). Indeed, several studies have found that oxidative modifications of glycolytic, TCA cycle and mitochondrial proteins occur in neurodegenerative disorders (di Domenico et al., 2017; Allan Butterfield & Boyd-Kimball, 2018) disrupting neuronal energy metabolism and worsening OS.

Moreover, a 2019 study has aimed to elucidate the mechanisms that control the energetic demand under nutrient and ER stress (Balsa et al., 2019). The authors showed that ER stress and glucose deprivation stimulate mitochondrial bioenergetics, leading to the formation of respiratory supercomplexes (SCs) through protein kinase R-like ER kinase (PERK). In fact, the genetic ablation or the pharmacological inhibition of PERK blocks nutrient and ER-mediated increase in SC level and reduces oxidative phosphorylation-dependent ATP production. SCs are promoted through the PERK-eiF2a-ATF4 axis, which increases supercomplex assembly factor I (SCAF1 or COX7A2L), along with the enhancement of mitochondrial respiration (Balsa et al., 2019) (Figure 15). Interestingly, PERK activation is able to rescue bioenergetic defects caused by complex I missense mutations derived from mitochondrial disease patients. These findings have described an energetic communication between ER and mitochondria, with potential implications in cell survival and diseases associated with mitochondrial failures, such as ALS.

In a 2021 study, induced pluripotent stem cells from healthy controls, familial ALS, and sporadic ALS patients were differentiated toward spinal MNs, cortical neurons, and cardiomyocytes. Metabolic flux analyses reveal an MN-specific deficiency in mitochondrial respiration in ALS, with similar results in familial or sporadic ALS MNs (Hor et al., 2020). This impairment of mitochondrial respiration was linked to hyper-acetylation of mitochondrial proteins. Particularly, Sirtuin-3 (SIRT3) is a mitochondrial protein acting as a deacetylase to preserve mitochondrial function and integrity. Interestingly, SIRT3 activation via nicotinamide or a small molecule activator was able to reverse the defective metabolism in ALS MNs (Hor et al., 2020).

In addition, autosomal dominant mutations in coiled-helix-coiled-helix domains containing protein 10 (CHCHD10) have recently been reported as a rare genetic cause of

ALS. (Purandare et al., 2018; Snowden et al., 2015). CHCHD10 is a soluble 14 kDa mitochondrial protein that is upregulated in stress conditions and localizes to the mitochondrial intermembrane space forming a complex with its paralogue CHCHD2 (Straub et al., 2018; Huang et al., 2018).

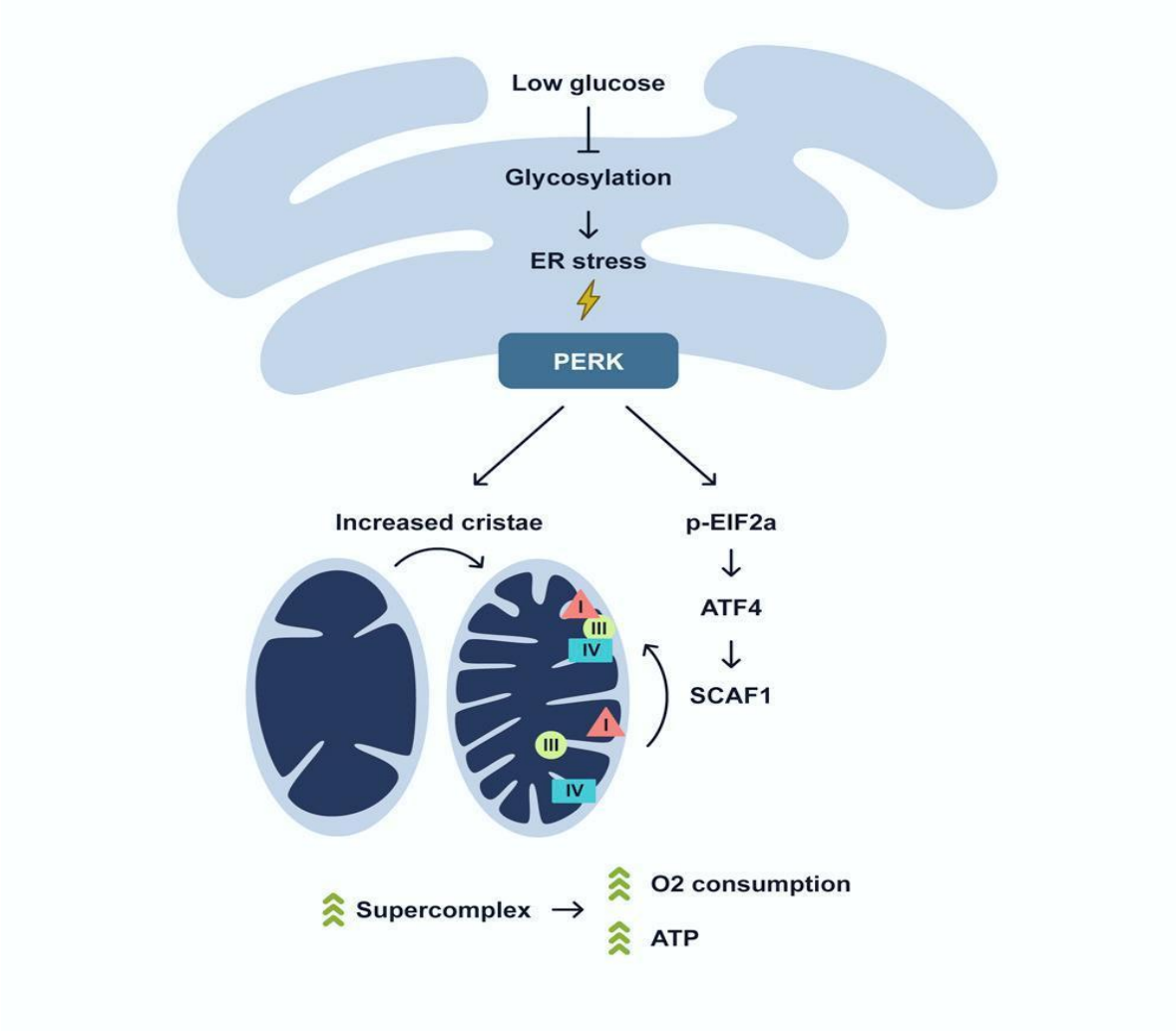

Figure 15. **When glucose becomes limiting for glucosamine synthesis and protein glycosylation, the ER activates a metabolic and energetic response mediated by PERK.** This process doesn't produce a complete remodeling of the mitochondrial proteome but reorganizes the electron transport chain (ETC) complexes and promotes the expansion of mitochondrial cristae. ETC supercomplexes assembly occurs through the PERK-eiF2a-ATF4 axis, with consequent increase in O_2 consumption and ATP generation (Adapted from Balsa et al., 2019).

The exact function of CHCHD10 remains unknown. Most predicted pathogenic variants are present in the N-terminal half of the protein. Four different studies have reported the

mutation c.44C > A (predicting p. R15L) in sALS and fALS (Müller et al., 2014); (Johnson et al., 2014; J. Zhang et al., 2015.; Khan et al., 2017). In a 2021 study cellular and metabolic remodeling caused by the CHCHD10 variant p.R15L was investigated (Straub et al., 2018). Researchers collected metabolomic, transcriptomic and proteomic datasets on patient fibroblasts. They cultured patient and rescued cells (expressing wild-type CHCHD10) in a medium containing either glucose or galactose as a nutrient source. Glucose-free galactose medium causes an energetic stress, as it forces cells to exclusively rely on OXPHOS for ATP production (Straub et al., 2018). The data demonstrate a global remodeling of mitochondrial and cellular metabolic pathways, and the activation of an unfolded protein (UPR) stress response mediated by the IRE1/XBP1 pathway in the ER, and by ATF4 and ATF5 in mitochondria, in patient cells under energetic stress conditions (Straub et al., 2018). The authors proposed that motor neurons, the cells that are specifically affected in ALS, are more susceptible to mitochondrial dysfunction and may suffer damage much earlier in limited nutrient conditions than do fibroblasts (Straub et al., 2018). It is known that aging results in decreased neuronal uptake of glucose, therefore rendering motor neurons harboring CHCHD10 p.R15L variant more susceptible to cell death in the aging individual (Yin et al., 2016). Thus, targeting mitochondrial metabolism and the UPR response could be very useful for the development of potential treatments in ALS models of CHCHD10. In this sense, we should remember the interaction between age and ALS incidence (Huang et al., 2018).

In 2012, it was also shown that glucose and pyruvate deprivation in cells depending on glucose for survival induces abnormal levels of phospho-tyrosine signaling and oxidative stress (Spitz et al., 2000; Akin-Burns et al., 2009) resulting in the activation of diverse intracellular kinases including ERK and JNK. This results in a positive feedback amplification loop, until ROS accumulate above a toxicity threshold resulting in cell death.

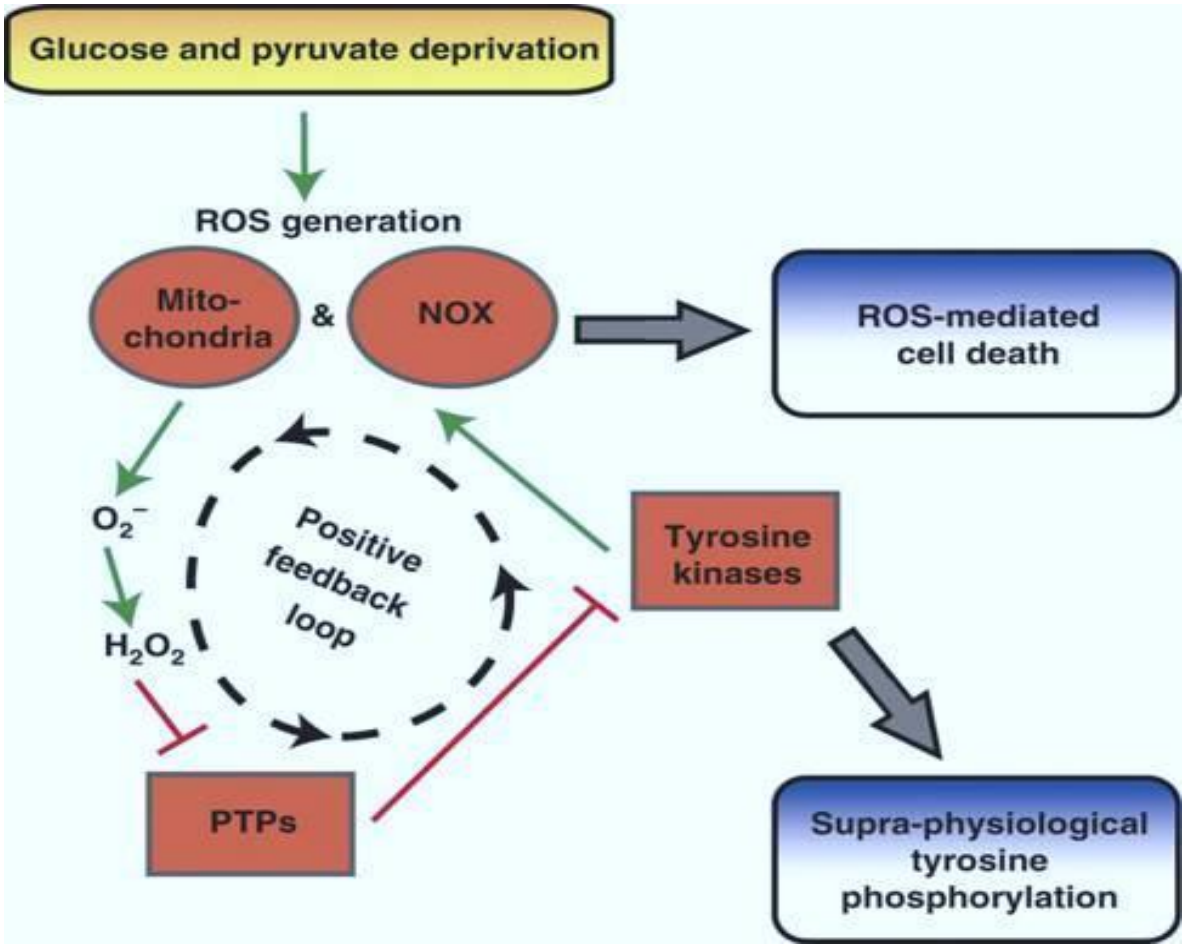

Figure 16. Glucose withdrawal initiates a positive feedback loop resulting in supra-physiological phospho-tyrosine signaling and ROS-mediated cell death. In cells dependent on glucose for survival, glucose and pyruvate deprivation causes OS driven by NOX and mitochondria. This OS provokes a positive feedback loop in which NOX and mitochondria generate superoxide anion (O_2^-), which dismutes to hydrogen peroxide (H_2O_2) and inhibits PTPs by oxidation (e.g., PTP-1B and PTEN). Without the negative regulation of PTPs, TKs including EGFR and Src activate NOX at focal adhesions, further amplifying ROS generation. This glucose withdrawal-induced positive feedback loop results in supra-physiological levels of tyrosine phosphorylation and ROS-mediated cell death (Adapted from Graham et al., 2012).

1.5. Lipid droplets: more than energy storage

Lipid droplets (LDs) are spherical organelles in which intracellular neutral lipid such as triacylglycerols (TAGs) and cholesteryl esters (CEs) are stored (Welte, 2015). The core of a lipid droplet is formed by hydrophobic molecules such as TAGs and CEs in association with retinyl esters (Meyers et al., 2017); the outer surface encloses an amphipathic lipid monolayer embedded with LD-associated proteins. Figure 17 illustrates the general structure of a lipid droplet. Depending on the cell type, different proteins can be found in

the LD core. This unique monolayer is a specific feature of LDs, and it lets the differentiation from organelles similar in size, such as lysosomes and endosomes, which show a lipid bilayer. Among LD-associated proteins, perilipins have been well described for their crucial roles in LD metabolic regulation (Sztalryd & Brasaemle, 2017). The exterior protein components of LDs are involved in many unique interactions and explain the numerous cellular roles of LDs in energy homeostasis, cellular communication, and disease.

For instance, LDs serve as lipid reservoirs for cells and a source of substrates for membrane formation and energy metabolism (Walther & Farese, 2012a). Adipose tissue is the richest in LDs. Here, fatty acids accumulate in times of nutrient excess and are mobilized when energy demand increases (Missaglia et al., 2019). But LDs also have an important role in physiological processes beyond simple fatty acid storage and supply, such as in inflammation and insulin signaling. For instance, LDs in various immune cell types contain a large pool of intracellular arachidonic acid (AA), which is a reserve of precursors for eicosanoid synthesis (Bozza & Viola, 2010; Saka & Valdivia, 2012; Dichlberger et al., 2016). LDs also contain enzymes involved in AA processing, indicating that these organelles serve as a supply site for inflammation (Bozza et al., 2011). In addition, LDs have been involved in ectopic lipid accumulation (Puri et al., 2007) and insulin resistance (Gemmink et al., 2017). It has been found that the overexpression of LD-associated proteins such as CIDE-A increases fat accumulation in mice, and human expression of LD proteins in adipose tissue shows a positive correlation with clinical insulin resistance (Puri et al., 2008).

LDs arise from the cytoplasmic leaflet of the ER membrane by budding (Walther et al., 2017). The acyl-glycerols enclosed in a LD are synthesized via diacylglycerol transferases (DGATs), which convert acyl-CoA-bound fatty acids, and DAGs into the TAGs that constitute the LD core (Harris et al., 2011). CEs which are also incorporated into the core of developing LDs (Zhu et al.,2018). Once dissociated from the ER membrane, LDs may continue to grow via LD fusion and further TAG incorporation. Fusion of LDs with the aid of members of Cell death-inducing DFF45-like effector (CIDE) family proteins (Gao et al., 2017) integrate smaller LDs into larger LDs. Re-localization of TAG synthesis enzymes like DGAT2 and GPAT4 from the ER to the LD surface allows direct synthesis of TAGs from cellular lipid sources (Wilfling et al., n.d.). During periods of stress and starvation, cellular debris can be incorporated into LDs, and it is thought that this process aims to protect the cells from lipotoxicity (Rambold et al., 2015). LDs harbor a variety of protein and lipid signatures, and these specific features can be useful to determine LD localization

and utilization. For example, perilipin 2 (PLIN2) shows low influence over lipolysis, so LDs that contain PLIN2 may be broken down more easily. On the other hand, PLIN1 and PLIN5 actively promote lipolysis when activated. Thus, LDs with varying PLIN proteins behave differently depending on the tissues and the environmental conditions (Sztalryd & Brasaemle, 2017).

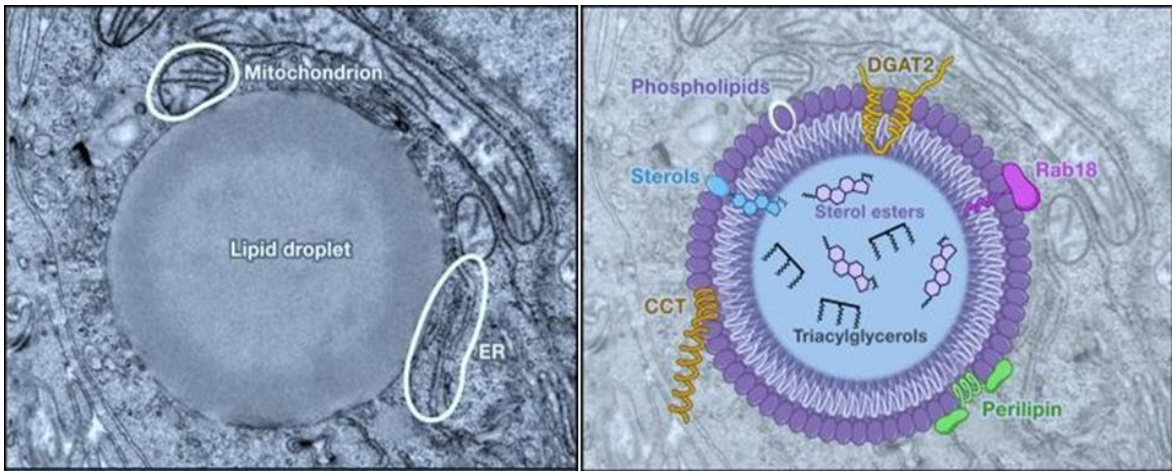

Figure 17. **Left panel| Electron micrograph of a lipid droplet in a cultured hepatoma cell.** The membrane monolayer surrounding the lipid droplet is visible, as well as the tight associations with mitochondria and ER membranes. **Right panel| Structural components of a lipid droplet**. The diagram shows the polar surface lipids of the monolayer (phospholipids and sterols), the nonpolar lipids of the core (sterol esters and triacylglycerols), and a number of proteins embedded in the surface of the droplet. These proteins include DGAT2, Rab18, perilipin, and CCT. Proteins can interact with the lipid droplet through amphipathic α helices, embedding of hydrophobic regions directly in the droplet, and lipid anchors. (Electron micrograph by S. Stone and J. Wong; image adapted from Farese & Walther, 2009)

In 2017, Kleckler and colleagues proposed a mechanism in which cells prepare for starvation synthesizing lipids as energy-rich storage compounds under conditions of ample nutrient supply. These can be stocked within LDs (Klecker et al., 2017). Upon nutrient depletion, cells survive by converting these internal energy supplies into FAs, which are used for ATP production by β oxidation in mitochondria (Walther & Farese, 2012) This process occurs along with cellular self-eating, or autophagy with the formation of autophagosomes, double-membrane bounded structures that engulf cytoplasmic cargo (Figure 18). Subsequently, autophagosomes fuse with the lysosome, where the cargo is dismantled into its molecular building blocks, mostly amino acids, and fatty acids (FAs). These are either recycled or utilized for energy generation (Kaur & Debnath, 2015).In this context, LDs not only fuel mitochondrial energy generation during starvation but also protect mitochondria by sequestering excess fatty acids that are released by autophagy and might damage organellar membranes (Nguyen et al., 2017).

Moreover, the potential link between ROS and lipid droplet formation has been investigated. Indeed, a study focusing on non-alcoholic fatty liver disease (NAFLD) has tested the capacity of OS induced by hydrogen peroxide on hepatocytes to induce LD upregulation, observing that ROS up-regulates the expression of PLIN2 in hepatocytes, whereas PLIN2 promotes the formation of lipid droplets resulting in lipid accumulation in liver tissues (Jin et al., 2018).

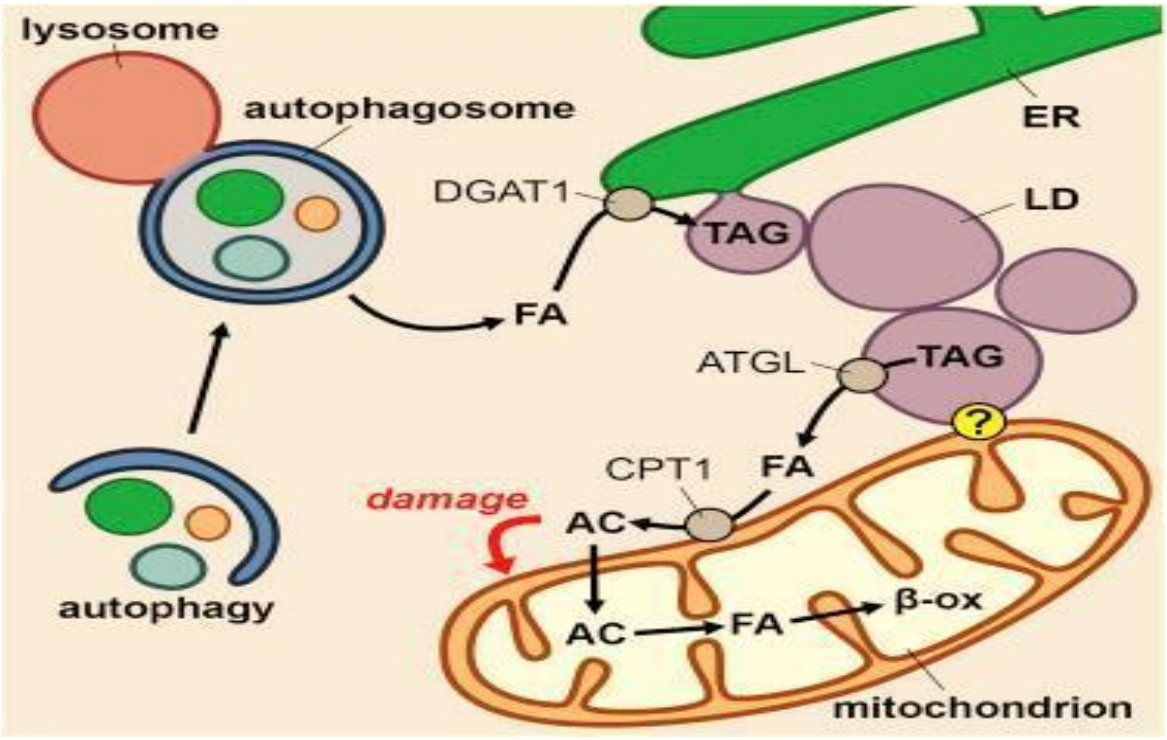

Figure 18. **Fatty Acids are forced to make a pit stop in LDs on their way from autophagosomes to mitochondria**. In starved cells, FAs are released during the autophagic degradation of membranous organelles. Instead of being directly transported to mitochondria to generate energy by β oxidation, FAs are rerouted to the ER, where they are used by diacylglycerol acyltransferase 1 (DGAT1) to synthesize TAGs, which are stored in ER-derived LDs. Simultaneously, TAG stores within LDs are used by the lipolytic enzyme adipose triglyceride lipase (ATGL) to generate FAs. These are subsequently converted to acylcarnitine (AC) by carnitine palmitoyltransferase 1 (CPT1) and transported into mitochondria, where they fuel ATP production by β oxidation. Interestingly, LDs and mitochondria are frequently found in close proximity, most likely because they form contact sites to facilitate efficient FA transport (Adapted from Klecker et al., 2017).

1.5.1. Lipid droplets in the CNS

Normal neuronal function and synaptic plasticity require lipid homeostasis (Montesinos et al., 2020), and processes such as lipid storage, breakdown and metabolism are tightly regulated through the dynamic interaction between perilipins and lipases on the LD surface (Olzmann & Carvalho, 2019). LD breakdown is generally driven by ATGL, another LD outer layer protein (Etschmaier et al., 2011). Lipophagy is a further LD breakdown

process, in which an LD is incorporated in an autophagosome and fuses with a lysosome to breakdown LD through lipid acid lipases (Cingolani & Czaja, 2016) Under conditions of metabolic stress, lipases cleave triglycerides into FAs, which are then processed in the mitochondria to liberate the energy stored in droplets via beta-oxidation into acetyl-CoA, TCA cycle and oxidative phosphorylation (Zechner et al.,2012), as introduced above. LDs have been shown to provide energy substrates (Cabodevilla et al., 2013); (B. Farmer et al., 2019), lipid signaling molecules (Arrese et al., 2014), and membrane infrastructure materials (Zehmer et al., 2009) for various cell types.

LDs have been found in all brain cell types. A recent study demonstrated that the majority LDs in the brain co-localize with ionized calcium binding adaptor molecule 1 (Iba1), a microglia/macrophage-specific protein. This finding may depict microglia as a main source of LDs (Marschallinger et al., 2020). Moreover, the lipid-associated microglia showed a unique transcriptomic signature compared to non-LD-laden microglia, suggesting that LDs in microglia could act as a cause or result of significant transcriptional modulations. Ependymal cells of the cerebral ventricular system have also been shown to accumulate LDs (L. K. Hamilton & Fernandes, 2018). Lesions to the CNS can induce LDs in neurons and astrocytes (Ioannou et al., 2019), and glial cells have been shown to form LDs from phagocytosed myelin fragments (S. C. Lee & Raine, 1989). Additionally, a study examining cell types that harbor PLIN positive droplets found that Iba1+, GFAP+, NeuN+ (a neuron specific antibody), and S100β+ (a calcium binding protein that is localized in astrocytes) cells harbor droplets (Shimabukuro et al., 2016). Together, these studies demonstrate that several cell types in the brain can form LDs.

LDs may affect cellular physiology and function in the CNS. In fact, the brain is the second most lipid-rich organ (J. A. Hamilton et al., 2007), with 20% of the body's total cholesterol (J. Zhang et al., n.d.). Alteration in the lipid composition of CNS cells has been shown to affect cell function and normal neural activity (Puchkov and Haucke, 2013; Bruce et al., 2017). It is known that neurodegenerative diseases, such as AD and PD, are characterized by lipid dysregulation as a metabolic feature.

More specifically, when the CNS is in a pathological state (i.e., cancer, neurodegenerative diseases, and ageing), its content of LDs increases, mainly in glial cells (astrocytes, microglia) and much less in neurons (Bailey et al., 2015; (Dienel, 2012; Marschallinger et al., 2020) (Figure 19). These findings support the role of astrocytes in variety of homeostatic function in the CNS. Being an abundant subtype of neuroglia, astrocytes may operate with neurons as a coupled metabolic unit (Dienel, 2019; Bélanger

et al., 2011b), as depicted in section 1.3. In fact, astrocyte processes surround blood capillaries and neuronal synapses (Tsacopoulos & Magistretti, 1996), being well positioned to transport glucose, free fatty acids (FFAs), and ketone bodies, from the systemic circulation to neurons and to store blood-derived glucose in the form of glycogen (Brown and Ransom, 2007). Under glutamatergic or noradrenergic stimulation during times of stress, astrocytes metabolize glycogen to glucose and lactate in the aerobic glycolysis (Bélanger et al., 2011; Dienel & Cruz, 2016; Pellerin & Magistretti, 1994). Lactate is considered to be used by astrocytes as a fuel to provide glucose for neurons (Dinuzzo et al., 2010; DiNuzzo et al., 2012) or it is released from astrocytes. When released, lactate may exit CNS and enter the systemic circulation (Dienel, 2012), it may enter neurons, where it is oxidized (i.e., the astrocyte-neuron lactate shuttle [ANLS] hypothesis; (Bélanger et al., 2011c), or it may act as a signaling molecule by binding to lactate receptors (Barros & Deitmer, 2010; Abrantes et al., 2019; Mosienko et al., 2015; Tang et al., 2014; Vardjan et al., 2018).

Studies utilizing astrocyte-neuron co-culture systems derived from Drosophila tissue have linked glial lactate transport to neurons via ANLS to increased FFA production in neurons (Ioannou et al., 2019; Liu et al., 2017). Neurons are exposed to reactive oxygen species (ROS) generated during β-oxidation of FFAs (K. D. Bruce et al., 2017), thus excessive FFAs and ROS can be lipotoxic for neurons. It is believed that FFAs are transferred from neurons to astrocytes, where they are stored in LDs as a defense against lipotoxicity (Ioannou et al., 2019). LD-stored FFAs can then be used by astrocytes for energy production in β-oxidation (Ioannou et al., 2019). It is still not completely clear whether LDs also supply astrocytes with lipids (FFA and cholesterol) for the synthesis of membranes and/or with lipids that act as signaling molecules. Whether the case is, it is clear that lipid metabolism of astrocytes could be of interest.

In vitro studies of LDs and *ex vivo* brain imaging have also associated LD formation with inflammation, as both a cause and an effect (Bozza & Viola, 2010). Lipopolysaccharide (LPS), a common pro-inflammatory stimulus, has been shown to increase the number and size of LDs in microglia (Khatchadourian et al., 2012). PLIN2 was shown to colocalize with these droplets; thus, PLIN2 may be considered a marker for both LDs and inflammation in the brain (Marschallinger et al., 2020).

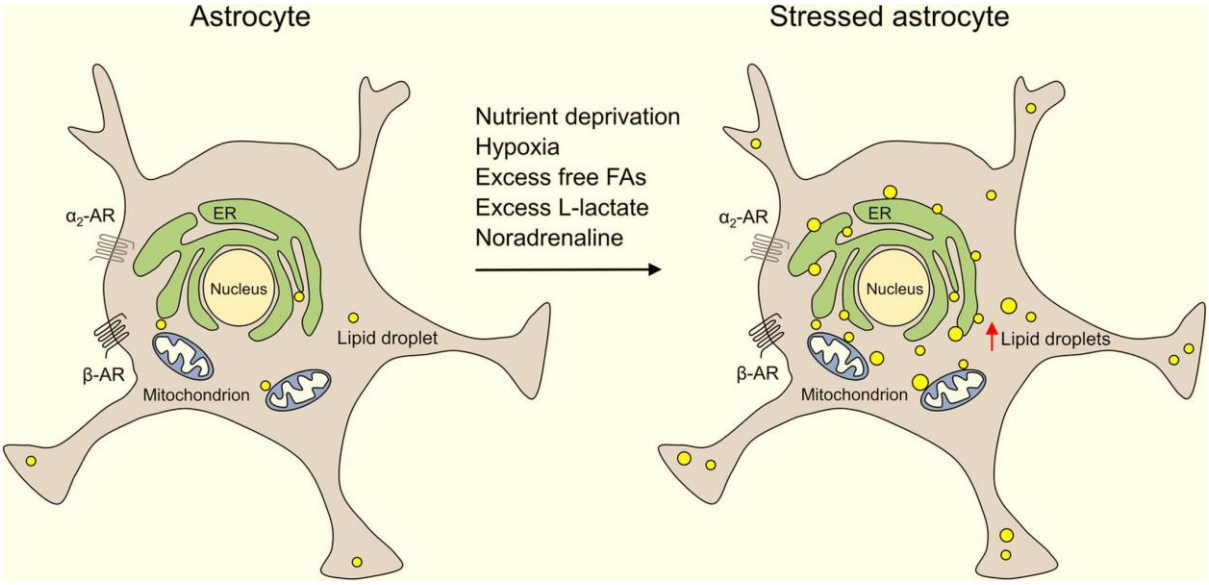

Figure 19. Stressed astrocytes accumulate LDs. LDs in astrocytes are organelles with limited mobility, in close proximity to mitochondria and ER to enable a stronger interaction between these organelles and more efficient β-oxidation and LD biogenesis, respectively. Noradrenaline, a brain stress–response system neuromodulator, metabolic stress (nutrient deprivation, excess of free FAs, and l-lactate), and hypoxic stress increase LD accumulation in astrocytes by increasing the number and the size of LDs. Noradrenaline increases LD accumulation activating β- and α2-ARs. Accumulation of LDs in stressed astrocytes may be useful as a support for energy provision but may also provide neuroprotection against the stress-induced lipotoxicity. AR, adrenergic receptor; ER, endoplasmic reticulum; FAs, fatty acids; LD, lipid droplet (Adapted from Smolič et al., 2021).

Another study claimed that palmitate treatment of isolated primary astrocytes increased the release of inflammatory markers including TNF-alpha, IL-1 beta, IL-6, and MCP-1 in addition to increase Oil Red O (a fat-soluble dye) staining and PLIN1 and PLIN2 transcription. These data suggest that LD-associated astrocyte inflammation may induce microglia to amplify the inflammatory response. Nevertheless, it remains to elucidate whether inflammation causes LDs, LDs cause inflammation, or both (Kwon et al., 2017).

1.5.1.2. Lipid droplets in neurodegeneration and ALS pathology

As previously mentioned**,** the appearance of LDs in neurons is not observed under physiological conditions but is associated with neural diseases. LD dynamics is still unclear as well as the effect of LDs on neuronal functions. In 2020, Yang et al. discovered that mutations of two key lipolysis genes *atgl-1* and *lid-1* lead to LD appearance in neurons of *Caenorhabditis elegans*. This lipid accumulation protects neurons from hyperactivation-triggered neurodegeneration, with a mild decrease in touch sensation. They also claimed that reduced biosynthesis of polyunsaturated fatty acids (PUFAs) causes similar effects and synergizes with decreased lipolysis. Furthermore, they

demonstrated that reduced incorporation of PUFAs into phospholipids increases neuronal protection. These findings suggest that lipolysis has a crucial role in cell-autonomous regulation of neural functions and neurodegeneration (L. Yang et al., 2020), most probably by supplying an extra amount of energy.

LDs have also been shown to accumulate in tumors, such as astrocytomas (Rémy et al., 1997; Zoula et al., 2003), in the brains of patients with AD (Derk et al., 2018; Gómez-Ramos & Morán, 2007; L. K. Hamilton et al., 2015) as well as in patients with PD, where LDs may be the sites of α-synuclein aggregation (Colebc et al., 2002). Moreover, LDs have been linked to MN diseases, including multiple sclerosis (Grajchen et al., 2018; Ponath et al., 2017), hereditary spastic paraplegia (Fowler et al., 2019; Papadopoulos et al., 2015; Renvoisé et al., 2016) and ALS (Chaves-Filho et al., 2019; Pennetta & Welte, 2018; Velebit et al., 2020).

Several studies interested in lipid metabolism have elucidated the connections between LDs and ALS pathology (Pennetta & Welte, 2018). For instance, mutations in the human VAMP-associated protein B (hVAPB) can cause ALS, with a disease-causing mechanism that is still unclear (Sanhueza et al., 2015). In this study, researchers performed a genome-wide screen in Drosophila to identify pathways involved in hVAPB-induced neurotoxicity and found that the list of modifiers was rich in proteins involved in LD dynamics. One of the reported modifiers was acyl-CoA synthetase long-chain (Acsl). This enzyme promotes LD biogenesis and its downregulation results in decreased size and number of mature LDs (Kassan et al., 2013). Furthermore, another group showed that gain of function mutations in the LD protein seipin promotes motor neuron disease symptoms in mice (Yagi et al., 2011; Sanhueza et al., 2015). Together these studies suggest that impaired LD biogenesis may be an important pathological aspect of hVAPB-mediated ALS.

A mutation in the gene SPG11 may also contribute to an early onset form of ALS affecting lysosome recycling (Branchu et al., 2017a). It is known that an intracellular lipid accumulation is followed by lipid clearance from lysosomes into droplets in wild-type (WT) mice. However, in Spg11 knockout mice, the rate of lipid clearance is slower, and LDs show a significant decrease in size and number (Branchu et al., 2017a). In another study, investigators found that loss of C9orf72 led to an increase in LDs, and that starvation-induced changes in lipid metabolism were mediated by coactivator-associated arginine methyltransferase (CARM-1). Since CARM-1 regulates lysosomal function and lipid

metabolism, these results suggest that the dysregulation of lipid metabolism, including the aberrant accumulation of LDs, could contribute to ALS pathology (Farmer et al., 2020).

LDs and peroxidation have been linked to AD; similarly, there also appears to be a connection between LDs and cellular stress in ALS. In Drosophila, ROS accumulation increased glial LD content, and when glia was unable to produce LDs, neuroblasts experienced peroxidative damage (Bailey et al., 2015). Also, a link between LDs, lipid peroxidation and ALS has also been proposed by Simpson and colleagues, showing a positive correlation between lipid peroxidation markers in ALS patient cerebrospinal fluid and disease burden (Simpson et al., 2004). Thus, LD dynamics may contribute to ALS. The mechanism that underlies pathological modifications may involve a context in which glial cells are unable to protect neurons through normal lipid accumulation and storage mechanisms (Pennetta & Welte, 2018).

A further link between ALS and disrupted organismal lipid metabolism is suggested by emerging data on TDP-43 function. As previously stated, TDP-43-mediated ALS may be caused by loss of its normal function, gain of new toxic functions, or possibly a combination of both mechanisms (Polymenidou & Cleveland, 2017; Robberecht & Philips, 2013). In TDP-43-overexpressing mice neurological symptoms, motor deficits, increased fat accumulation, and adipocyte hypertrophy have been detected (Stallings et al., 2013). On the other hand, TDP-43 depletion postnatally in mice causes weight loss, body fat reduction, decreased adipocyte LD content, increased FA consumption, and rapid death (Chiang et al., 2010). A mechanistic base for these crucial physiological changes has been proposed, involving lipid metabolism. In skeletal muscles, TDP-43 depletion determines a blockage in insulin-induced trafficking of the glucose transporter Glut4 to the plasma membrane, through the downregulation of TBC1D, a Rab-GTPase activity. As a consequence, the impairment of glucose uptake leads to a metabolic switch towards lipids consumption for energy production. The augmented fatty acids oxidation in the skeletal muscle can possibly explain the increased fat mobilization from the adipose tissue (Chadt et al., 2008). TBC1 could directly influence fat storage, considering that the related isoform AS160/TBC1D4 is involved in the regulation of both Glut4 translocation and LD generation in adipocytes (L. Wu et al., 2014).

Interestingly, in a yeast model for ALS, TDP-43 toxicity is worsened by seipin depletion (Armakola et al., 2012). Seipin is a homo-oligomeric integral membrane protein in the ER with a crucial role in LD biogenesis; it has been linked distal hereditary motor neuropathy

type V (dHMN-V) and Silver syndrome, two motor disorders (Welte, 2015).Therefore, LDs production seems protective in this context.

The hVAPB/ALS8 gene also controls Glut4 trafficking in myoblasts and adipocytes, affecting LD size, number, and composition (Al-Anzi et al., 2015; Foster et al., 2000; Jansen et al., 2011). It has been found that mutations in genes which are involved in LD biogenesis and dynamics modify ALS8 phenotypes in flies (Sanhueza et al., 2015), while in *C. elegans* and mice, VAPB depletion determines LD accumulation in muscles (Han et al., 2013).

In humans, spatacsin mutations induce slowly progressive juvenile-onset autosomal recessive ALS. Spatacsin is a 2443-amino acid protein codified by the SPG11 gene, which interacts with proteins involved in membrane-trafficking. Examination of the cellular alterations observed in *Spg11* knockout mice suggests that the loss of spatacsin leads to the accumulation of lipids in lysosomes by perturbing their clearance from these organelles (Branchu et al., 2017). Thus, the existence of a potential link between lysosomal dysfunction, lipid metabolism and neurodegeneration has been demonstrated, pinpointing a critical role of spatacsin in lipid turnover (Branchu et al., 2017).

A metabolic switch from glucose toward lipids is also emerging in the G93A SOD1 mouse model of ALS. Indeed, their spinal cord neurons display decreased glucose usage (Miyazaki et al., 2012) while a fat-rich diet is able to restore normal body mass, delays disease onset and MN degeneration, and extends life expectancy (Schmitt et al., 2014). The switch toward lipids usage in SOD1 mice is further suggested by the fact that denervation of glycolytic muscle fibers is subsequent to the increased expression of lipid-handling genes (Palamiuc et al., 2015).Thus, an increase in fatty acids requirements could be the reason why hyperlipidemia displays a positive correlation with survival in ALS patients in addition to increased circulating levels of ketone bodies (KBs) (Schmitt et al., 2014). In line with these findings, an investigation carried out in our laboratory, has globally shown a sex-specific benefit of dietary docosahexaenoic acid (DHA) supplementation in the G93A ALS mouse model, compared with mice fed an isocaloric control or a n-3 fatty acids depleted diet (Torres et al., 2020). These changes were associated with an increased DHA concentration in the LSC and were compatible with *in vitro* results showing DHA neuroprotective properties. These results suggest the need for further study on the interaction of gender-influenced biological parameters and DHA in ALS pathogenesis (Torres et al., 2020).

Recapitulating, several emerging findings correlates ALS to systemic impairment of lipid metabolism; nevertheless, further investigation is needed to establish whether LD defects contribute to ALS pathology or have a more direct causative role. In this regard, Pennetta and Welte have proposed that LD dysfunction in various peripheral organs could suppress the physiological energy delivery to neurons and muscles (Figure 20A) (Pennetta & Welte, 2018). Additionally, LDs may have a protective role against oxidative injury in ALS due to mitochondrial dysfunction (Figure 20B). This is suggested by the finding of markers of lipid peroxidation in the cerebrospinal fluid of ALS patients, indicating that accumulation of these toxic molecules could be involved in ALS pathology (Simpson et al., 2004; Smith et al., 1998).

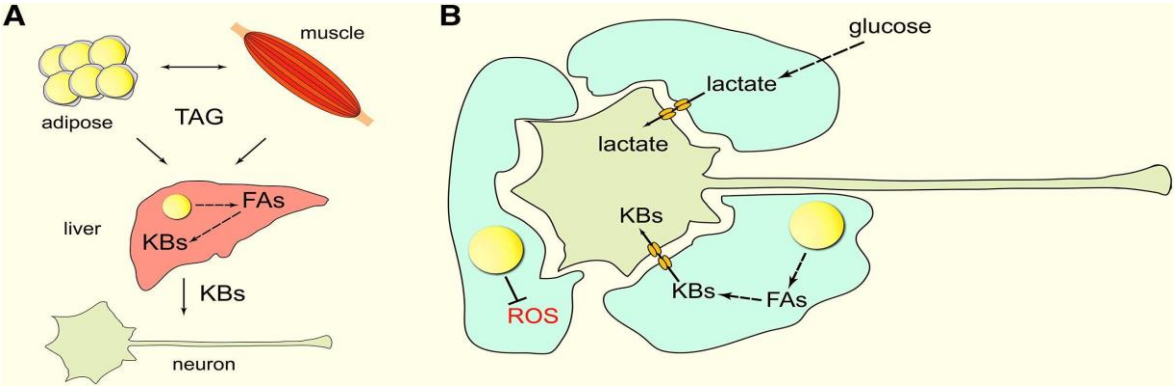

Figure 20. Lipid droplets in peripheral organs and in glia can affect motor neuron diseases. (A) TAGs are enclosed in LDs in adipose tissue, muscle, and liver and can be exchanged between these tissues via the bloodstream. In the liver, FAs can be generated from TAGs and converted into KBs. KBs travel through the blood to neurons, where they are used as energy substrates. **(B)** Glial cells convert glucose into lactate that is then transferred to neurons as energy substrates. FAs in glial LDs are metabolized into KBs that are also transferred to neurons and used as energy substrates. LDs in glia also show a protective role against oxidative stress due to ROS. (Adapted from Pennetta & Welter, 2018).

HYPOTHESIS

HYPOTHESIS

The correct balance between production and degradation of proteins (proteostasis) is pivotal for the health and survival of cells. Proteostasis is maintained thanks to an intricate network of protein quality control pathways that aim to prevent protein aggregation and maintain proteome health. Collapse of proteostasis has been implicated in the etiology of a number of neurodegenerative diseases, including ALS. Strong evidence links dysfunctional proteostasis to the etiology of ALS; this is especially true for proteins such as TDP-43, which aggregates as a consequence of impaired proteostasis in MNs, this feature being a well-recognized hallmark of ALS. Many kinds of cellular stress have been related to proteostasis alteration in ALS. In this work we focus on the effects that the induction of oxidative, proteasomal, ER and mitochondrial stresses exert on the distribution of important proteins, namely p-TDP43, p-ERK, p-JUN and REST, within the nuclear, cytoplasmic, and mitochondrial compartments of a cell.

Firstly, we hypothesize a direct relationship between cellular stress and protein mislocalization/ redistribution, including potential interactions with mitochondria.

Secondly, we theorize the association of stress-induced mislocalization of TDP-43 is associated with changes in REST-regulated genes and a significant effect of cellular stress on mitochondrial dynamics.

Moreover, we propose that metabolic challenges can produce a heterogeneous response in mitochondrial impairment in cellular lines carrying different TDP-43 mutations.

Finally, we postulate that mitochondrial impairment upon cellular stress is related to changes in LDs dynamics, both in neuronal and glial cells. Particularly, we speculate a protective role for LDs accumulation in these cells upon stress insult.

OBJECTIVES

OBJECTIVES

In order to contrast the above-mentioned hypotheses, we set the following research objectives.

1. To set up a high content screening system, based on immunofluorescence (IF) and computerized analysis of confocal microscope images, to evaluate alterations in protein mislocalization/redistribution and colocalization with mitochondria, following the induction of ALS-related stresses. These analyses were conducted in the nonneuronal HMEC-1 cell line.

2. To validate the results derived from the completion of objective 1 in the subcellular fractionation brains derived from TDP-43 ^{Q331K} mice overexpressing the human mutated TDP-43 gene

3. To investigate on the potential link between cell stress-induced mislocalization of TDP-43 and changes in REST-regulated genes.

4. To establish a potential relationship between cellular stresses and alterations in mitochondrial dynamics, by the mean of computerized analyses of mitochondrial and mitochondrial networks abundance in HMEC-1 cells.

5. To characterize mitochondrial impairment in MEFs carrying different ALS-related TDP-43 mutations upon the induction of metabolic acute stress based on glucose/galactose switch and pyruvate deprivation.

6. To establish the potential link between mitochondrial dysfunction and alteration in LDs dynamics in the above mentioned MEFs and in Neuro-2A cell line upon the induction of osmotic stress, which we had previously related to TDP-43 cytoplasmic mislocalization and aggregation.

7. To explore LDs dynamics in a Sprague-Dawley primary astrocyte culture, upon the exposure to oleic acid (a potent inducer for LDs accumulation) and oxidative or osmotic stresses.

MATERIALS AND METHODS

2. MATERIALS AND METHODS

2.1 Human samples

Samples derived from post-mortem tissue were kindly donated by the Tissue Bank of Neuropathology Institute of Bellvitge Hospital (Isidro Ferrer Abizanda. MD. PhD, Pathological Anatomy Service, University of Barcelona, Bellvitge Campus) accordingly to the ethical rules of the institutional Committee for Clinical Investigation, the World Medical Association, and the quality assessment criteria of the sample. These samples belonged to 4 patients who received a sALS diagnosis based on neurological and neuropathological features (Johnsen et al., 2019). Control samples derived from control individuals without any clinical evidence of the illness and with a normal neuropathological profile, were processed in parallel. Patients or their legal representatives signed an informed consent giving permission for samples storage and analysis. For ALS diagnosis, several pathological studies were carried out (Ilieva et al., 2007). Brains were rapidly removed, frozen in dry ice and stored at -80ºC until use. Table 1 contains a resume of the features of patients and controls.

Table 1. Features of patients and controls

Sex	Age at death	Diagnosis	Origin of the disease
M	64	ALS	Bulbar
M	68	ALS	Bulbar
M	59	Control	-
M	62	Control	-

2.2 Cell lines and cell culture conditions

For this study, different cell lines were employed to carry out the experiments. Furthermore, a cortical rat astrocytes primary cell culture was set up for LipidTOX™ staining experiments. Details of each one and their maintenance can be found below.

2.2.1 HMEC-1

HMEC-1 cells are normal human mammary epithelial cells isolated from reduction mammoplasty tissue. This cell line (HMEC-1) was purchased from the ATTC® (Cat.#CRL 3243) and was grown in DMEM high glucose (Gibco™, Cat.# 41966029) supplemented with 10% fetal bovine serum (FBS), heat inactivated and penicillin/streptomycin (P/S) (Gibco™, Cat.#15140122) as antibiotics to prevent bacterial contamination.

2.2.2 SH-SY5Y

Originally derived from a human metastatic bone tumor biopsy, SH-SY5Y (ATCC® CRL-2266™) cells are a subline of the parental line SK-N-SH (ATCC HTB-11™). SK-N-SH were subcloned three times; first to SH-SY, then to SH-SY5, and finally to SH-SY5Y. SH-SY5Y cells were deposited to the ATCC® in 1970 by June L. Biedler (Kovalevich & Langford, 2013).

The culture medium was DMEM (Gibco, Invitrogen) supplemented with 4.5g/L glucose, 2mM glutamine, 10% fetal bovine serum heat inactivated and P/S (GibcoTM, Cat.#15140122) as antibiotics to prevent bacterial contamination.

2.2.3 Neuro-2A

Neuro-2A is a mouse neural crest-derived cell line that has been extensively used to study neuronal differentiation, axonal growth and signaling pathways. Cells show neuronal and amoeboid stem cell morphology (Tremblay et al., 2010).

Culture medium: Advanced MEM (GibcoTM Cat.# 12492013) supplemented with 10% fetal bovine serum, heat inactivated and P/S (GibcoTM, Cat. #15140122) as antibiotics to prevent bacterial contamination. Moreover, PlasmocinTM (InvivoGen, Cat. ant-mpp) was used prophylactically at concentration of 5 µg/ml to prevent mycoplasma contamination. Cells were maintained in 100mm Petri-dishes and split each 2-3 days in a 1:10 ratio. Subsequent incubation was carried out in a 37°C incubator supplemented with 5% CO_2.

2.2.4 HEK-293

HEK-293 cell line and its derivatives are widely used in cellular biology and biotechnology. HEK293 cells derived from human embryonic kidney cells grown in tissue culture. They are informally known as HEK cells. This particular line was initiated by the transformation and culturing of normal HEK cells with sheared adenovirus 5 DNA. The transformation resulted in the incorporation of approximately 4.5 kilobases from the viral genome into human chromosome 19 of the HEK cells. The line was cultured by scientist Alex Van der Eb in the early 1970s at his lab at the University of Leiden, Holland. The transformation was executed by Frank Graham, another scientist Van der Eb's lab. The source of the cells was a healthy aborted fetus of unknown parenthood. The name HEK293 is thusly named because it was Frank Graham's 293rd experiment (Toth & Wold, 2002).

The culture medium was DMEM supplemented with 4.5g/L glucose, 2mM glutamine, 10% fetal bovine serum heat inactivated and P/S (Gibco™, Cat.#15140122) as antibiotics to prevent bacterial contamination. Cells were maintained in 100mm Petri-dishes and split each 2-3 days in a 1:10 ratio. Subsequent incubation was carried out in a 37°C incubator supplemented with 5% CO_2.

2.2.5 Mouse embryonic fibroblasts

Wild-type *Tardbp* mouse embryonic fibroblasts (MEFs) and their knock-in counterpart carrying the *Tardbp* M323K, F210I and Q331K pathogenic variants were kindly provided by Abraham Acevedo (Hospital Universitario de Canarias, Fundación Canaria de Investigación Sanitaria FUNCANIS). Immortalization of the four cell lines was induced using simian virus 40 (SV40).

Cells were growth in DMEM supplemented with 4.5g/L glucose, 2mM glutamine, 10% fetal bovine serum heat inactivated and P/S (Gibco™, Cat.#15140122) as antibiotics to prevent bacterial contamination. Cells were maintained in 100mm Petri-dishes and split each 2-3 days in a 1:10 ratio. Subsequent incubation was carried out in a 37°C incubator supplemented with 5% CO_2.

2.2.6 hiPS cell-derived motor neurons

Human induced pluripotent stem cells (hiPSCs) were obtained from NINDS Human Genetics DNA and Cell line Repository at Coriell Institute which bearing FUS mutation (C.G1566A [P.R522R], Cat.#ND35663), C9ORF72 expansion ([GGGGCC]n, Cat.#2765), and Cat.#ND41865 control cell line. The different media compositions can be found in Table 2. Consequently, hiPSCs were grown in standard human embryonic stem (ES) cell media supplemented with 6 ng/ml basic fibroblast growth factor on in-activated mouse embryonic fibroblasts (Sigma) as feeder cells. Differentiation towards motor neurons was carried with a modification of the Du et al. protocol (Du et al., 2015). Briefly, undifferentiated hiPSC cultures were digested with Accutase solution (Sigma-Aldrich) for 5 min, seeded for 40 min in mouse embryonic fibroblasts-conditioned hES media supplemented with 10μM Y27632 (Cayman Chemicals) to remove as many fibroblasts as possible, and then the cell suspension was transferred to Geltrex® (Thermo Fisher Scientific)-coated tissue culture dishes for 24–48 hr until stem colonies were visible.

Medium was then changed to neuroepithelial medium for 6 days and then replaced sequentially with motor neuron progenitor (MNP) medium the first, second, and sixth days.

At this point, progenitors were either expanded on MNPs at the second day or further differentiated into neurospheres and MNs using MN induction medium and MN maturation medium, respectively. Non-tissue culture dishes without coating were used for neurosphere formation. Both neuroepithelial and MNPs were split into new Geltrex®-coated dishes when 70%-100% confluent and seeded at 50,000–75,000 cells/cm^2 using Y27632 10μM during the first 24 hr. Media was changed every other day. After 6 days in MN induction media, neurospheres were collected in 15 ml centrifuge tubes and spun for 3.5 min at 0.1g; the supernatant was discarded, and the spheres digested for 5-7 min in Accumax solution (Sigma). Cell clusters were disaggregated pipetting until a homegenous single cell suspension was obtained. Cells were then washed with DMEM/F12 (Thermo Fisher Scientific) and re-suspended for seeding in MN maturation media supplemented with Y27632, laminin (2.5 μg per 1 ml of media; Thermo Fisher Scientific) and 0.1 μM Compound-E (Stem Cell Technologies). After plating in poly-L-lysine (Sigma) coated dishes, media was replaced every 72 hours. Seeding density was maintained at 50,000–100,000 cells/cm^2.

Table 2. Media used for human motor neuron differentiation from iPSC.

Component / Media	**NEPM**	**MNP medium 1st**	**MNP media 2nd**	**MN induction medium**	**MN maturation media**
DM/F12	20 mL	20 mL			
Neurobasal	20 mL	20 mL			
Neurobasal +			40 ml	40 ml	40 ml
B27+ supplement	800μL	800μL	800μL	800μL	800μL
Ascorbic acid	0.1 mM	0.1 mM	0.1 mM	0.1 mM	0.1 mM
L-Glutamine solution (Thermo Scientific, Cat.#25030024)	1:200	1:200	1:200	1:200	1:200
Non-essential amino acids solution (Sigma, Cat.# M7145)	1:100	1:100	1:100		
CHIR	3 μM	1 μM	3 μM	3 μM	

Component / Media	NEPM	MNP medium 1st	MNP media 2nd	MN induction medium	MN maturation media
SB43	2 µM	2 µM	2 µM	2 µM	
DMH1	2 µM	2 µM	2 µM	2 µM	
Retinoic acid		0.1 µM	0.1 µM	0.5 µM	0.5 µM
Purmorphamine					
Valproic acid			0.5 mM		
Compound E					0.1 µM
CNTF					20 ng/ml
IGF1					20 ng/ml
Penicillin/Streptromycin (Thermo Scientific Cat.#15140122)	1:400	1:400	1:400	1:400	1:400

For all cell lines used in this study, Plasmocin™ (InvivoGen, Cat.# ant-mpp) was used prophylactically at concentration of 5 µg/ml g/ml to prevent mycoplasma contamination. Cells were maintained in 100mm Petri-dishes and split each 2-3 days in a 1:10 ratio. Subsequent incubation was carried out in a 37°C incubator supplemented with 5% CO_2.

2.3 Primary cell culture

2.3.1 Primary rat cortical astrocyte culture

Astrocytes cultures were obtained from brain cortical tissue of 1 day-old Sprague-Dawley rats. At least 4 pups are used for each culture. Pups were subjected to decapitation and subsequent brain extraction. Brain structures were separated under a under a stereomicroscope. In order to retrieve the cortices, the posterior end of the brain was grabbed with the fine forceps, a midline incision between the hemispheres was performed, a second set of forceps was inserted to the created grove in order to peel away the plate-like structure of the cortex from the brain. The meninges were carefully dissected from the cortex hemispheres by pulling with the fine forceps. This step avoids contamination of the final astrocyte culture by meningeal cells and fibroblasts. Finally, each cortex hemisphere was cut into small pieces using sharp blades (approximately 4 to 8 times).The prepared cortex hemispheres were transferred to a solution made of 35 mL of calcium-free Krebs Ringer Buffer (KRB), 120 mM NaCl, 4.8 mM KCl, 1.2 mM KH_2PO_4,

25 mM $NaHCO_3$, 14,3 mM glucose, 0.03% Mg_2SO_4 and 0,03% bovine serum albumin (BSA). Brain tissue was centrifuged at 300g for 1 minute and the resulting supernatant was discharged. After this, 10 mL of calcium-free KRB solution containing 0.025% of trypsin were added to the cells following incubation at 37 ºC for 10 minutes to allow tissue dissociation. In order to inhibit trypsin digestion, 10 mL of calcium free KBR supplemented with 0.052% of soybean trypsin inhibitor (Gibco™, Cat.# 17075029), 0.008% DNase (Thermo Fisher, Cat.# 90083) and 0.03% extra of Mg_2SO_4 were added. Next, the cells were centrifuged for 1 minute at 300 g, the supernatant was discharged, and the cells were resuspended in 5 mL of KRB buffer. The cells were physically disaggregated using a glass pipette and filtered through a 40 µm nylon mesh. The obtained cells were centrifuged for 5 minutes at 250 g. Supernatant was removed and cells were resuspended in DMEM medium (GibcoTM, Cat.# 41966029) supplemented with 10% Fetal Bovine Serum (FBS), 20U mL^{-1} penicillin and 20 µg mL^{-1} streptomycin.

The cells were resuspended in Trypan Blue solution (0.4% liquid, Cat.# T8154, Sigma-Aldrich) and counted in a Neubauer chamber. Astrocytes were seeded at 300.000 cells/ mL in T150 flasks and incubated at 37ºC with 5% of CO_2 in a humified atmosphere. The growth medium was changed at 3 hours after seeding in order to diminish oligodendrocyte and microglial growth. After this first change, medium was changed every 7 days, until confluency. Then, the flasks were agitated on a mechanical shaker at 400 rpm during 3 hours in order to eliminate superficial microglia. Cells were washed twice with phosphate buffered saline (PBS) containing 2.5 mM KCl, 136.87 mM NaCl, 1.47 mM K_2HPO and 40.8 mM NaH_4PO_4 at a pH 7.4, supplemented with 20 U mL^{-1} penicillin and 20 µg mL^{-1} streptomycin. Then, 3 mL of trypsin/EDTA (Sigma, Cat.# T4049-100ML) were added to each flask and incubated for 5 minutes at 37º C. Flasks were shaked manually to improve detachment and DMEM medium was added to stop trypsin action. Cells were harvested and centrifuged at 250 g for 5 minutes; the supernatant was removed, and cells were seeded at a density of 40,000 cells/well in 12-well plates or at a density of 250,000 cells/well in 6-well plates. Cells were incubated at 37ºC with 5% of CO_2 in a humified atmosphere.

2.4 Cell culture treatments

2.4.1 Cellular stress-inducing treatments

In this study we carried out a series of treatments aiming to clarify the linkage between different cellular stresses and protein mislocalization. Tables 3 and 4 enclose a detailed description of experimental treatments.

Table 3. Cell lines and treatments

Type of stress	Reagent	Doses	Time of treatment	Cell line
Oxidative stress	Hydrogen peroxide	40 µM	30 minutes	HMEC-1
		200 µM	60 minutes	
Endoplasmic reticulum stress	Thapsigargin	5µM	2 hours	HMEC-1
			4 hours	
Osmotic stress	Sorbitol	400 mM	3 hours	HEK-293
		400 mM	3 hours	SHSY5Y
		400 mM	0.5 hours	Neuro2A
			1 hour	
			1.5 hours	
			2 hours	
			2.5 hours	
			3 hours	
Proteasome inhibition	Epoxomicin	2.5µM	4 hours	HMEC-1
			2 hours	
Mitochondrial stress	Rotenone	4µM	4 hours	HMEC-1
			2 hours	

Table 4. Primary rat cortical astrocyte culture treatments

Type of stress	Reagent	Doses	Time of treatment
Oxidative stress	Hydrogen peroxide	10 µM	2 hours
			4 hours
Osmotic stress	Sorbitol	400 mM	3 hours

Table 5. hiPS cell-derived motor neurons treatments

Type of stress	Reagent	Doses	Time of treatment
Osmotic stress	Sorbitol	400 mM	3 hours

2.5 Microscopy

2.5.1 Immunofluorescence microscopy

In this study, indirect immunofluorescence was performed to assess both the localization and endogenous expression levels of proteins of interest. In this technique, a secondary fluorophore-coupled antibody, which specifically binds to the primary antibody, is used to visualize the structure of interest.

2.5.1.2 Confocal fluorescence microscopy

For microscopy, 50,000 cells were seeded on glass coverslips. After treatments, cells were rinsed 3 times with pre-warmed PBS and fixed with 3.7% formaldehyde in PBS for 10 minutes at room temperature. Following this, cells were permeabilized with Triton X-100 (0.1% (v/v) in PBS) for 30 minutes at room temperature. In the next step, cells were blocked in a solution of 5% normal goat serum (NGS) for 1 hour at room temperature. After that, cells were incubated overnight at 4º C with the suitable primary antibodies dissolved in PBS, in a humid chamber. After this period, cells were rinsed with 1x PBS and were incubated with the appropriate secondary antibody along with DAPI (Sigma, Cat# D9542) at 1µg/mL, 15 minutes at room temperature, to stain nuclei. Lastly, cells were washed submerging the coverslips briefly in PBS, twice and blotting them on filter paper to remove the excess buffer. Coverslips were mounted in Fluoromount-G solution (0100-01, Southern Biotech, Birmingham, AL, USA) on glass slides and allowed to dry at room temperature for 30 minutes before storing them at 4º C in the dark until imaging.

Confocal microscopy images were acquired with an Olympus FV10i laser scanning confocal microscope or an Olympus FV1000 confocal microscopy, 60x magnification. For the evaluation of nuclear and cytosolic protein intensity as well as for the quantification of protein colocalization with the mitochondria, we employed a dedicated pipeline created on the open-source software Cell Profiler 2.1.1 for Windows (Kamentsky et al., 2011). Ten fields per condition were analyzed. In table 6 the primary and secondary antibodies used in the immunofluorescence experiments are listed. Figure 21 shows some representative output images produced by Cell Profiler algorithm. This pipeline can be downloaded from Mendely data (Rossi, Chiara (2022), “CellProfiler pipeline for confocal images analysis_1”, Mendeley Data, V2, doi: 10.17632/235yr4pkr8.2).

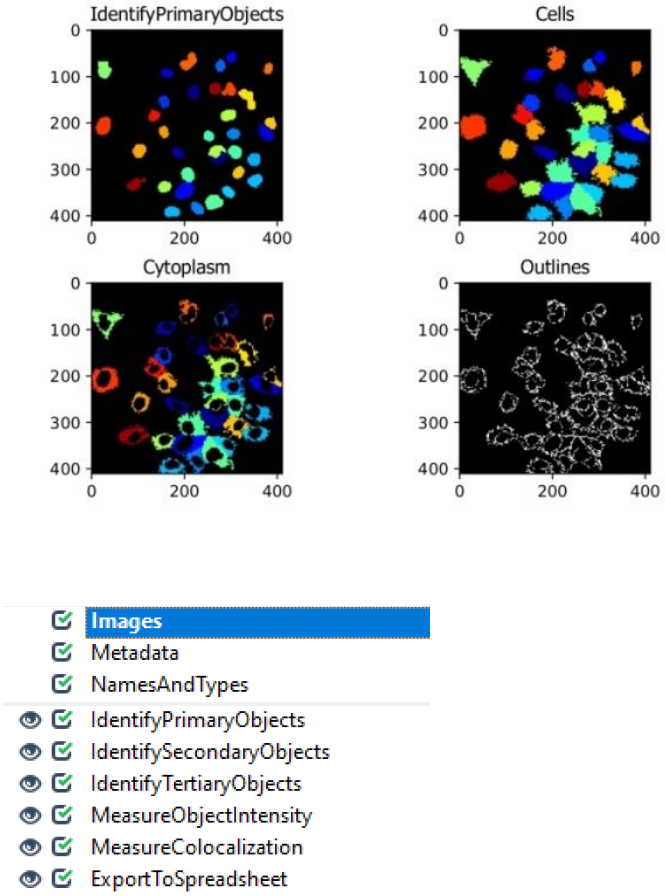

Figure 21. Cells profiling workflow using the Cell Profiler software. Cells components are identified as primary objects starting from DAPI stained nuclei as an input to identify cell body (secondary objects) and cytoplasm (tertiary object) by propagation and segmentation. Once cellular components have been correctly depicted, the software is able to perform a series of measurements such as immunostaining intensity or channels overlapping to estimate protein colocalization.

Table 6. Primary and secondary antibodies used in immunofluorescence experiments

Antibody	Dilution in PBS	Purchased from	Catalogue number
TDP43	1:200	Proteintech	10782-2-APS
p-TDP43 (pS409/S410)	1:200	Cosmo Bio Co.	TIP-PTD-M01
p-JUN	1:100	Cell Signaling	9164
REST/NSRF	1:100	Abcam	ab21635
p-ERK 1/2	1:100	Cell Signaling	4370
ATP-5A	1:100	Abcam	ab14748

Antibody	Dilution in PBS	Purchased from	Catalogue number
AGPS	1:100	Santa Cruz	SC-374201
NDUFS3	1:100	Invitrogen	459130
Alexa Fluor-488 goat anti-rabbit IgG	1:800	Molecular Probes	A32742
Alexa Fluor-546 goat anti-mouse IgG	1:800	Molecular Probes	A11030

2.6 Analysis of mitochondrial network morphology changes

Analysis of mitochondrial network morphology changes was performed using the macro MiNa (Mitochondria Network Analysis) for ImageJ (Valente et al., 2017). After cellular stress-inducing treatments performed on HMEC-1 cells (see Table 2 for details), mitochondrial immunofluorescence staining of the mitochondrial epitope ATP5A and confocal microscopy imaging as previously described in section, images were processed by the MiNa workflow in order to estimate the number individual mitochondria and mitochondrial networks. All the analyses were carried out on 60X confocal images, selecting a region of interest (ROI) containing an equal number of cells, for each microscopy field.

2.7 Protein immunodetection

2.7.1 Protein extraction from cultured cells

Cellular lysates were obtained after treating cells and analyzed by western blot after electrophoresis, under denaturalizing conditions. Treatments were carried out in 6-wells plate to obtain a suitable protein yield to be detected by western blotting. At the end of the treatment period, culture medium was aspired, and the plate was put on ice. Cells were washed 3 times with ice-cold PBS to discard medium proteins. Subsequently, 350 µL of RIPA lysis buffer supplemented with protease and phosphatase inhibitors (Thermo Scientific Cat.#78440) were pipetted in each well and cells were harvested by scraping. The resulting lysate was transferred to an eppendorf tube and sonicated for 1 minute to disrupt cellular membranes and release the cells contents. Samples were stored at -20º C until analysis.

2.7.1.2 Protein quantification and preparation for SDS-PAGE

Protein quantification was carried out with the Quick Start™ Bradford Protein Assay (BIO-RAD, Cat.#500-0006).

The exact protein concentration of the sample was determined by interpolation from a standard curve made by measuring the absorbance of a dilution series of protein standards of known concentrations within the linear response range of the Bradford protein assay. Bovine serum albumin (BSA) was used as a standard. Sample concentration was equalized with MilliQ water followed by the addition of loading buffer (Tris-HCl 62.5 mM pH 6.8; SDS 2% (w/v); Glycerol 10% (v/v); 2-β-mercaptoethanol 20% (v/v) and blue bromophenol 0.02% (w/v). Samples were stored at -20ºC until analysis.

2.7.1.2.3 Western-Blot analysis

Protein samples, prepared as described above, were run on SurePAGE™ Precast gels (4–20%, 15 wells GenScript, Piscataway, NJ, USA). Gels were blotted onto PVDF membranes by transfer at a constant 100 volts, 1 h at RT. The membranes were then blocked by non-fat dry milk solution (5%) in 1x TBS (Tris Buffered Saline) and incubated in the desired primary antibody overnight.

Membranes were then washed in 1x TBST with Tween 20 (0.05%) three times, 5 min each before incubating with the appropriate secondary antibody for 1 h at room temperature. Following the secondary antibody incubation, membranes were washed in 1x TBST with Tween 20 (0.05%) three times, 5 min each and one final time, 5 min, with TBS 1x. Blots were incubated in the Immobilon ECL Ultra Western HRP Substrate (Merck Millipore, Burlington, NJ, USA). A Chemidoc MP Imaging System (Biorad, Hercules, California, USA) was employed to reveal chemiluminescence.

For Jun/ p-c-Jun Westerns, protein samples were run on SurePAGE™ Precast gels (4–20%, 15 wells GenScript, Piscataway, NJ). Cruz Marker™ molecular weight standards (sc-2035, Santa Cruz Biotechnologies, Dallas, TX, USA) were loaded in the gels. Gels were blotted onto low fluorescence PVDF membranes (Immobilon®-FL PVDF: sc-516541). Nonspecific binding was blocked in incubating membranes with UltraCruz® Blocking Reagent (sc-516214) for 1 h at room temperature, with shaking.

In this case, the blocked membranes were incubated with the appropriates Alexa Fluor® conjugated primary antibodies (Anti-p-c-Jun Antibody (KM-1) Alexa Fluor® 790 and Anti c-Jun Antibody (G-4) Alexa Fluor® 680, from Santa Cruz) diluted 1:1000 in UltraCruz® Blocking Reagent. Cruz Marker™ MW Tag-Alexa Fluor® 680 (sc-516730) and Cruz Marker™ MW Tag-Alexa Fluor® 790 (sc-516731) at 1:1000 were added to obtain molecular weight distribution.

Membranes were incubated in this mixture for 2 h at room temperature, in the dark, with shaking. Membranes were then washed three times for 5 min each with TBST and once for 5 min with TBS. Blots when then placed on the top of blotter paper and dried for 5–10 min. The western blot was imaged using the infrared (IR) laser-based instrumentation LI-COR Odyssey (Lincoln, NE, USA). Coomassie Brilliant Blue staining was utilized as a control to assess total protein loading.

Table 7 shows the primary and secondary antibodies used in immunodetection by Western Blot analysis.

Table 7. Primary and secondary antibodies used in Western Blot

Antibody	Dilution in PBS	Purchased from	Catalogue number
TDP-43	1:1000	Proteintech	10782-2-APS
p-TDP-43	1:1000	Cosmo Bio Co.	TIP-PTD-M01
p-ERK 1/2	1:2000	Cell Signaling	4370
c-JUN Alexa Fluor® 680	1:0000	Santa Cruz Biotechnology	KM-1
p-c-JUN Alexa Fluor® 790	1:0000	Santa Cruz Biotechnology	G-4
REST/NSRF	1:1000	Abcam	ab21635
Mitofusin-2	1:1000	Sigma	M6319
Porin	1:1000	Abcam	ab15895
Histone H3	1:1000	Sigma	SAB4500352
GAPDH	1:5000	Thermo Fisher Scientific	MA5-15738

2.8 Reverse transcriptase quantitative PCR (RT-QPCR)

RNA was extracted from cells and brain lysates using TRI Reagent (Thermo Fisher Scientific, Waltham, MA, USA, AM9738) following the manufacturer's instructions. RNA concentrations were measured using a NanoDrop ND-1000 (Thermo Fisher Scientific). One microgram of RNA was used for retrotranscription to cDNA employing TaqMan Reverse Transcription Reagent and random hexamers (Thermo Fisher Scientific, N8080234).

RT-qPCR experiments were performed using a CFX96 instrument (Bio-Rad, Hercules, CA, USA) with SYBR Select Master mix for CFX (Thermo Fisher Scientific, #4472937).

Each 20 µL reaction mix contained 4-µL cDNA, 10-µL SYBR Select Master Mix, 0.2 nM of forward primer and 0.2 nM of reverse primer solutions and 4-µL PCR grade water. RT-qPCR run protocol was as follows: 50 °C for 2 min and 95 °C for 2 min, with the 95 °C for 15 s and 60 °C for 1 min steps repeated for 40 cycles, and a melting curve test from 65°C to 95 °C at a 0.1 °C/s measuring rate. Primers employed in these experiments, previously described (Lu et al., 2014) are listed in Supplemental Table ST1 (Annex I).

2.9 Acute metabolic switch assay and flow cytometry analysis

Flow cytometry analysis was used in acute metabolic switch assay to detect mitochondrial toxicity in previously described knock-in MEFs. Briefly, MEFs were seeded on 12-well plates with 70,000 cells/wells in DMEM (Gibco™ Cat.# 11960044) supplemented with 2mM glutamine, 10% fetal bovine serum heat inactivated, sodium pyruvate 1mM and P/S at 20 µg/mL (Gibco™, Cat.#15140122) as antibiotics to prevent bacterial contamination. Cells were incubated in a 37°C incubator supplemented with 5% CO_2. After a period of 24 hours to allow cells attachment, MEFs were grown in either glucose or galactose-containing media. The galactose medium consisted of DMEM without glucose and sodium pyruvate (Gibco™ Cat.#11966025) supplemented with10mM galactose, 2mM glutamine, 10% fetal bovine serum and penicillin/streptomycin at 20 µg mL^{-1}.

After 6 or 12 hours, cells were harvested in 15 mL centrifuge tubes by trypsinization after recollecting the supernatant in order to retain floating dead cells. Then, cells were centrifuged at 1000 rpm for 4 minutes; the resulting supernatant was discharged while the pellet was resuspended in 250µL of PBS supplemented with 2% FBS and 50 nM Acridine Orange 10-Nonyl Bromide (NAO) (ThermoFisher Cat.#A1372). NAO is a green, fluorescent mitochondrial dye whose staining is not dependent on mitochondrial membrane potential, and it's used in order to measure changes in mitochondrial mass. Following resuspension, cells were transferred to flow cytometry tubes and incubated at 37ºC for 30 minutes. After this period, propidium iodide (Invitrogen, Cat.#P1304MP) was added to each cell sample at a concentration of 1.25µg/mL. Propidium Iodide (PI) is a standard reagent used for assessing cell viability and exclusion of non-viable cells in flow cytometry. PI binds to double stranded DNA but is excluded from cells with intact plasma membranes. Samples were incubated on ice, in the dark, for 10 minutes in order to achieve NAO/PI double staining. Next, samples were analysed using a FACS-Canto II digital flow cytometer (BD Biosciences, Franklin Lakes, New Jersey, USA). Controls for

this experiment were set consisting of non-stained cells as negative control, PI dead stained cells and OA stained cells as positive controls.

2.10 Seahorse XFp Real-Time ATP Rate Assay

Seahorse XFp Real-Time ATP Rate Assays (Seahorse, Agilent Technologies, Santa Clara, CA) were performed according to the manufacturer's protocol on an XFp instrument. One day prior to the assay, cells were seeded in Seahorse culture plates at a density of 12000 cells/ well in DMEM supplemented with 4.5g/L glucose, 2mM glutamine, 10% fetal bovine serum heat inactivated and P/S (GibcoTM, Cat. #15140122). For acute metabolic switch assay with the previously mentioned mouse embryonic fibroblasts (section 2.2.5), the day of assay, control cells normal growth medium (DMEM, Cat.#15140122) was replaced by fresh medium while, for experimental cells, normal growth medium was replaced by galactose medium as previously described for 6 hours (section 2.9).

At day of assay, XF assay medium was supplemented with 10 mM glucose, 1mM pyruvate, and 2mM glutamine and the pH adjusted to 7.4. XF medium was substituted to normal growth medium or treatment medium, in the case of metabolic switch assay, 1 hour before the Seahorse assay. Cell number per well was used for data normalization. After the assay, cells were stained with NucBlue™ Live ReadyProbes™ (ThermoFisher, Cat.# R37605) reagent and imaged under an Olympus IX71 inverted fluorescence and phase contrast microscope with a 10x air objective (NA 0.30). We then proceeded to cell counting and the resultant values were entered in the normalization section of the XF Real-Time ATP Rate template in the Seahorse Wave software.

2.11 Mitochondrial Transmembrane Potential and Complex I levels measurements

For Mitochondrial Transmembrane Potential assay, cells were seeded at a density of 50.000 per well on a 12 well plate. Cells were allowed to attach for 24 hours; after this period of time, the acute metabolic stress assay was performed as previously described (section 2.9). On the day of imaging, culture medium was removed, and cells were incubated with NucBlueTM Live Cell Stain ReadyProbesTM (Invitrogen, Cat.#R37605) and Image-IT™ TMRM Reagent (InvitrogenTM Cat.# 15656139) (100 nM) in Hank's Balanced Salt Solution (HBSS), 1X (Cat.#14025-092), for 45 minutes at 37ºC. Images of 10 fields per well were acquired under an Olympus IX71 inverted fluorescence and phase contrast microscope with a 20x air objective (NA 0.45). Images were analysed with a

dedicated pipeline created on the open-source software Cell Profiler 4.2.1 for Windows (Kamentsky et al., 2011) The pipeline was uploaded on Mendeley data (Rossi, Chiara (2022), “CellProfiler pipeline for confocal image analysis_4”, Mendeley Data, V1, doi: 10.17632/3g6f298wyr.1). Complex I levels in confocal images were estimated following the analysis with a dedicated pipeline on CellProfiler, which can be find on Mendeley data (Rossi, Chiara (2022), “CellProfiler pipeline for confocal image analysis_3”, Mendeley Data, V2, doi: 10.17632/p4g5zwz67r.2).

2.12 Caspase 3/7 activation assay

The examination of caspase 3/7 activation was performed on previously described MEFs following metabolic switch assay (section 2.9). Briefly, MEFs were seeded in a 12-wells plate format at a density of 70,000 per well in DMEM high glucose medium (Cat.#11965084, Invitrogen, Waltham, MA, USA) and metabolic switch assay was performed for 6 hours. After this, cells were stained with the CellEvent™ Caspase-3/7 Green ReadyProbes™ Reagent (ThermoFisher Scientific, Cat.# R37111) adding two drops of the reagent per mL of culture medium and incubating at 37 ºC for 30 minutes. Then, nuclei were counterstained with NucBlue™ Live ReadyProbes™ (ThermoFisher, Cat.# R37605) reagent and cells were imaged under an Olympus IX71 inverted fluorescence and phase contrast microscope with a 20x air objective (NA 0.45). Caspase-3/7 activation was estimated by calculating the ratio between green, fluorescent cells (apoptotic) and total cells (NucBlue™ stained nuclei).

2.13 Thin layer chromatography analysis for ACAT assay

Acyl-coenzyme A: cholesterol acyltransferase (ACAT) activity was measured as previously reported (Lada et al., 2004) in a method based in the conversion of the fluorescent 7-nitro-2-1,3-benzoxadiazol-4-yl-cholesterol (NBD-Chol) to its ester. Briefly, cells were seeded in a 12-wells plate format at the density of 70,000 per well in DMEM high glucose medium (Cat.#11965084, Invitrogen, Waltham, MA, USA,) supplemented with 10% fetal bovine serum, heat inactivated (Invitrogen), 2-mM L-Glutamine (Invitrogen) and 20-U/mL penicillin and 20-µg/mL streptomycin (Invitrogen). The cells were kept at 37 °C in humidify atmosphere with 5% of CO_2.

After 24 hours, cells were rinsed with warm PBS and incubated in serum and phenol red free medium (Opti-MEM™, Invitrogen, Waltham, MA, USA) for two hours before any treatment together with the administration of NBD-cholesterol (Molecular Probes, Eugene, OR, Cat.#N1148). For metabolic switch assay experiments with MEFs (section 2.2.6),

cells were incubated with glucose or galactose medium, as previously described (section). A stock solution of NBD-cholesterol (1mg/mL in ethanol) was employed to achieve a final concentration of 4µM. At the end of treatment, cells were washed twice with ice cold PBS and collected in a chloroform-methanol mixture (1:5 ratio) after shaking for 5 minutes. Tubes were then centrifuged 2 minutes, 13000 rpm, at 4º. Supernatants were collected in a new tube, while the resulting pellet was used to quantify total protein concentration by Bradford assay (Quick Start™ Bradford 1x Dye Reagent, Bio-Rad #5000205) after resuspension in RIPA buffer and addition of protease inhibitor (Cat #78429, Thermo Fisher Scientific, Waltham, MA USA).

Subsequently, 120 µL of 100% chloroform and 240µL of a 0.1% acetic acid solution in double distilled water were added to each supernatant, followed by vortexing for 60 seconds and centrifugation for 2 minutes (13,000 rpm at 4ºC), leading to formation of two phases. The lower (i.e. organic) phase was recollected and transferred in a new tube, while the upper was discarded. The lower phases were then dried by centrifugal evaporation under vacuum (Speedvac) for 30 minutes, resulting in a lipid pellet that was resuspended in 50 µL of a 2:1 chloroform/methanol mixture.

A 10 µL volume for each lipid samples was applied to a thin-layer chromatography (TLC) plate, (Merck Millipore, Kenilworth, NJ 07033 U.S.A. Cat. #Z740227-25EA) kept at 50ºC on a heat plate. NBD-Chol (Retention factor [RF]: 0.05) and esterified NBD-Chol (Retention factor: 0.18) were used as standards to confirm the migration patterns. Esterified NBD-Chol standard was obtained by the esterification of NBD Cholesterol. Briefly, we evaporated 500 microliters of 1 mM NBD-Chol solution (Molecular Probes, Eugene, OR, Cat.#N1148). Then, in a glass tube, we added 4 mg Chol (Sigma-Aldrich, Burlington, MA, United States, Cat.# C75209) 50 mg Oleic Anhidride (Sigma-Aldrich, Burlington, MA, United States, Cat.#75095) and 11 mg 4-Dimethylaminopyridine (Sigma-Aldrich, Burlington, MA, United States, Cat.# 107700). We resuspended the NBD Chol (Molecular Probes, Eugene, OR Cat.#N1148) in 2 mL of chloroform ($CHCl_3$) and added this to the tube with the remaining reactants. We heated at 80ºC for 30 min. For the development of the TLC plate, we employed a mobile phase with the following composition: petroleum ether: diethyl ether: acetic acid (200:100:1). Separated lipids were imaged in the Chemidoc MP Imaging System (Bio-Rad Laboratories, Hercules, California, United States) following air-drying of the TLC plate and choosing Alexa Fluor 488 as a fluorescent dye in the imaging system. Resulting Chol-NBD and esterified Chol-NBD blots were quantified by densitometric analysis using the Image Lab software (version 4.1, Bio-

Rad). Chol NBD/ esterified Chol NBD ratios were normalized to total protein content determined with the Quick Start™ Bradford Protein Assay (BIO-RAD, Cat.#500-0006).

2.14 Nuclei extraction from human cortical tissue

Cell nuclei were extracted from portions of frontal cortex gently donated by the Bellvitge hospital in Barcelona applying a variation of the Blobber and Potter protocol (Blobel & Potter, 1966). We started from approximately 0.260 g of frozen tissue, which was left thawing at room temperature. Subsequently, thawed tissue was cut in minute pieces with a scalpel and transferred to a 2 mL Eppendorf tube, where tissue was homogenized in two volumes of 0.25 M sucrose in cold TKM buffer (10 mM KCl, 10 mM Tris-Cl (pH 7.5), 1mM $MgCl_2$) and commercial protease and phosphatase inhibitors (Thermo Scientific Cat.#78440). Tissue was firstly homogenized with a Polytron mechanical homogenizer with a plastic pestle using 20-40 strokes. The resulting homogenate was transferred to Dounce homogenizer with a crystal pestle applying 20-40 strokes with the tight pestle. The resultant homogenate was transferred to an ultracentrifuge tube (Beckman Coulter, Cat.#344057), and 1080 µL of 2.3 M sucrose in TKM buffer were added and the tube was gently inverted 4-5 times to mix well its content. At that point, a pipette was introduced towards the bottom of the ultracentrifuge tube and 540µL of 2.3 M sucrose in TKM buffer were carefully added leading to the formation of two well distinguishable sucrose phases with the homogenate filling the upper part of the tube. Ultracentrifuge tubes were equilibrated in order to not unbalance the centrifuge and were centrifuged at 124,000 g, for 30 minutes at 4º C in Optima L-100XP ultracentrifuge (Beckam Coulter) equipped with a SW55 Ti rotor. The resultant pellet was resuspended in 50 µL of TKM buffer supplemented with phosphatase and protease inhibitors (Thermo Scientific, Cat.#78440). Nuclei isolation was tested by fluorescence microscopy, following staining with DAPI at 1µg/mL.

2.14.1 Isolated nuclei microscopy

Isolated nuclei were fixed in 4% paraformaldehyde (PFA) (w/v) in PBS, applying a 1:3 nuclear suspension volume/ PFA volume ratio. This mixture was pipetted on a rounded coverslip, 12 mm in diameter, situated on 2 cm^2 culture plates. Plates were centrifuged in a plate centrifuge, 3 minutes at 1,000 rpm. Coverslips were then transferred on a suitable surface coated with parafilm. Nuclei were incubated in a blocking and permeabilization solution (Triton X-100 0.1%, Normal goat serum 10%, in PBS), for 30 minutes. Following this, coverslips were gently washed in PBS and incubated in 300 µL of Nile Red (Sigma Cat.# N-3013) dissolved in PBS at 1µg/mL for 10 minutes at 37º. Incubation with Nile Red

was followed by 3 PBS washes; nuclei were mounted on glass slides in Fluoromount-G solution and preparations were allowed to dry at room temperature for 30 minutes.

Microscopy images were taken on an FV10i laser scanning confocal microscopy, and they were analyzed using the ImageJ software for Windows (Schneider et al., 2012).

2.15 Nile Red staining for lipids

Nile Red is a dark purplish-red powder (Sigma, Cat.# N-3013). The stock solution was prepared in acetone (1mg/ml) and kept in a tightly sealed, lightproof container at -20ºC. Working solution was prepared adding 1 µL of Nile Red Stock Solution to 999 µL PBS, resulting in a final concentration of 1µg/mL.

Cells or isolated nuclei were stained on 12 mm diameter glass coverslips in 24-well plates format. Isolated nuclei or cells were fixed in 4% PFA (w/v) in PBS at room temperature for 15 minutes. Nile Red working solution was added in each well (1mL/well) and plates were incubated for 10 minutes at 37ºC. Then cells were rinsed in PBS and coverslips were mounted on glass slides in Fluoromount-G solution and allowed to dry at room temperature for 30 minutes.

Microscopy images were acquired with an Olympus FV10i laser scanning confocal microscope and an Olympus FV1000 confocal microscopy, 60 x magnifications. For lipid droplets count per nucleus, confocal images were analyzed with the Find Maxima macro for ImageJ open-source software (Schneider et al., 2012).

2.16 Incorporation of 22-NBD Cholesterol in living MEFs to stain LDs

22-NBD Cholesterol was administered to living MEFs, simultaneously with the induction of metabolic switch, as described in section 2.9. Briefly cell cultured were supplied with a final concentration of 4µM starting from a stock solution of NBD-cholesterol (1mg/mL in ethanol). At the end of treatment, cells were washed twice with ice PBS and rapidly imaged under an Olympus IX71 inverted fluorescence and phase contrast microscope with a 20X air objective.

2.17 Primary rat cortical astrocyte treatment with oleic acid

Fatty acid-free bovine serum albumin (BSA FAF) (Cat.# 10775835001) and oleic acid (Cat.# O1008-25G) were purchased from Sigma-Aldrich (St. Louis, MO, USA). Oleic acid was supplemented with BSA FAF, which functioned as a carrier to ensure sufficient dissolution (mol/mol <2). A 0.7 M stock solution of oleic acid was prepared in chloroform

and stored at -20ºC; before usage, the chloroform was evaporated with gas nitrogen, and the resultant powder was dissolved in 1 mL of filtered fatty acid-free BSA 1mM in DMEM medium (GibcoTM, Cat.# 41966029). The obtained mixture was added to astrocytes (100 µL/ well in 12-well plates).

2.17.1 LipidTOX™ staining of primary cortical rat astrocytes

LipidTOX™ (Cat.# H34475, Invitrogen) is a neutral lipid stain that has an extremely high affinity for neutral lipid droplets and can be detected by fluorescence microscopy or an HCS reader. For LipidTOX™ staining, primary cortical rat astrocytes were seeded on glass coverslips in 24-well plates at a density of 25,000 cells/ well and treated with oleic acid and stress inducers (see Table 2) in OptiMEM. Subsequently, cells were rinsed twice with PBS and fixed with 3.7% Formaldehyde in PBS for 10 minutes at room temperature. The fixative solution was removed, and the formaldehyde-fixed cells were gently rinsed with PBS 2–3 times to remove residual formaldehyde before labeling with the neutral lipid staining solution. The labeling solution was prepared by diluting the 1000X LipidTOX™ neutral lipid stain 1:1000 in PBS to make a 1X working solution. A volume of 500 µL of the obtained working solution was added to each well. Plates were sealed with plate-sealing film and incubated at room temperature for 30 minutes. After this time, cells were lightly permeabilized with 0.1% saponin in PBS and stained with DAPI at 1µg/mL for 15 minutes at room temperature. Coverslips were briefly rinsed in PBS by submersion, mounted in Fluoromount-G solution (Cat.# 0100-01, Southern Biotech, Birmingham, AL, USA) on glass slides and allowed to dry at room temperature for 30 minutes before storing them at 4º C in the dark until imaging.

Microscopy images were acquired with an Olympus FV10i laser scanning confocal microscope and an Olympus, 60x magnification. For the evaluation and subsequent quantification of neutral lipids staining, we used a dedicated pipeline created on the open-source software Cell Profiler 2.1.1 for Windows (Kamentsky et al., 2001). For LipidTOX™ intensity per cell, confocal images were analyzed with a dedicated pipeline created on the open-source software Cell Profiler 2.1.1 for Windows (Kamentsky et al., 2011). The pipeline is available at Mendely data (Rossi, Chiara (2022), “CellProfiler pipeline for confocal images analysis_2”, Mendeley Data, V1, doi: 10.17632/vh6bgbnk2n.1).

2.18 Statistical Analysis

All statistics were performed using the GraphPad Prism version 9.1.2 for Windows software (GraphPad Software, San Diego, CA, USA). Differences between groups were analyzed by the Student’s t-tests, One-way, Two-way, and Three-way ANOVA analyses,

with adequate post-hoc analyses, once normality of variables was tested by Kolmogorov-Smirnov test. Correlations between variables and linear regression analyses were also performed by using the same software. The 0.05 level was selected as the point of minimal statistical significance in every comparison.

RESULTS

3. RESULTS

3.1. Changes in nuclear/extranuclear ratio of transcriptional factors upon ALS-related stress conditions

3.1.1 Effect of oxidative stress on protein delocalization and colocalization with mitochondria

As already mentioned in the Introduction chapter (section 1.1.3.5), hyperphosphorylated TDP43, (p-TDP-43) can be found in pathological inclusions (Jo et al., 2020) representing a hallmark of ALS pathology. Nevertheless, cellular stress response pathways have been widely implicated in neurodegeneration and aging (Taylor et al., 2016). In particular, the mitogen-activated protein kinase (MAPK) pathway is notably involved in ALS etiology and progression (Sahana & Zhang, 2021) (section 1.2.1). Also, changes in subcellular localization of RE-1 silencing transcription factor (REST) have been traditionally linked to AD; however, recent studies have claimed its implication in ALS progression (section 1.3.1).

In order to characterize the extranuclear location of the transcriptional factors p-TDP43, p-ERK, p-Jun and REST, we performed a screening based on confocal microscopy and automatized image analyses of an epithelial cell culture treated with hydrogen peroxide, thapsigargin, epoxomicin, or rotenone at different concentrations and times to recreate oxidative, endoplasmic-reticulum, proteasomal and mitochondrial stresses.

Oxidative stress induced by H_2O_2 in HMEC-1 cell line led to changes in the nuclear and non-nuclear distribution of p-TDP-43, while the nuclear intensity of p-TDP-43 was decreased in the milder oxidative conditions tested (Figures 22 and 26).

In contrast with p-TDP-43, despite an initial cytosolic increase of p-ERK in the same conditions, this protein was rapidly cleared (Figures 23 and 26), being mainly non-nuclear.

The cytoplasmic staining of REST and p-Jun showed the same tendencies, i.e., after an initial decrease, there was a tendency for increasing their values (highly significant in the case of REST), as shown in representative confocal images in Figure 24 and 25, respectively (see Figure 26 for quantitative results).

These changes in protein distribution were quantified analyzing the confocal images of HMEC-1 cell culture with the free open-source software CellProfiler™.

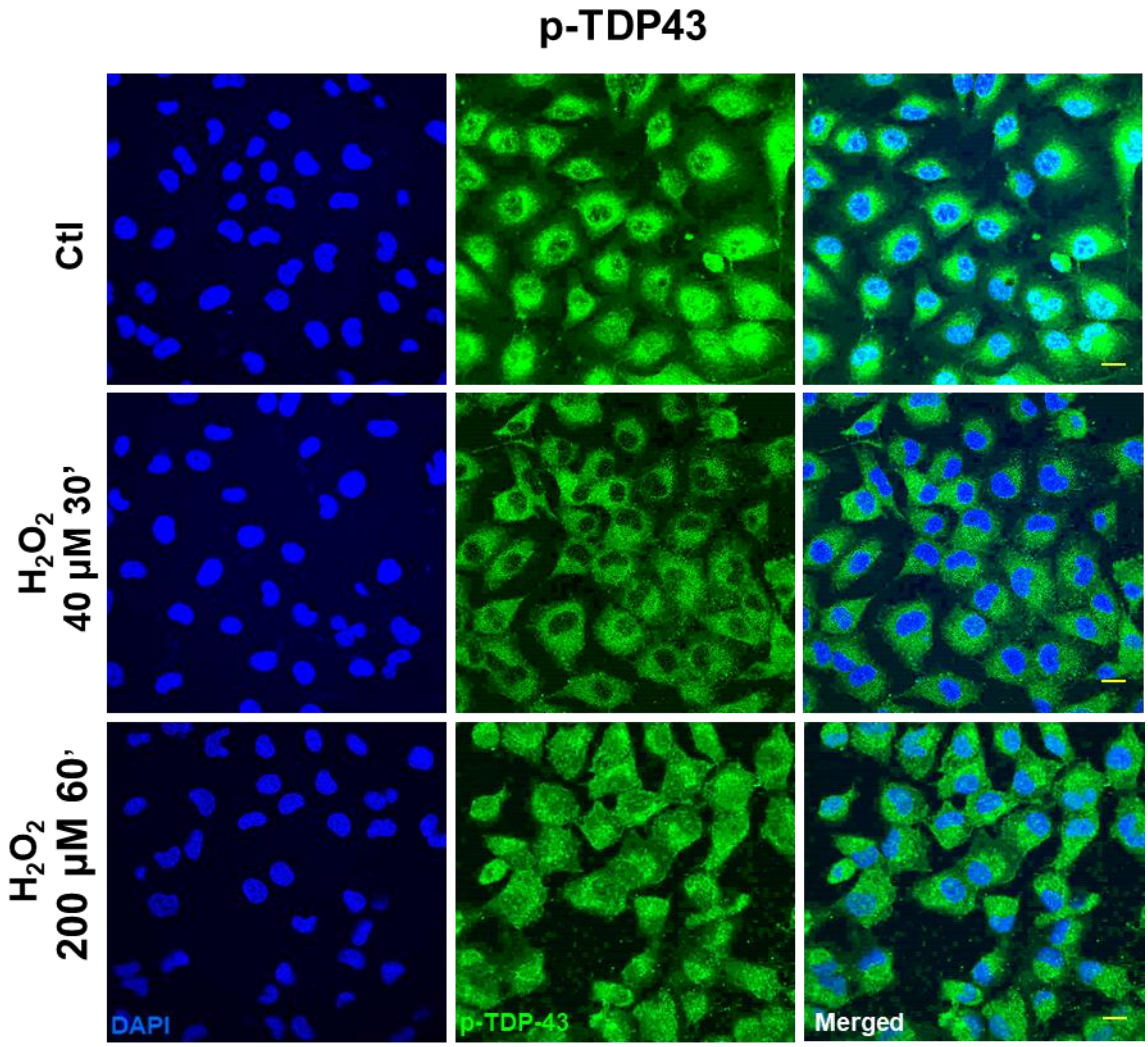

Figure 22. **Oxidative stress induces changes in the levels of proteins implicated in neurodegeneration.** Representative confocal microscopy images of HMEC-1 cells immunostained with anti-phospho-TDP43 antibody showing diverse effects of oxidative stress (H_2O_2, doses and times indicated) in nuclear and non-nuclear (cytosol) immunostaining. Bars are 60 micrometers long.

The nonhomogeneous distribution of cytoplasmic locations after oxidative stress (evident in p-TDP-43, p-Jun, and REST) suggested their colocalization with an organelle fraction. We performed coimmunostaining with several mitochondrial epitopes to test if this non-nuclear localization involved a mitochondrial residence (Gautam et al., 2019). Complex V coimmunostaining with these factors indicated that the degree of colocalization increased significantly in all the cases after oxidative stress (Figure 27, 29 and 30) exceeding z'-values of 0.5 (roughly meaning that at least 50% of both epitopes could coincide at the resolution of the confocal microscopy), except for p-ERK (Figure 28). Although the colocalization of this protein increased significantly after oxidative stress, and in line with

the p-ERK decreased values in the cytoplasm, the z'-values did not reach 0.3 in this case. The correlation analyses of nuclear vs. cytoplasmic intensity showed linear relationships between these parameters, though their responses to oxidative stress were strongly dependent on the factor (Supplemental Figure SF1).

Colocalization of the proteins of interest with the mitochondrial compartment was estimated analyzing the confocal images of HMEC-1 cell culture with the free open-source software CellProfiler. Figure 31 shows the results of these measurements.

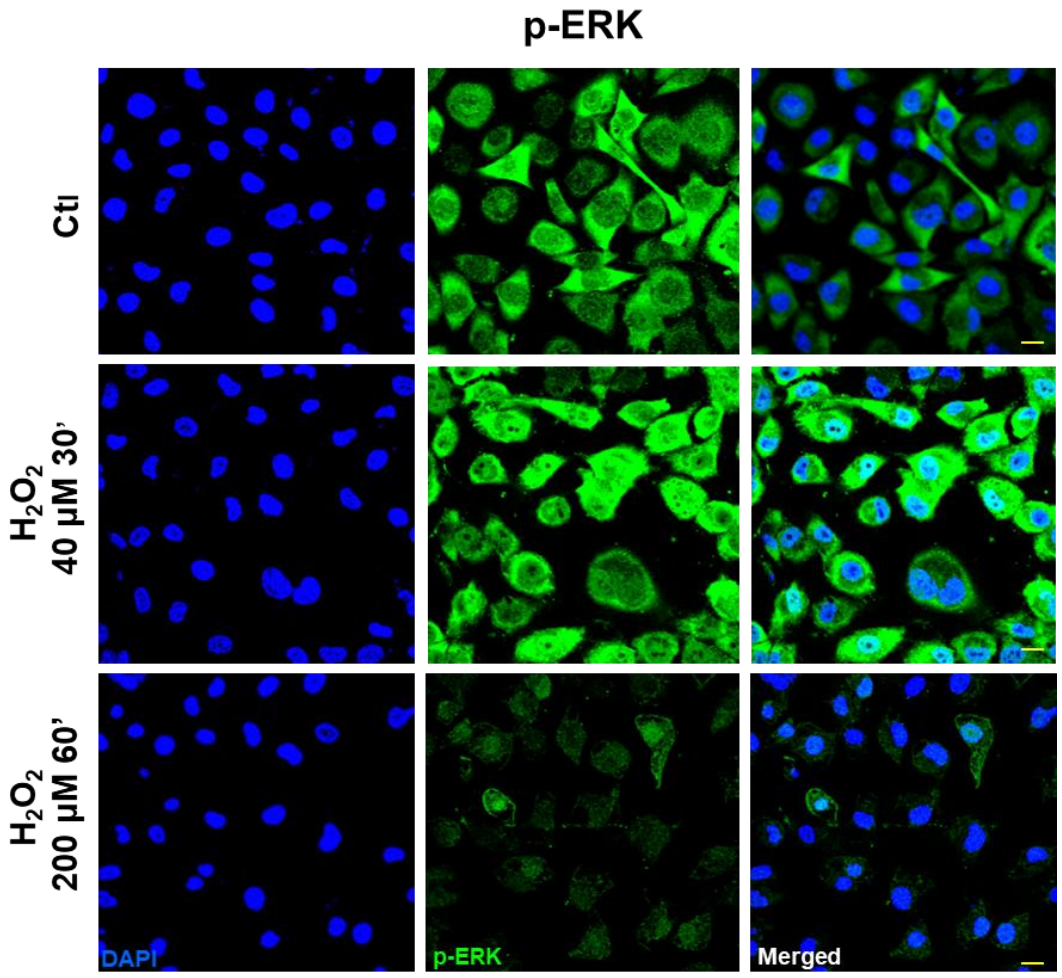

Figure 23. **Oxidative stress induces changes in the levels of proteins implicated in neurodegeneration**. Representative confocal microscopy images of HMEC-1 cells immunostained with anti-phospho-ERK antibody showing diverse effects of oxidative stress (H_2O_2, doses and times indicated) in nuclear and non-nuclear (cytosol) immunostaining. Bars are 60 micrometers long.

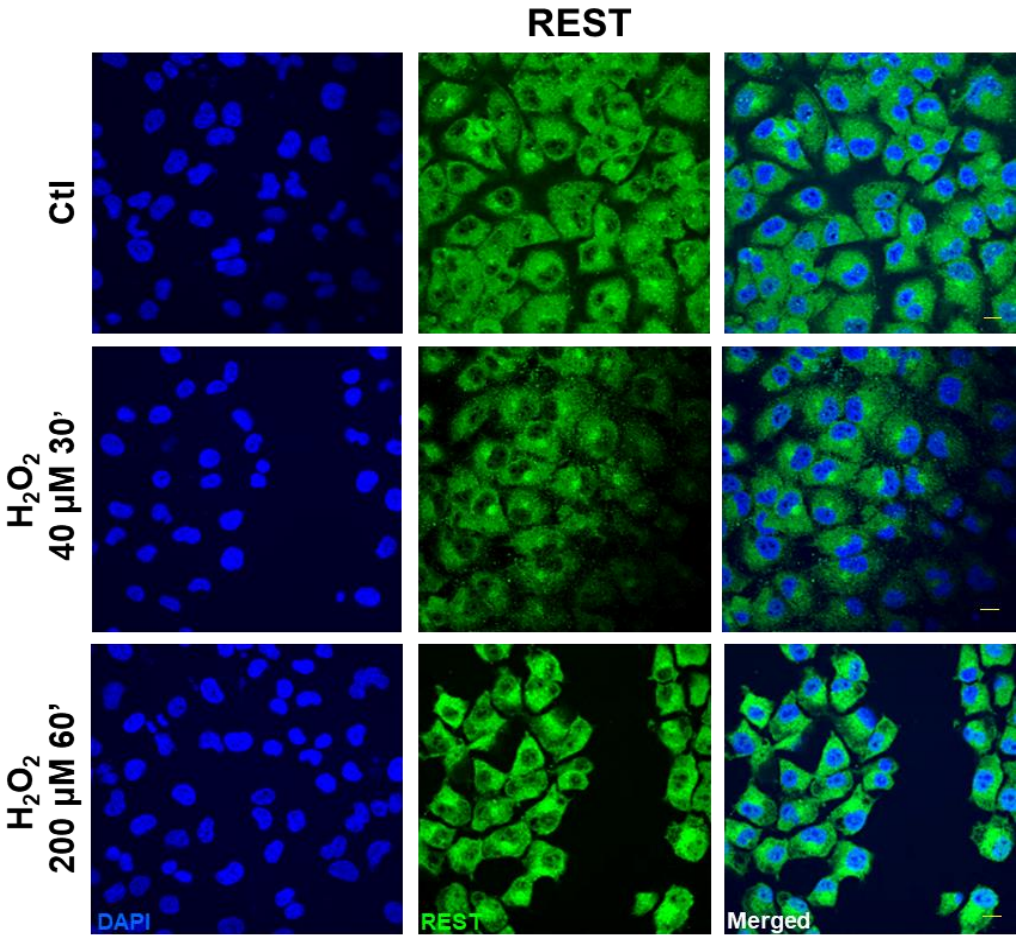

Figure 24. **Oxidative stress induces changes in the levels of proteins implicated in neurodegeneration.** Representative confocal microscopy images of HMEC-1 cells immunostained with anti-REST antibody showing diverse effects of oxidative stress (H_2O_2, doses and times indicated) in nuclear and non-nuclear (cytosol) immunostaining. Bars are 60 micrometers long.

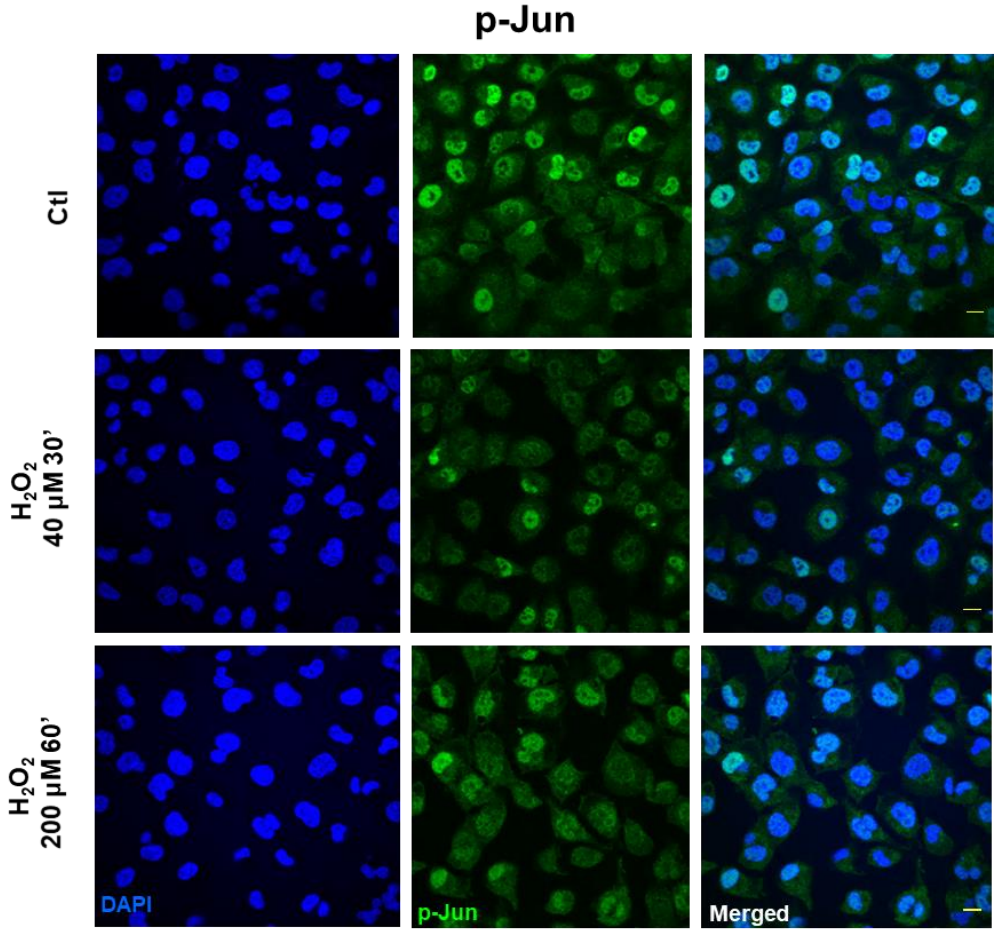

Figure 25. **Oxidative stress induces changes in the levels of proteins implicated in neurodegeneration**. Representative confocal microscopy images of HMEC-1 cells immunostained with anti-phospho-Jun antibody showing diverse effects of oxidative stress (H_2O_2, doses and times indicated) in nuclear and non-nuclear (cytosol) immunostaining. Bars are 60 micrometers long.

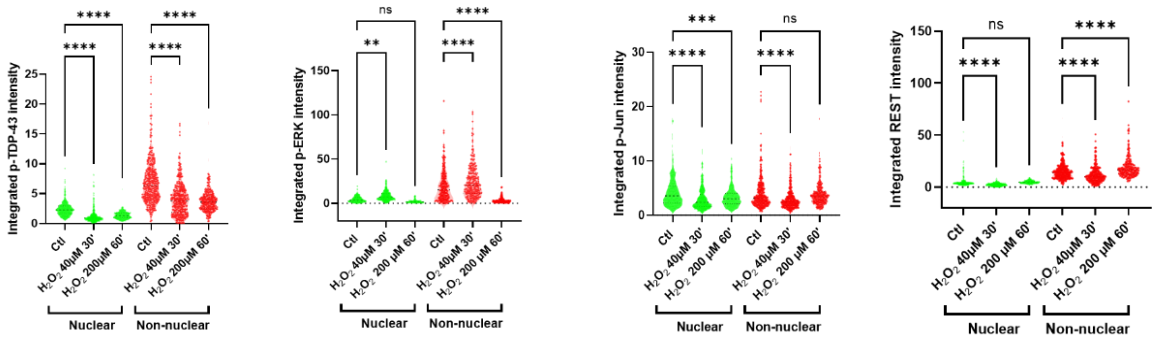

Figure 26. Quantification of the changes in the levels of proteins implicated in neurodegeneration in their nuclear and non-nuclear (cytosol) immunostaining after the induction of oxidative stress by H_2O_2 (times of treatment and doses indicated). Bars indicate the mean with the standard deviation shown by the lines (*n* = 200–296 cells for p-TDP-43, *n* = 191–255 for p-ERK, *n* = 234–326 for p-Jun, and *n* = 217–415 for REST, obtained in at least 4 independent replicates). * Indicates $p < 0.05$, ** $p < 0.01$, *** $p < 0.001$, and **** $p < 0.0001$ by Sidak's post-hoc multiple comparison test after a 2-way ANOVA.

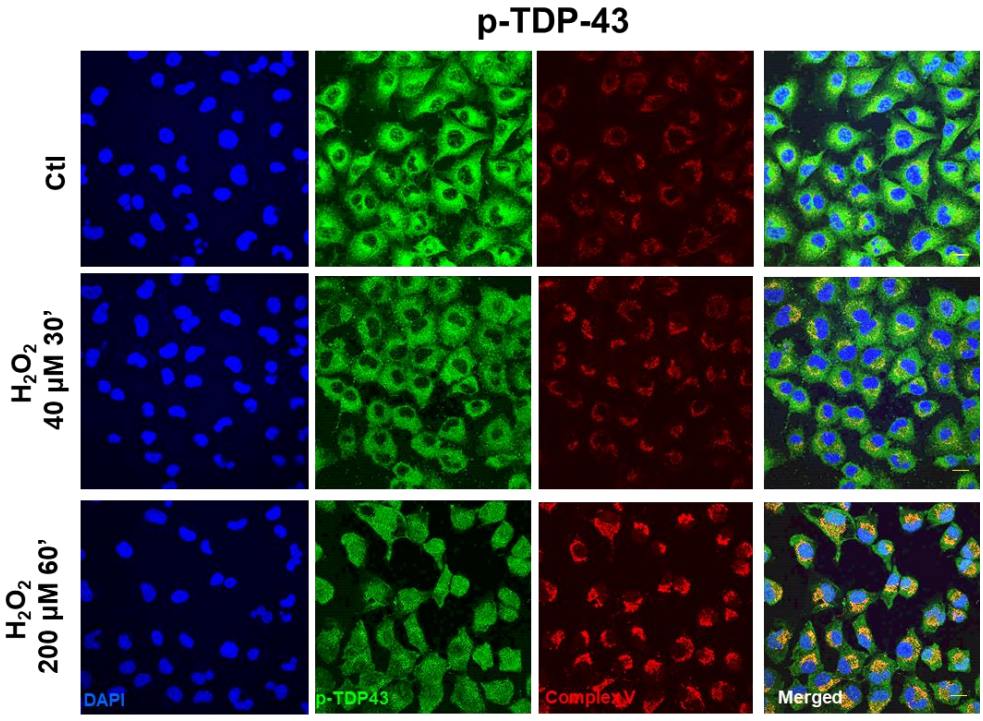

Figure 27. **Oxidative stress induces changes in the colocalization levels of proteins implicated in neurodegeneration with mitochondria.** Representative confocal microscopy images of HMEC-1 cells immunostained with anti-phospho-TDP43 antibody showing diverse effects of oxidative stress (H_2O_2, dose and time indicated) on colocalization with the mitochondrial epitope Complex V. Bars are 60 micrometers long.

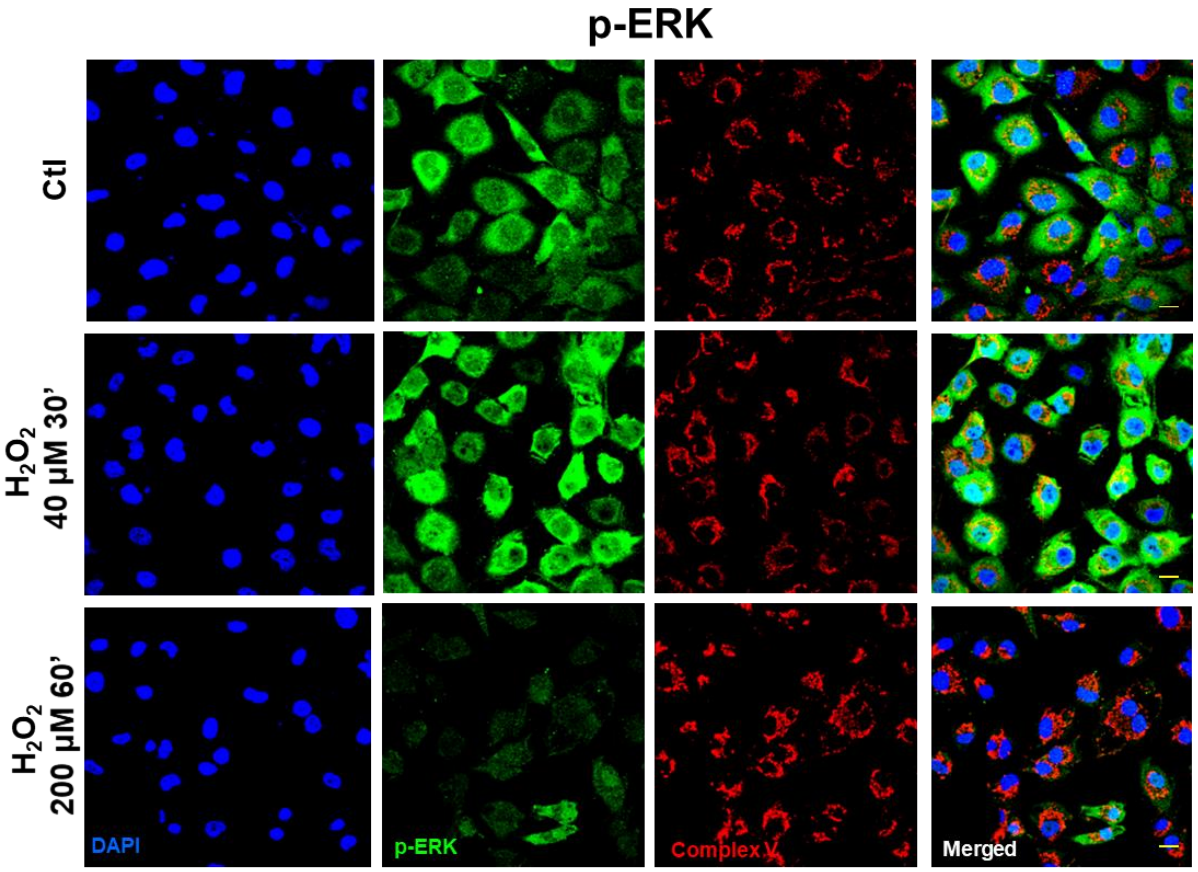

Figure 28. **Oxidative stress induces changes in the colocalization levels of proteins implicated in neurodegeneration with mitochondria**. Representative confocal microscopy images of HMEC cells immunostained with anti-phospho-ERK antibody showing diverse effects of oxidative stress (H_2O_2, dose and time indicated) on colocalization with the mitochondrial epitope Complex V. Bars are 60 micrometers long.

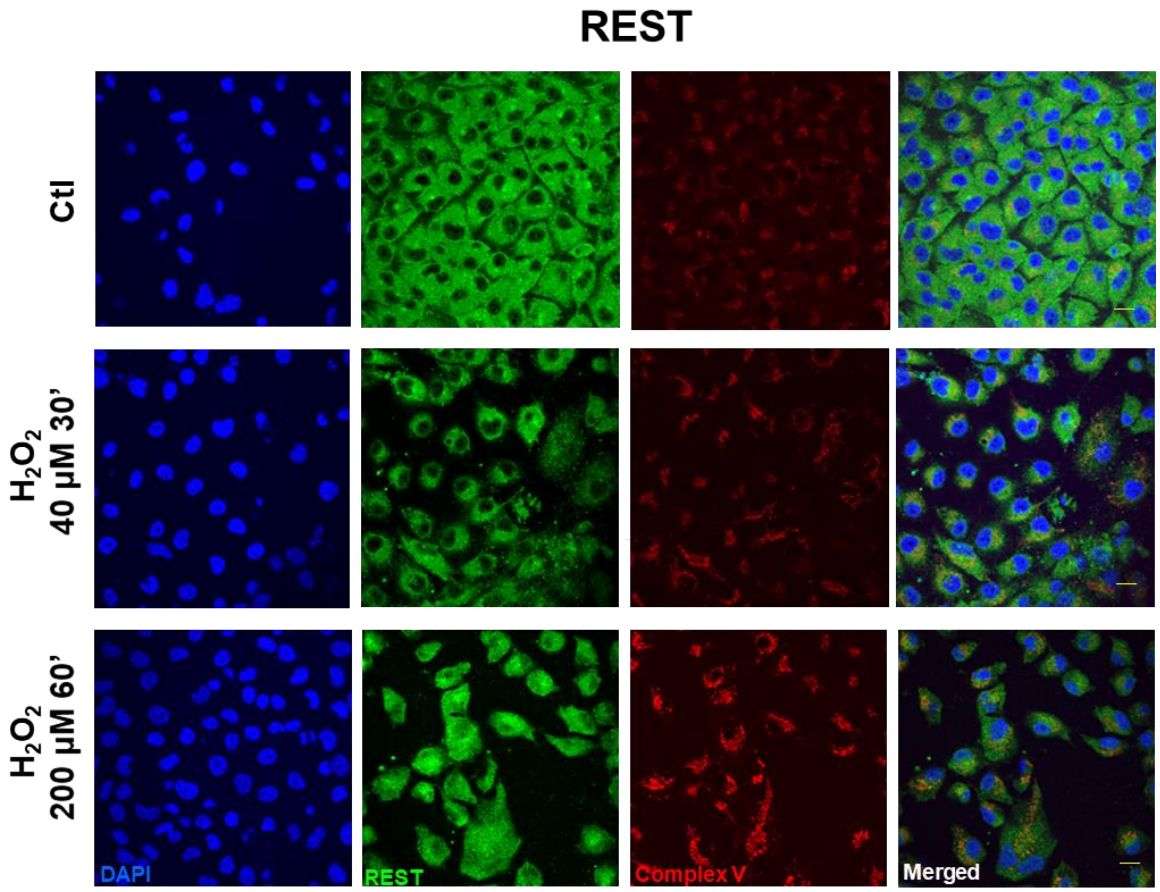

Figure 29. **Oxidative stress induces changes in the colocalization levels of proteins implicated in neurodegeneration with mitochondria**. Representative confocal microscopy images of HMEC cells immunostained with anti-phospho-ERK antibody showing diverse effects of oxidative stress (H_2O_2, dose and time indicated) on colocalization with the mitochondrial epitope Complex V. Bars are 60 micrometers long.

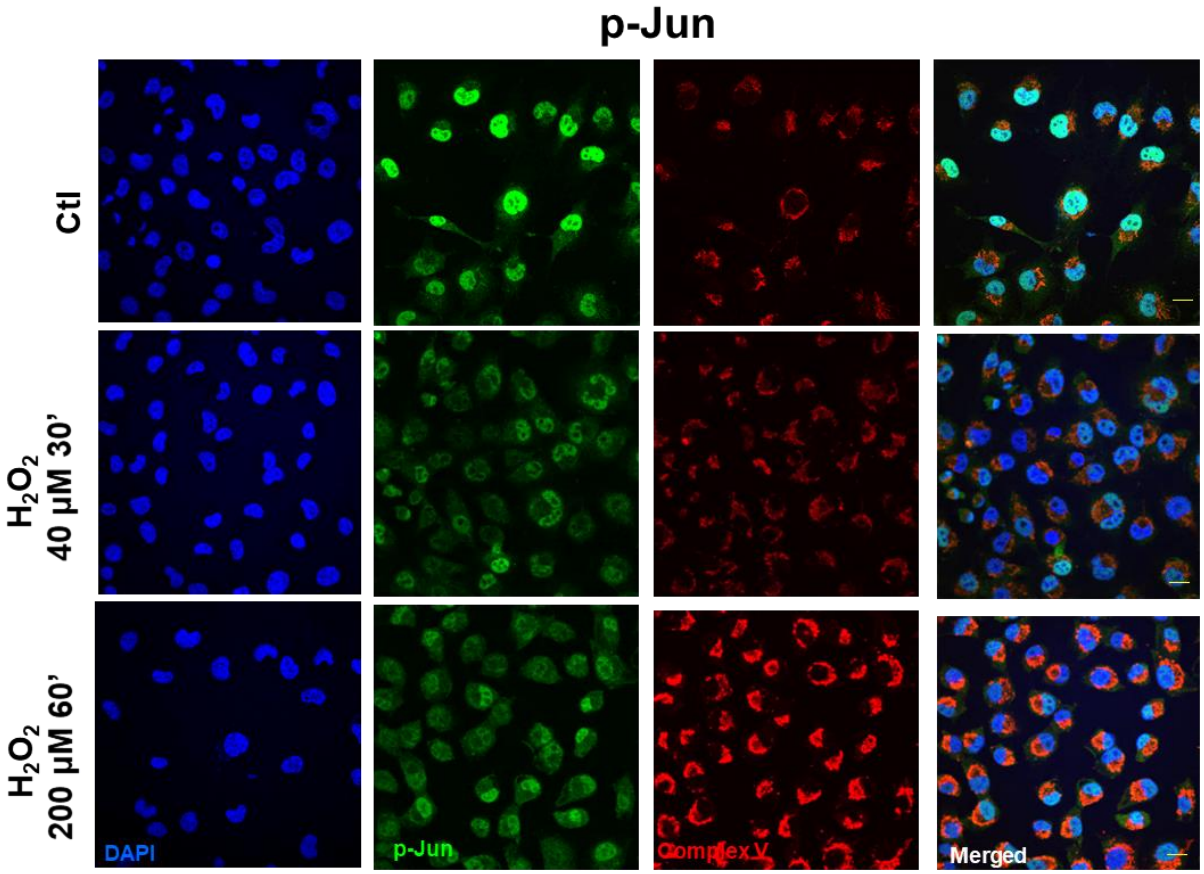

Figure 30. **Oxidative stress induces changes in the colocalization levels of proteins implicated in neurodegeneration with mitochondria**. Representative confocal microscopy images of HMEC cells immunostained with anti-phospho-Jun antibody showing diverse effects of oxidative stress (H_2O_2, dose and time indicated) on colocalization with the mitochondrial epitope Complex V. Bars are 60 micrometers long.

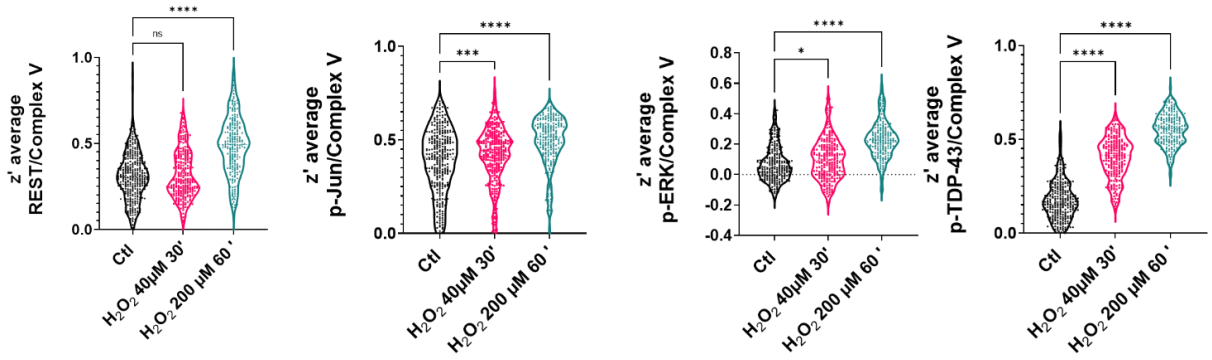

Figure 31. Degree of colocalization of different proteins implicated in neurodegeneration with the mitochondrial epitope Complex V after the induction of oxidative stress by H_2O_2 (time of treatment and doses indicated). Changes in colocalization were estimated by calculation of the z' factor, shown in the violin graphs. * Indicates $p < 0.05$, ** $p < 0.01$, *** $p < 0.001$, and **** $p < 0.0001$ by Dunnett's post-hoc multiple comparison test after an ANOVA.

3.1.2 Effects of ER stress on p-ERK and p-Jun delocalization

We also examined if other ALS-related cell stressors, such as ER stress, could induce similar delocalizations of the evaluated proteins. We have previously shown that proteasomal and ER stress induce a cytosolic mislocalization of TDP-43 (Ayala et al., 2011). Using similar conditions, we first evaluated if the cells exposed to proteasomal stress (epoxomicin) in similar conditions to the ones already reported to mislocalize TDP-43 also changed p-ERK and p-Jun. The results (Figure 32) indicated that these proteins exhibited differential dynamics. Thus, in p-ERK, the nuclear levels were always inferior to the cytosolic ones (90% of the total variance explained by the cellular location, p < 0001). Further, proteasomal stress induced by epoxomicin decreased the levels of p-ERK significantly (either at the nuclei and in the cytosol, 7% of the total variance, p < 0.0001). In p-Jun, there was a significant interaction between stress and the subcellular location, i.e., the effect on epoxomicin depended on the location. Therefore, epoxomicin treatment decreased the cytosolic levels of p-Jun (Figures 32A and 32C) in a close relationship with the increased levels in the nuclei (51% of the total variance explained by the interaction of stress and the subcellular location). In the case of ER stress (thapsigargin), we observed similar results in p-ERK. Thus, the total levels were decreased after the stress, both at the nuclear and cytosolic levels (Figure 32A). Similarly, the cytosol vs. nuclear location was the factor explaining the most variance (79% of the total variance, p < 0.0001). For p-Jun, while its preferential nuclear location was maintained, the ER stress induced by thapsigargin induced a significant early increase in the nuclei (similar to proteasome stress), but later on, the levels were decreased, in line with the changes in the cytosol

(Figure 32B). Therefore, cytosol vs. nuclear location explained most of the variance (90% of variance, $p < 0.0001$).

We then evaluated the potential colocalization of these proteins with the mitochondrial components. The results of the confocal microscopy (Figures 33A, 33B and 33C) suggested that the degree of colocalization was affected by cell stressors. In the case of proteasome stress, the degree of p-ERK colocalization increased significantly at the longer times evaluated (Figures 33A and 33C), while this was not present for p-Jun at 2 hours. Later, proteasome stress led to a decrease in the degree of colocalization (Figure 34A). For ER stress, at the shorter term, the z'-values increased for p-ERK, but later on, they showed a significant decrease (Figures 33B and 33C). Both at short and longer times, in the case of p-Jun, decreased degrees of colocalization were evident (Figures 33B and 33C).

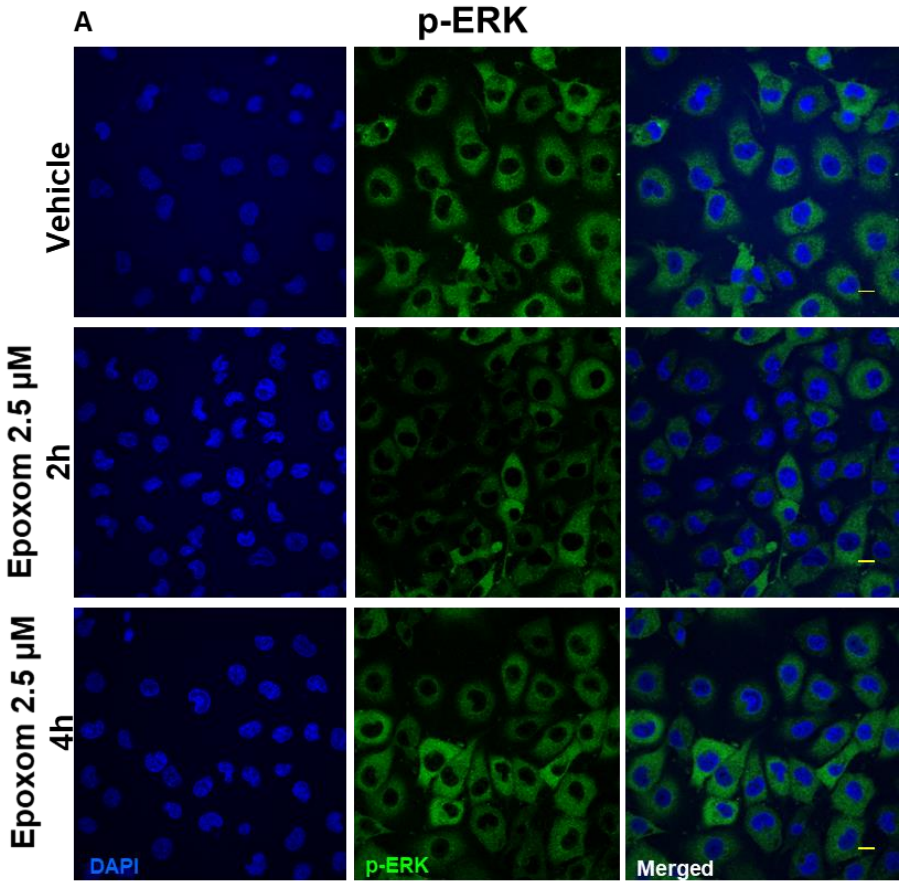

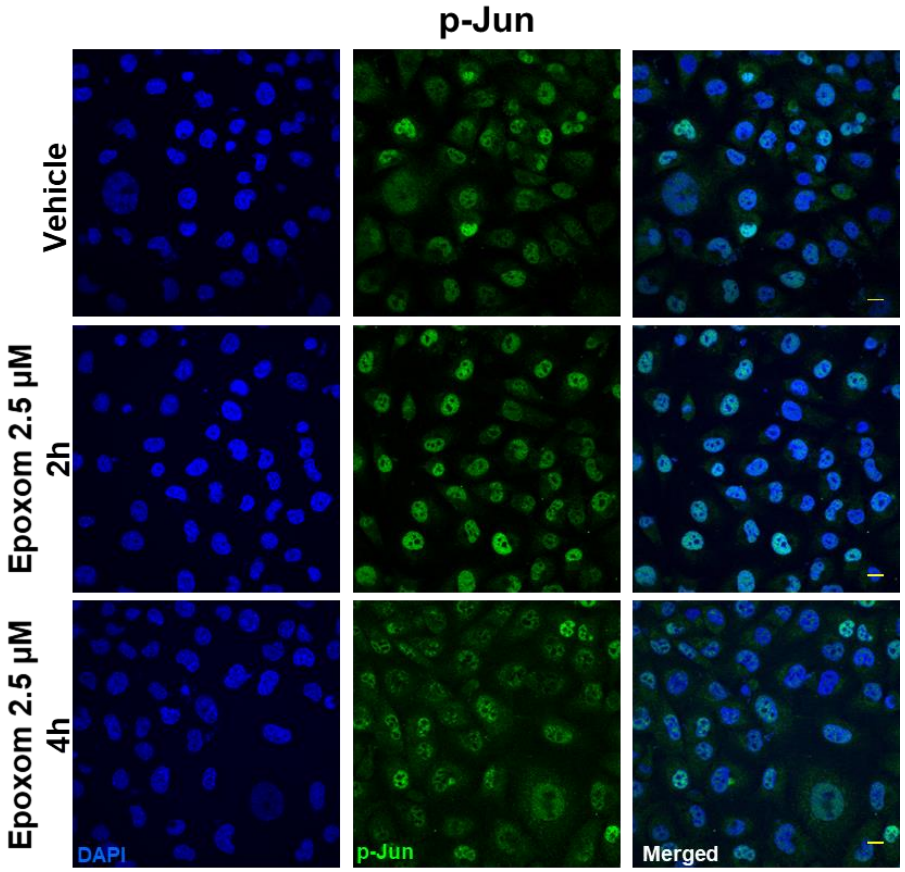
p-Jun
Vehicle
Epoxom 2.5 µM 2h
Epoxom 2.5 µM 4h
DAPI
p-Jun
Merged

B

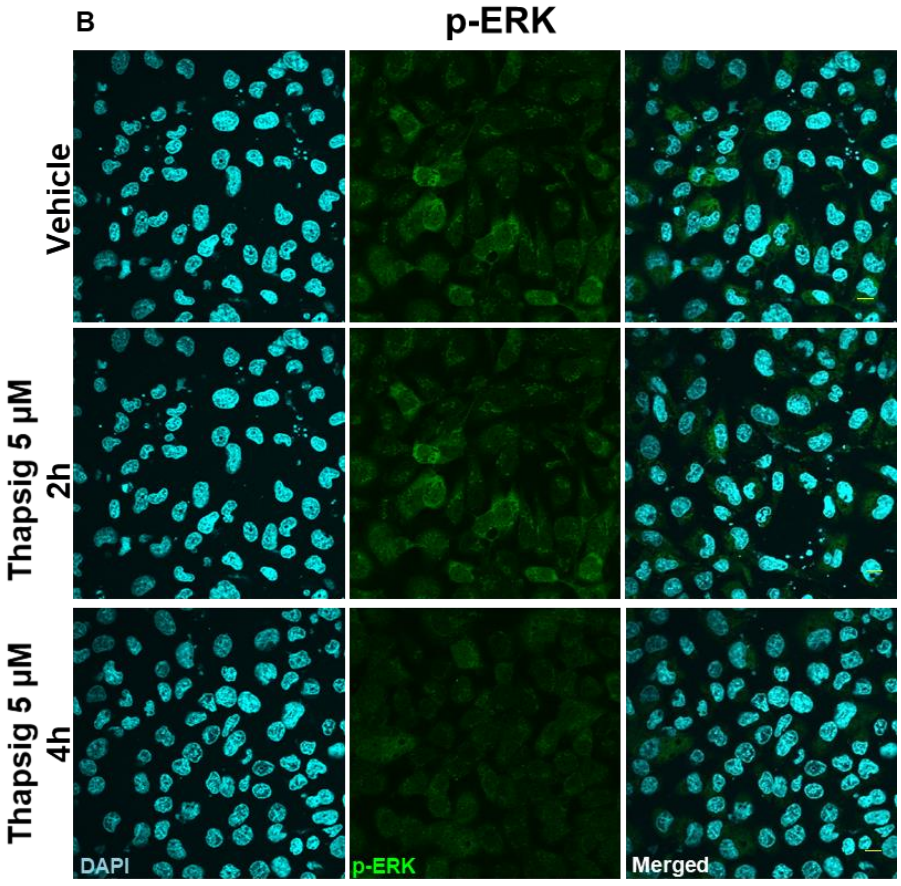
p-ERK
Vehicle
Thapsig 5 µM 2h
Thapsig 5 µM 4h
DAPI
p-ERK
Merged

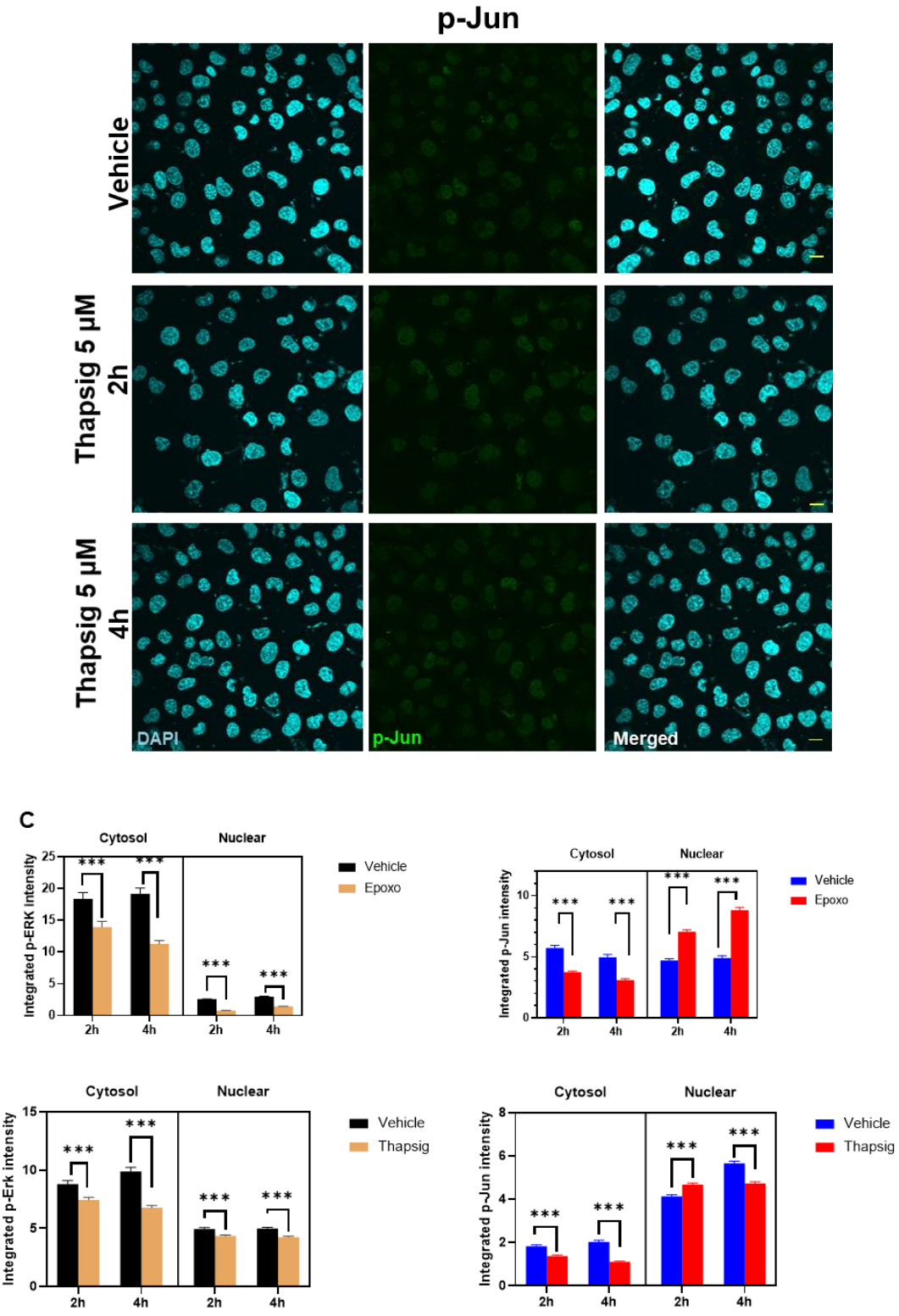

Figure 32. Proteasome and ER stress induces changes in the levels of p-ERK and p-Jun. Representative confocal microscopy images of HMEC cells immunostained with antibodies against p-ERK and p-Jun showing diverse effects of proteasome inhibition (epoxomicin) in **(A)** and ER stress (thapsigargin) in **(B)** in nuclear and non-nuclear (cytosol) immunostaining, quantified in **(C)**. Images shown are for 2 and 4 hours of incubation. In (c), the bars indicate the mean with the standard deviation shown by lines. N = 195–283 cells for p-ERK and N = 285–394 for p-Jun upon proteasomal stress, while N= 519–658 cells for p-ERK and N= 415–

553 for p-Jun upon ER stress. *** Indicates p < 0.001 by Sidak's post-hoc multiple comparison test after a 2-way ANOVA. The bars in the (A) and (B) micrographs are 60 micrometers long.

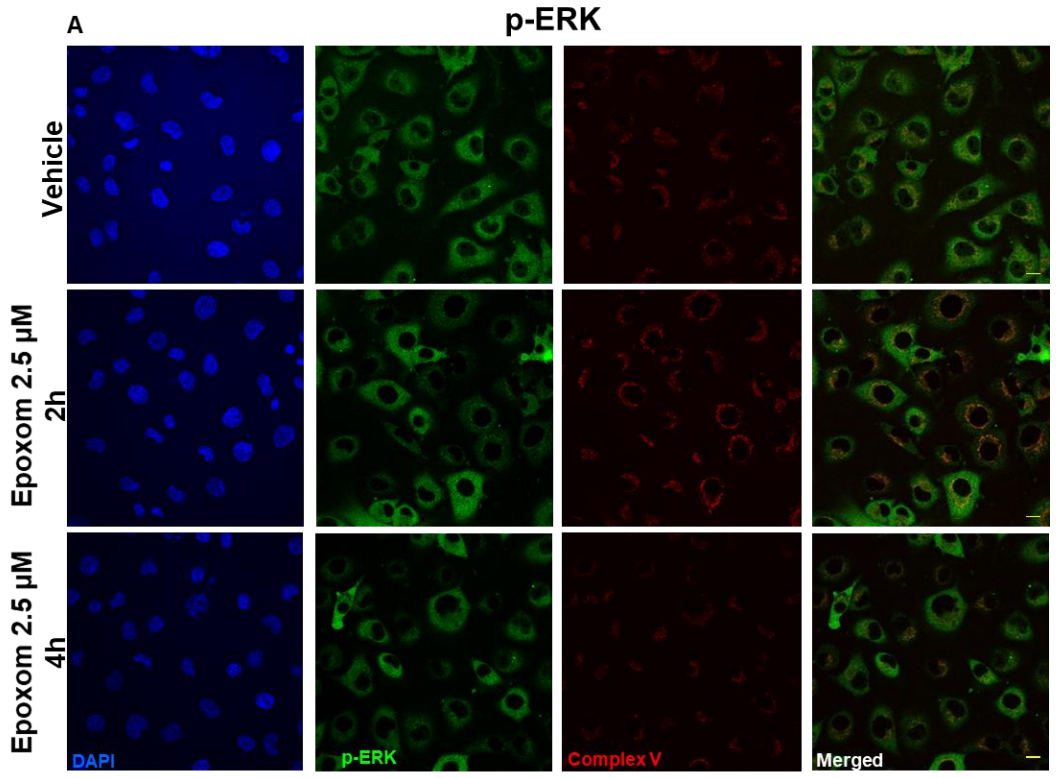

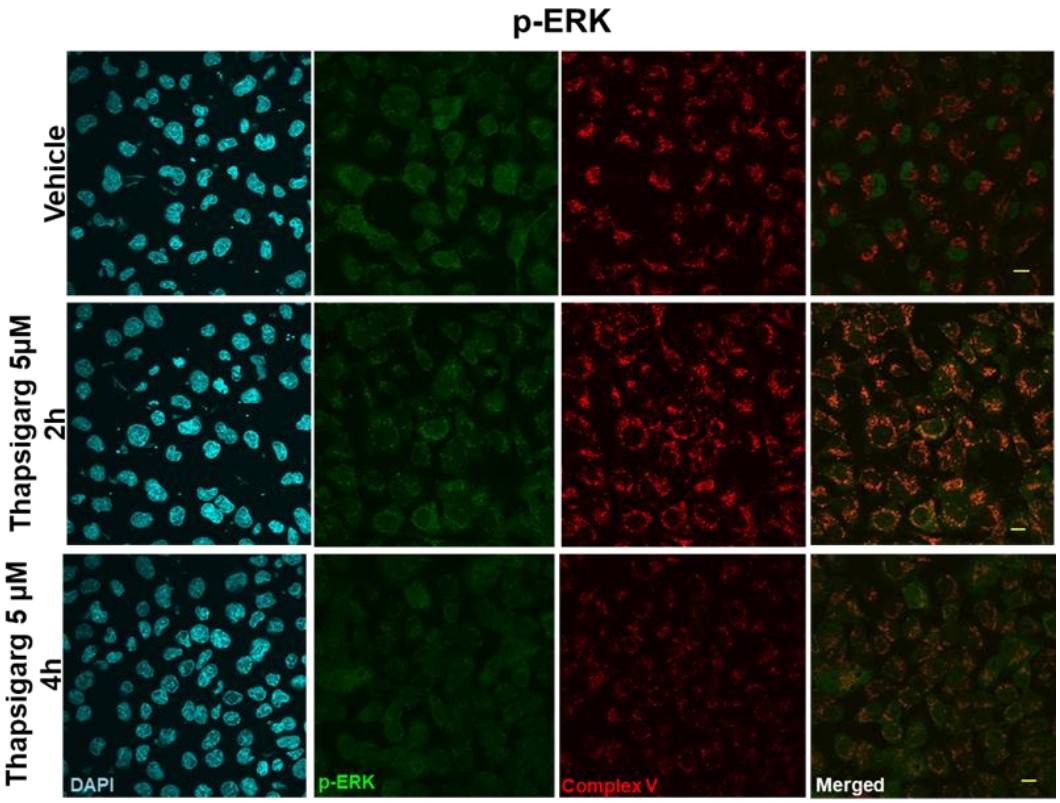

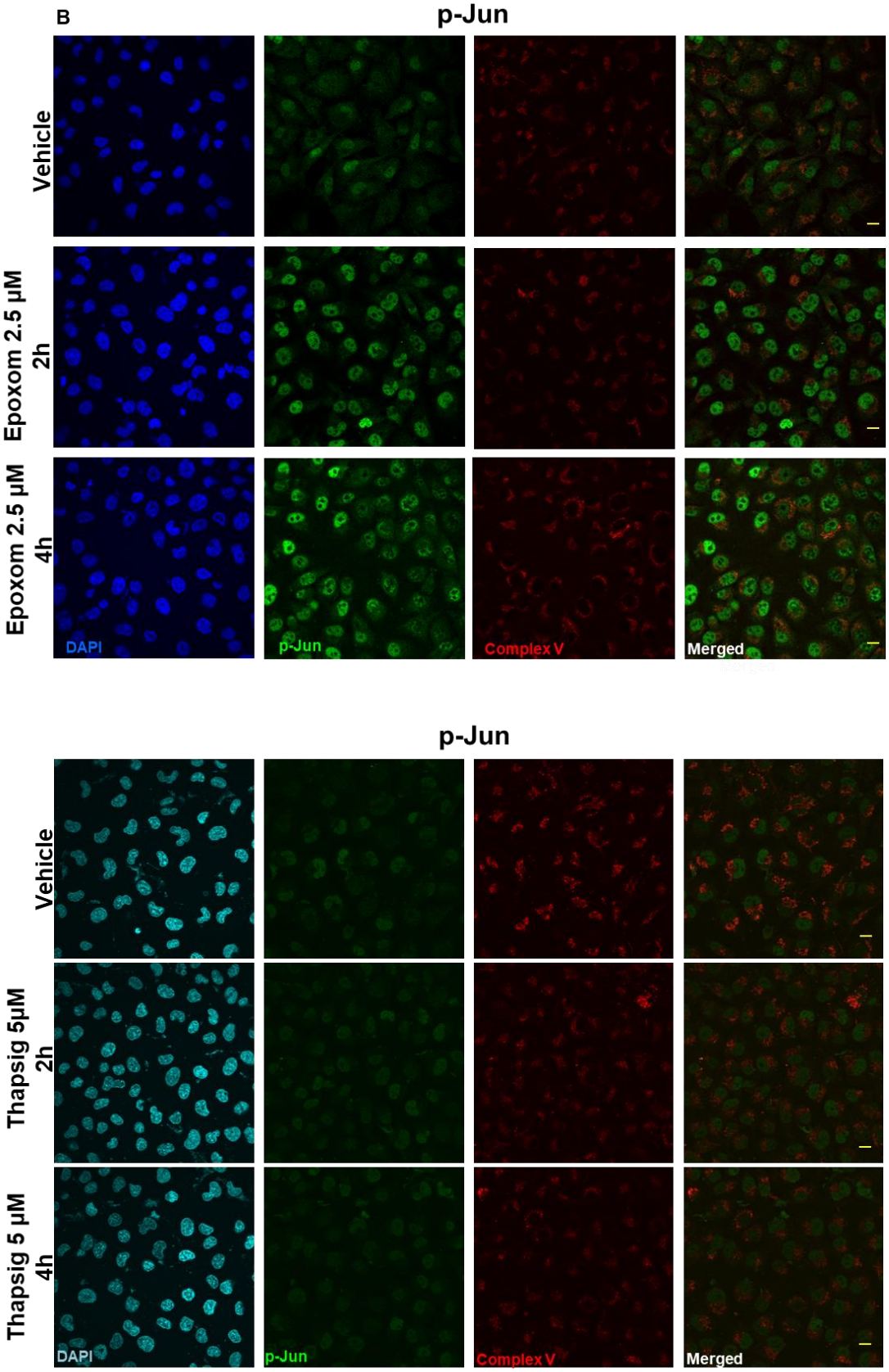
B
p-Jun
Vehicle
Epoxom 2.5 µM 2h
Epoxom 2.5 µM 4h
DAPI
p-Jun
Complex V
Merged
p-Jun
Vehicle
Thapsig 5µM 2h
Thapsig 5 µM 4h
DAPI
p-Jun
Complex V
Merged

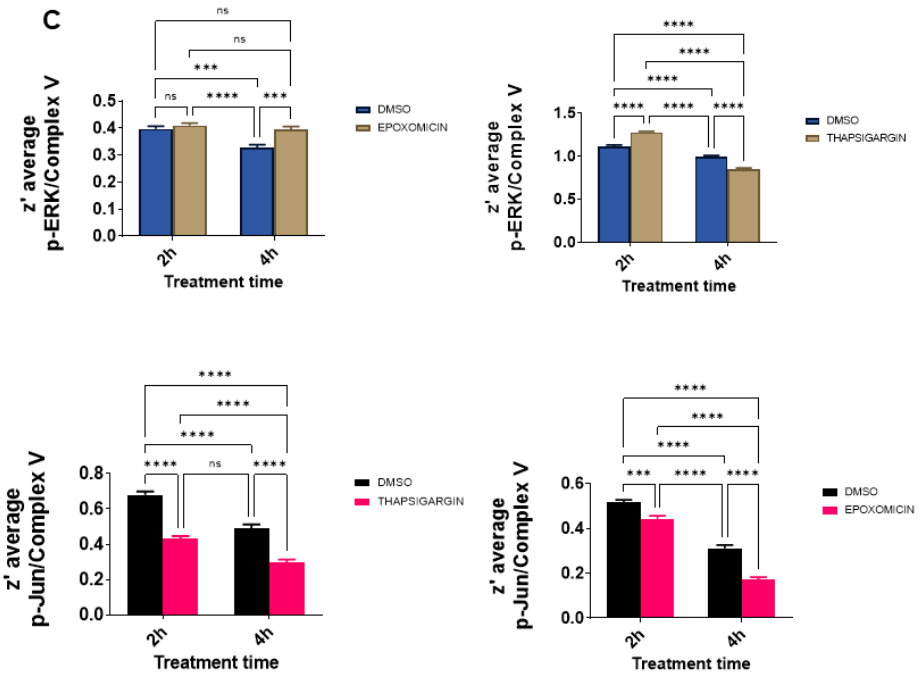

Figure 33. Proteasome and ER stress induces changes in the colocalization degree of p-ERK and p-Jun with mitochondrial epitopes. Representative confocal microscopy images of HMEC cells immunostained with antibodies against p-ERK and mitochondrial epitopes in **(A)** and against p-Jun and mitochondrial epitopes in **(B)**, showing diverse effects of proteasome inhibition (epoxomicin) and ER stress (thapsigargin) in the degree of colocalization estimated by calculation of the z' factor **(C)**. Images shown are for 2 and 4 hours of incubation. In (C) bars indicate mean with standard deviation shown by lines (n = 195 to 658 cells for p-ERK and n = 285–553 for p-Jun); *** indicate $p < 0.001$, and **** $p < 0.0001$ by Bonferroni's post-hoc multiple comparison test after 2-way ANOVA. Bars in (A) and (B) micrographs are 60 micrometers long.

3.1.3 Effect of mitochondrial stress on protein delocalization and colocalization with mitochondria

As already mentioned in Introduction (section 1.2.2.5) there is strong evidence linking mitochondrial dysfunction and ALS, with mitochondria playing a pivotal role in excitotoxicity, oxidative stress, and apoptosis. Nevertheless, the intimate mechanism correlating mitochondrial failure with motor neuron degeneration in ALS is still elusive (Singh et al., 2021). Here, we tested the effect of mitochondrial stress on protein mislocalization to investigate on the eventual changes in subcellular distribution of the proteins named before (p-TDP43, p-ERK, REST and p-Jun). To recreate mitochondrial stress in cell culture we employed rotenone, a strong inhibitor of the mitochondrial complex I.

Similarly to the heterogenous response we observed for the other stressors mentioned above, in this new set of experiments the results also appear to be influenced by

treatment time and the cytosol vs. nuclear location. This phenomenon is evident for p-TDP43, with rotenone inducing a significant decrease in the cytosolic levels of this protein during the first 2 hours of treatment, while the tendency was reversed at 4 hours, with a significant increase in the cytosolic compartment (Figures 34A and 35A). Concerning the nuclear content of p-TDP43, its levels were significantly decreased at both times of treatments, as shown in Figures 34A and 35A. The cytosol vs. nuclear location was the factor explaining the most variance.

In the case of p-ERK, mitochondrial stress induced a significant decrease in the levels of this protein in the cytosolic compartment at the shorter time (2h), while the phenomenon is still observable at 4 hours, even if in a non-significant trend. Nuclear content was significantly increased both at 2 and 4 hours of treatment (Figures 34B and 35B). Variability is mainly explained by the interaction between treatment and cytosol vs. nuclear location.

REST levels in the cytosol were subjected to a significant increase at 2 hours, while an opposite trend was observed at 4 hours. Concerning the nuclear content of this protein, we reported a significant increase at both times of treatment (Figures 34C and 35C), with the higher percentage of variation being explained by the interaction of the treatment and the subcellular location of the protein.

Moving to p-Jun, nuclear levels were decreased at both times of treatment, even if the phenomenon was not statistically significant at 4 hours. The nuclear content of this protein was increased at 2 hours, while an opposite tendency was observed at 4 hours, whit a significant decrease (Figures 34D and 35D). Subcellular location accounted for the main source of variation.

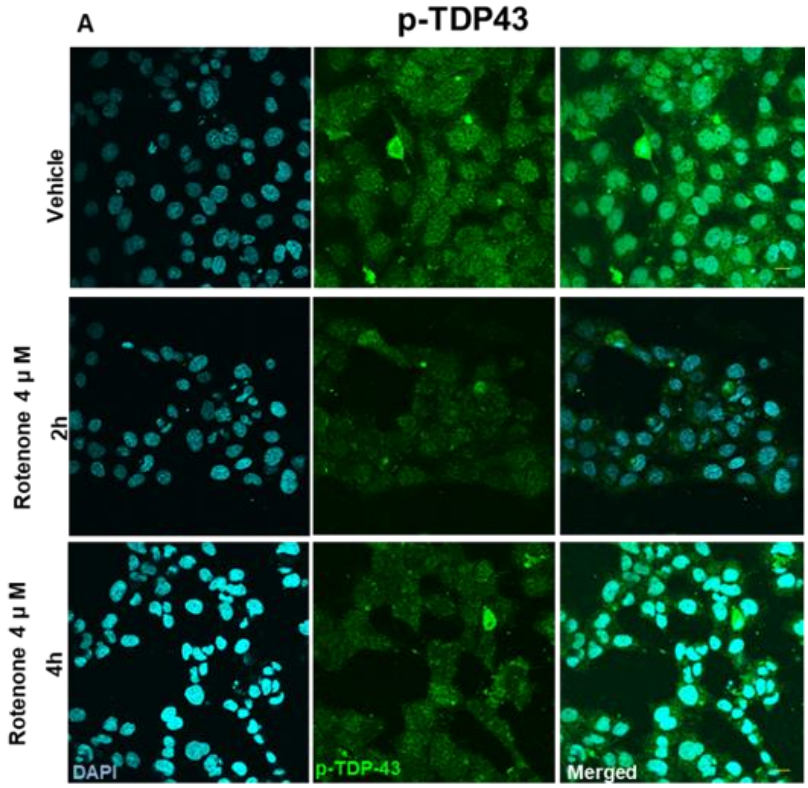
A
p-TDP43
Vehicle
Rotenone 4 µ M
2h
Rotenone 4 µ M
4h
DAPI
p-TDP-43
Merged

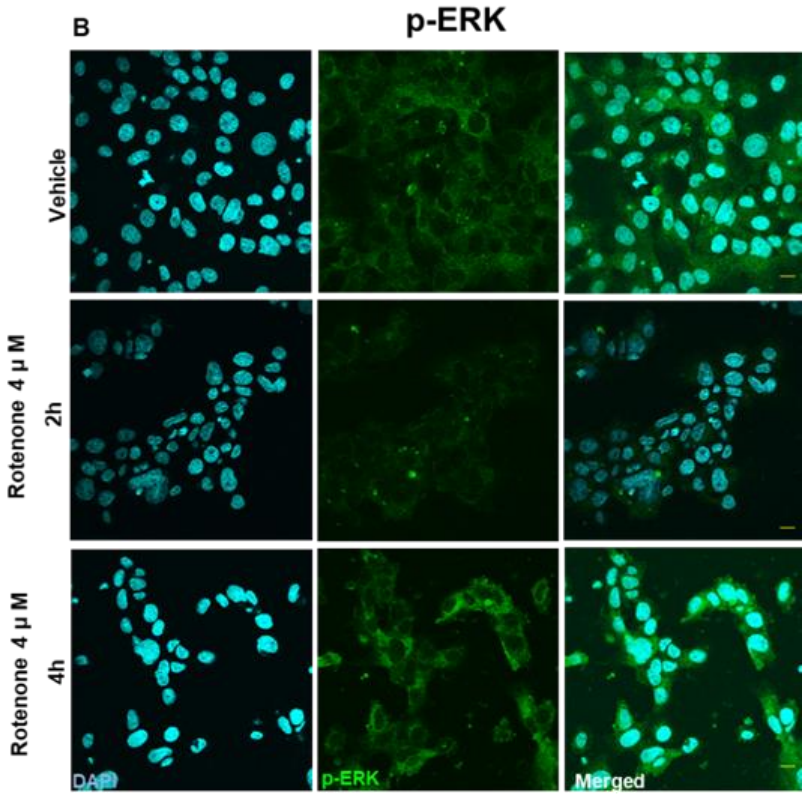
B
p-ERK
Vehicle
Rotenone 4 µ M
2h
Rotenone 4 µ M
4h
DAPI
p-ERK
Merged

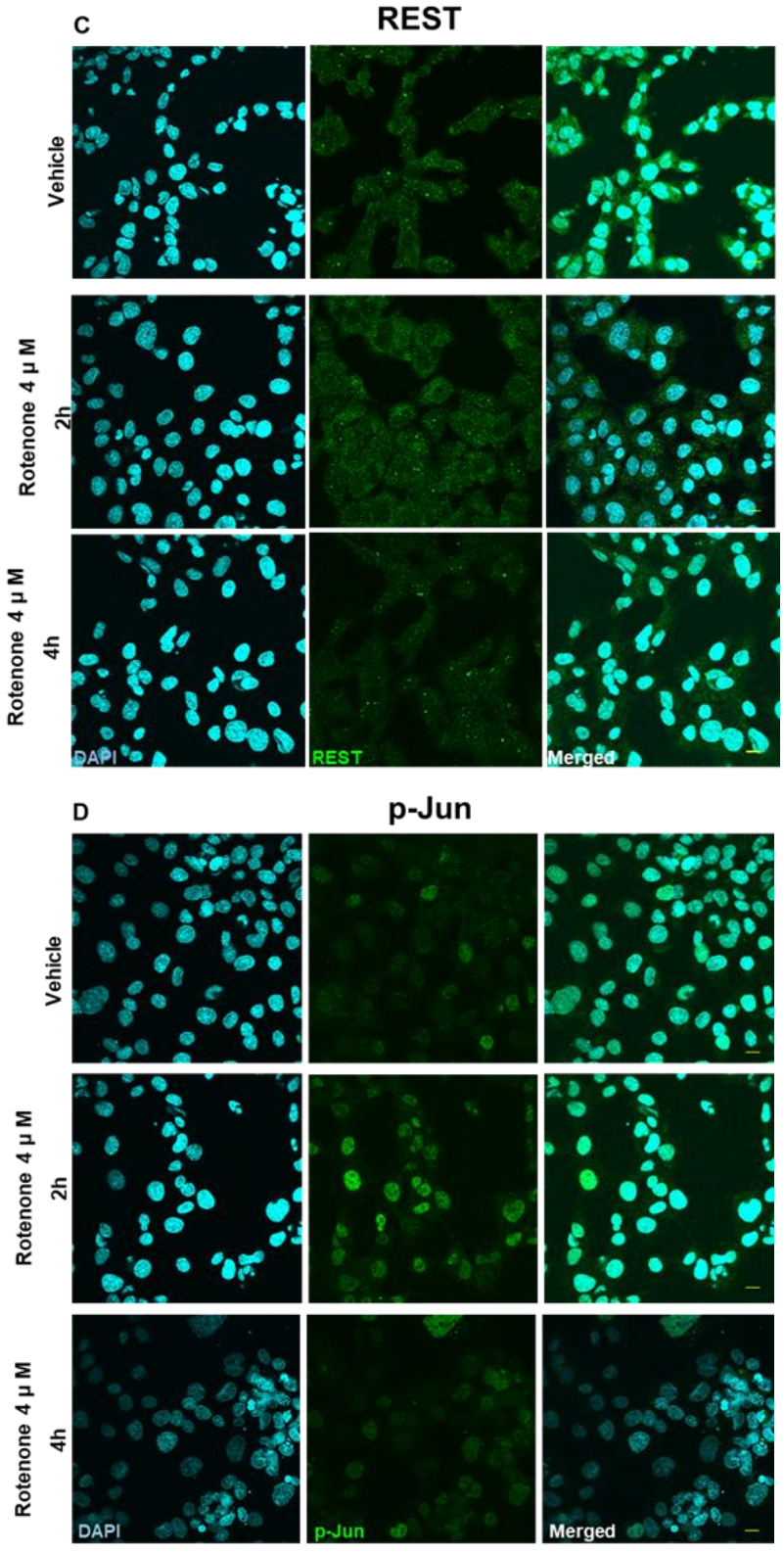

Figure 34. **Mitochondrial stress induces changes in the levels of proteins implicated in neurodegeneration.** Representative confocal microscopy images of HMEC-1 cells immunostained with antibodies against p-TDP-43 **(A)**, p-ERK **(B)**, REST**(C)**,p-Jun **(D)** top to bottom. Diverse effects of mitochondrial stress (rotenone, dose and time indicated) are shown in nuclear and non-nuclear (cytosol) immunostaining. Bars are 60 micrometers long.

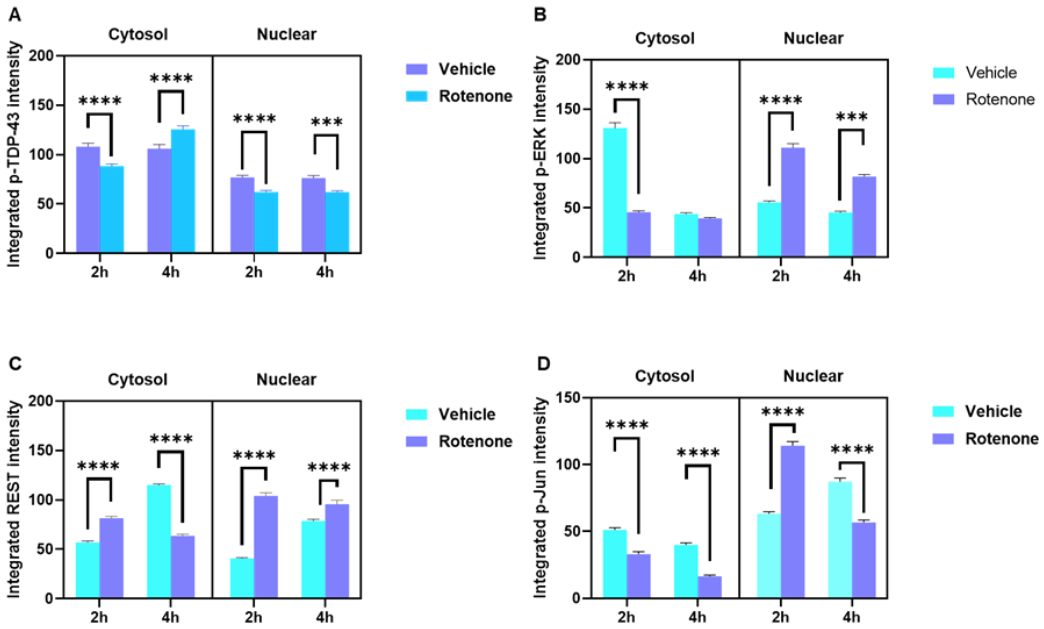

Figure 35. Quantification of the changes in the levels of proteins implicated in neurodegeneration in their nuclear and non-nuclear (cytosol) immunostaining after the induction of complex I dysfunction by rotenone (4μM, 2 and 4 hours). Bars indicate the mean with the standard deviation shown by the lines (n = 387- 405 cells for p-TDP-43 **(A)**, n = 450–462 for p-ERK **(B)** , n = 467-469 for REST **(C)** and n =508-470 for p-Jun **(D)**, obtained in at least 4 independent replicates). * Indicates $p < 0.05$, ** $p < 0.01$, *** $p < 0.001$, and **** $p < 0.0001$ by Sidak's post-hoc multiple comparison test after a 2-way ANOVA.

The induction of mitochondrial stress in HMEC-1 cell culture also determined changes in the interaction between the proteins of interest and the mitochondrial epitope Complex V. As shown in Figures 36A and 37A, colocalization between p-TDP43 and Complex V increased significantly at 4 hours of treatment, while the same tendency was observed at the shorter time (2h), being non-significant.

An opposite trend was observed for p-ERK. Its level of colocalization with mitochondria significantly increased at 2 hours of treatment, with the same tendency being reported at 4 hours being non-significant (Figures 36B and 37B)

The transcriptional factor that showed the higher increase in its mitochondrial colocalization was REST, which levels of interaction with Complex V epitope appear to be significantly increased both at 2 and 4 hours of treatment (Figure 36C and 37C).

Lastly, concerning p-Jun, a significant increase in mitochondrial colocalization only was observed at 4 hours of treatment with rotenone. At the shorter time of treatment, we observed a similar tendency even if it was not statistically significant (Figure 36D and 37D).

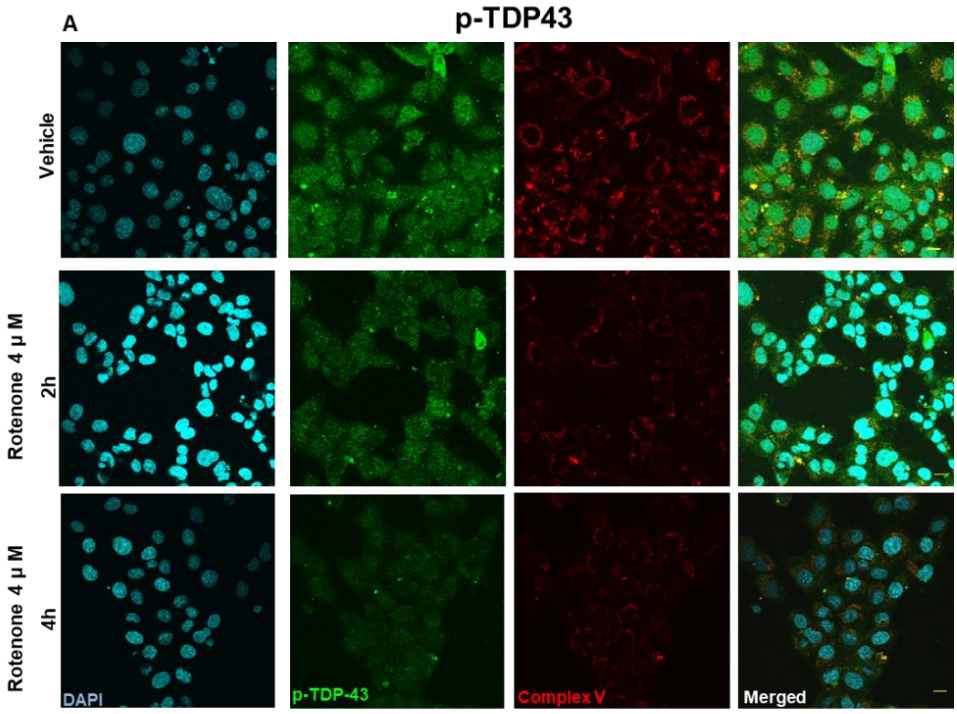
A
p-TDP43
Vehicle
Rotenone 4 µ M
2h
Rotenone 4 µ M
4h
DAPI
p-TDP-43
Complex V
Merged

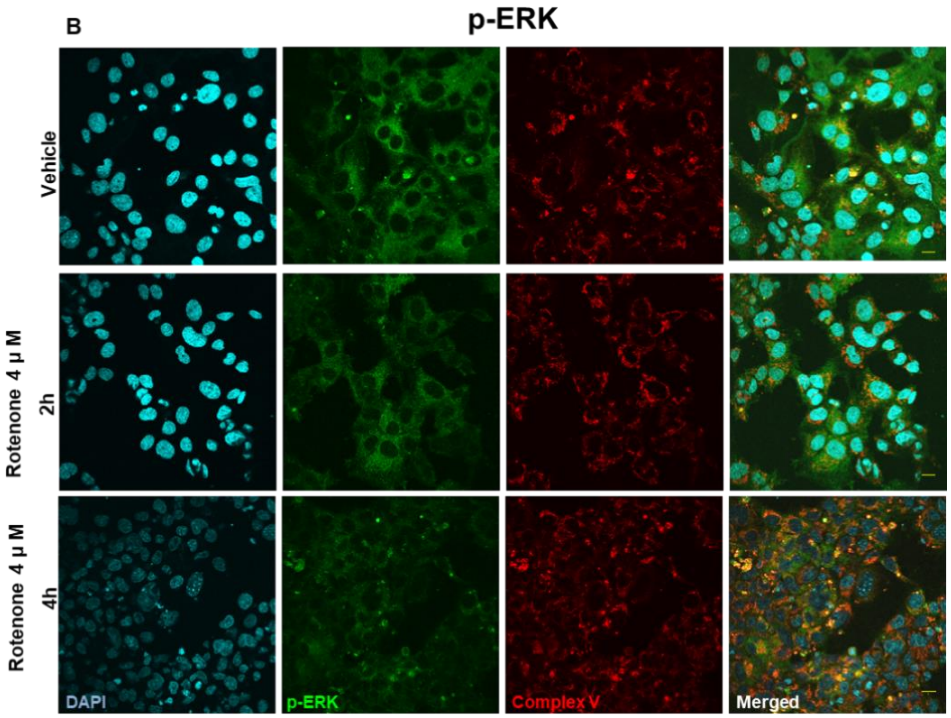
B
p-ERK
Vehicle
Rotenone 4 µ M
2h
Rotenone 4 µ M
4h
DAPI
p-ERK
Complex V
Merged

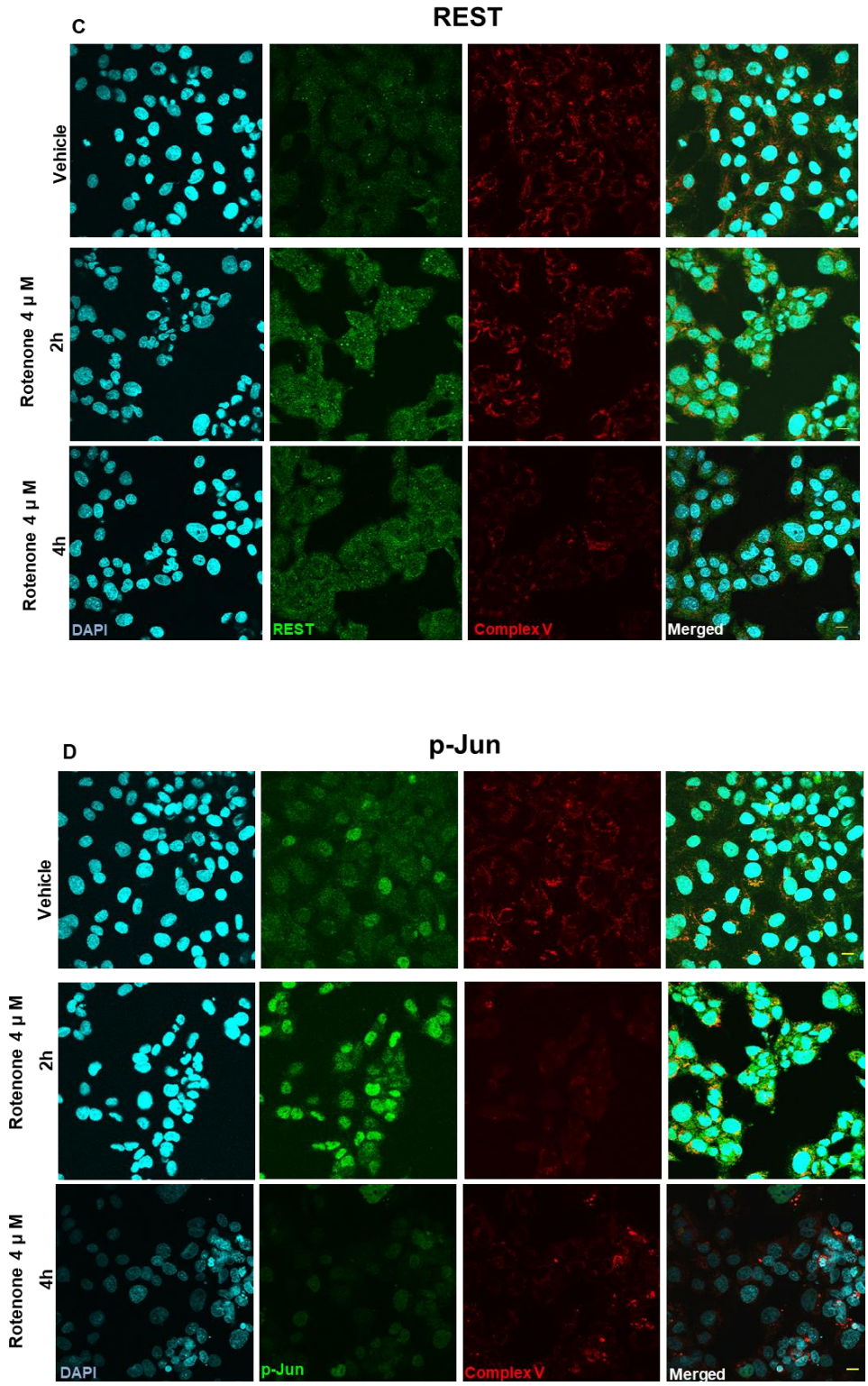

Figure 36. Complex I dysfunction induces changes in colocalization of ALS-related proteins with mitochondrial epitopes. Representative confocal microscopy images of HMEC cells immunostained with antibodies against p-TDP43 (A), p-ERK (B), REST (C) and p-Jun (D) showing diverse effects of mitochondrial stress induced by rotenone on p-TDP43 colocalization with the mitochondrial epitope Complex V. Bars are 60 micrometers long.

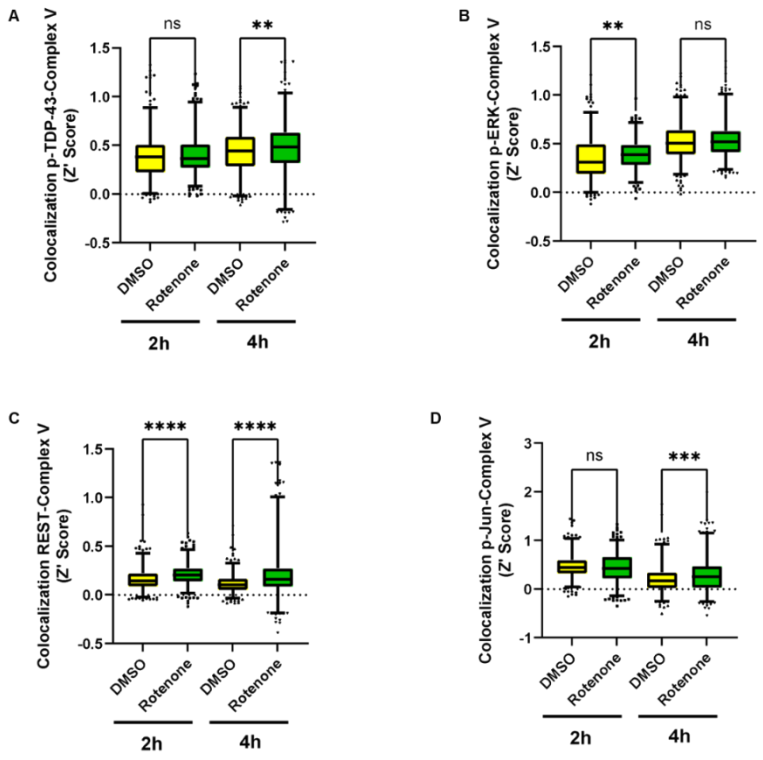

Figure 37. Quantification of the degree of colocalization between the proteins of interest p-TDP43 (A), p-ERK (B), REST (C) and p-Jun (D) and the mitochondrial epitope Complex V estimated by calculation of the z' factor. In the graphs, the bars indicate the mean with the standard deviation shown by lines. ** indicates, $p < 0.01$*** Indicates $p < 0.001$ and **** $p < 0.0001$ by Sidak's post-hoc multiple comparison test after a 1-way ANOVA. The bars in confocal microscopy images are 60 micrometers long.

3.1.4 Validation of the results in a murine model of ALS-related neurodegeneration

To validate these results in an independent setup, we evaluated the above described mislocalization phenomena in a murine model of ALS-related neurodegeneration.

For this purpose, we employed TDP-43^{Q331K} mice overexpressing the human mutated TDP-43 gene. The results of the subcellular fraction in the brain agree with the in vitro findings. Thus, both TDP-43 and ERK are present in crude mitochondria, a subcellular fraction enriched in mitochondria but also containing other membranes (Figure 38 and Supplemental Figure SF2, Annex I). Indeed, as expected, human TDP-43 (h-TDP-43) was highly enriched in the cytosol, nuclei, and crude mitochondria fraction. Demonstrating that TDP-43 location in the crude mitochondria was not an artifact of the overexpression of this gene, endogenous murine Tdp-43 (mTdp-43) was also present, as evidenced by Western blotting (Figure 28). The analyses of variance demonstrated that the TDP-43 amount was significantly affected by transgenesis (22% of the total variation, $p < 0.001$, after a three-

way ANOVA. In contrast, the subcellular location strongly influenced the p-TDP-43 levels (47% of the variation, $p < 0.0001$), followed by sex (13.6% of the variation, $p < 0.0035$), but not the transgenesis (Figure 38). In general, the values of p-TDP-43 were higher in female mice (Figure 38 and Supplemental Figure SF3 for males, Annex I), and in both genders, the levels of p-TDP-43 were higher in the crude mitochondria than in cytosol (Figure 38).

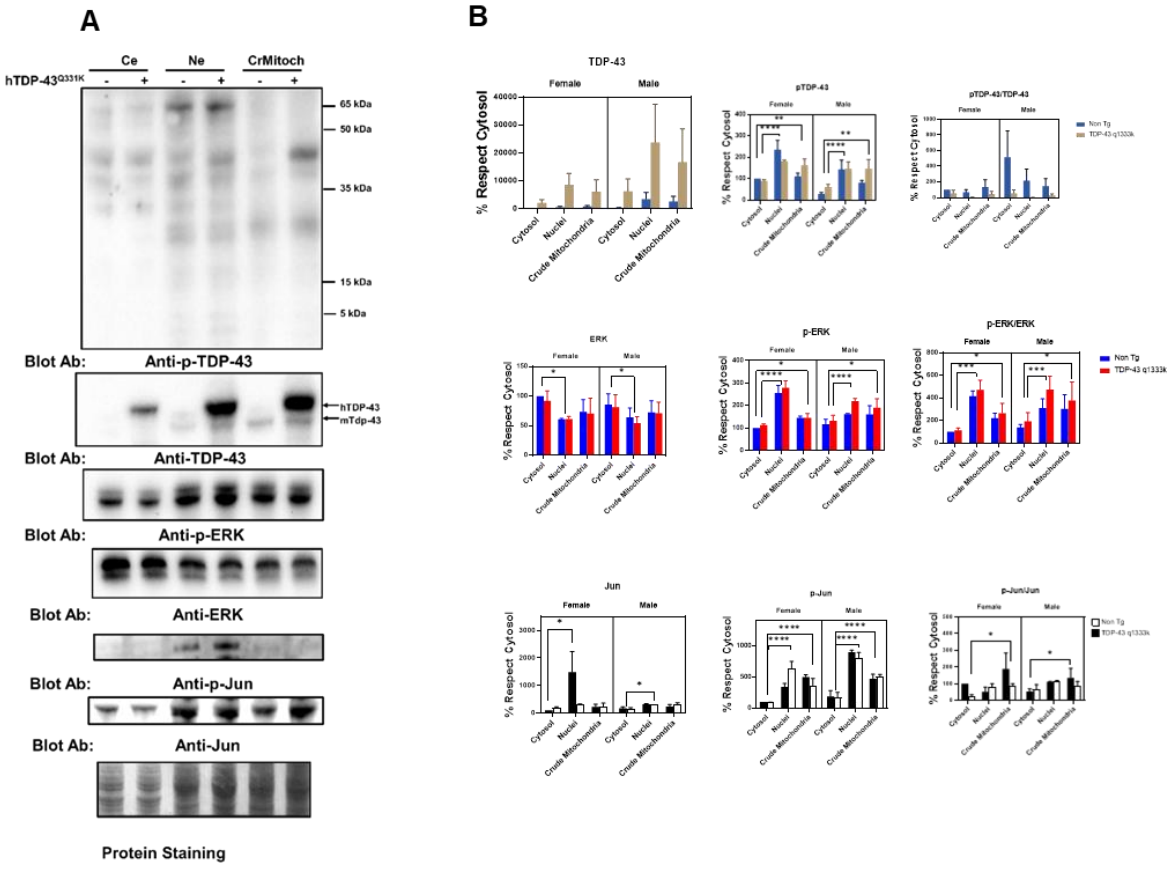

Figure 38. Cellular subfractionation evidence for the in vivo colocalization of the proteins implicated in neurodegeneration with the mitochondrial components. As shown by the Western blot analyses of brain lysates after subcellular fractionation, in addition to the nuclear-enriched (Ne) and cytosolic-enriched (Ce) compartments' crude mitochondrial fractions (CrMitoch), both non-transgenic and transgenic hTDP-43 mice show the presence of p-TDP-43, p-ERK, and Jun. The levels were quantified by densitometry in the brains from 90-day-old mice. The Western blots shown are for female specimens. Right panels **(B)** indicate the quantitative analyses. Bars indicate the mean values with lines showing the standard deviation. * Indicates $p < 0.05$, ** $p < 0.01$, *** $p < 0.001$, and **** $p < 0.0001$ by Dunnett's post-hoc multiple comparison test after a three-way ANOVA (n = 4 different mice from each genotype and sex). The ANOVA values are shown in the text. Concerning ERK, the findings in the spinal cord of that murine model reinforce the in vitro data. Thus, in line with the colocalization of p-ERK with complex V, the crude mitochondria showed a relevant concentration of p-ERK. However, the nuclear fractions showed a high concentration of p-ERK, while the total ERK levels were significantly lower in the nuclei than cytosol (Figure 38A). Densitometry analyses indicated that the total ERK levels were not significantly influenced by the sex, transgene expression, or subcellular fraction. However, when evaluating p-ERK, the subcellular location influenced, to the greatest extent, its levels (52% of the variation, $p < 0.0001$), with sex interacting with the subcellular location also being a relevant factor (13.8%, $p < 0.008$).

Concerning p-Jun, we detected its presence mainly in nuclear fractions, with almost no detection in the crude mitochondrial fraction or cytosol. After densitometry, most of the variance was explained by the subcellular location (63% of the variance, $p < 0.0001$), with sex also influencing the values (9.6%, $p < 0.006$). TDP-43 overexpression only explained 4% of the total variance in the sex and subcellular location ($p < 0.04$). Nonetheless, we evidenced the presence of Jun in the three fractions examined. Thus, densitometry showed that the subcellular location explained more than 16% of the total variance ($p < 0.03$, Figure 40) , with no significant influence of the sex or TDP-43 overexpression.

Finally, the analyses of the subcellular fractionation of murine brains revealed that the crude mitochondrial fractions, in line with the immunostaining measurements, contained a non-negligible amount of REST (Figures 39A and 39B). Crude mitochondria were the subcellular fraction with a higher concentration of REST. Regarding the influence of specific factors, neither sex nor TPD-43 overexpression was a significant factor contributing to the variance, in contrast with the subcellular location (39% of the variation, $p < 0.0043$).

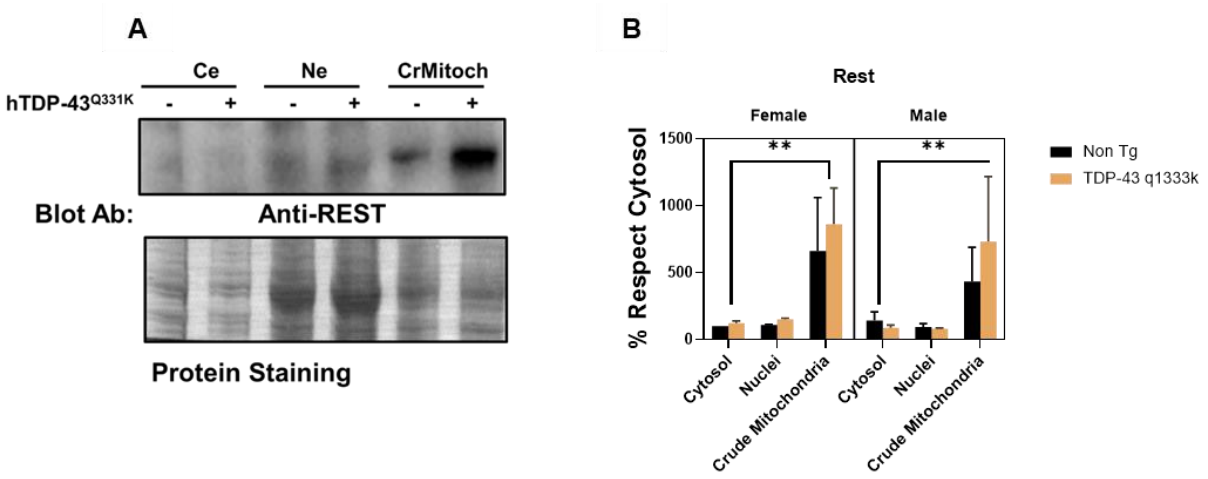

Figure 39. (A) Representative Western blots from brain lysates, indicating that REST is localized within crude mitochondria (CrMitoch), in comparison with enriched nuclei (Ne) or cytosolic extract (Ce). (B) Levels were quantified by densitometry in brains from 90-day-old mice. Western blots shown are for female specimens. Bars indicate the mean values with lines showing the standard deviation. (n = 4 different mice from each genotype and sex).

3.1.5 Effect of REST target genes on SHSY-5Y under TDP-43 aggregation induced by osmotic stress

Besides a nonsignificant trend for an increase in REST in transgenic mice, we evaluated the potential effect of a mutated TARDBP overexpression in well-established REST targets by RT-qPCR. The results showed that one downstream REST, CYCS mRNA, was increased almost significantly in the TARDBP transgenic mice (Figure 40B).

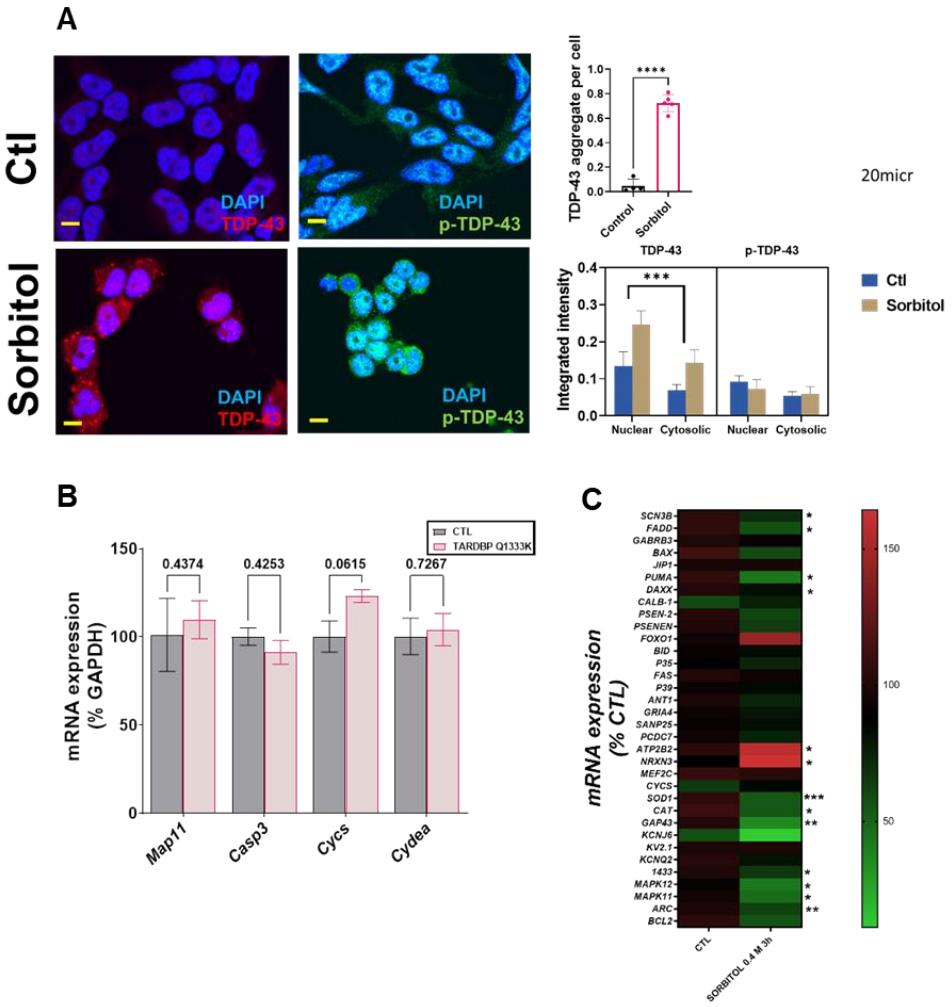

Figure 40. Cell stress-induced mislocalization of TDP-43 is associated with changes in REST-regulated genes. (A) Shows representative immunofluorescence images of HEK-293 under osmotic stress (Sorbitol, 0.4 M, 4 h), demonstrating that both TDP-43 and p-TDP-43 are localized in a non-nuclear location as aggregates after sorbitol incubation (graphs in the right panel). **(B)** Shows the effect of mutated TARDBP overexpression in the mRNA levels of REST-regulated genes in brain lysates, quantified by RT-qPCR. Bars indicate mean values with lines showing the standard deviation (n = 3 mice from each genotype). **(C)** Shows a heatmap of the mRNA expression levels of REST-regulated genes in SHSY-5Y cells under osmotic stress, with the scale on the right showing the relative overexpression (in red) or downregulation (in green), quantified by RT-qPCR. * Indicates $p < 0.05$, ** $p < 0.01$, *** $p < 0.001$, and **** $p < 0.0001$ by Dunnett's post-hoc multiple comparison test after a three-way ANOVA (in (A) for the integrated intensity of p-TDP-43 or TDP-43 in confocal immunofluorescence analyses), for the Student's t-test (in (C) for the number of aggregates; n = 150 different cells quantified in each condition or 4 independent RT-qPCR experiments in (B) or in (D)). The bars in (A) are 20 micrometers long.

To further confirm the interaction between TDP-43 and REST, we set up an in vitro model of TDP-43 and p-TDP-43 aggregation in HEK-293 cell line. Thus, after sorbitol incubation (Figure 40A), both the number of TDP-43 aggregates and global intensity of TDP-43, but not p-TDP-43, were increased, with a high amount of TDP-43 in nuclear location. Thus, both the subcellular location (18% of the variance, $p < 0.0001$) and sorbitol incubation (11.2% of the variance, $p < 0.0165$) strongly influenced the TDP-43 immunostaining intensity. In this particular model, we explored the effect of REST targets on SHSY-5Y cells. The results of the RT-qPCR revealed that TDP-43 aggregation induced by sorbitol incubation was associated with significant decreases in the mRNA levels of SCN3B, FADD, PUMA, DAXX, SOD1, CAT, GAP43, 1433, MAPK11, MAPK12, and ARC, known REST targets. Sorbitol incubation also increased some REST targets such as NRX3 and ATP2B2 (Figure 40C).

To evaluate if TDP-43 aggregation can be related to mitochondrial dysfunction, we evaluated if sorbitol incubation in these conditions led to alterations in the cellular ATP production. The results (Supplemental Figure SF4) suggest that both mitochondrial and glycolysis-linked ATP production is severely affected by sorbitol incubation.

To establish if the stress mentioned above could be behind the changes in the transgenic TDP-43 model, we also studied the effects of the proteasome and ER stress in the levels and distribution of REST in the non-neuronal cell line studied. For epoxomicin treatment, an early (2-h) increase in the REST intensity in the cytosol was followed by a decrease in the nuclear amount (at 4 h, Figure 41A). The degree of colocalization with the mitochondrial markers diminished as well (data not shown). Additionally, the results showed that ER stress increased the cytosolic and nuclear amounts of REST at longer times studied (Figure 41B) and also due to changes in the degree of colocalization with the mitochondria (z-values decreased by 20% in the epoxomicin treatment).

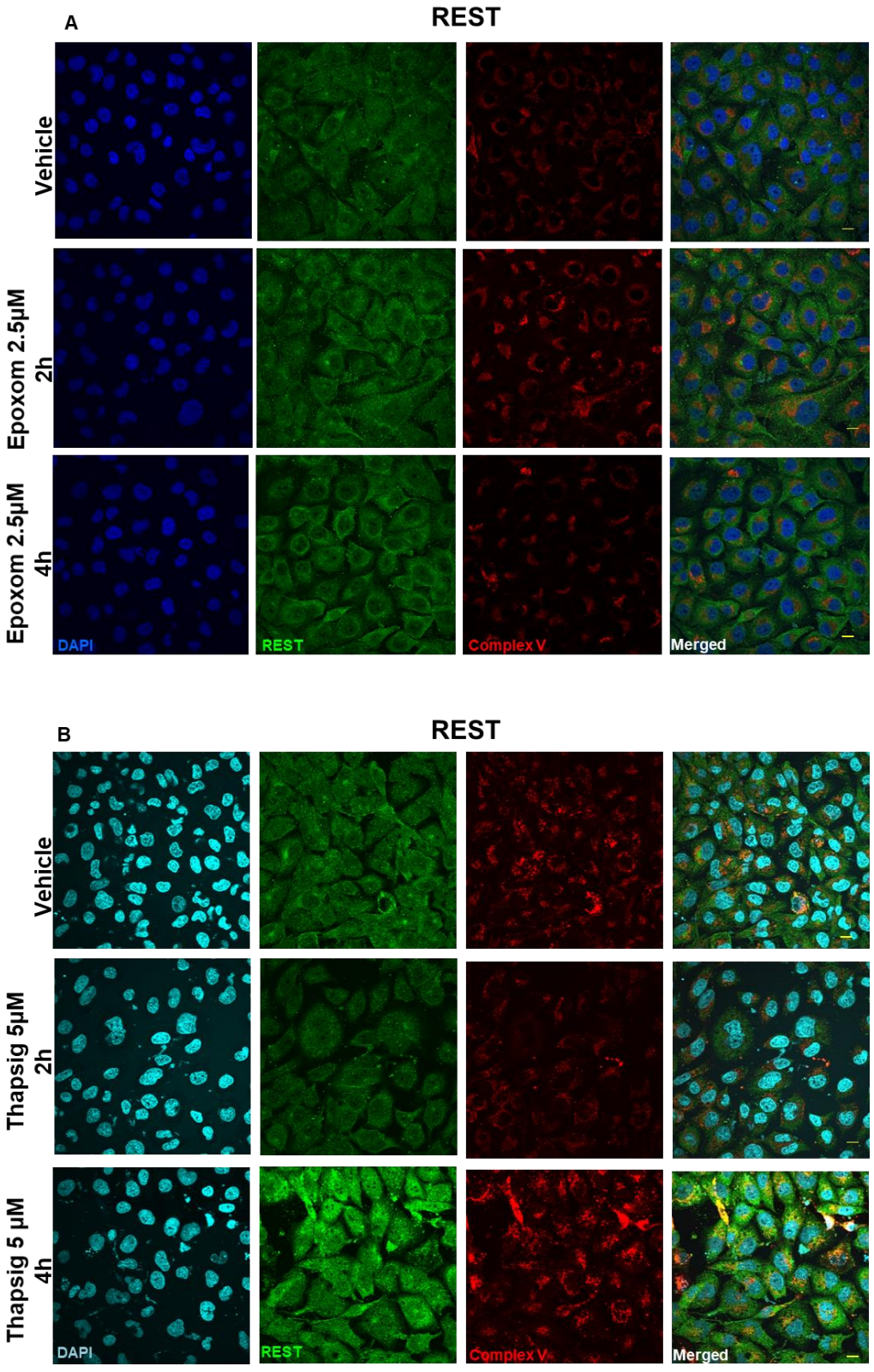
A
REST
Vehicle
Epoxom 2.5μM 2h
Epoxom 2.5μM 4h
DAPI
REST
Complex V
Merged
B
REST
Vehicle
Thapsig 5μM 2h
Thapsig 5 μM 4h
DAPI
REST
Complex V
Merged

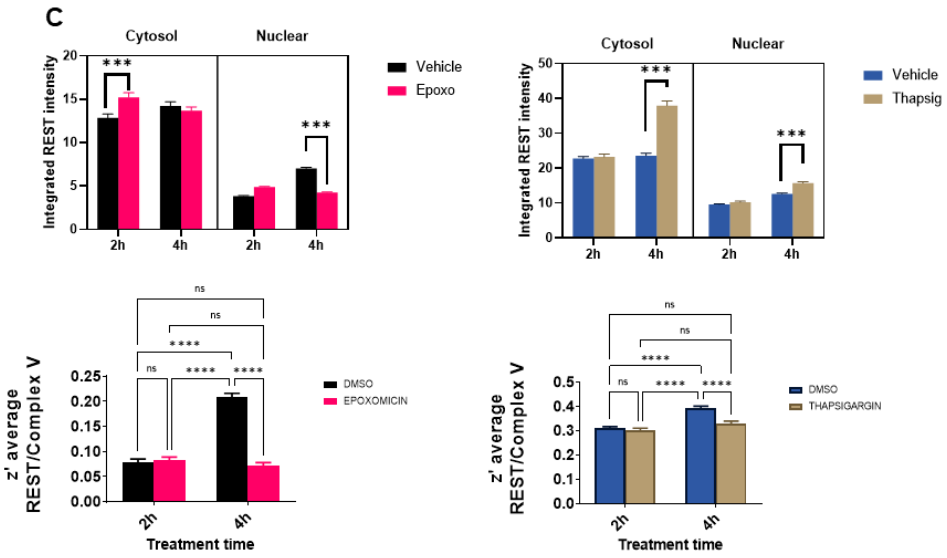

Figure 41. ER and proteasome stress induces changes in the levels of REST and its colocalization with the mitochondrial epitopes. Representative confocal microscopy images of HMEC cells immunostained with antibodies against REST, and the mitochondrial complex V showing the diverse effects of proteasome stress **(A)** and ER stress **(B)** (n = 365–559 different cells). Images shown are for 2 and hours of incubation. In **(C)**, the bars indicate the mean with the standard deviation shown by lines. *** Indicates $p < 0.001$ by Sidak's post-hoc multiple comparison test after a 2-way ANOVA. The bars in the (A) and (B) micrographs are 60 micrometers long.

3.2 Effect of ALS-related cellular stresses on mitochondrial dynamics in HMEC-1 cell line

As already mentioned before, mitochondrial dysfunction is a common event in the pathogenesis of neurodegenerative diseases such as ALS (Song, 2012). Mitochondrial fission is mediated by dynamin-related protein 1 (DRP1) while fusion is linked to mitofusin 1/2 (MFN1/2) and optic atrophy 1 (OPA1), which are essential for mitochondrial function. Mutations in the mitochondrial fission and fusion machinery lead to neurodegeneration. Thus, whether defective mitochondrial dynamics participates in ALS requires further investigation (Song, 2012).

In this work, we aimed to clarify if ALS-related cellular stress can have an impact on mitochondrial dynamics. Thus, we employed automatized analysis of the mitochondrial channel in confocal images of HMEC-1 cells to investigate on potential changes in mitochondrial morphology or networks formation, following the induction of oxidative, proteasomal, ER and mitochondrial stress. Figure 36 summarizes the effect of oxidative stress on the number of individual mitochondria, the number of mitochondrial networks and the network index (defined as the ratio between the individual mitochondria number and the number of mitochondrial networks per cell) in HMEC-1 cells, following treatment

with H_2O_2, fixation and staining of the mitochondrial channel in red (Complex V epitope). The effect of oxidative stress on mitochondrial dynamics appears to be negligible upon the milder condition tested (Figures 42A, 42B and 42C H_2O_2 4µM/ 30'). In fact, changes in three parameters mentioned above are non-significant. The opposite is true upon the harshest oxidative stress induction (Figures 42A, 42B, and 42C, H_2O_2 200µM/ 60') with a significant increment not only in the number of individual mitochondria per confocal field (Figure 42B), but also in the number of mitochondria networks (Figure 42C).

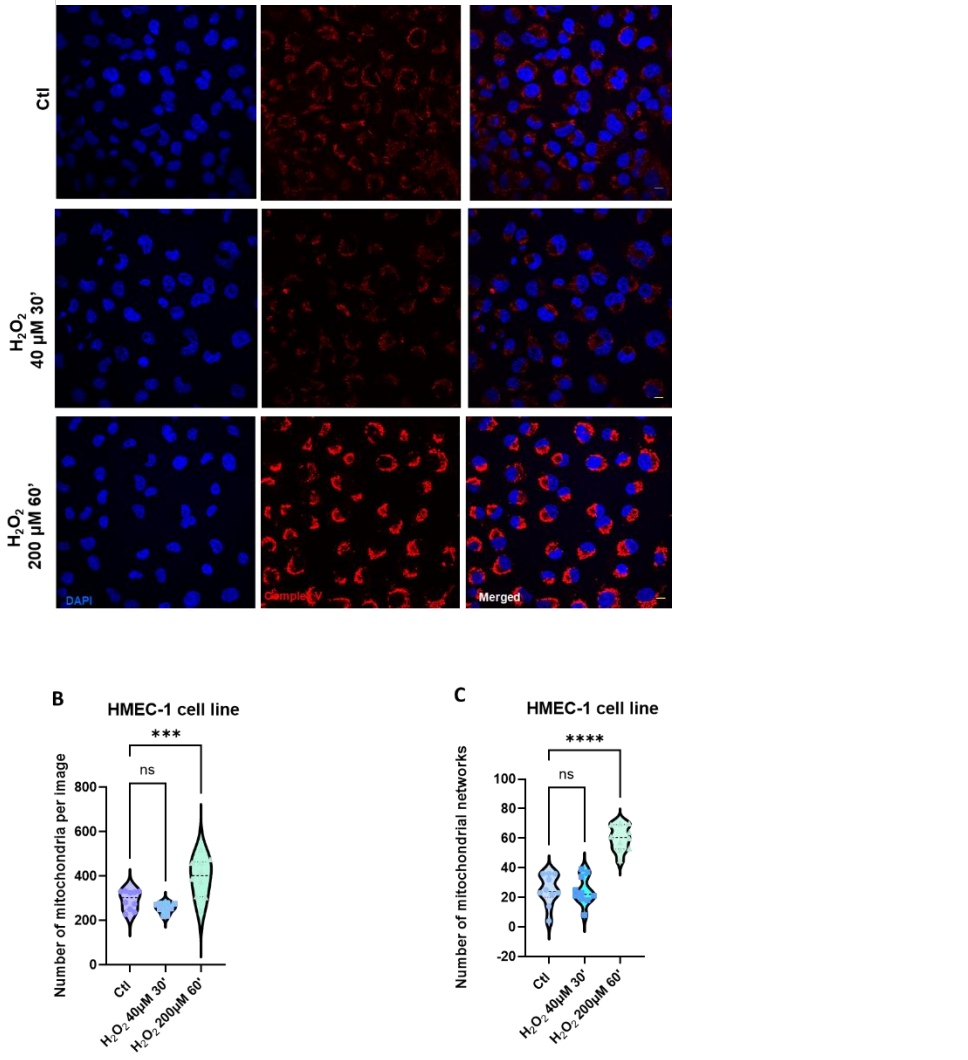

Figure 42. Oxidative stress induces changes in mitochondrial dynamics in HMEC-1 cell line. **(A)** Representative confocal microscopy images of HMEC-1 cells immunostained with anti-ComplexV antibody. Images were processed with MiNA macro in ImageJ to study mitochondrial dynamics. **(B)** Oxidative stress induces changes in the number of mitochondria per confocal field in HMEC-1 cell line. **(C)** Oxidative stress induces changes in the number of mitochondrial networks per confocal field in HMEC-1 cell line. *** indicates $p < 0.001$, and **** $p < 0.0001$ by post hoc test after one-way ANOVA. Bars in (A) are 60 micrometers long.

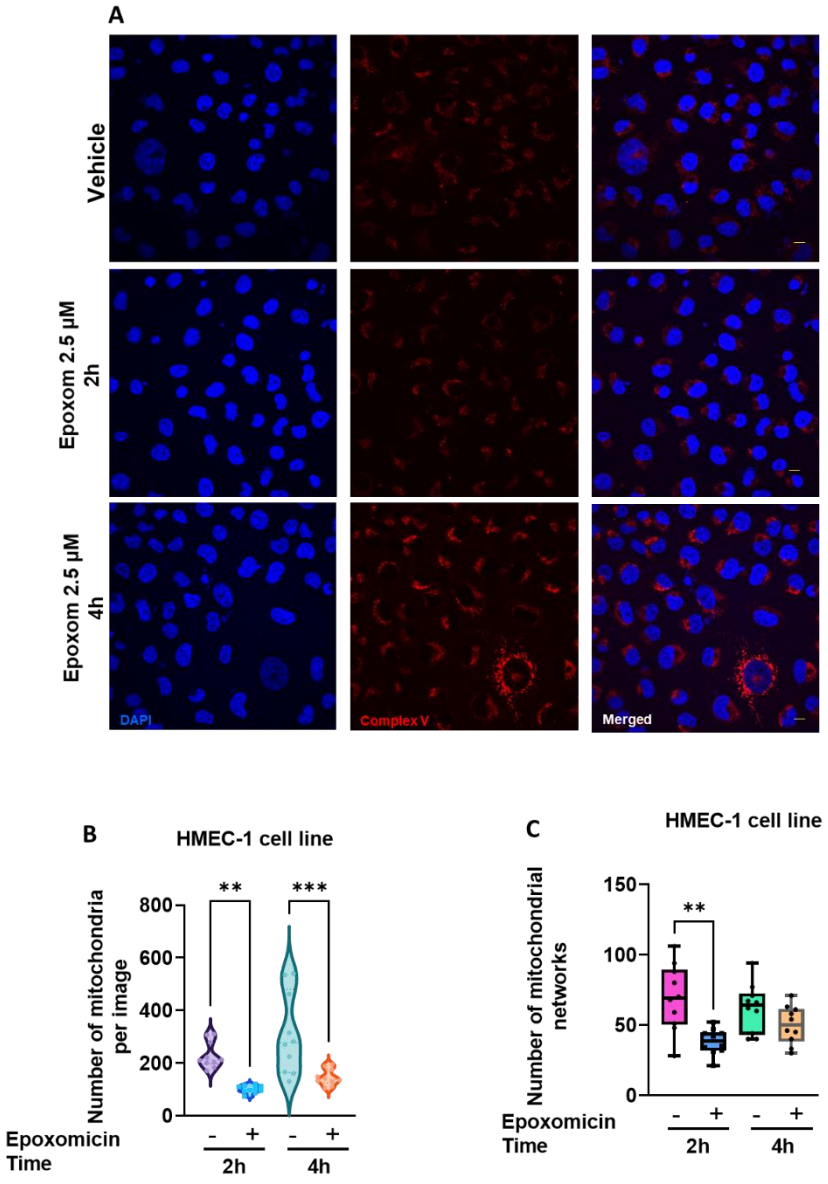

Figure 43. Proteasomal stress induces changes in mitochondrial dynamics in HMEC-1 cell line. (A) Representative confocal microscopy images of HMEC-1 cells immunostained with anti-ComplexV antibody. Images were processed with MiNA macro in ImageJ to study mitochondrial dynamics. **(B)** Proteasomal stress induces changes in the number of mitochondria per confocal field in HMEC-1 cell line. **(C)** Proteasomal stress induces changes in the number of mitochondrial networks per confocal field in HMEC-1 cell line. ** Indicates $p < 0.01$, and *** $p < 0.001$, by one-way ANOVA. Bars in (A) are 60 micrometers long.

Concerning proteasomal stress, the number of individual mitochondrial diminished significantly both at 2 hours and 4 hours of treatment with epoxomicin (Figures 43A and 43B), while reorganization in networks was significantly decreased only at the shorter time of treatment; this tendency was preserved at the longer time of treatment even if differences between control and treated cells were non-significant (Figures 43A and 43C).

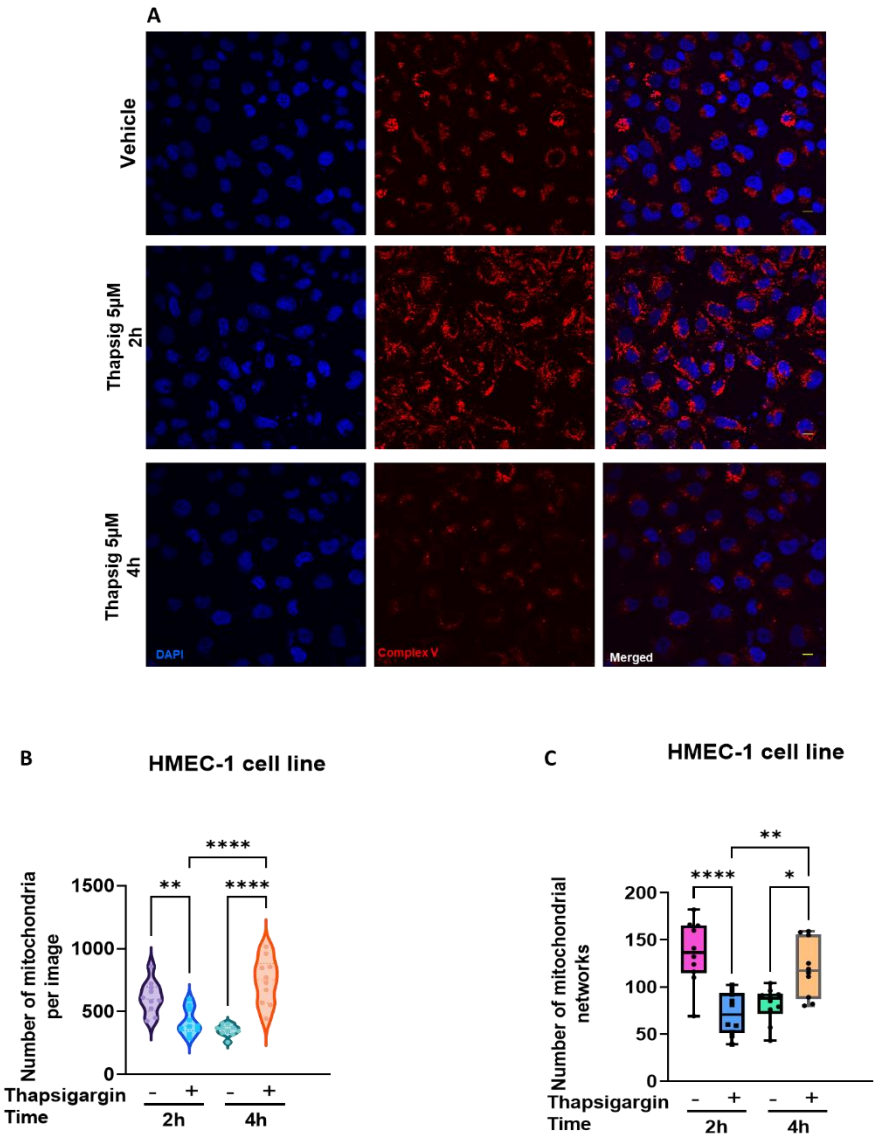

Figure 44. ER stress induces changes in mitochondrial dynamics in HMEC-1 cell line. **(A)** Representative confocal microscopy images of HMEC-1 cells immunostained with anti-ComplexV antibody. Images were processed with MiNA macro in ImageJ to study mitochondrial dynamics. **(B)** ER stress induces changes in the number of mitochondria per confocal field in HMEC-1 cell line. **(C)** ER stress induces changes in the number of mitochondrial networks per confocal field in HMEC-1 cell line. * Indicates $p < 0.05$, ** $p < 0.01$, *** $p < 0.001$, and **** $p < 0.0001$ by one-way ANOVA. Results derive from 4 independent replicates. Bars in (A) are 60 micrometers long.

ER stress induced by treatment with thapsigargin determined a significant decrease in the number of individual mitochondria per image at the shorter time of treatment. Nevertheless, the phenomenon was reversed at 4 hours, with a strongly significant increase, both in comparison with cells treated for 2 hours and cells exposed to vehicle (DMSO) for 4 hours (Figure 44A and 44B). Regarding the number of mitochondrial networks, after a strongly significant ($p< 0.0001$) decrease of this parameter following treatment for 2 hours, the tendency was preserved at 4 hours, even if with a p value lower

than 0.05. Also, the number of mitochondrial networks is higher ($p<0.01$) in cells exposed to the stressors for 4 hours than in cells treated for 2 hours (Figures 44A and 44C).

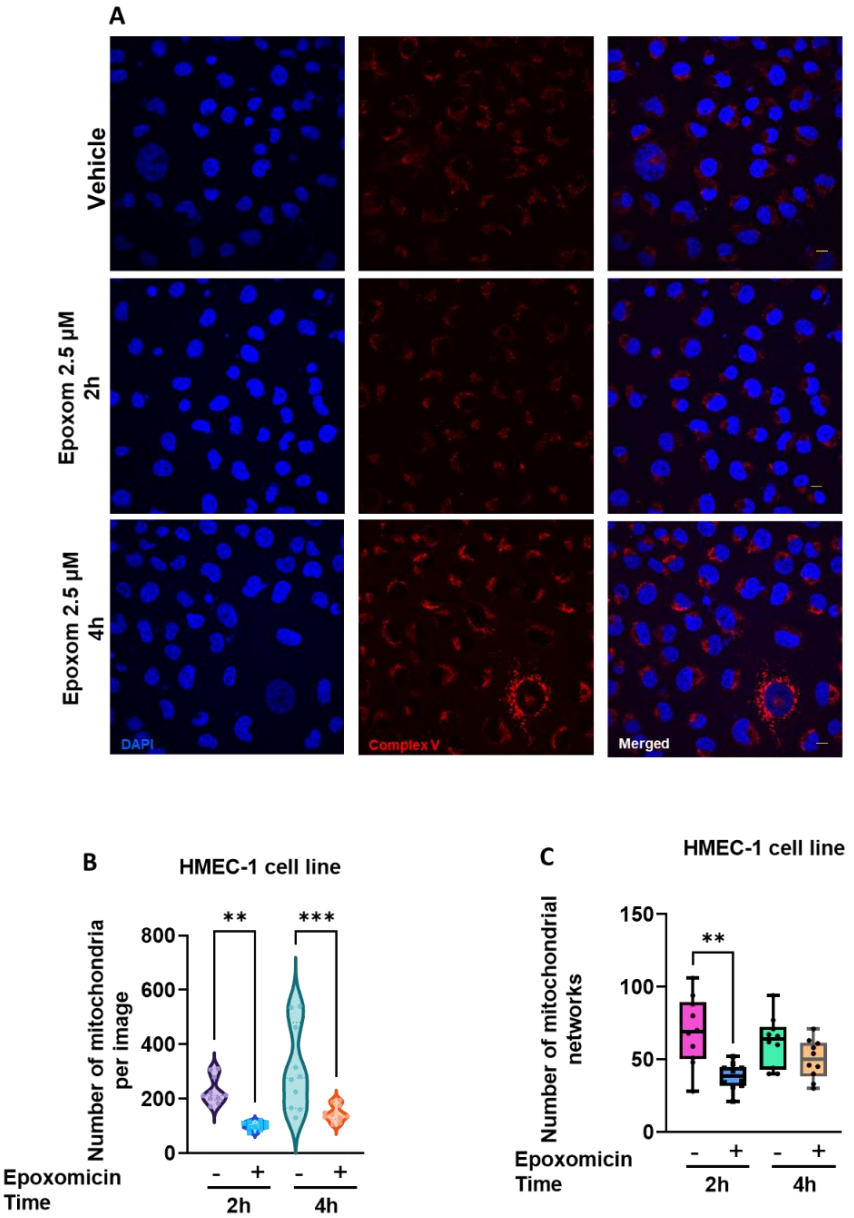

Figure 45. Complex I dysfunction induces changes in mitochondrial dynamics in HMEC-1 cell line. (A) Representative confocal microscopy images of HMEC-1 cells immunostained with anti-ComplexV antibody. Images were processed with MiNA macro in ImageJ to study mitochondrial dynamics. **(B)** Mitochondrial stress induces changes in the number of mitochondria per confocal field in HMEC-1 cell line. **(C)** Mitochondrial stress induces changes in the number of mitochondrial networks per confocal field in HMEC-1 cell line. * Indicates $p < 0.05$, ** $p < 0.01$, and *** $p < 0.001$ by one-way ANOVA. Bars in (A) are 60 micrometers long.

Lastly, we explored the effect of Complex I dysfunction induced by rotenone, on mitochondrial dynamics. In this scenario, the number of individual mitochondrial per

confocal field was diminished ($p < 0.05$) at 2 hours of treatment, while an opposite trend was observed at 4 hours ($p < 0.05$) (Figures 45A and 45B). Concerning the number of mitochondrial networks (Figures 45A and 45C) we didn't observe any significant changes between control and treated cells, suggesting that the treatment affected the number of individual mitochondria with no influence on their organization in networks.

3.3 *Tardbp* genotype and mitochondrial dysfunction in mutant MEFs

3.3.1 Effects of *Tardbp* genotype on cellular respiration and mitochondrial mass of mutant MEFs

Taking advantage of the availability of immortalized MEFs carrying three different *Tardpb* mutations (Q331K, F201I and M323K, see sections 1.2.2.2 and 2.2.6) and the correspondent WT line, we decided to further explore mitochondrial alterations linked to ALS pathophysiology. It has already been reported that ectopic transient expression of TDP-43-Q331K shows increased cytoplasmic accumulation in SH-SY5Y cells (Guerrero et al., 2019). On the contrary in mice carrying F201I and M323K mutations, researchers didn't observe any increase in the aggregative potential of TDP-43 *in vivo*, being the characterization of the pathological motor phenotype still elusive in these models (Rouaux et al., 2018). In particular, we focused on the potential link between *Tardpb* genetic background and mitochondrial dysfunction in terms of cellular respiration and mitochondrial mass. To unmask mitochondrial dysfunctions in terms of respiration and mass, we designed the experimental setting considering two groups of cells for each of the four phenotypes. Control cells were grown as described in section 2.2.6, while their experimental counterpart was exposed to acute metabolic switch (section 2.9).

Cellular respiration was measured in terms of ATP production and divided in the glycolytic and mitochondrial components by respirometry (see section 2.10). Figure 46A shows the results of our experiments on mutant MEFs in comparison with WT. Comparing WT MEFs with the Q331K genotype, we observed a slightly significant increase in ATP production by glycolysis in Q331K mutants upon normal growing conditions; the same trend was preserved in glucose and pyruvate deprived cells ($p<0.01$). Moving to mitochondrial ATP production, a slight decrease in Q331K cells was observed in the control group; the tendency was confirmed for the deprived cells being $p<0.001$. On the other hand, the comparison between WT MEFs and F201I or M323K genotype, didn't produce any significant difference neither in the glycolytic ATP production or in the mitochondrial counterpart.

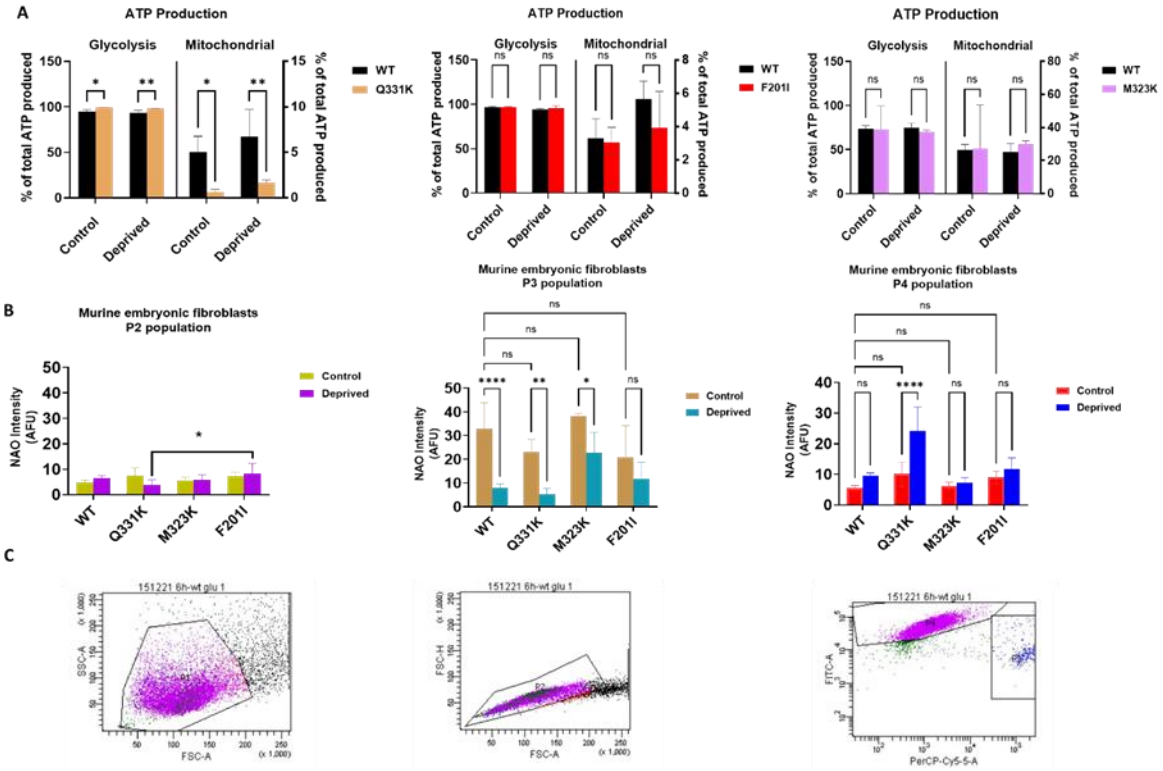

Figure 46. Influence of *Tardbp* genotype on cellular respiration and mitochondrial mass. ATP production rates were estimated by respirometry, separating glycolytic from mitochondrial energy production. **(A)** ATP production measurements were performed comparing WT MEFs with Q331K, F210I and M323K Tardbp mutants, cultured in presence of glucose and pyruvate as anergy substrate (control condition) or replacing glucose with galactose in absence of pyruvate (deprived condition), for 6 hours. Bars indicate the mean with the standard deviation shown by the lines. **(B)** Mitochondrial mass was evaluated in WT and mutant MEFs by flow cytometry after staining with Nonyl Acridine Orange (NAO) in three cellular populations, indicated as P4, P3 and P2, based on cell viability following counterstaining with Propidium Iodide (PerCP-Cy5-5/ PI). Bars indicate the mean with the standard deviation shown by the lines. **(C)** Representative scatter plots derived from flow cytometry analysis of WT MEFs cultured in presence of glucose as energy substrate after double staining with NAO and PI. Starting population P1 (first scatter plot on the left) can be split in sub-populations based on cellular affinity for PI and NAO. P2 indicated the analyzed MEFs population after aggregates exclusion, while P4 and P3 correspond, respectively, to live cells population (high sensitivity for NAO, indicated as FITC in the third scatter plot from the left) and apoptotic cells (high sensitivity to PerCP-Cy5-5, third scatter plot from the left). * Indicates $p < 0.05$, ** $p < 0.01$, *** $p < 0.001$, and **** $p < 0.0001$ by 2way ANOVA. Results derive from 4 independent replicates.

Figure 46B summarizes the results obtained from the measurement of mitochondrial mass by flow cytometry (see section 2.9) comparing each of the genotype upon normal growth conditions with its counterpart following the induction of metabolic stress. Cells were classified in three different population, namely P2, P3 and P4. In the P2 population (the entire pool of cells analyzed after the exclusion of aggregates, see Figure 46C), we didn't observe significant changes in mitochondrial mass between control and deprived cells, except for a slightly significant ($p<0.005$) increase in F201I line, compared with Q331K upon metabolic switch assay. In P3 population (see the legend of Figure 46 and Figure 46C for details), a strongly significant decrease in NAO affinity and, consequently, in mitochondrial mass was observed in WT cells upon metabolic switch when compared to its control ($p< 0.001$). The same tendency with $p <0.01$ was maintained for the Q331K genotype, being mitochondrial mass lower following metabolic stress than upon standard growth conditions. Finally, turning to P4 population (see the legend of Figure 48 and Figure 48C for details), a remarkably significant ($p< 0.0001$) increase in mitochondrial mass was observed for Q331K genotype following metabolic stress.

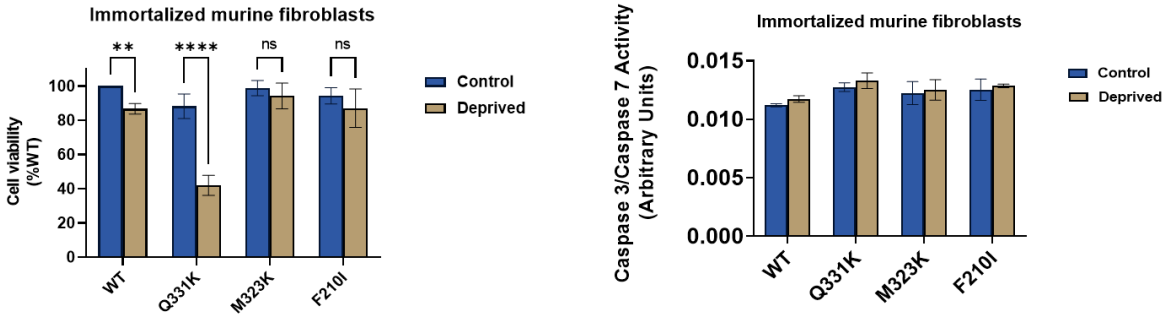

Figure 47. Influence of Tardbp genotype on cellular viability and Caspase3/Caspase 7 activity in MEFs. Cellular viability was estimated by flow cytometry following cellular staining with Propidium Iodine. **(A)** Differences in cell viability of Tardbp mutant MEFs in comparison with WT, upon normal growing conditions (availability of glucose and pyruvate, here indicated as control) or following the induction of metabolic stress (glucose replacement with galactose/ no pyruvate, deprived condition). Bars indicate the mean with the standard deviation shown by the lines. Cell viability of mutant MEFs is expressed as a percentage of WT viability (%WT). **(B)** Caspase3/Caspase 7 activity was estimated by flow cytometry upon the same conditions described in (A), following staining with CellEvent™ Flow Cytometry assay kit. Bars indicate the mean with the standard deviation shown by the lines. ** Indicates $p < 0.01$ and **** $p < 0.0001$ following 2way ANOVA. Results derive from 4 independent replicates.

As described in the legend of Figure 46, WT and mutant MEFs where counterstained with IP in order to measure cell viability by flow cytometry. Figure 47 shows the results of cell viability measurement, reported as a percentage of WT cell viability upon normal growth conditions for mutant lines. Thus, deprived WT show a significant decrease in viability in comparison with control WT ($p < 0.001$), while deprived Q331K genotype

underwent the greater decrease in viability ($p < 0.0001$) when compared with its control. However, non-significant changes were observed concerning viability for M323K and F201I genotypes (Figure 47A).

In order to characterize the cellular death, we observed for WT and Q331K MEFs, we measured the apoptosis indicator Caspase3/Caspase7 activity by flow cytometry, as described in section 2.13. Results show a slightly but not significant increase in the activity of these caspases for each of the genotypes following metabolic switch assay (Figure 47B).

3.3.2 Effects of *Tardbp* genotype on mitochondrial membrane potential and Complex I levels

In post-mortem spinal cord of sporadic ALS patients the activity of all electron transport chain (ETC) complexes, complex I, II, III, and IV was found to be reduced (Wiedemann et al., 2002) In addition, the activity of complexes I and IV were reported to be impaired in skeletal muscle while complex I activity and ATP levels were reduced in lymphocytes of sporadic ALS patient (Smith et al., 2019) Also, in skin fibroblasts obtained from biopsies of sporadic ALS patients the mitochondrial membrane potential (MMP) was increased compared to healthy controls (Ghiasi et al., 2013). Starting from this well-established finding documented in literature, we measured mitochondrial potential in the above mentioned *Tardbp* mutant MEFs, in order to investigate on changes in parameter, which maintenance is pivotal to preserve mitochondrial health (Zorova et al.,2018). Membrane potential was quantify as described in section 2.11. Results in Figure 48A and 48B show non-significant changes in the membrane potential for WT and M323K *Tardbp* genotypes, when comparing control cells with cells exposed to metabolic switch for 6 hours. Interestingly M323K and F210I genotypes showed a very different behaviour, being the membrane potential significantly and strongly decreased in cells cultured in absence of pyruvate and having galactose as energy source ($p<0.0001$ in both cases).

Turning to Complex I, images obtained from confocal microscopy of MEFs were analyzed following indirect immunofluorescence (section 2.5.1.2). Figure 49A shows representative images of MEFs cultured in presence of glucose and pyruvate or in absence of pyruvate and with galactose substituting glucose for 12 hours. Quantification of the membrane potential (Figure 49B) displays non-significant differences for WT, while membrane potential is significantly decreased when comparing control M323K MEFs with deprived counterpart ($p< 0.01$). The remaining genotypes, Q331K and F210I behave

contrarily, showing a slightly significant increase in the case of deprived Q331K MEFs and a strongly significant increase of the potential in the case of deprived F210I MEFs.

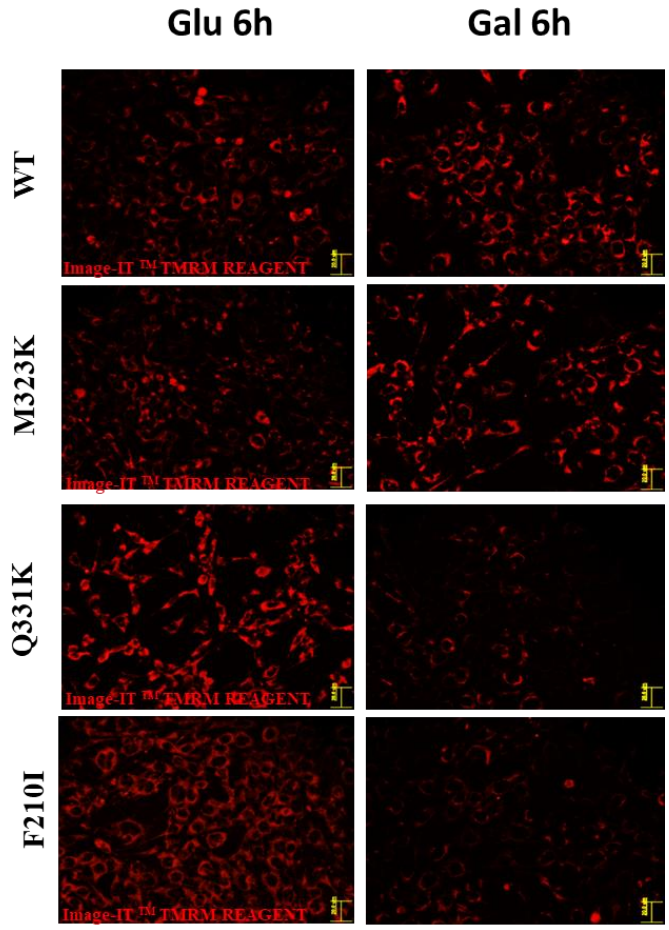

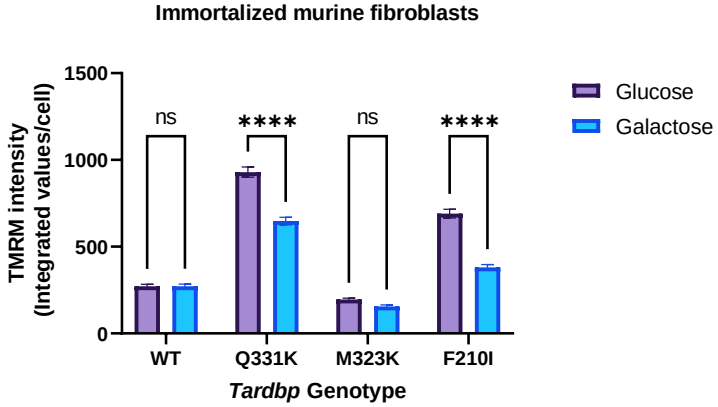

Figure 48. *Tardbp* influences mitochondrial function. **Mitochondrial membrane potential measured using the red-fluorescent probe TMRM in MEFs with different *Tardbp* genetic background cultured either with glucose or galactose as a source of energy for 6 hours. (A)** Representative fluorescence images of living MEFs cultured in standard medium (DMEM supplemented with glucose and pyruvate, left panel) or upon metabolic switch conditions (DMEM containing galactose in alternative to glucose and no pyruvate, right panel). **(B)** Graphical representation of TMRM quantification per cell using a dedicated pipeline in CellProfiler. Results derive from 3 independents replicates. Bars indicate mean values with lines showing the standard deviation. * Indicates $p < 0.05$, ** $p < 0.01$, *** $p < 0.001$, and **** $p < 0.0001$ by Post-hoc analyses after 2way ANOVA. Bars in (A) are 20 micrometers long.

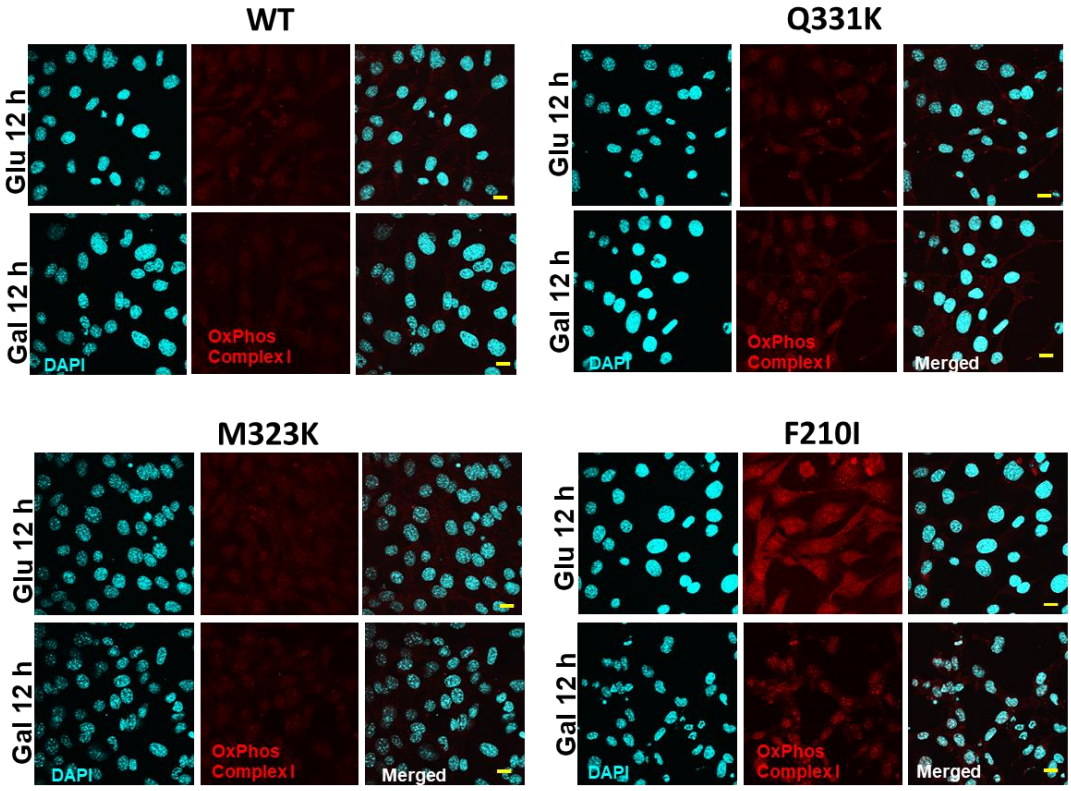

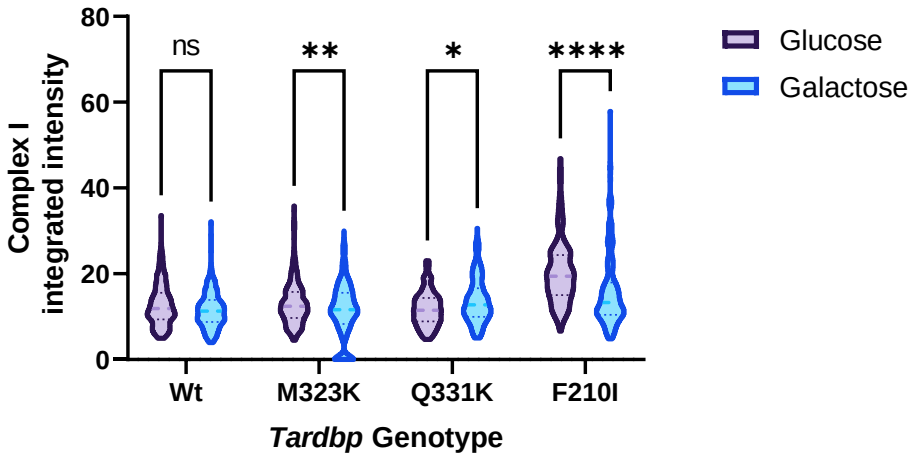

Figure 49. *Tardbp* influences Complex I subunit content. OxPhos Complex I quantification by confocal images analysis of MEFs with different *Tardbp* genetic backgrounds upon normal growth condition (glucose + pyruvate containing medium) or metabolic stress (glucose and pyruvate deprivation) for 12 hours. **(A)** Representative immunofluorescence images of living MEFs cultured in standard medium (DMEM supplemented with glucose and pyruvate, left panel) or upon metabolic switch conditions (DMEM containing glucose in alternative to glucose and no pyruvate, right panel). **(B)** Graphical representation of Complex I quantification per cell using a dedicated pipeline in CellProfiler. Results derive from 4 independent replicates. * Indicates $p < 0.05$, ** $p < 0.01$, *** $p < 0.001$, and **** $p < 0.0001$ by post hoc analyses after a 2way ANOVA. Bars in (A) are 60 micrometers long.

3.4.1 Tardpb genotype influences LDs formation in MEFs upon metabolic switch

It is well known that mitochondria and LDs are essential organelles involved in cellular lipid metabolism and energy homeostasis (L. Cui & Liu, 2020). In stressed cells, lipid droplets guard energy and redox homeostasis and avoid lipotoxicity by sequestering toxic lipids into their neutral lipid core. Their mobility and dynamic interactions with mitochondria enable an efficient delivery of fatty acids for optimal energy production (Jarc & Petan, 2019).

After exploring the link between metabolic stress and mitochondrial dysfunction in our model of mutant *Tardbp*, we decided to investigate on lipid metabolism, tracing the formation of LDs following the induction of metabolic switch; thus, we aimed to establish whether *Tardbp* genetic background could make a difference in the enhancement of LDs production as a consequence of cellular stress. Figure 50 displays the results obtained by the employment of the green, fluorescent 22-NBD Cholesterol as a marker of intracellular LDs in living cells after the exposure of MEFs to metabolic switch for 6 hours (see sections 2.9 and 2.16). As reported in Figure 44B, we detected a strongly significant increase in the number of LDs per cell when comparing controls with stressed MEFs, being this true for all the *Tardbp* genotypes considered in this study. The main sources of variation for this experiment can be ascribed to TDP-43 mutation (accounting for the 47.52 % of total variation) and to the energetic status (accounting for the 42.22% of total variation).

3.4.2 Tardpb genotype influences ACAT 1/2 activity in MEFs upon metabolic switch

The most abundant neutral lipids in LDs are triacylglycerol and cholesterol esters (see section 1.5). While in adipocytes, caveolae may contribute to triacylglycerol synthesis (Öst et al., 2005), in most cells neutral lipid synthesis is conducted by enzymes permanently or transiently located in the ER. LDs accumulate free cholesterol in adipocytes (B R Krause & A D Hartman, 1984) and cholesterol esters in most cells, especially in macrophages and steroidogenic cells. The synthesis of cholesterol esters is mediated by acyl-CoA:cholesterol *O*-acyltransferase (ACAT1 and ACAT2).

In cells lacking LDs, these enzymes are distributed homogenously along the ER. When LD formation is promoted with fatty acids, enzyme segregation occurs, with some remaining in the ER and others dynamically accumulating on the LDs (Pol et al., 2014).

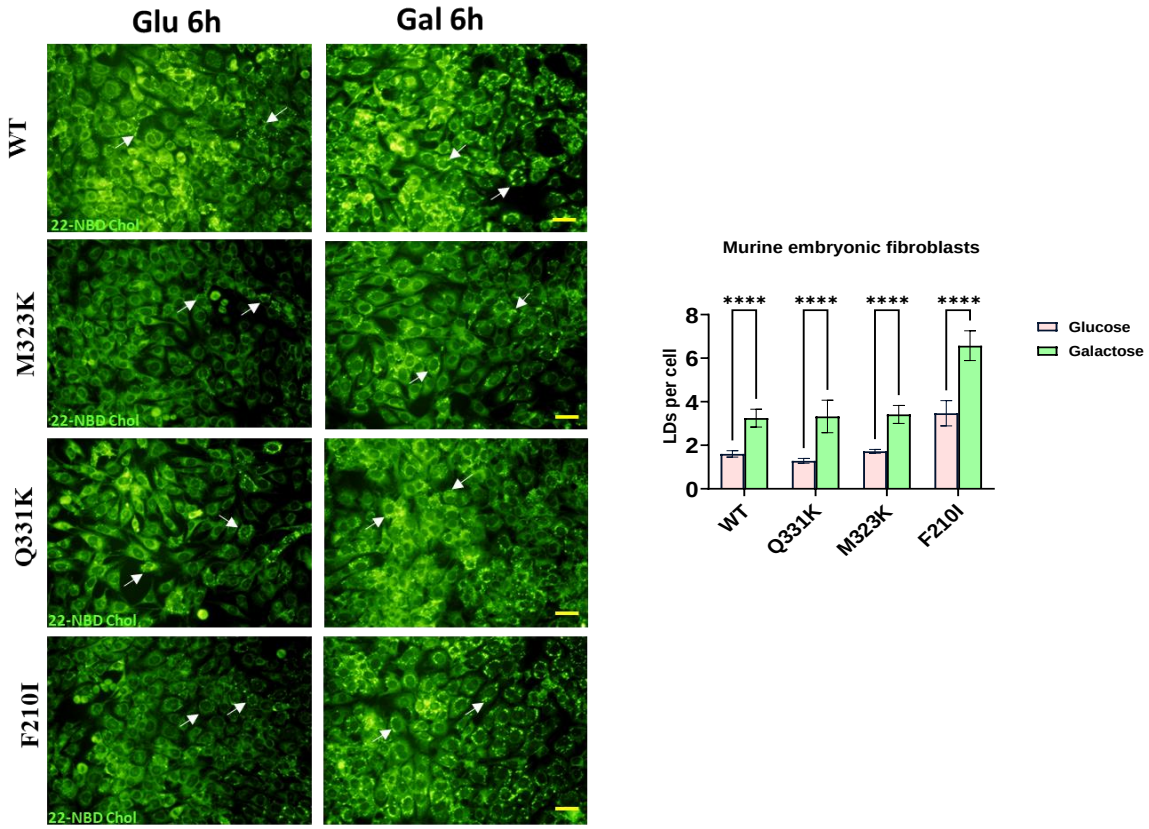

Figure 50. *Tardbp* influences LDs formation in MEFs. **(A)** Representative fluorescence images of living MEFs cultured in standard medium (DMEM supplemented with glucose and pyruvate, left panel) or upon metabolic switch conditions (DMEM containing galactose in alternative to glucose and no pyruvate, right panel). White arrows indicate LDs. Cells were imaged following the addition to 22-NDD Cholesterol to the growth medium. **(B)** Graphical representation of LDs counting per cell following the analysis of fluorescence images with the ImageJ Find maxima function. Results derive from 3 independents replicates. **** indicates $p < 0.0001$ by Post-hoc analyses after 2way ANOVA. Bars in (A) are 60 micrometers long.

In our model, ACAT 1/2 activity was measured by TLC as described in section 2.14.

Figure 51 contains the results of these analyses, with a representative image of a TLC plate in Figure 51A, showing the incorporation of 22-NBD Cholesterol in control and glucose/pyruvate deprived MEFs. As shown in Figure 51B, ACAT activity (expressed as the ratio between 22-NBD Cholesterol and its esterified form, adjusted by protein content), was significantly increased in deprived WT and Q331K MEFs, in comparison with their controls. This trend is preserved for M323K and F201I, but in these cases the increase is non-significant. Variability is mostly due to TDP-43, accounting for 25.65% of total variation, and energy status (42.58% of total variation). Figure 51C compares the changes

in ACAT activity considering only the deprived cells and comparing the three *Tardbp* genotypes with WT cells. Thus, a strongly significant increase is evident for Q331K and F210I MEFs, in which ACAT activity was enhanced by 70% and 75%, respectively. M323K genotype behaved contrarily, with a decrease in ACAT activity by 9%.

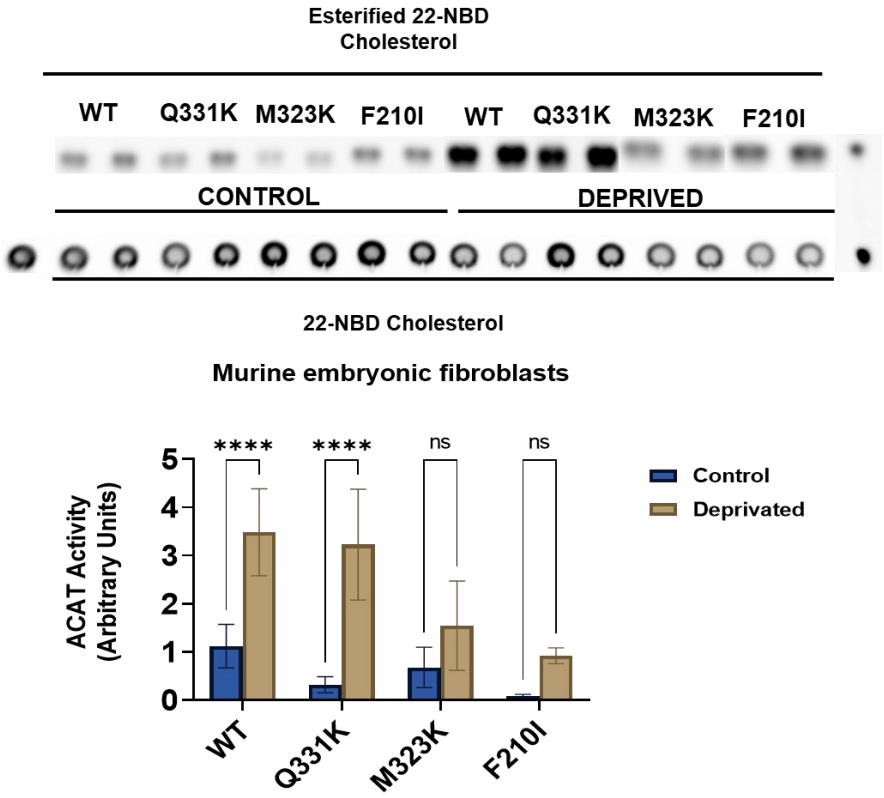

Figure 51. *Tardbp* influences ACAT activity. (A) Representative image of a TLC plate showing the incorporation of 22-NBD Cholesterol in MEFs and its esterification following the induction of metabolic stress (glucose and pyruvate deprivation), in comparison with control MEFs (glucose and pyruvate availability). The first and the last positions in the charging line of the TLC plate corresponds to 22-NBD Cholesterol and 22-NBD esterified Cholesterol, respectively, used as standards to confirm the migration patterns of MEFs lipids. **(B)** ACAT activity was estimated by employing the Cholesteryl Ester/Cholesterol ratio after TLC and adjustment by protein amount. n=9 different experiments. **(C)** Comparison of the increase in ACAT activity induced by metabolic stress for deprived MEFs with different *Tardbp* genetic background, in comparison with wild-type. Bars indicate mean values with lines showing the standard deviation. ** Indicates $p < 0.01$, and **** $p < 0.0001$ by post hoc analyses after 2way ANOVA (in B) or one way ANOVA (in C). Results derive from 4 independents replicates.

3.4.3 Osmotic stress induces LDs synthesis in N2A cell line

As already mentioned in section 1.2.2.3, osmotic stress is highly involved in ALS pathology. The causes for neuropathological TDP-43 aggregation in ALS are still unknown, but it has been suggested that SGs formation is important in this process. Thus, in human embryonic kidney HEK293E cells, various SG-forming conditions induced very strong TDP-43 ubiquitylation, insolubility, and reduced splicing activity (Hans et al., 2020). In this cells, OsmS-induced SG formation and TDP-43 ubiquitylation occurred rapidly and coincided with colocalization of TDP-43 and SG markers (Hans et al., 2020). Moreover, we found that both TDP-43 and p-TDP-43 are localized in a non-nuclear location as aggregates after sorbitol incubation (see Figure 40A). Starting from this interesting background in literature, we decided to check LDs accumulation in N2A cell line following the incubation with sorbitol at 0.4 M (the same concentration that induces TDP-43 and p-TDP43 in HEK293 cells) in a time course experiment. In this case, LDs were marked by staining with Nile Red, as described in section 2.16.

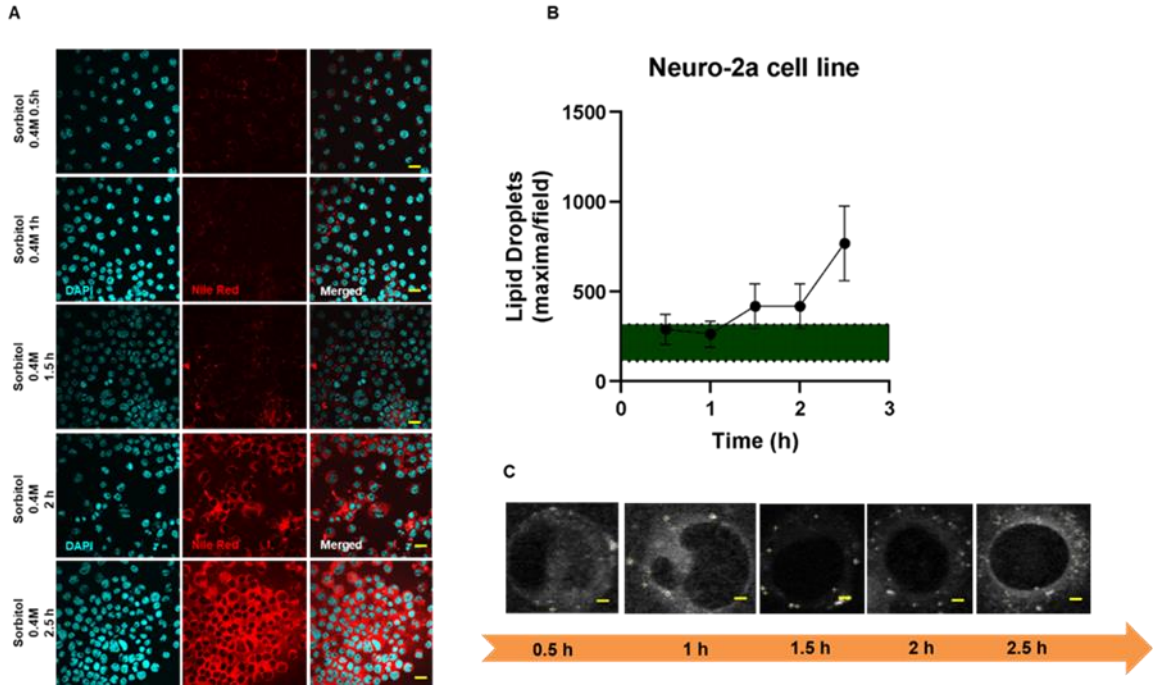

Figure 52. Osmotic stress increases LD in human cells. Nile Red staining of LDs in the N2a cell line treated with the osmotic stress inductor sorbitol in a time course experiment. **(A)** Representative confocal microscopy images of N2a cells grown on glass coverslips cells and treated with sorbitol 0.4 M at different times before fixation and Nile Red staining (red channel) **(B)** Number of LDs increases with treatment time. Intracellular Nile Red positive structures were automatically counted in ImageJ using the Find maxima function for image analysis. Number of LD in control situation is shown by the green band (mean± SD). **(C)** Representative images resulting from the ImageJ "Find maxima" algorithm to quantify number of lipid droplets per confocal field. White dots represent maxima per cell. Bars in (A) and (C) are 60 micrometers long.

As shown in Figure 52 we found that longer exposure to osmotic stress induced by incubation with sorbitol caused a progressively higher accumulation of Nile Red staining (Figure46A) and LD compatible structure per cell, as determined analyzing confocal images with the “Find maxima” algorithm in ImageJ following the selection of a ROI containing an equal number of cells for each microscopy field (Figure 52B). The higher number of LDs per cell was reached at 2.5 hours of sorbitol exposure with a 164.399% increase at 2.5 hours in comparison with 0.5 hours of incubation.

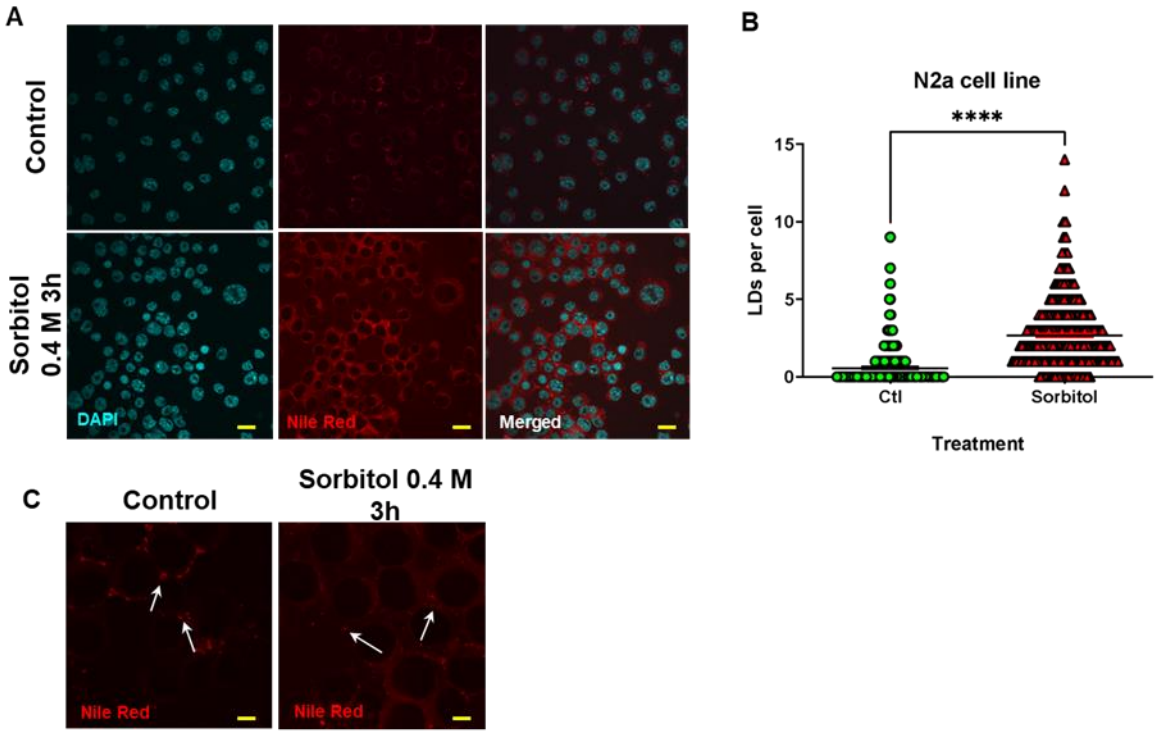

Figure 53. Osmotic stress induces LDs formation in N2A cell line. (A) Representative confocal microscopy images of N2A cells stained with the lipophilic staining Nile red showing the formation of LDs after the induction of osmotic stress by sorbitol treatment (dose and time indicated). (B) LDs counting per cell showing a significative increase in LDs/cell in stressed cells (n=881-801 cells for control cells and treated cells obtained in 4 independent replicates, respectively).**(C)** Representative confocal microscopy of the red channel in (A) at a higher magnification, comparing control and treated cells with white arrows indicating LDs. * Indicates $p < 0.05$, ** $p < 0.01$, *** $p < 0.001$, and **** $p < 0.0001$ by unpaired t-test. Bars in (A) and (B) are 60 micrometers long.

Figure 53A displays some representative photos obtained by confocal microscopy after the incubation of N2A cells with sorbitol 0.3 M for 3 hours, whit Figure 47C containing a higher amplification of control and treated cells. In Figure 53B, LDs counting per cell was carried out using ImageJ “Find maxima” function; the number of LDs compatible-structures was significantly (434%) higher in stressed cells than in control.

Similarly to MEFs, in this model we also quantified the grade of activation of ACAT1/2.

In Figure 54A, the increase in 22-NBD Cholesterol esterification is evident for stressed cells in a representative image of the TLC plate where total lipids extracted from control and experimental cells were applied.

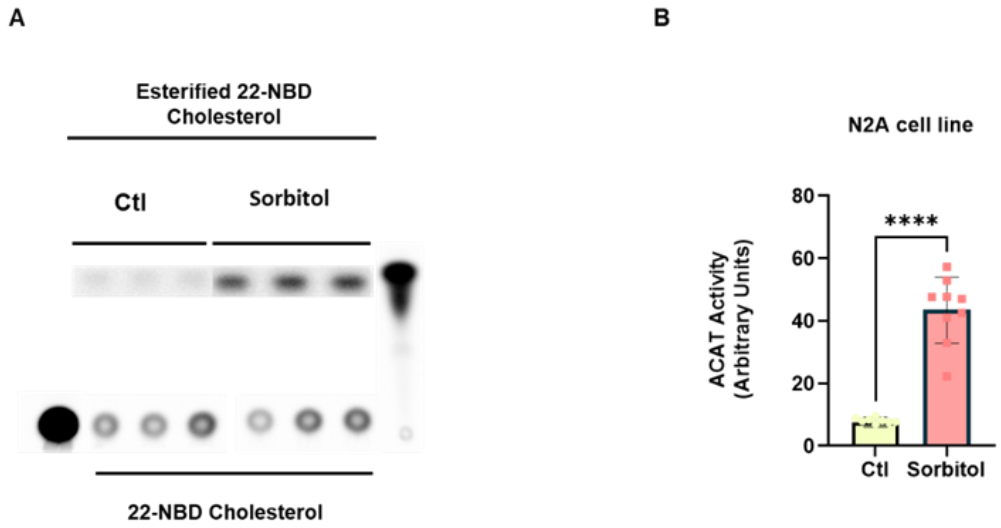

Figure 54. Osmotic stress increases ACAT activity in N2A cell line. (A) Representative image of the TLC plate showing the incorporation of 22-NBD Cholesterol in N2a cells and its esterification following the induction of osmotic stress by sorbitol treatment (0.4 M, 3h), in comparison with non-treated cells. The first and the last positions in the charging line of the TLC plate corresponds to 22-NBD Cholesterol and 22-NBD esterified Cholesterol, respectively, used as standards to confirm the migration patterns of N2a lipids. **(B)** ACAT activity was estimated by employing the Cholesteryl Ester/Cholesterol ratio after TLC and adjustment by protein amount. n=4 different experiments. **** indicates $p<0.0001$ by Student's t unpaired test.

Quantitative results are reported in Figure 54B, showing a highly significant increase in ACAT activity for stressed cells in comparison with unstressed (472.105%).

3.5 LDs in nuclei isolated from frontal cortex tissue

The impairment of nucleocytosolic transport is a well described process that appears to be impaired in ALS. In our group the influence of this defect on nuclear lipidome has been recently investigated, finding significant differences between samples derived from ALS patients in comparison with healthy controls (Ramírez-Nuñez et al., 2021). In figure 55A, representative confocal images of isolated nuclei show Nile Red-positive structure, mainly in the perinuclear location, in isolated nuclei extracted from frontal cortex tissue of ALS patients and controls. Features of patients and controls can be found in section 2.1, while the protocol to carry out nuclei isolation is described in detail in section 2.15.

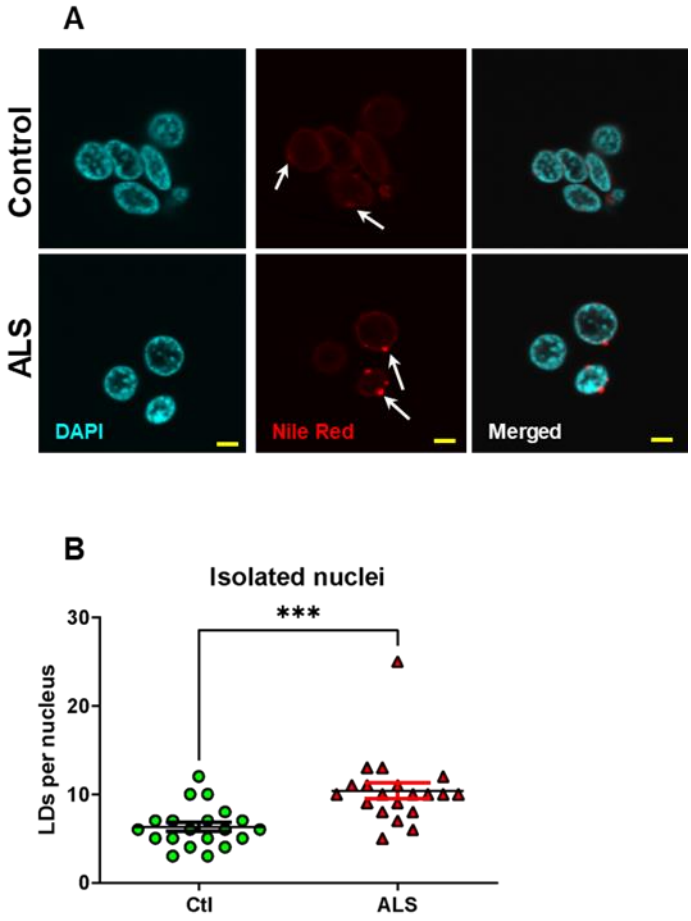

Figure 55. Nile Red staining of LDs in isolated nuclei extracted from frontal cortex tissue. (A) Representative confocal microscopy images of isolated nuclei derived from portions of frontal cortex of ALS patients in comparison with healthy controls . White arrows indicated perinuclear LDs. (B) LDs counting per nucleus showing a significative increase in LDs/nucleus in ALS nuclei (n=20-20 isolated nuclei for control and ALS samples obtained in 4 independent replicates, respectively). * Indicates $p < 0.05$, ** $p < 0.01$, *** $p < 0.001$, and **** $p < 0.0001$ by unpaired t-test. Bars in (A) are 60 micrometers long.

The quantitative analysis of confocal images determined a highly significant increase (65%) in the number of LDs per nucleus in ALS samples as displayed in Figure 55B.

3.6 Lipid metabolism alterations in hiPS-derived motor neurons

3.6.1 AGPS levels were decreased in ALS-related motor neurons derived from hIPS cells

As already mentioned above, our group recently focused on differential lipids in the nuclear lipidome signature of ALS samples in comparison with matched control, concluding that near 40% of potential identities of differential lipids comprised several plasmalogen-type lipids (Ramírez-Nuñez et al., 2021). For this reason, we explored the potential changes of alkylglycerone phosphate synthase (AGPS), one of the rate-limiting peroxisomal enzymes for plasmalogen synthesis (Grimm et al., 2011); AGPS abundance was monitored in hIPS cells-derived motor neurons from control cell lines in comparison with ALS-related genetic backgrounds expressing *FUS* mutation and *C9ORF72* expansion. Figure 56A displays representative confocal images of the three neuronal lines analyzed following indirect immunofluorescence. As shown in Figure 56B, AGPS immunoreactivity was significantly decreased in ALS or frontotemporal dementia-related cells when compared with control cell lines. Interestingly, when evaluating the correlation between AGPS mean immunoreactivity and nuclear perimeter, this was found only in control and C9ORF72 cells.

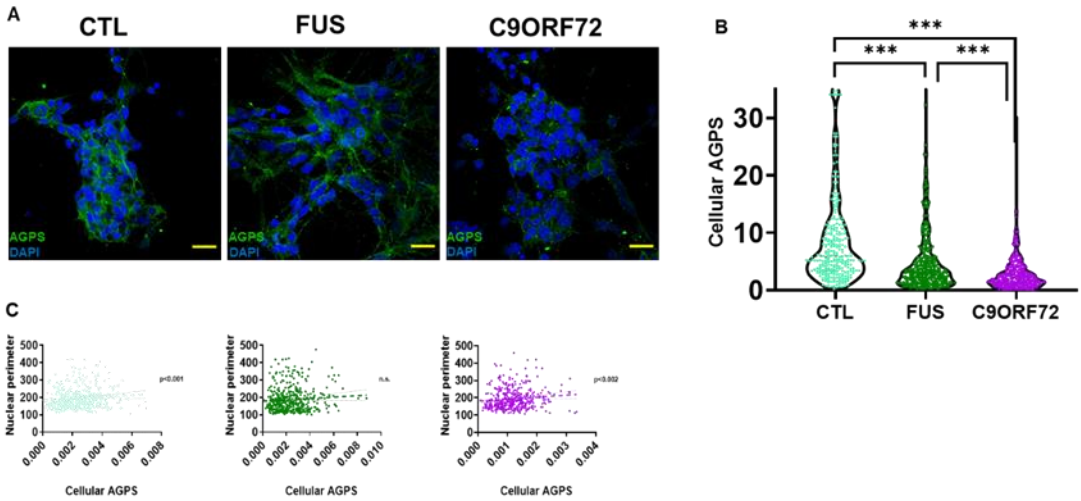

Figure 56. ALS influences AGPS levels in hiPS cell-derived MNs. (A) Representative confocal microscopy images of Ctl, FUS, and c9orf72 hiPS cell-derived MNs immunostained with the anti-AGPS antibody (in green). (B) Quantification of cellular AGPS levels (n = 281 for Ctl cells, n = 344 for FUS cells, n= 428 for C9ORF72 cells, obtained in at least 4 independent replicates). *** Indicates $p < 0.001$ by post hoc analyses after one-way ANOVA. **(C)** Significant correlation between AGPS mean immunoreactivity and nuclear perimeter occurs in control and C9ORF72 cells, but not in FUS mutated cells.

3.6.2 ACAT activity increases following osmotic stress in human motor neurons

Considering the significant differences in nuclear lipidome we detected comparing ALS-derived samples in comparison with controls, and the increased levels of AGPS in human MNs carrying FUS mutation or C9ORF72 expansion, we also investigated potential alterations in ACAT activity in this model, performing the TLC-based assay described in section 2.14. In particular, we focused on OsmS induced by sorbitol, since the changes in the lipid profile are well documented in cells exposed to increased osmolarity (Robciuc et al., 2012). In Figure 57A we enclosed a representative image of the TCL plate showing difference in 22-NBD Cholesterol esterification when comparing CTL MNs with *FUS* or *C9ORF72* mutants. Quantitatively (Figure 57B), OsmS increased ACAT activity in control cells, while the same tendency was evident for mutants exposed to sorbitol, even if differences are non-significant. Although, we observed a significant increase in ACAT activity for *FUS* MNs in comparison with controls in absence of osmotic stress.

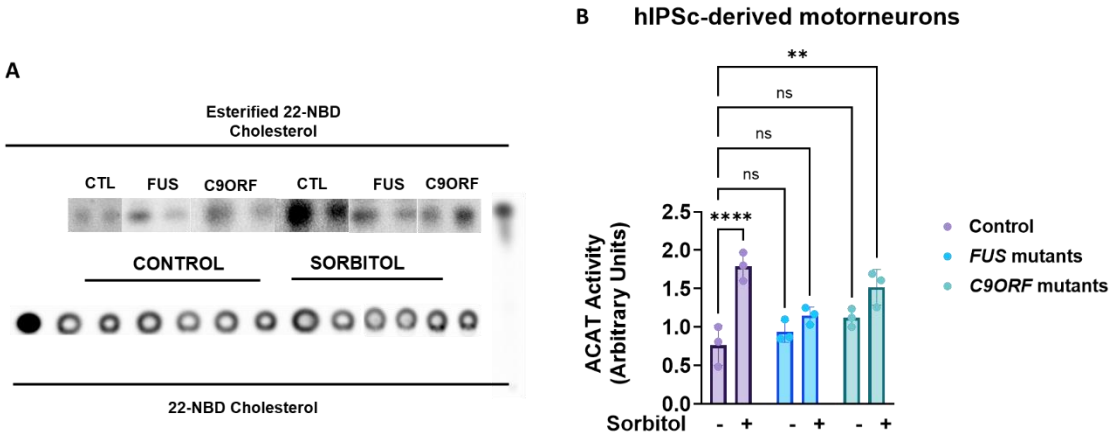

Figure 57. Osmotic stress increases ACAT activity human MNs, depending on ALS status. **(A)** Representative image of the TLC plate showing the incorporation of 22-NBD Cholesterol in hIPSc-derived MNs and its esterification following the induction of osmotic stress by sorbitol treatment (0.4 M, 3h), in comparison with non-treated cells. The first and the last positions in the charging line of the TLC plate corresponds to 22-NBD Cholesterol and 22-NBD esterified Cholesterol, respectively, used as standards to confirm the migration patterns of lipids. **(B)** ACAT activity was estimated by employing the Cholesteryl Ester/Cholesterol ratio after TLC and adjustment by protein amount. n=4 different experiments. *** indicates $p<0.001$ and ** $p<0.01$ by post hoc analyses after two way ANOVA.

3.7 LDs and cellular stress in astrocytes upon oxidative or osmotic stress

Astrocytes have been described in literature as important players in synaptic function, and, consequently, they have an important role on brain function and animal behavior. The Tripartite Synapse concept considers astrocytes as integral elements involved in synaptic function (Durkee & Araque, 2019) . In fact, they establish bidirectional communication with neurons, whereby they respond to synaptically released neurotransmitters and, in turn, release gliotransmitters that influence neuronal and synaptic activity Also, astrocyte–neuron signaling is not based on broad, unspecific interaction; indeed, it is a synapse-, cell- and circuit-specific phenomenon with a high degree of complexity (Durkee & Araque, 2019) . As mentioned in section 1.5.1, noradrenaline, a brain stress–response system neuromodulator, metabolic and hypoxic stress increase LD accumulation in astrocytes by increasing the number and the size of LDs. Noradrenaline increases LD accumulation activating β- and α2-ARs. This accumulation of LDs in stressed astrocytes may be useful as a support for energy provision but may also provide neuroprotection against the stress-induced lipotoxicity. In the context of these recent findings, we explored the potential relationship between oxidative and osmotic stress in a primary rat cortical astrocyte culture, obtained as described in section 2.3.1. Both control and stressed cells were charged with oleic acid, a potent inducer for LD accumulation through its esterification to glycerol by DGAT in primary cortical astrocytes (Nakajima et al., 2019) as described in section 2.17. Following the incubation with oleic acid, cells were exposed to oxidative or osmotic stress (Figures 58 and 59), fixed, and stained with LipidTOX™ (see section 2.17.1) Concerning H_2O_2 exposure, at the shorter time of treatment (2hours, see Figure 58B) the introduction of oleic acid alone in the culture medium, increased the number of LDs per confocal field in comparison with control cells, while the combination of H_2O_2 and oleic acid showed the opposite effect, decreasing the number of LDs; nevertheless, these changes were not statistically significant. At 4 hours of treatment, the same trend was confirmed, with oleic acid alone enhancing LD accumulation; in combination with H_2O_2 once again, LD accumulation decreases. In this case, the described changes were significant in comparison with unstressed astrocytes. Moreover, the was a significant enhancement in LD accumulation upon oleic acid administration alone at 4 hours in comparison with the shorter treatment.

The same experimental setting was employed to set the effects of Osms on LD formation (Figure 59A and 59B). In presence of oleic acid alone, we observed a significant increase

in LD accumulation in comparison with control cells, while combining sorbitol with oleic acid, maintained the level of LDs similar to the one reported for the control (Figure 59B).

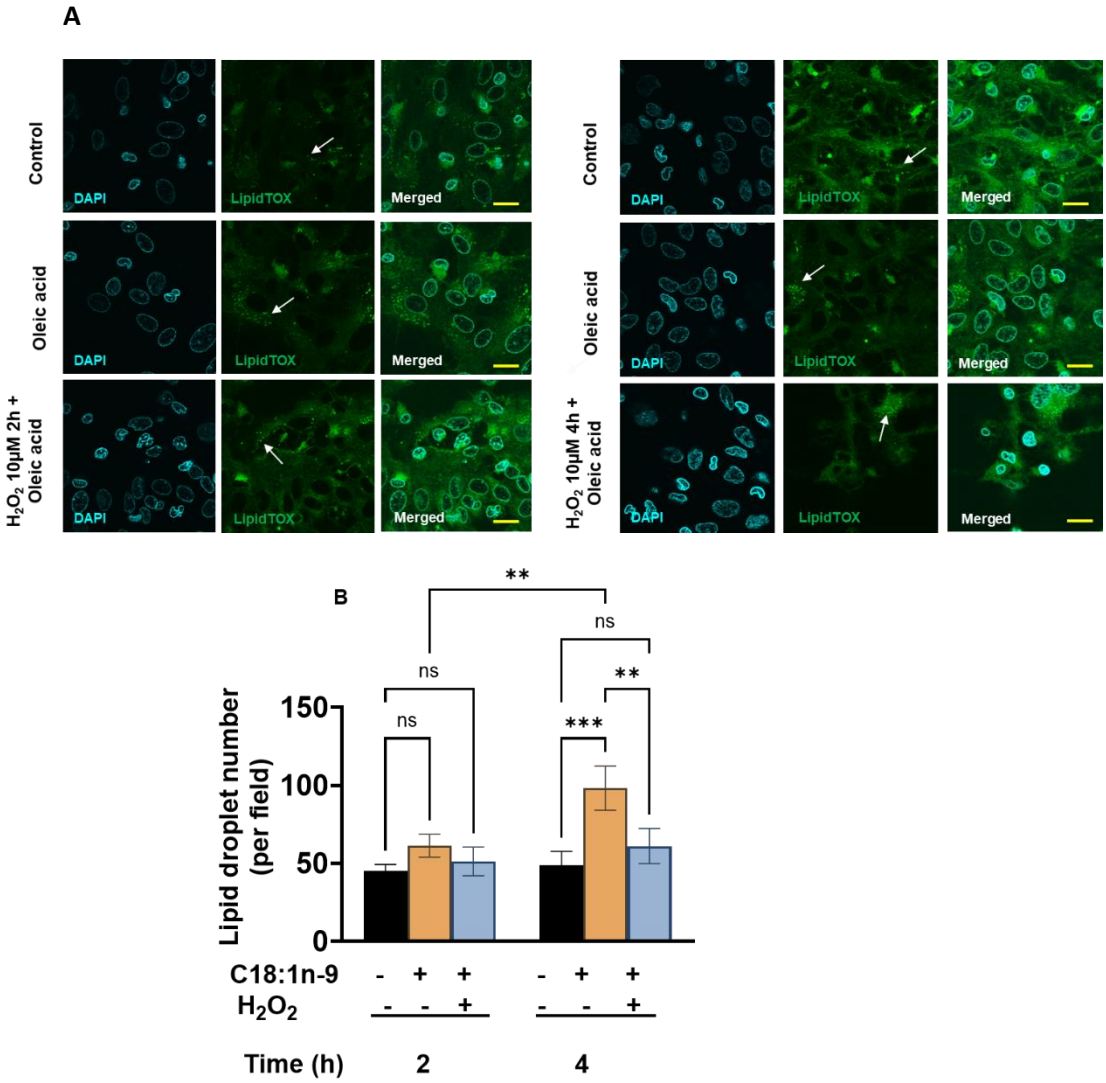

Figure 58 Oxidative stress interferes with LD formation in primary astrocytes. LipidTox™ staining of Sprague-Dawley neonatal rat astrocytes following treatment with oleic acid as an inductor of LDs formation, H_2O_2 as an oxidative stress inductor and a combination of both. **(A)** Representative confocal images of fixed astrocytes stained after treatment with oleic acid and H_2O_2 for 2 and 4 hours. White arrows indicate intracellular LDs. White arrows indicate intracellular LDs. **(C)** Graphical representation of LDs counting per confocal field with an equal number of cells in Sprague-Dawley rat astrocytes after oleic acid treatment and/ or oxidative stress induction. Results derive from 4 independent replicates. * Indicates $p < 0.05$, ** $p < 0.01$, *** $p < 0.001$, and **** $p < 0.0001$ by one-way ANOVA in A and B or by 2way ANOVA in (C). Bars in (A) and (B) are 60 micrometers long.

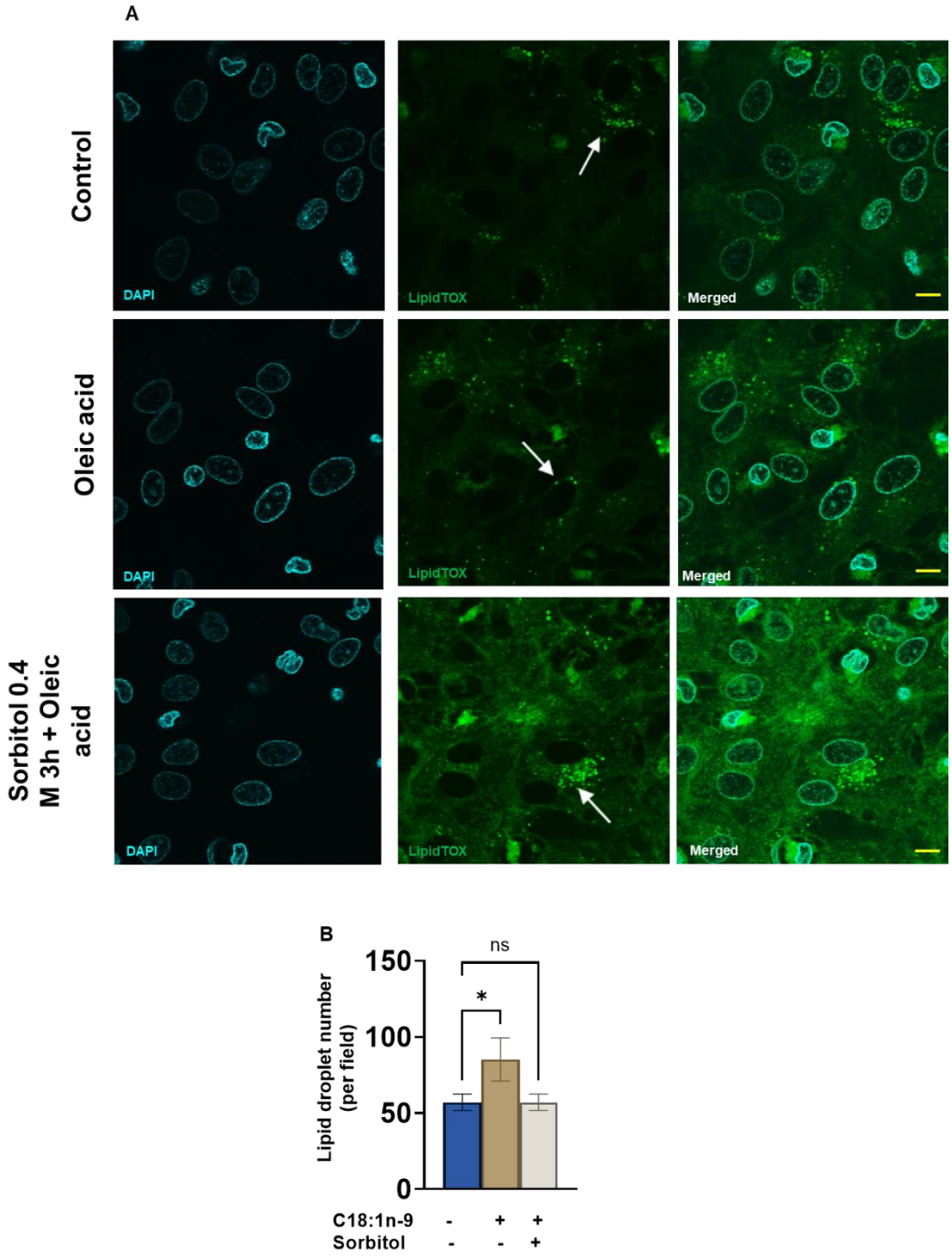

Figure 59. Osmotic stress interferes with LD in primary astrocytes. LipidToxTM staining of Sprague-Dawley neonatal rat astrocytes following treatment with oleic acid as an inductor of LDs formation, sorbitol as an osmotic stress inductor and a combination of both. **(A)** Representative confocal images of fixed astrocytes stained after oleic acid and sorbitol treatment for 3 hours. White arrows indicated intracellular LDs. **(B)** Graphical representation of LDs counting per confocal field in Sprague-Dawley rat astrocytes after oleic acid treatment and/ or osmotic stress induction. Results derive from 4 independent replicates. * Indicates $p < 0.05$, and *** $p < 0.001$ by post hoc analyses after one-way ANOVA in (B) or by 2way ANOVA in (C). Bars in (A) are 60 micrometers long.

DISCUSSION

4. DISCUSSION

4.1 ALS-related cellular stress and protein mislocalization

This work shows that several proteins implicated in ALS (TDP-43, ERK, Jun) and other neurodegenerative processes, such as AD (Jun, REST), show a sensitivity to cell stress. Several neurodegenerative diseases exhibit protein aggregates where these proteins may be present(Spires-Jones et al., 2017) . As already stated, both sporadic and familial ALS patients share the presence of protein aggregates in their motor neurons; in addition, misfolded proteins are associated with synapse loss and cellular death (Blokhuis et al., 2013). It is well established that cellular stress can trigger protein misfolding and aggregation by several means. Proteasomal or lysosomal removal of damaged proteins may be altered by OS (Pajares et al., 2015). In turn, the accumulation of misfolded proteins leads to the formation of oligomers and higher aggregates that can interact with metal ions and catalyze RS production, as already described in neurodegenerative diseases (NDDs) (Cheignon et al., 2018). Moreover, the formation of protein aggregates can impair mitochondrial bioenergetics or alter the removal of dysfunctional mitochondria through mitophagy, a selective form of autophagy in which mitochondria are specifically degraded (Devi et al., 2006; Grassi et al., 2018), leading to their accumulation, which further enhances reactive species (RS) generation and neuronal death. Characteristic protein aggregates of NDDs can also disrupt the mitochondria-ER association, leading to disrupted Ca^{2+} homeostasis and lipid metabolism, among others.

Here, we evaluated four different major cellular stressors, namely OS, proteasome inhibition, ER stress and mitochondrial stress, demonstrating that the effects on cellular distribution showed stress and protein specificity.

In the case of p-TDP-43, the results showed that, following oxidative stress, both nuclear and cytoplasmic levels of this protein decreased. Further, its degree of colocalization of within the mitochondria after oxidative and mitochondrial stresses also increased. These findings are related with the recent description of TDP-43 and p-TDP43 coexisting with intensively stained key subunits of mitochondrial oxidative phosphorylation complexes I-V in skeletal muscle fibers of patients with inclusion body myositis (IBM) (Huntley et al., 2019). The same researchers also showed increased levels of TDP-43, truncated TDP-43 and p-TDP-43, but decreased levels of key subunits of mitochondrial oxidative phosphorylation complexes I and III in IBM patients compared to aged matched control subjects(Huntley et al., 2019). OS could play a fundamental role in this mislocalization and aggregation processes involving the mitochondrial compartment, but it is also known that

TDP-43 may be an OS inducer, in turn (Zuo et al., 2021). Aggregated TDP-43 may act in the sequestering of a series of nuclear-genome-encoded mitochondrial proteins, causing a general mitochondrial imbalance and ultimately increasing OS in a vicious cycle (Zuo et al., 2021) In general, several reports have described the occurrence of TDP-43 in mitochondrial fractions (Yu et al., 2020) and other membranal fractions(Gautam et al., 2019).

Regarding hyperosmotic stress induced by sorbitol incubation, the results showed that the cytosolic levels of TDP-43 as well its aggregation, increased in the HEK-293 cell line. Of note, TDP-43 may show differences in behavior with p-TDP-43 in osmotic stress-inducing experiments. Thus, while TPD-43 is accumulated after sorbitol stress in the cytosol, this phenomenon was nonsignificant in p-TDP-43. The *in vivo* evidence presented shows that this is also the case in the brain lysates, where p-TDP-43 and TDP-43 show differential responses to the overexpression of mutated TARDBP. Whatever the case, the subcellular fractionation data agree with the enrichment of both endogenous murine TDP-43 and hTDP-43 in mitochondrially enriched fractions.

These phenomena may be explained by the previously detected involvement of TDP-43 in both assembly and maintenance of SGs. Furthermore, TDP-43 also regulates the expression of key SG nucleating proteins, such as rasGAP SH3 domain binding protein 1 (G3BP) and T cell-restricted intracellular antigen-1 (TIA-1) (McDonald et al., 2011). ALS-linked mutations can influence stress granule dynamics. In fact, under sorbitol-induced osmotic stress, the G348C mutant TDP-43 was found to be localized into progressively larger stress granules (Dewey et al., 2011). On the contrary, the R361S mutant of TDP-43 was shown to disrupt the stress granule assembly (McDonald et al., 2011). The role of TDP-43 assembling in these stress granules is thought to be protective against cellular stress (Colombrita et al., 2009)

In our results, both the functional and morphological analyses showed that the conditions linked to TDP-43 aggregation (especially in sorbitol incubation) were associated with major changes in the mitochondrial ATP production. Thus, TDP-43 aggregation appears to be linked to mitochondrial dysfunction at least in human neuroblastoma SHSY-5Y cell line, which we employed in respirometry experiments to evaluate ATP production rate. In our model, sorbitol treatment induces a strongly significant decrease in ATP production in comparison with control cells.

Nevertheless, it’s worth noting that different cell lines respond differently to the combination of osmotic and oxidative stress induced by sorbitol treatment. This is the

case of HeLa and HCT116. In these models, sorbitol promoted the phenotypic manifestations of early apoptosis followed by complete loss of viability in a time-, dose-, and cell type-specific fashion, by eliciting distinct yet partially overlapping molecular pathways (Criollo et al., 2007). In HCT116 but not in HeLa cells, sorbitol caused the mitochondrial release of the caspase-independent death effector AIF, whereas in both cell lines cytochrome c was retained in mitochondria. Despite cytochrome c retention, HeLa cells exhibited the progressive activation of caspase-3, presumably due to the prior activation of caspase-8. Accordingly, caspase inhibition prevented sorbitol-induced killing in HeLa, but only partially in HCT116 cells (Criollo et al., 2007). Both the knock-out of Bax in HCT116 cells and the knock-down of Bax in A549 cells by RNA interference reduced the AIF release and/or the mitochondrial alterations. While the knock-down of Bcl-2/BclX(L) sensitized to sorbitol-induced killing, overexpression of a Bcl-2 variant that specifically localizes to mitochondria (but not of the wild-type nor of an endoplasmic reticulum-targeted form) strongly inhibited sorbitol effects. Thus, hyperosmotic stress kills cells by triggering different molecular pathways, which converge at mitochondria where pro- and anti-apoptotic members of the Bcl-2 family exert their control (Criollo et al., 2007). The decreasing in ATP production rate for cells exposed to osmotic stress is in line with these findings, suggesting the induction of mitochondrial impairment under osmotic stress conditions which simultaneously determine p-TDP43 and TDP-43 aggregation in the cytosol.

Regarding p-ERK, in response to increased oxidative stress, we noticed a decrease in the cytosolic and nuclear locations after a transient increase. Nonetheless, the degree of colocalization with mitochondria increased significantly, suggesting the close occurrence of p-ERK with mitochondrial epitopes again. In contrast with p-TDP-43, the slopes relating to nuclear and extranuclear p-ERK were inversely related to the oxidative stress intensity, suggesting the nuclear retention of this factor or rapid cytosolic clearance of it. The same phenomenon (decreased both in the cytosol and in nuclei) was present after proteasome and ER stress. This later cell stress also decreased the colocalization within the mitochondrial epitopes. Interestingly, after the epoxomicin treatment, we observed an increase in the degree of mitochondrial colocalization. Under conditions of mitochondrial stress, we observed a transient increase in cytosolic levels following a 2 hours exposure to rotenone; this effect was then lost at 4h exposure. On the other hand, nuclear intensity significantly increased at both treatment times. Regarding colocalization with mitochondria, our data show again a transient increase at the shorter treatment time, followed by non-significant differences with control cells at 4h. The subcellular

fractionation in the TDP-43 model suggested that p-ERK could be significantly enriched with mitochondria, independently of the TARDBP overexpression.

Interestingly, researchers in our laboratory have investigated the relationship between cell stress and pathological changes of TDP-43 showing that it also includes a dysfunction in the survival pathway mediated by mitogen-activated protein kinase/ extracellular signal-regulated kinases (ERK1/2). In summary, these previous findings, have demonstrated that cellular stressors are key factors in neurodegeneration associated with TDP-43 and have disclosed the identity of ERK1/2 as novel players in the pathogenesis of ALS(Ayala et al., 2011). Thus, under stress conditions, neurons and other spinal cord cells showed cytosolic aggregates containing ERK1/2 (Ayala et al., 2011). Moreover, aggregates of abnormal phosphorylated ERK1/2 were also found in the spinal cord ALS, specifically in motor neurons with abnormal immunoreactive aggregates of phosphorylated TDP-43 (Ayala et al., 2011) These aggregates may be related potentially to mitochondrial interactions. In this regard, we show that there are no interactions between p-ERK and TDP-43 overexpression in the evaluated murine model.

Also, it is known that there are mitochondrial substrates for p-ERK kinase activity (Tomer et al., 2018). Recent data underlines that ERK signaling specificity requires the spatial compartmentalization of ERK activity for signals like EGF to govern diverse functional responses via compartmentalized ERK activity (Keyes et al., 2020). Previous data showed that p-ERK mitochondrial location could be a consequence of tumoral transformation (Rasola et al., 2010) demonstrating that a fraction of active ERK1/2 associates with succinate dehydrogenase and some mitochondrial chaperones, such as TRAP1 (Masgras et al., 2017). We have previously shown that motor neurons in the spinal cord from ALS patients exhibit p-ERK aggregates in extranuclear locations (Ayala et al., 2011).

Concerning the enrichment in p-ERK that we observed in mitochondria, a closely related phenomenon was found in substantia nigra neurons from patients with PD. Phospho-ERK immunoreactivity was often associated with mitochondrial proteins (MnSOD, 60 kDa and 110 kDa mitochondrial antigens), and some vesicular-appearing phospho-ERK granules appeared to envelop enlarged mitochondria by confocal laser scanning microscopy(Zhu et al., 2003). Ultrastructural immuno-gold studies have revealed phosphor-ERK labeling in mitochondria. As mitochondrial pathology may play a pivotal role in PD and other related neurodegenerative diseases such as ALS, these results suggest, all together, a potential link between mitochondrial dysfunction and ERK signaling pathways (Zhu et al., 2003).

Concerning p-Jun, no clear accumulation in the extranuclear location was present after oxidative stress, though the mitochondrial colocalization increased. After proteasome inhibition and ER stress, the extranuclear levels of this factor were decreased with concomitant retention in the nuclei (thought at later stages, the ER stress decreased the levels of nuclear p-Jun slightly). In clear contrast with oxidative stress, both ER stress and proteasome inhibition decreased the mitochondrial colocalization. Indeed, the subcellular fractionation suggested that, while Jun accumulated with crude mitochondria, this was not the case with p-Jun. Mitochondrial stress affected p-Jun cytosolic accumulation, which significantly diminished at both treatment times, while a significant increment in the nuclear location was only observed at 2h exposure.

It is already known that JNK is located in the mitochondria (Heslop et al., 2020). Other studies demonstrate that the cytosolic location of c-Jun depends on its interaction with other transcription factors (Liu et al., 2006). In particular, it has been demonstrated that opening of voltage dependent anion channels (VDAC) by the erastin-like compound X1 and the multikinase inhibitor sorafenib promotes OS and mitochondrial dysfunction in hepatocarcinoma cells. Particularly, X1 and sorafenib induce mitochondrial dysfunction by increasing ROS formation and activating c-Jun N-terminal kinases (JNKs), leading to translocation of activated JNK to mitochondria(Heslop et al., 2020). Of note, the major location of p-Jun in brain lysates is the nuclei, but we detected a consistent signal in the cytosol and in the crude mitochondrial fractions. Previous in vitro studies showed that c-Jun interacts with phospholipids (del Boca et al., 2005). Interestingly, other in vivo reports indicated that cytoplasmic c-Jun is associated with the mitochondria (Haase et al., 1997). Indeed, it is known that c-Jun may interact with mitochondrial DNA motifs, the mitochondrial location validated by electron microscopy(Blumberg et al., 2014)Despite some doubts for the mitochondrial location of typically nuclear transcription factors, such as NF-kB (Albensi, 2019), it may be adequate to validate the reported findings further and establish the interaction of c-Jun with mitochondria. Further c-Jun binding sites occur within mtDNA genes and are negatively selected (Blumberg et al., 2014).

Turning to REST, its accumulation has been previously reported in a cytosolic location in neurodegenerative processes. Our results regarding the response to cell stress showed that its behavior was similar to p-Jun, showing an initial decrease in the cytosol followed by a slight increase in both the nuclei and cytosol. Epoxomicin treatment decreased the nuclear levels after the long exposure, while ER stress increased their values in the cytosol and nuclei. Indeed, the degree of colocalization increased after oxidative stress. In response to mitochondrial stress, this protein showed significant changes both in the

cytosolic and nuclear locations. In particular, nuclear REST increased at both treatment times, while cytosolic REST increase at 2 hours treatment was followed by a reserved trend at 4 hours, with a significant decrease.

Previous data reported the relationship between changes in the REST expression and protein aggregates (Barrachina et al., 2007). Particularly, several genes under the control of this negative regulator are upregulated, suggesting its impairment in human pathology (Barrachina et al., 2007). Amongst the controlled genes, the authors indicated increased ubiquitin car-boxy-terminal hydrolase L1, a component of the aggregates (Barrachina et al., 2007).This protein is involved in the ubiquitin-proteasome pathway of proteostasis, suggesting that REST could influence proteostasis. Our data indicate that the reverse is also true, i.e., proteasome could control the REST protein levels and their subcellular location.

The accumulation of REST in a cytosolic location in neurodegenerative processes has been previously described (Kawamura et al., 2019). Our data regarding the response to cell stress showed that its behavior was similar to p-Jun, showing an initial decrease in the cytosol followed by a slight increase in both the nuclei and cytosol. Epoxomicin treatment decreased the nuclear levels after the long exposure, while ER stress increased their values in the cytosol and nuclei. Indeed, the degree of colocalization increased after oxidative stress. Previous data also reported the relationship between changes in the REST expression and protein aggregates(Barrachina et al., 2007).Particularly, several genes under the control of this negative regulator are upregulated, suggesting its impairment in human pathology. Amongst the controlled genes, the authors indicated increased ubiquitin carboxy-terminal hydrolase L1, a component of the aggregates (Barrachina et al., 2007).This protein is involved in the ubiquitin-proteasome pathway of proteostasis, suggesting that REST could influence proteostasis. Our data indicate that the reverse is also true, i.e., proteasome could control the REST protein levels and their subcellular location.

To the best of our knowledge, we have not found previous evidence of REST in the mitochondria. Previous evidence in human substantia nigra (Kawamura et al., 2019) showed a cytoplasmic staining profile in neurons. Nonetheless, REST was found as aggregates closely related to autophagy impairment (Ramesh & Pandey, 2017). Thus, defects in the protein quality control system induce REST mRNA expression; its gene product mainly appears in aggregates. In brain subcellular fractionation experiments, we did not evidence changes in the total levels of REST. Nonetheless, we show that all stress

evaluated, including ER, proteasomal, and oxidative stress, changes its cellular distribution, increasing the colocalization with mitochondrial epitopes. Indeed, recent data showed that CRISPR-mediated REST KO induced mitochondrial dysfunction and impaired mitophagy in vitro. Furthermore, REST overexpression impedes mitochondrial toxicity and mitochondrial morphology disruption through the transcription factor PGC-1α (Ryan et al., 2021).

4.1.2 Cell stress-induced mislocalization of TDP-43 and changes in REST-regulated genes

Interestingly, the in vivo data showed that the overexpression of mutated TARDBP increased the degree of REST enrichment in mitochondrial fractions. The interaction between TDP-43 alterations and REST is new, and it is reinforced by the fact that several REST-regulated genes appear affected under osmotic stress conditions, where TDP-43 is mislocalized. These genes included SCN3B, encoding a voltage-gated sodium channel (O'Malley & Isom, 2015) and two genes implicated in apoptosis (PUMA and FADD)(Sharifi et al., 2015) with downregulation in both cases. Interestingly, in the human cells evaluated, sorbitol decreased the expression of transcripts encoding antioxidant enzymes, such as SOD1 and catalase. Furthermore, in these cells, an increased expression of the ATP2B2 mRNA was found, encoding a plasma membrane Ca++ pump. Additionally, we noticed a decreased ARC mRNA expression in the cells, implicating altered mRNA traffic (one of the functions of TDP-43). We also detected an increased NRXN3 expression, encoding Neurexin 3-α. This factor encodes a cell adhesion component whose paralogs have been recently implicated in synaptic strength, in close collaboration with the factors regulating RNA/aggregation toxicity (Arsović et al., 2020). We also detected a tendency for decreased p35 mRNA after osmotic stress, not achieving a signification threshold. Of note, P35 is a neuron-specific cyclin-dependent kinase 5 activator. When p35 is cleaved by calpain into p25, the protein is relocalized from the cell periphery to the nucleus and perinuclear region. Patients with AD accumulate the p25 form in their brain neurons (Shah et al., 2014). This build-up is linked to an increase in CDK5 kinase activity, leading to abnormally phosphorylated microtubule forms. CDK5 kinase overactivation is linked to TDP-43 pathological effects in neuronal cells(Rao et al., 2016). We also detected a tendency for increased Foxo 1 mRNA. It is known that this key metabolic transcription factor promotes neuron death (Yuan et al., 2008). Therefore, decreased values of antiapoptotic factors (PUMA and FADD) may be responses to this increased expression.

Noteworthy, we used proliferative cell lines (HMEC-1 human mammary epithelial cells, human embryonic kidney HEK-293 cells, and SHSY-5Y human neuroblastoma cells). It is

known that these cellular types show a different response against oxidative and osmotic stress, besides having proliferation, which is not the case of neurons. Therefore, we need to show caution in the potential extrapolation of these results.

Accounting for the fact that one of their primary functions is working as transcription factors (in the case of Jun and REST), interacting with RNA (in the case of TDP-43) or transmitting extracellular signals to intracellular targets (in the case of ERK) , their localization in the extranuclear placements (particularly in close relationships with mitochondrial epitopes) suggests the existence of pathogenic mechanisms operating in common. All these proteins require nucleocytosolic transport; therefore, a loss in this cellular property's homeostasis may partially explain their presence in the cytosol. Indeed, we have recently reported that the nuclear envelope (where the proteins responsible for nucleocytoplasmic shuttling reside) showed altered properties in ALS patients and models (Ramírez-Nuñez et al., 2021).

Also, it is of note that rotenone, the mitochondrial stress inducer we employed in our experiments, show an oxidant effect which has been demonstrated in a PD cellular model, by the fact that the addition of antioxidants to rotenone treated cells have been shown to decrease some PD symptoms (Chernivec et al., 2018). Thus, the increment of colocalization with mitochondria and the significant changes in nuclear and cytosolic levels observed after rotenone treatment for all the proteins of interest in this work, could be due to the oxidant effect of this proven complex I inhibitor, positioning these findings in a more extensive context where, as mentioned above, OS induces mislocalization and aggregation (Zhang et al., 2021).

As for the limitations of our work, we must remark that this evidence was present in an endothelial-like cell phenotype. Therefore, neuronal, or glial cells could exhibit different dynamics. Nonetheless, some of the findings in the endothelial cell culture were replicated independently in lysates of the brain cortex of a murine model. We shall also indicate that the subcellular fractionation was more enriching than a strict purification of the indicated compartment. However, we can exclude nuclear contamination of the mitochondrial fraction (based on purity markers).

4.3 Effect of cellular stress on mitochondria dynamics

Following the induction of cellular stress to investigate on protein mislocalization and potential colocalization with the mitochondrial epitope ATP5A, we performed a computerized analysis of mitochondrial dynamics in HMEC-1 cell line. Stress induction was due to the exposure of cells to the same stressors above mentioned (oxidative, proteasomal inhibition, mitochondrial and ER stress). As already mentioned in section 1.2.2.1 OS appears to be implicated in the loss of MNs and mitochondrial dysfunction, contributing to neurodegeneration in ALS (Cunha-Oliveira et al., 2020).

In our model, acute exposure to H_2O_2 leads to significative changes in mitochondrial dynamics. Particularly, at the longest treatment time, we observed a significant increment in number of individual mitochondria as well as in the number of mitochondrial networks. These findings comply with the well-established relationship between oxidative stress and mitochondrial impairment in MNDs. It is known that mitochondrial morphology changes rapidly in response to external insults and alterations in metabolic status via fission and fusion processes that maintain mitochondrial quality and homeostasis. Damaged mitochondria are removed by a process known as mitophagy, which involves their degradation by a specific autophagosomal pathway (Misrani et al., 2021). Over the last few years, remarkable efforts have been made to investigate the impact on the pathogenesis of AD of various forms of mitochondrial dysfunction, such as excessive ROS production, mitochondrial $Ca2^{+}$ dyshomeostasis, loss of ATP, defects in mitochondrial dynamics and transport, and mitophagy. Recent research suggests that restoration of mitochondrial function by physical exercise, an antioxidant diet, or therapeutic approaches can delay the onset and slow the progression of AD (Misrani et al., 2021). Abnormal mitochondrial dynamics have been also repeatedly reported in ALS and increasing evidence suggests altered mitochondrial dynamics as possible pathomechanisms underlying mitochondrial dysfunction in ALS (Jiang et al., 2015). Although there is only one study showing abnormal mitochondrial outer membrane protrusions within axons of anterior root in ALS patients using biopsied tissues (Hirano et al., 1984) abnormal mitochondrial morphology has been well documented in ALS experimental models. Studies from multiple groups showed that mitochondria became fragmented in cell and animal models expressing ALS-associated mutant SOD1 (Song et al., 2013; vande Velde et al., 2011). In addition, it has been found that ALS-associated mutant TDP-43 overexpression also caused mitochondrial fragmentation in motor neurons in vitro and in mice (Magrané et al., 2014). Studies in past decades reveal that mitochondria are highly dynamic organelles, and mitochondrial morphology results from the delicate balance of

fission and fusion process (Bleazard et al., 1999; Chan, 2006). Mitochondrial fission involves the division of a single mitochondrion into 2 individual fragmented and disconnected mitochondria by the fission proteins, dynamin-related protein 1 (Drp1), human fission protein 1 (hFis1), mitochondrial fission factor (Mff) and the mitochondrial dynamics proteins of 49 kD (MiD49) and 51 kD (MiD51). Fusion is also modulated by several proteins(Hernandez-Resendiz et al., 2020); In fact, it depends on the tethering of two adjacent mitochondria via the OMM fusion GTPase proteins, mitofusin 1 (Mfn1) and mitofusin 2 (Mfn2), which then mediate fusion of the OMMs in a GTP-dependent manner. Subsequently, the inner mitochondrial membrane (IMM) fusion GTPase protein, optic atrophy 1 (OPA1), mediates fusion of the IMMs resulting in sharing of mitochondrial matrix material, and the formation of a single elongated mitochondrion (Hernandez-Resendiz et al., 2020). The mitochondrial fragmentation observed in ALS experimental models suggested a tipped balance of mitochondrial fission and fusion towards excessive fission due to increased fission, reduced fusion, or both.

Thus, our results may be compatible with a prevalence of fission on fusion processes, under OS induction. On the other hands, we also observed how mitochondria appear to undergo a rapid reorganization to form networks. At the network scale, a large, stable mitochondrial reticulum can provide a structural pathway for energy distribution and communication across long distances yet also enable rapid spreading of localized dysfunction (Glancy et al., 2020). Highly dynamic mitochondrial networks allow for frequent content mixing and communication but require constant cellular remodeling to accommodate the movement of mitochondria. However, increasing the number of contact sites between mitochondria and any given organelle reduces the mitochondrial surface area available for contact sites with other organelles as well as for metabolite exchange with cytosol (Glancy et al., 2020). The precise mechanisms guiding the coordinated multi-scale mitochondrial configurations observed in different cell types have yet to be elucidated, but it is clear that mitochondrial structure is controlled at every level to optimize mitochondrial function in order to meet specific cellular demands(Glancy et al., 2020). Whether the increasing in network number in our model aims to be protective against oxidative insult or, on the contrary, facilitates the spreading of dysfunction, need to be clarified.

Regarding proteasomal stress induced by epoxomicin, the results show a significant decrease in the number of individual mitochondria at both treatment times (2 and 4 hours). The number of networks showed the same tendency, decreasing at both treatment times,

being the change statistically significant only at 2 hours. Consequently, in this case, fusion or mitophagy could prevail on fission.

A recent study depicted a similar scenario in which proteasome inhibition triggers disintegration of the mitochondrial network and a reduced energy output, associated with OS (Sulkshane et al., 2020). The researchers employed HeLa cells devoid of Parkin, the primary E3 ligase responsible for mitophagy. Thanks to comparative proteomics, they elucidated changes to mitochondria in response to proteasome inhibition and highlighted potential roles of the UPS in ensuring unhindered protein import to mitochondria. Indeed, a general outcome of proteasome inhibition is accumulation of damaged proteins inducing an unfolded protein response and elevation of heat shock proteins (Q. Ding & Keller, 2001). Thus, in line with this, Sulkshane and collegues found that certain cytosolic chaperones and heat shock response proteins were enriched at mitochondria following proteasome inhibition (Sulkshane et al., 2020). It is of note that prolonged proteotoxic stress activates additional pathways of protein degradation such as autophagy in order to overcome reduced proteasome capacity (Park & Cuervo, 2013). Proteasome activity has also been proven to play an important role upon mild mitochondrial stress in *Caenorhabditis elegans* (Sladowska et al., 2021). It has been suggested that impairments in mitochondrial import machinery can activate a universal stress response that results in an increase in the activity of cytosolic degradation machinery, namely the proteasome. To date, this phenomenon has been described only in yeast and named unfolded protein response activated by protein mistargeting (UPRam) (Wrobel et al., 2015). The UPRam was defined as a response to the accumulation of mitochondrial precursor proteins in the cytosol, one characteristic feature of which is activation of the proteasome at the level of proteasome complex rearrangements. Non-imported mitochondrial precursor proteins can also cause clogging of the main gateway to mitochondria, the TOM translocase. In yeast, clogging of the translocase activated a transcriptional response that induced the clearance and proteasomal degradation of proteins that failed to be imported (Weidberg & Amon, 2018).

Impaired proteasome function also contributes to ALS pathogenesis. Apoptosis is promoted by accumulation of abnormal proteins and through depletion of HSPs that have direct inhibitory effects on apoptotic pathways in addition to their protein chaperoning activity (Michael Y. Sherman Alfred & L. Goldberg, 2001). The proteasome is the major pathway for degradation of transcription factors and other short-lived regulatory proteins, thus proteasomal inhibition could alter transcription of multiple gene families including those that promote cell death (Almond & Cohen, 2002). Another important function of

proteasome is degrading misfolded proteins shuttled into the cytoplasmic from the endoplasmic reticulum (ER); both ER and Golgi networks are disrupted in ALS and experimental models of mutant SOD1, implicating multiple compartments in failure of protein quality control (Turner & Atkin, 2006). In ALS, proteasome inhibitors also disrupt mitochondrial homeostasis (Ling et al., 2003). Motor neurons in ALS patients and in $SOD1^{G93A}$ and $SOD1^{G37R}$ transgenic mice do exhibit mitochondrial abnormalities (Hervias et al., 2006) and the relationship between mitochondrial and proteasomal dysfunction in ALS deserves investigation. In our model, it should be interesting to further explore the mechanisms that produce the observed mitochondrial dynamics alterations under proteasomal inhibition and their consequences such as potential changes in the mitochondrial proteome. A further effort in elucidated the crosstalk between proteasome impairment and mitochondrial dysfunction is worth it considering its potential therapeutic implications. Indeed, a currently active line of investigation is exploring the effects of phytochemicals, specifically polyphenols (PPs) as modulators of the proteasome activity. It has been shown that PPs modify the UPS by means of accumulation of ubiquitinated proteins, suppression of neuronal apoptosis, reduction of neurotoxicity, and improvement of synaptic plasticity and transmission (Momtaz et al., 2020).

Exploring the effect of ER stress induced by thapsigargin on mitochondrial dynamics, we found that the number of individual mitochondria was decreased at the shorter treatment time (2h), being this change transient, since this trend was reversed at the longer treatment time (4h) with a significant increase in the number of individual mitochondria. Thus, upon these conditions, the outcome is similar to the one observed for proteasomal inhibition, with a prevalence of fusion or mitophagy on fission at 2 hours and a prevalence of fission mechanisms at 4 hours. Mitochondrial networks diminished at 2 hours while they underwent a slightly, significant increase at 4 hours. Also, when comparing the two treatment times, we observed a significant increase of mitochondrial networks at 4 hours in comparison with 2 hours.

To understand how the induction of ER stress can have consequences on mitochondrial dynamics, we should keep in mind the close physical and functional relationship exiting between these two organelles.

The isolation of ER-mitochondria contacts was performed ~45 years ago by density gradient differential centrifugation from rat liver (Jain & Shivanna, 1989). Vance subsequently coined the term mitochondria associated ER membranes (MAMs) (A E Rusiñol et al., 1994). These functional sites participate in lipid metabolism, calcium

signaling, mitochondrial fission and fusion, ER stress, apoptosis, and autophagy (Gordaliza-Alaguero et al., 2019). The distance between ER and mitochondria were estimated to be around 100 nm but later digital imaging microscopy and electron tomography studies proved that they were at a distance of 10 to 25 nm during resting conditions, hence, they are referred to as 'tethering of organelles' (Giacomello & Pellegrini, 2016). However, during environmental stress, the contact sites become tighter (~10nm) (Gordaliza-Alaguero et al., 2019).

As already stated, the observed decrease in the number of mitochondria and network upon ER stress at 2 hours could be due to mitophagy. The PINK1/PARKIN pathway is the most well studied pathway of mitophagy. It has been found that PINK1 and BECN1 re-localize at MAMs during mitophagy and promote the ER mitochondria tethering (W. X. Ding & Yin, 2012). It is not surprising that later it was found few MAM proteins are actively involved in the mitophagy process. For example, FUNDC1 is a novel MAM protein required for hypoxia-induced mitophagy (Wu et al., 2016). Numerous studies have convincingly demonstrated the crucial role of macro-autophagy and mitophagy in the commitment and differentiation of stem cells. MAM protein, Atad3a engages in the maintenance of human progenitor cells via the PINK/PARKIN arm of mitophagy(G. Jin et al., 2018) Deletion of Pink1 in Atad3a-deficient mice rescued mitophagy related defects which in turn resulted in the restoration of the progenitor and hematopoietic stem cell pools (G. Jin et al., 2018). In the lights of these findings, we may hypothesize that ER stress could be "transferred" to mitochondria through the activation of the above mentioned mitophagy pathway at MAMs. Summarizing, the links between mitochondria and ER are established through specialized ER-mitochondria encounter structures (ERMES) comprising both ER and mitochondrial transmembrane proteins that provide a tethering force between the two organelles to ensure proximity and communication (Franzini-Armstrong, 2007). Mitofusin-2 (Mfn2) is an ERMES component that serves to tether mitochondria to the ER. Mfn2 also serves to fuse mitochondria, which together with other fusion proteins [e.g., Mfn1, optic atrophy 1 (Opa1)] elongate mitochondria making them more filamentous, whereas fission proteins such as dynamin related protein 1 (Drp1) and fission 1 protein (Fis1) act to fragment mitochondria. Together these fusion/fission proteins act to dynamically remodel mitochondria under a variety of conditions and their alternate action could explain the transient changes we observed in our model, depending on treatment time.

However, an enhanced understanding of the factors that control the communication between ER and mitochondria can lead to targeted therapeutic interventions as these

molecules, such as IRE1α and PERK are highly involved in the development neurodegenerative diseases through different pathways (Kumar & Maity, 2021).

Finally, we report that the induction of mitochondrial stress by rotenone exposure did not cause any significant change in the number of mitochondrial networks or in the network index, while the number of individual mitochondria was slightly but significantly diminished at 2 hours; this phenomenon appears to be transient, considering that at 4 hours the opposite is true, with a slightly but statistically significant increase in the number of individual mitochondria.

In relation with these findings, a very comprehensive exploration on the effect of rotenone on mitochondrial dynamics has been conducted by Chernicev et al. in 2018. In the mentioned work, rotenone was used to induce parkinsonian cellular conditions in *Dictyostelium discoideum. The authors have reported* that rotenone disrupts the actin and microtubule cytoskeleton, but mitochondrial morphology remains intact. Furthermore, they showed that rotenone stimulates mitochondrial velocity while inhibiting mitochondrial fusion, increases reactive oxygen species (ROS) but has no effect on ATP levels (Chernivec et al., 2018). Thus, the effect on the mitochondrial dynamics may be indirectly due to the negative effect of rotenone on the integrity of the cytoskeleton. In our model, the inhibition of fusion could explain the increase in the number of individual mitochondria we observed at 4 hours. This negative effect on fusion could be maybe not observable at 2 hours, where the fusion mechanisms seem to be active.

Specifically, the loss of microtubules causes a decrease in mitochondrial velocity, fission, and fusion, while loss of actin decreases the percentage of moving mitochondria (Woods et al., 2016). Also, rotenone was found to affect dynamics but not equivalently to the simple loss of the cytoskeleton. Indeed, immunofluorescence analysis of the microtubule cytoskeleton demonstrated that increasing concentrations of rotenone, as expected, alters the microtubules, driving them toward less assembled shorter structures (Chernivec et al., 2018). Moreover, rotenone unbalances fission and fusion, by significantly decreasing fusion, and increasing mitochondrial velocity, with no effect on the percentage of moving mitochondria. These effects are likely due to a combination of cytoskeletal defects and the increase in ROS. Perhaps the direct effect is on fusion; therefore, indirectly velocity is increased in an effort for the mitochondria to find each other to maintain the fusion processes (Chernivec et al., 2018). Alternatively, the disruption of the mitochondria's main transport mechanism could decrease the ability of two organelles to effectively come in contact with each other thus decreasing fusion. Interestingly, Peng

et al., 2017 saw a similar phenotype in PC12 cells with expression studies indicating an increase in fission proteins and a decrease in fusion proteins (Peng et al., 2017). It's worth noting that Chervicev and colleagues used rotenone at much more higher concentrations (ranging from 150µM to 500µM) than the one we employed in our experiments (4µM). A dose-dependent response in mitochondrial dynamics changes was observed while examining alteration of microtubules (Chernivec et al., 2018), so it would be interesting to test a range of increasing concentrations of rotenone in our model to check mitochondrial dynamics more extensively. Indeed, despite many drug-based and gene therapy approaches targeting mitochondrial dysfunction in ALS, neither treatments aimed at increasing mitochondrial function and survival nor those aimed at reducing oxidative stress have yielded significant results in clinical trials, despite promising trials in animal models (Goyal & Mozaffar, 2014). For example, several drugs targeting mitochondrial function and/or ROS such as Coenzyme Q10, Dexpramipexole, Olesoxime and Creatine all showed initial success in animal models but were unsuccessful in human clinical trials (Goyal & Mozaffar, 2014). For these reasons, further insights on mitochondrial alterations are strongly needed.

4.4 Acute metabolic switch and mitochondria dysfunctions

Using galactose instead of glucose in the culture medium of hepatoma cell lines, such as HepG2 cells, has been utilized for a decade to unmask the mitochondrial liability of chemical compounds (Kamalian et al., 2019).

Considering the well-established role mitochondrial dysfunction in neurodegenerative processes (Yang et al., 2020)and the results about mitochondrial dynamics and stress described above, we induced a metabolic switch in murine immortalized fibroblasts lines carrying three different variants of TDP-43, namely TDP-43^{M323K}, TDP-4^{F210I} and TDP-43 ^{Q331K} in comparison with TDP-43^{WT}. Specifically, cells underwent modification in their growth conditions, consisting of a glucose-galactose switch and pyruvate deprivation. Thus, mitochondrial dysfunction at various levels was evaluated comparing cells growth upon glucose/pyruvate availability and their "switched" counterparts.

4.4.1 Measurement of viability, cellular respiration, and mitochondrial mass

With the aim of an extensive characterization of the potential mitochondrial impairment depending on *Tardbp* genetic background, we firstly estimated MEFs viability after 6 hours under metabolic switch induction. Thus, cells were stained with propidium iodide (PI), a popular red-fluorescent nuclear and chromosome counterstain. Since propidium iodide is

not permeant to live cells, it is commonly used to detect dead cells in a population (Bahmani et al., 2011). PI staining was measured by flow cytometry. The results display heterogeneity based on *Tardbp* genetic background. More specifically, we observed a significant decrease in the number of viable cells when comparing WT TDP-43 genotype upon glucose availability with its counterpart upon glucose/pyruvate deprivation. The same trend, with a greater significance, was observed for the TDP-43 ^{Q331K} genotype, with an evident decrease in cellular viability under metabolic switch induction in comparison with growth in the glucose/pyruvate medium. Contrastingly, no significant differences were detected for the TDP-43 ^{F210I} and TDP-43 ^{M323K} genotypes. TDP-43 mutation, as well as energy status and the interaction between these two factors, appeared to determine such significant changes in cell viability. Previous findings have shown that replacing glucose with galactose in the culture environment cells become more sensitive to mitochondrial perturbations caused by mitotoxicants (Orlicka-Płocka et al., 2020). Interestingly, in 2012 Graham et al. reported that glucose and pyruvate deprivation provokes a systems-level positive feedback loop between ROS generation, protein tyrosine phosphatases (PTPs), and tyrosine kinase (TK) signaling in cells dependent on glucose for survival. The same authors also observed that glucose withdrawal induces supra-physiological levels of phospho-tyrosine signaling, in line with previous reports about the induction of oxidative stress (Spitz et al., 2000; Aykin-Burns et al., 2009) and the activation of diverse intracellular kinases including ERK, JNK, and Lyn (S. R. Lee et al., 1998; Blackburn et al., 1999) by glucose withdrawal. It is also known that ROS can inhibit PTPs, inducing further TK signaling (Y. J. Lee et al., 1998; Mahadev et al., 2001; Meng et al., 2002). Taken together, this systems perspective reveals that glucose and pyruvate deprivation activates a positive feedback amplification loop, as indicated by supra-physiological levels of phospho-tyrosine signaling, until ROS accumulate above a toxicity threshold resulting in cell death. We speculate that a similar mechanism could determine loss of cell viability both in TDP-43 WT and TDP-43 ^{Q331K} genotypes in our model. Nevertheless, further experiments are required to contrast this hypothesis, such as checking for upregulation of phospho-tyrosine signaling.

Regarding TDP43^{M323K} and TDP-43 ^{F201I} genotypes, the non-significant changes in cell viability could suggest a better adaptation for these genotypes to metabolic stress. As already mentioned, M323K mutation is located within the low complexity domain (LCD), while the F210I mutation was found in the second RNA-binding domain (RRM2) of TDP-43. The LCD mutation results in a TDP-43 GOF that affects the splicing of a subset of genes not previously known to be controlled by TDP-43, whereas the RRM2 mutation

behaves as a LOF, strongly reducing the RNA-binding capacity of the protein (de Giorgio et al., 2019). In order to characterize the type of cellular death detected for WT and Q331K genotype, we carried out an assay based on the flow cytometric detection of activated caspase-3 and caspase-7. The involvement of these two effectors of apoptosis was better explained in a work published in 2006; researchers studied the effect of caspase 3 and 7 deletion in mice fibroblasts, founding that these cells were highly resistant to both mitochondrial and death receptor–mediated apoptosis, displayed preservation of mitochondrial membrane potential, and had defective nuclear translocation of apoptosis-inducing factor (AIF). In addition, the early apoptotic events of Bax translocation and cytochrome c release were also delayed. They concluded that caspases 3 and 7 are critical mediators of mitochondrial events of apoptosis (Lakhani et al., 2006). Nevertheless, in our model we didn't observe any significant change in the activation of caspase 3/7, when comparing control cells with their deprived counterpart. Thus, the mortality we observed in deprived cells with WT and Q323K *Tardbp* mutations seems to be not related with the activation of these caspases, being probably due to some form of caspase-independent cell death. In fact, an increasing number of studies substantiate the existence of caspase-independent forms of programmed cell death. According a recent classification based on both morphological and biochemical criteria, three different forms of programmed cell death exist in addition to passive necrosis: 1) classical, caspase-dependent apoptosis associated with membrane blebbing, huge chromatin condensation/fragmentation, phosphatidylserine exposure, disruption of the cell into apoptotic bodies, activation of executioner caspases and internucleosomal DNA cleavage, 2) apoptosis-like PCD characterized by less compact chromatin condensation, phosphatidylserine exposure, but absence of executioner caspase activation, and 3) necrosis-like PCD which occurs in the absence of both chromatin condensation and caspase activation. In addition to this tripartite classification, there are more specialized forms of PCD not fitting into any of the three above models (Lakhani et al., 2006). Yet another type of PCD is represented by autophagy, which is characterized by prominent cytoplasmic vacuolization, cells are destroyed by degradation of cellular components via an autophagosomic-lysosomal pathway (Lakhani et al., 2006). Indeed, cell death in ALS and in general was previously believed to exist as a dichotomy between apoptosis and necrosis (Morrice et al., 2017). However, a new form of programmed cell death has been recently related to ALS, namely "necroptosis"; this could be a primary mechanism driving motor neuron cell death in different forms of ALS (Morrice et al., 2017). It could be interesting to characterize the type of cellular death we observed for this two *Tardbp* genotype, considering that several forms of caspase-independent cell death are now well

described in literature, which is the case of necroptosis. Considering the lack of molecular markers for necroptosis, this form of cellular death can be detected using a combination of approaches. For cultured cells, extracellular release of HMGB1, loss of cell viability, and depletion of ATP can be used as markers of necroptosis, but do not distinguish necroptosis from other types of necrotic death. More definitive evidence for necroptosis is the requirement of RIP1, RIP3, and/or MLKL (Chen et al., 2016). An additional insight on differential response to metabolic stress in mutant MEFs, comes from the respirometry experiments and the flow cytometric evaluation of the mitochondrial mass we conducted in this model. Results from respirometry experiments show significant higher glycolytic ATP production rate for Q331K MEFs in comparison with WT, both upon normal and deprived growth conditions. On the other hand, the mitochondrial contribution to ATP synthesis was decreased in Q33K genotype in comparison with WT, both upon normal and deprived growth conditions. For the remaining *Tardbp* genotypes no significant changes in the glycolytic or mitochondrial ATP rate were detected in comparison with WT. This findings are in contrast with the substitution of galactose for glucose in cell culture media as a way to enhance mitochondrial metabolism in a variety of cell lines (Elkalaf et al., 2013). Nevertheless, in our model, not only glucose was substituted with galactose as energetic substrate, but cells were exposed to pyruvate deprivation at the same time. As already depicted In section 1.5, Graham et al. showed in 2012 that glucose and pyruvate withdrawal in cells dependent on glucose for survival activates a positive feedback amplification loop, as indicated by supra-physiological levels of phospho-tyrosine signaling, until ROS accumulate above a toxicity threshold resulting in mitochondrial dysfunction and finally in cell death (Graham et al., 2012). A similar mechanism could explain the lack of significant enhancement of mitochondrial ATP production upon metabolic switch both in WT and Q331K genotypes. Concerning the maintenance of the same glycolytic ATP production rate both comparing control and deprived WT MEFs or control and deprived Q331K MEFs, the phenomenon could be related to the findings published by Reitzer et al. in 1979 for cultured HeLa cells. Indeed, these researchers suggested that glutamine provides energy by aerobic oxidation from citric acid cycle metabolism, provides more than half of the cell energy when high concentrations of glucose are present in the culture medium, and greater than 98% when fructose or galactose is the carbohydrate (Reitzer et al., 1979).

Mitochondrial mass was measured following the protocol described in section 2.9. Flow cytometry allowed the split cellular populations in sub-populations based on the affinity for IP and NAO, differentiating living cells (P4 population) from “apoptotic” (P3 population)

cells. Thus, when comparing control MEFs with their deprived counterpart in the P3, we observed a significant decrease of mitochondrial mass (NAO affinity) for WT, Q331K and M323K genotypes, while the same tendency was reported for F201I MEFs, with no statistical significance. For cells belonging to P4 population, affinity for NAO was significantly increased only in the case of Q331K genotype, being changes for the remaining genotype non-significant. Mitochondrial depletion in P3 population is again in line with Graham et al. studies about pyruvate and glucose withdrawal in cells using glucose as their main source of energy, and it is also in accordance with respirometry results, i.e. with the incapacity of deprived MEFs (independently from the genotype) to enhance their mitochondrial ATP production rate. Among cells that can survive to metabolic switch (P4 population), Q331K genotype seems to acquire resistance to mitochondrial dysfunction, increasing mitochondrial mass in response to stress induction. Interestingly, in mesenchymal stromal/stem cells (MSC), a similar phenomenon was observed in presence of augmented superoxide production and decreased mitochondrial membrane potential due to senescence. Authors related these changes in morphology to slightly levels increase in mitochondrial fusion proteins, MFN1and Dynamin-related OPA1 (Stab et al., 2016). In our model, increased mitochondrial mass could represent, for Q331K-cells, an attempt to survive in presence of high levels of ROS due to metabolic switch that doesn't result in a significantly increased mitochondrial metabolism. It would be interesting to evaluate the levels of fusion-related proteins to characterize mitochondrial dynamics in our models.

4.4.2 Alterations of the mitochondrial membrane potential

The mitochondrial membrane potential (ΔΨm), which is an essential component in the process of energy storage during oxidative phosphorylation (Zorova et al., 2018). Indeed, together with the proton gradient (ΔpH), ΔΨm forms the transmembrane potential of hydrogen ions which is harnessed to make ATP (Zorova et al., 2018). Thus, with the aim to investigate the potential changes of this parameter, we quantified ΔΨm in MEFs lines, as described in section 2.11. Secondly, we performed an immunofluorescence-based analysis to quantify respiratory Complex I level, the largest and most complicated enzyme of the electron transport chain (Brandt, 2006).

Interestingly, determination of the ΔΨm in our model, upon the two differential growth conditions mentioned above, showed that alterations in this pivotal indicator for mitochondrial function vary with genetic background. In fact, upon galactose/no pyruvate exposure, the WT and the TDP-43^{F210I} genotypes didn't show a significant alteration in their ΔΨm; on the other hand, both TDP-43 ^{Q331K} and TDP-43 ^{F210I} genotypes manifest a

significant reduction of the ΔΨm. In particular, TDP-43^{Q311K} suffers a weaker (approx. 30%) decrease in ΔΨm than TDP-43^{F210I} (approx. 40%). This finding is in line with the results of the investigation mentioned above with decreased ΔΨm being detected as a consequence of ROS production in senescence (Brandt, 2006).

It is to note that the three TDP-43A mutations we considered are located in different regions of the TDP-43 protein. More specifically, F210I is located in the RRM2 region, while Q331K and M323K occur in the glycine-rich LDC, at the C-terminal. Thus, their effect on TDP-43 is different; in a well-established splicing assay and RNA-seq it has been shown that the F210I mutation leads to a dose-dependent TDP-43 LOF, whereas the M323K mutation leads to a GOF (Fratta et al., 2018).

The LOF effect for F201I mutant was expected, because the mutation reduces TDP-43 RNA binding capacity; thus, this mouse model provides a novel tool to study chronic LOF *in vivo* and notably, in contrast to homozygous TDP-43 null mice, which do not survive beyond embryonic day 6 (Kraemer et al., 2010; Sephton et al., 2010).

Conversely, the splicing GOF effect produced by *M323K mutant* was unexpected and, although GOF effects had been previously described in transgenic models where TDP-43 is overexpressed, the *physiological setting* of the mutations in these mice shows for the first time that C-terminal TDP-43 mutations result in a splicing GOF (Fratta et al., 2018).

In the case of TDP-43^{Q331K}, this mutant as been related with abnormal nucleic acid binding that results in an increased aggregation rate of the protein (Lim et al., 2016). Indeed, a recent study unraveled the role of nuclear TDP-43 in facilitating the nuclear translocation of the XRCC4-DNA ligase 4 complex for the repair of DNA double-strand breaks (DSBs) via NHEJ and the effect of the Q331K mutation in disrupting this process, causing defective DSB repair, which may play a critical role in neurodegeneration.

Regarding our results on ΔΨm, an interesting link can be made with the findings of a recent study focusing on the prevention of mitochondrial impairment by inhibition of protein phosphatase 1 (PP1) in ALS (Choi et al., 2020). Since mitochondrial bioenergetics is expected to influence axonal growth, the authors of this study tested whether a blockade of PP1 or Dynamin-related protein 1 (Drp1) activity rescued the impairment of mitochondrial function induced by the overexpression of SOD1 G93A or TDP-43 ^{Q331K}, which rapidly reduced complex I activity and ΔΨm (Choi et al., 2020). Their results showed that suppression of the PP1-Drp1 cascade effectively prevented ALS-related symptoms, including mitochondrial fragmentation, axonal degeneration, and cell

death, in primary neuronal culture models, iPSC-derived human MNs, and zebrafish models *in vivo* (Choi et al., 2020).

It would be of interest to test if the same is true for TDP-43 ^{Q331K} and TDP-43 ^{F210I} upon metabolic switch induction. In this sense we should be aware of the fact that, as previously shown by others in different cell lines or primary fibroblasts (Marroquin et al., 2007; Rossignol et al., 2004) replacing glucose with galactose in the medium forces the cells to become more oxidative in order to maintain ATP levels. Moreover, adding pyruvate deprivation to glucose-galatose switch can increase ROS (Graham et al., 2012).Thus, the effect on ΔΨm may be enclosed in a vaster landscape in which metabolic switch may activate a series of pathways resulting in cell death.

To the best of our knowledge, we are not aware of reports about the link between TDP43^{F201I} mutant and reduced ΔΨm; however, mitochondrial impairment, including the presence of smaller mitochondria with swollen and degenerated cristae, were observed in cell and animal models of overexpressed TDP-43 ^{A315T} (Wang et al., 2019) and, to a lesser extent in models with WT TDP-43 overexpression. These degenerative changes were accompanied by reduced ΔΨm, increased ROS, reduced mitochondrial ATP and activation of the UPR (Wang et al., 2019).

In the light of our results on ΔΨm upon metabolic challenge, we may conclude that different *Tardpb* genotype affect in a specific way cell resistance to mitochondrial insult, with TDP-43 ^{M323K} and WT TDP-43 showing a better management of it in terms of ΔΨm preservation. These findings may be starting points to further investigate on the differential outcomes of TDP-43 mutations in ALS physiopathology and more personalized therapeutic approaches.

4.4.3 Metabolic switch and respiratory Complex I

To further investigate on the relationship between metabolic switch and mitochondrial impairment unmasking, we performed an immunofluorescence to quantify respiratory complex I, the largest and most complicated enzyme of the electron transport chain (Heidari et al., 2009; Wiedemann et al., 1998)

A series of studies have been performed on the presence of mitochondrial defects in lymphocytes and skeletal muscle of ALS patients and other neurological disease like Friedreich's ataxia and PD (Heidari et al., 2009; Wiedemann et al., 2002). Furthermore, defect of complex I either alone or in combination with other complexes is shown in the

patients with neurological disease including AD (Kish et al., 1992), PD (Schapira et al., 1990) multiple sclerosis (Hargreaves et al., 2018)and Friedreich's ataxia (Heidari et al., 2009).

Our results, similarly to the determination of ΔΨm alteration discussed above, show heterogeneity depending on the genetic *Tardpb* background. Thus, while WT TDP-43 doesn't show a significant alteration in the immunodetection of complex I upon metabolic switch, TDP-43 ^{Q331K}, TDP-43 ^{M323K} and TDP43^{F210I} genotypes showed significant changes, even though at different extent. Particularly, TDP-43 ^{M323K} displays significant decrease in complex I immunostaining upon glucose switch and pyruvate deprivation; contrastingly, TDP43^{F210I} and TDP-43 ^{Q331K} exhibit an increase in complex I abundance, which appears to be strongly significant for TDP43^{F210I} and slight but still significant for TDP43^{Q331K}.

As already mentioned, recent studies postulate that the cellular ROS levels and reactive oxygen species-related damage have important influence on mitochondrial morphology. Since OS may lead to protein damage and alterations in membrane integrity might also affect complex I function (Ghiasi et al., 2013). In addition, it has been reported a statistical correlation between complex I activity and patients' disease progression time, although this correlation is not quite linear, probably due to differences between age of patients (Beal, 2005; Ghiasi et al., 2013).

Also, galactose is extensively used for modeling aging-related pathophysiological processes in rodents (Sadigh-Eteghad et al., 2017). OS has been proposed as the main driver mediating galactose-induced senescence, although exact pathophysiological mechanisms mediating detrimental effects are yet to be elucidated (Azman & Zakaria, 2019). Proposed mechanisms by which galactose may induce redox dyshomeostasis include: (i) increased leakage of electrons from the mitochondrial electron transport chain (Yanar et al., 2011), (ii) wasting reducing equivalents (nicotinamide adenine dinucleotide phosphate; NADPH) that are required for biosynthetic and redox reactions in the process of metabolism of galactose to galactitol catalyzed by aldehyde reductase osmotic stress induced by accumulation of galactitol (iv) generation of advanced glycation end products (AGE) (Azman & Zakaria, 2019) and (v) accumulation of H_2O_2, a byproduct of galactose oxidation catalyzed by galactose oxidase (GO) (Cui et al., 2004).

Thus, concerning our results, we may postulate that respiratory complex I in the WT TDP-43 genotype is the less sensitive to the potential detrimental effects of galactose

administration and pyruvate deprivation; in the TDP-43 ^{M323K} it would be intriguing to measure complex I activity in a specific assay (e.g., using ferricyanide as an artificial electron acceptor) to establish whether the observed lowering in complex I abundance correlates with a lower activity.

It is more challenging trying to elucidate the mechanisms that lead to the incremented Complex I we observed in TDP-43 ^{F201I} and TDP-43 ^{Q331K} genotypes. A recent study has claimed that, consequently to the exposure of N2A cells to proteasomal inhibition, respiratory complexes (RCs) tend to an increased supraorganization with increased pelletable aggregation of RC subunits inside mitochondria (Rawat et al., 2021). More specifically, Complex II (CII) and complex V (CV) subunits are increasingly incorporated into oligomers, while Complex I (CI), complex III (CIII) and complex IV (CIV) subunits are engaged in supercomplex formation (Rawat et al., 2021). Notably, in the same study the abundance of RC subunits slightly increased after 8 h treatment with MG132, a potent, reversible, and cell-permeable proteasome inhibitor (Rawat et al., 2021). Based on our data, we cannot postulate a relationship between increased levels of complex I and RCs reorganization, but we think that further investigation on the cellular stress derived from metabolic switch could clarify if TDP-43 ^{F201I} and TDP-43 ^{Q331K} genotypes are prone to RCs reorganization to handle stress.

Once again, heterogeneity of results offers an opportunity for a better understanding of the effect of different mutations in TDP-43 on ALS physiopathology and the development of better focused therapeutic targets.

4.4.4 LDs replenishment and metabolic switch

LDs are cytosolic fat storage organelles present in most eukaryotic cells which far from being inert fat reservoirs, are emerging as major regulators of cellular metabolism. They act as hubs that coordinate the pathways of lipid uptake, distribution, storage, and use in the cell (see section 1.5). Recent studies have revealed that they are also essential components of the cellular stress response in which LDs maintain energy and redox homeostasis protecting against lipotoxicity by sequestering toxic lipids into their neutral lipid core. Their mobility and dynamic interactions with mitochondria enable an efficient delivery of fatty acids for optimal energy production (Jarc & Petan, 2019). In this project, we explored LDs formation as a consequence of metabolic insult in the previously described MEFs lines. Cells were incubated with 22-NBD Cholesterol together with the induction of metabolic stress in order to mark LDs accordingly to the protocol in section

2.16. All *Tardbp* genotype showed a remarkably significant increase in the number of LDs per cell. The response is heterogeneously depending on the considered genetic background, with the highest increase being reported for Q331K genotype upon metabolic stress. These results were corroborated by a specular increase in ACAT1/2 activity, which was strongly enhanced in deprived WT and Q331K genotypes in comparison with control counterparts. The same trend was reported for M323K and F201I MEFs, without reaching significance. The pivotal role of LDs in protecting mitochondria against stressful insults is well documented (Klecker et al., 2017).

Also, LDs formation has been related with OS. Thus, enhancement in LDs synthesis following metabolic stress, appears to be compatible with the detrimental effects of metabolic switch on mitochondrial, as previously described. Indeed, Q331K genotype experimented the higher increase in mitochondrial mass following glucose/galactose switch and pyruvate deprivation; this is in line with the induction of LDs, which could act in close contact with mitochondria apportioning energy-generating substrates to cellular defense. Similar adaptative mechanisms have been described *in vivo*. Membrane phospholipids are also a source of LDs, as claimed by a study on the formation of LDs, in mice exposed to hyperoxia, hypoxia, myocardial ischemia, and sepsis. All these stressors enhanced the formation of LDs, as assessed by transmission electron microscopy, with severe mitochondrial swelling. Moreover, the disruption of mitochondria by depleting mitochondrial DNA significantly augmented the formation of LDs, causing transcriptional activation of fatty acid biosynthesis and metabolic reprogramming to glycolysis (S. J. Lee et al., 2013). It would be interesting to establish whether the link between mitochondrial dysfunction and LDs formation can be confirmed also in our model.

4.5 LDs and osmotic stress in N2A cell line

LDs dynamics have been well studied in *Saccharomyces cerevisiae*, where they are modulated by the growth phase; In this organism the role of the TORC1 pathway on LD metabolism has been studied, since in mammals LD synthesis is inhibited by rapamycin, a known inhibitor of the mTORC1 pathway (Madeira et al., 2015). Interestingly, rapamycin treatment resulted in a fast LD replenishment and growth inhibition in this model. In addition, the discovery that osmotic stress (1 M sorbitol) also induced LD synthesis but not growth inhibition suggested that the induction of LDs in yeast is not a secondary response to reduced growth (Madeira et al., 2015). OsmS induced by sorbitol, is one of the stressors related with TDP-43 and p-TDP43 translocation out of the nucleus, as shown in Figure 40A. For this reason, we quantified LD formation in N2A cell line, following the

induction of osmotic stress by incubation with sorbitol at the same time and concentration producing TDP-43/p-TDP43 aggregation in the cytosol of HEK-293 cells. In a time, course experiment, we found that LDs marked with the lipophilic staining Nile Red (accordingly to the protocol in section 2.15), increase their number per cell with treatment time. At 3 hours, LD replenishment in treated cells was significantly higher in comparison with unstressed cells. Thus, in this particular cell model, osmotic stress induces changes in neutral lipid homeostasis. These results are corroborated by the increase in ACAT1/2 experimented by stressed cells, in which the esterification of 22-NBD Cholesterol is notably enhanced.

In line with these findings, an interesting study conducted on the budding yeast *Saccharomyces cerevisiae* claimed that mitochondrial function is generally required for proper salt and osmotic stress adaptation considering that mutants with defects in many different mitochondrial components show hypersensitivity to increased NaCl and KCl concentrations (Pastor et al., 2009). In this sense, the rapid increment of LD formation in our model could support the already mentioned protective role of LDs against stressful insults. The negative effect of sorbitol on mitochondrial integrity has been documented; in 2008, Marfè et al. published a paper in which osmotic stress was depicted as an apoptosis-inductor in cancer cells. In particular they focused on the intracellular signaling pathways of sorbitol-induced apoptosis in human K562 cells using morphological analysis and DNA fragmentation technique. They conclude that sorbitol-induced apoptosis in K562 cells was accompanied by the up-regulation of Bax, and down-regulation of p-Bcl-2, respectively pro-apoptotic and anti-apoptotic effectors.

Moreover, the sorbitol treatment resulted in a significant reduction of mitochondria membrane potential and increase in the release of mitochondrial cytochrome c (Marfè et al., 2008). It would be of interest establish the mitochondrial effects of Osms on our model to clarify if LDs increase could act as a mechanism to rescue damaged mitochondria via energy supplementation to avoid death. Moreover, since sorbitol can drive TDP-43 redistribution to the cytoplasm in different cell models such as SHSY-5Y (Y. B. Lee et al., 2021), establishing the role of LDs upon OsmS could be a starting point to improve the knowledge of the molecular pathways linking mitochondrial health, cellular stress, and changes in lipid dynamics in ALS.

4.6 LDs in isolated nuclei are influenced by ALS status

LDs normally emerge from, and associate with, the ER interacting with other cytoplasmic organelles to deliver the stored lipids. Recently, LDs were found to reside also at the inner side of the nuclear envelope and inside the nucleus both in yeast and mammalian cells. This unexpected finding raises fundamental questions about the nature of the inner nuclear membrane, its connection with the ER and the pathways of LD formation (Barbosa & Siniossoglou, 2020).

Accordingly with this report, we observed Nile Red-positive structure, compatible with LDs in isolated nuclei proceeding from frontal cortex of ALS patients and controls following the procedure described in section 2.14. In ALS samples, the number of LDs per nucleus were significantly higher in comparison with control. This finding is in line with a description of nuclear lipidome dysfunction in ALS we published last year (Ramírez-Nuñez et al., 2021).

In addition to that, in recent years several nuclear envelope remodeling events that contribute to both normal nuclear homeostasis and disease have been described. These include nuclear envelope rupture and repair, nuclear pore complex biogenesis, and viral nuclear egress pathways (King & Lusk, 2016). It is likely that extensive nuclear envelope shape changes in these cases are coordinated with local modification of phospholipid composition. In such a scenario, nuclear LDs could provide a pool of lipids located at the inner nuclear membrane for these remodeling events (Barbosa & Siniossoglou, 2020).

4.7 AGPS levels and ACAT1/2 activity in hiPS-derived motor neurons

Alkylglycerone phosphate synthase (AGPS) is an enzyme found in structures called peroxisomes. Within peroxisomes, AGPS is responsible for a critical step in the production of lipid molecules called plasmalogens, which are component of the cellular membrane. They are also abundant in myelin. However, little is known about the functions of plasmalogens. Researchers suspect that these molecules may help protect cells from OS (Almsherqi, 2021). Plasmalogens may also play important roles in interactions between lipids and proteins, the transmission of chemical signals in cells, and the fusion of cell membranes (Almsherqi, 2021). We quantified AGPS levels in hiPS cell-derived MNs from cell lines expressing FUS mutation, and C9orf72 expansion finding a reduction in these ALS-related neuronal lines in comparison with control MNs. It is known that nuclear size, correlated with AGPS in our experiments, may be controlled by factors such as

nucleocytoplasmic transport, lipid biogenesis, and RNA processing (Cantwell & Dey, 2021), which also contribute ALS pathogenesis. Indeed, the high abundance of ether-lipids in nuclear envelope (Dean & Lodhi, 2018) suggests the existence of a correlation between nuclear envelope size and mechanisms for the synthesis of these specific lipids. In addition, a recent publication conferred a key role of lipid enzymes such as phospholipase A2 in transmitting nuclear envelope stretch to membrane remodeling activities (Venturini et al., 2020). Our results show a correlation between AGPS mean intensity and nuclei perimeter for control and C9orf72 cell lines, which was not observed for FUS mutant. This discrepancy may indicate that FUS mutation could interfere with the mechanisms connecting nuclear size with lipid metabolism.

In order to investigate on changes in neutral lipid metabolism in these MNs, we also measured their capacity of activating ACAT1/2 in response to OsmS as a potentially protective mechanism against a stressful insult. Interestingly, ACAT1/2 activity was significantly increased when comparing unstressed control MNs with stressed control MNs, while no significant increase for FUS or C9orf72 MNs. Nevertheless, the enzymatic activity was significantly increased in stressed FUS MNs when compared with unstressed controls, suggesting that genetic background could have a role in determining the intensity of this response. We didn't check for LD formation in this model, so we cannot directly relate the increase in neutral lipid synthesis with LD replenishment. Further insights on lipid metabolism alterations in hiPS-derived MNs are needed to better understand the relationship between ALS genetics and alterations of the lipid metabolism as a key factor in ALS pathology.

4.8 LDs in primary astrocytes upon oxidative and osmotic stress

As mentioned in section 1.5.1, LDs can accumulate in the NCS, when the brain is in a pathological condition. Glial cells are especially involved in this phenomenon, much more than neurons. Nevertheless, we know very little about the mechanisms underlying LDs accumulation in astrocytes. A recent study focused to the imaging of fluorescently labeled LDs by microscopy in isolated and brain tissue rat astrocytes and in glia-like cells in *Drosophila* brain to determine the (sub)cellular localization, mobility, and content of LDs under various stress conditions found in brain pathologies. In this model, LDs displayed a limited mobility close to mitochondria and ER. Interestingly the inhibition of DGAT1 and DGAT2 enzymes, both involved in LD metabolism, caused an evident reduction in the number of cells, indicating that LD turnover is a pivotal factor for cell survival in stressed astrocytes (Smolič et al., 2021).

In our experiment, a primary culture of rat astrocyte was treated with oleic acid as described in section 2.17, in order to enhance LD synthesis. Cells were contemporarily treated with H_2O_2 or sorbitol recreating OS and OsmS. Following the treatments, astrocytes where stained with LipidTOX™ (see section 2.17.1). In both cases, oleic acid alone enhanced LDs accumulation, while when it was administered in cell culture in combination with both sorbitol or H_2O_2, the number of LDs per cell tend to decrease. Thus, OS and OsmS could interfere with the enhancement of LDs formation promoted by exogen oleic acid. Clearly, these results need to be supported by more evidence; it would be appropriate to test LD accumulation upon a vaster range of concentration and treatment times for oxidative and osmotic stressors, among others. Also, it is of note that a much better insight on LD turnover ins astrocytes, could be obtained in an astrocyte-neuron co-culture system. In fact, as mentioned in section 1.5.1, several studies support the idea of a close communication between neurons and astrocytes in which excessive FFA produced in stressed neurons seems to be transferred to astrocytes where they are stored in LDs protecting against lipotoxicity (Ioannou et al., 2019).

CONCLUSIONS

5. CONCLUSIONS

1. The induction of different ALS-related cellular stresses is related with significant alteration in the nuclear/cytosolic ratio of the proteins of interest in this work (p-TDP43, p-ERK, p-Jun and REST) as well as with their colocalization with mitochondria. These changes are highly variable depending on the protein, the nature of stress and the treatment time.

2. Crude mitochondrial fractions (CrMitoch) derived from brain lysates after subcellular fractionation, show the presence of p-TDP-43, p-ERK, p-Jun and REST.

3. Changes in REST-regulated genes have been found to be associated with cell stress induction of TDP-43 mislocalization. The effect of TARDBP ^{Q331K} overexpression on the mRNA levels of REST-regulated genes in murine brain lysates is not significant.

4. Stress induction plays a significant impact on mitochondrial morphology and dynamics in HMEC-1 cells. The responses were highly dependent on the nature of stress and treatment time, with fast and transient modifications in the number of individual mitochondria or networks (e.g., in the case of OS, with opposite tendencies with the treatment lasting 2 or 4 hours).

5. *Tardbp* genotype influence survival, mitochondrial mass, respiratory capacity, Complex I abundance and ΔΨm following the induction of metabolic stress in MEFs carrying three TDP-43 variants (M323K, Q331K and F201I) in comparison with WT. Characterization of cell death in Q331K and Q331K genotypes were found to be caspases-independent.

6. Changes in LD metabolism occur in different cell lines upon different stressors: LDs accumulation increase with time in N2A cells upon OsmS and for all *Tardbp*-mutant MEFs following metabolic switch assay. A significant increase in ACAT1/2 activity has been found in line with LD replenishment both in N2A cells and in WT or Q331K MEFs.

7. AGPS levels were diminished in FUS and C9orf72 hiPS-derived MNs in comparison with WT. AGPS mean intensity correlated with nuclei perimeter for WT and C9orf72 cell lines, but for FUS MNs. This discrepancy may indicate that FUS mutation could interfere with the mechanisms connecting nuclear size with lipid metabolism.

8. ACAT1/2 activity significantly increased in WT hiPS-derived MNs upon OsmS in comparison with their unstressed counterpart. For C9orf72 and FUS MNs this tendency was confirmed but without reaching significance. Thus, changes ACAT1/2 activity in this context appear to be heterogeneously depending on genetic background.

9. Isolated nuclei from frozen nervous tissue (proceeding from ALS patients and healthy controls) show Nile Red-positive structures compatible with LDs. LDs counting per nucleus was significantly higher in ALS nuclei representing an aspect of pathological alteration of nuclear lipidome in ALS pathology.

10. OS and OsmS interfere with LD formation in astrocytes. These results are in contrast with LD accumulation documented in several cellular models upon stress but may also be explained with the importance of the interaction between neurons and astrocytes for the latter to act as energy rich reservoirs and contrast stress in the CNS.

BIBLIOGRAPHY

A E Rusiñol, Z Cui, M. H. C., & J E Vance. (1994). *A unique mitochondria-associated membrane fraction from rat liver has a high capacity for lipid synthesis and contains pre-Golgi secretory proteins including nascent lipoproteins - PubMed*. Journal of Biological Chemistry. https://pubmed.ncbi.nlm.nih.gov/7961664/

Abrantes, H. de C., Briquet, M., Schmuziger, C., Restivo, L., Puyal, J., Rosenberg, N., Rocher, A. B., Offermanns, S., & Chatton, J. Y. (2019). The Lactate Receptor HCAR1 Modulates Neuronal Network Activity through the Activation of G α and G βγ Subunits. *The Journal of Neuroscience : The Official Journal of the Society for Neuroscience*, *39*(23), 4422–4433. https://doi.org/10.1523/JNEUROSCI.2092-18.2019

Adams, C. J., Kopp, M. C., Larburu, N., Nowak, P. R., & Ali, M. M. U. (2019). Structure and molecular mechanism of ER stress signaling by the unfolded protein response signal activator IRE1. *Frontiers in Molecular Biosciences*, *6*(MAR), 11. https://doi.org/10.3389/FMOLB.2019.00011/BIBTEX

Aktekin, M. R., & Uysal, H. (2020). Epidemiology of amyotrophic lateral sclerosis. *Turk Noroloji Dergisi*, *26*(3), 187–196. https://doi.org/10.4274/TND.2020.45549

Al-Anzi, B., Arpp, P., Gerges, S., Ormerod, C., Olsman, N., & Zinn, K. (2015). Experimental and computational analysis of a large protein network that controls fat storage reveals the design principles of a signaling network. *PLoS Computational Biology*, *11*(5). https://doi.org/10.1371/JOURNAL.PCBI.1004264

Albensi, B. C. (2019). What is nuclear factor kappa B (NF-κB) doing in and to the mitochondrion? *Frontiers in Cell and Developmental Biology*, *7*(JULY), 154. https://doi.org/10.3389/FCELL.2019.00154/BIBTEX

Alberti, S., & Hyman, A. A. (2021). Biomolecular condensates at the nexus of cellular stress, protein aggregation disease and ageing. In *Nature Reviews Molecular Cell Biology* (Vol. 22, Issue 3, pp. 196–213). Nature Research. https://doi.org/10.1038/s41580-020-00326-6

Allan Butterfield, D., & Boyd-Kimball, D. (2018). Oxidative Stress, Amyloid-β Peptide, and Altered Key Molecular Pathways in the Pathogenesis and Progression of Alzheimer's Disease. *Journal of Alzheimer's Disease*, *62*(3), 1345–1367. https://doi.org/10.3233/JAD-170543

Almond, J. B., & Cohen, G. M. (2002). The proteasome: a novel target for cancer chemotherapy. *Leukemia 2002 16:4*, *16*(4), 433–443. https://doi.org/10.1038/sj.leu.2402417

Almsherqi, Z. A. (2021). Potential Role of Plasmalogens in the Modulation of Biomembrane Morphology. *Frontiers in Cell and Developmental Biology*, *9*, 1648. https://doi.org/10.3389/FCELL.2021.673917/BIBTEX

Alvarez-Miranda, E. A., Sinnl, M., & Farhan, H. (2015). Alteration of Golgi structure by stress: A link to neurodegeneration? *Frontiers in Neuroscience*, *9*(NOV), 435. https://doi.org/10.3389/FNINS.2015.00435/BIBTEX

Ames, A. (2000). CNS energy metabolism as related to function. *Brain Research Reviews*, *34*(1–2), 42–68. https://doi.org/10.1016/S0165-0173(00)00038-2

Andersen, P. M. (2006). Amyotrophic lateral sclerosis associated with mutations in the CuZn superoxide dismutase gene. *Current Neurology and Neuroscience Reports*, *6*(1), 37–46. https://doi.org/10.1007/S11910-996-0008-9

Andrew, A. S., Bradley, W. G., Peipert, D., Butt, T., Amoako, K., Pioro, E. P., Tandan, R., Novak, J., Quick, A., Pugar, K. D., Sawlani, K., Katirji, B., Hayes, T. A., Cazzolli, P., Gui, J., Mehta, P., Horton, D. K., & Stommel, E. W. (2021). Risk factors for amyotrophic lateral sclerosis: A regional United States case-control study. *Muscle & Nerve*, *63*(1), 52. https://doi.org/10.1002/MUS.27085

Andrew, A., Zhou, J., Gui, J., Harrison, A., Shi, X., Li, M., Guetti, B., Nathan, R., Tischbein, M., Pioro, E. P., Stommel, E., & Bradley, W. (2021). Pesticides applied to crops and amyotrophic lateral sclerosis risk in the U.S. *NeuroToxicology*, *87*, 128–135. https://doi.org/10.1016/J.NEURO.2021.09.004

Aoyama, K. (2021). Glutathione in the Brain. *International Journal of Molecular Sciences*, *22*(9), 22. https://doi.org/10.3390/IJMS22095010

Apolloni, S., Parisi, C., Pesaresi, M. G., Rossi, S., Carrì, M. T., Cozzolino, M., Volonté, C., & D'Ambrosi, N. (2013). The NADPH oxidase pathway is dysregulated by the P2X7 receptor in the SOD1-G93A microglia model of amyotrophic lateral sclerosis. *Journal of Immunology (Baltimore, Md. : 1950)*, *190*(10), 5187–5195. https://doi.org/10.4049/JIMMUNOL.1203262

Arai, T., Hasegawa, M., Akiyama, H., Ikeda, K., Nonaka, T., Mori, H., Mann, D., Tsuchiya, K., Yoshida, M., Hashizume, Y., & Oda, T. (2006). TDP-43 is a component of ubiquitin-positive tau-negative inclusions in frontotemporal lobar degeneration and amyotrophic lateral sclerosis. *Biochemical and Biophysical Research Communications*, *351*(3), 602–611. https://doi.org/10.1016/j.bbrc.2006.10.093

Armakola, M., Higgins, M. J., Figley, M. D., Barmada, S. J., Scarborough, E. A., Diaz, Z., Fang, X., Shorter, J., Krogan, N. J., Finkbeiner, S., Farese, R. v., & Gitler, A. D. (2012). Inhibition of RNA lariat debranching enzyme suppresses TDP-43 toxicity in ALS disease models. *Nature Genetics*, *44*(12), 1302–1309. https://doi.org/10.1038/NG.2434

Arsović, A., Halbach, M. V., Canet-Pons, J., Esen-Sehir, D., Döring, C., Freudenberg, F., Czechowska, N., Seidel, K., Baader, S. L., Gispert, S., Sen, N. E., & Auburger, G. (2020). Mouse Ataxin-2 Expansion Downregulates CamKII and Other Calcium Signaling Factors, Impairing Granule—Purkinje Neuron Synaptic Strength. *International Journal of Molecular Sciences*, *21*(18), 1–36. https://doi.org/10.3390/IJMS21186673

Attwell, D., & Laughlin, S. B. (2001). An energy budget for signaling in the grey matter of the brain. *Journal of Cerebral Blood Flow and Metabolism*, *21*(10), 1133–1145. https://doi.org/10.1097/00004647-200110000-00001

Audet, J. N., Gowing, G., & Julien, J. P. (2010). Wild-type human SOD1 overexpression does not accelerate motor neuron disease in mice expressing murine Sod1 G86R. *Neurobiology of Disease*, *40*(1), 245–250. https://doi.org/10.1016/J.NBD.2010.05.031

Auten, R. L., Whorton, M. H., & Mason, S. N. (2002). Blocking Neutrophil Influx Reduces DNA Damage in Hyperoxia-Exposed Newborn Rat Lung. In *Am. J. Respir. Cell Mol. Biol* (Vol. 26). www.atsjournals.org

Ayala, V., Granado-Serrano, A. B., Cacabelos, D., Naudí, A., Ilieva, E. v., Boada, J., Caraballo-Miralles, V., Lladó, J., Ferrer, I., Pamplona, R., & Portero-Otin, M. (2011). Cell stress induces TDP-43 pathological changes associated with ERK1/2 dysfunction: Implications in ALS. *Acta Neuropathologica*, *122*(3), 259–270. https://doi.org/10.1007/S00401-011-0850-Y/FIGURES/7

Ayala, Y. M., de Conti, L., Avendaño-Vázquez, S. E., Dhir, A., Romano, M., D'Ambrogio, A., Tollervey, J., Ule, J., Baralle, M., Buratti, E., & Baralle, F. E. (2011). TDP-43 regulates its mRNA levels through a negative feedback loop. *EMBO Journal*, *30*(2), 277–288. https://doi.org/10.1038/emboj.2010.310

Ayala, Y. M., Misteli, T., & Baralle, F. E. (2008). *TDP-43 regulates retinoblastoma protein phosphorylation through the repression of cyclin-dependent kinase 6 expression*. www.pnas.org/cgi/content/full/

Aykin-Burns, N., Ahmad, I. M., Zhu, Y., Oberley, L. W., & Spitz, D. R. (2009). Increased levels of superoxide and H2O2 mediate the differential susceptibility of cancer cells versus normal cells to glucose deprivation. *The Biochemical Journal*, *418*(1), 29–37. https://doi.org/10.1042/BJ20081258

Azman, K. F., & Zakaria, R. (2019). d-Galactose-induced accelerated aging model: an overview. *Biogerontology 2019 20:6*, *20*(6), 763–782. https://doi.org/10.1007/S10522-019-09837-Y

B R Krause, & A D Hartman. (1984). *Adipose tissue and cholesterol metabolism - PubMed*. Journal of Lipid Research. https://pubmed.ncbi.nlm.nih.gov/6368715/

Bahmani, P., Schellenberger, E., Klohs, J., Steinbrink, J., Cordell, R., Zille, M., Müller, J., Harhausen, D., Hofstra, L., Reutelingsperger, C., Farr, T. D., Dirnagl, U., & Wunder, A. (2011). Visualization of cell death in mice with focal cerebral ischemia using fluorescent annexin A5, propidium iodide, and TUNEL staining. *Journal of Cerebral Blood Flow and Metabolism*, *31*(5), 1311–1320. https://doi.org/10.1038/jcbfm.2010.233

Bailey, A. P., Koster, G., Guillermier, C., Hirst, E. M. A., MacRae, J. I., Lechene, C. P., Postle, A. D., & Gould, A. P. (2015). Antioxidant Role for Lipid Droplets in a Stem Cell Niche of Drosophila. *Cell*, *163*(2), 340–353. https://doi.org/10.1016/J.CELL.2015.09.020

Bak, L. K., Schousboe, A., & Waagepetersen, H. S. (2006). The glutamate/GABA-glutamine cycle: aspects of transport, neurotransmitter homeostasis and ammonia transfer. *Journal of Neurochemistry*, *98*(3), 641–653. https://doi.org/10.1111/J.1471-4159.2006.03913.X

Balch, W. E., Morimoto, R. I., Dillin, A., & Kelly, J. W. (2008). Adapting proteostasis for disease intervention. *Science (New York, N.Y.)*, *319*(5865), 916–919. https://doi.org/10.1126/SCIENCE.1141448

Balendra, R., & Isaacs, A. M. (2018). C9orf72-mediated ALS and FTD: multiple pathways to disease. In *Nature Reviews Neurology* (Vol. 14, Issue 9, pp. 544–558). Nature Publishing Group. https://doi.org/10.1038/s41582-018-0047-2

Ballas, N., & Mandel, G. (2005). The many faces of REST oversee epigenetic programming of neuronal genes. *Current Opinion in Neurobiology*, *15*(5), 500–506. https://doi.org/10.1016/J.CONB.2005.08.015

Balsa, E., Soustek, M. S., Thomas, A., Cogliati, S., García-Poyatos, C., Martín-García, E., Jedrychowski, M., Gygi, S. P., Enriquez, J. A., & Puigserver, P. (2019). ER and Nutrient Stress Promote Assembly of Respiratory Chain Supercomplexes through the PERK-eIF2α Axis. *Molecular Cell*, *74*(5), 877-890.e6. https://doi.org/10.1016/J.MOLCEL.2019.03.031

Barbalho, I., Valentim, R., Júnior, M. D., Barros, D., Júnior, H. P., Fernandes, F., Teixeira, C., Lima, T., Paiva, J., & Nagem, D. (2021). National registry for amyotrophic lateral sclerosis: a systematic review for structuring population registries of motor neuron diseases. *BMC Neurology*, *21*(1), 1–12. https://doi.org/10.1186/S12883-021-02298-2/TABLES/4

Barber, S. C., Mead, R. J., & Shaw, P. J. (2006). Oxidative stress in ALS: A mechanism of neurodegeneration and a therapeutic target. *Biochimica et Biophysica Acta (BBA) - Molecular Basis of Disease*, *1762*(11–12), 1051–1067. https://doi.org/10.1016/J.BBADIS.2006.03.008

Barbosa, A. D., & Siniossoglou, S. (2020). New kid on the block: lipid droplets in the nucleus. *The FEBS Journal*, *287*(22), 4838–4843. https://doi.org/10.1111/FEBS.15307

Barrachina, M., Moreno, J., Juvés, S., Moreno, D., Olivé, M., & Ferrer, I. (2007). Target genes of neuron-restrictive silencer factor are abnormally up-regulated in human myotilinopathy. *The American Journal of Pathology*, *171*(4), 1312–1323. https://doi.org/10.2353/AJPATH.2007.070520

Barros, L. F., & Deitmer, J. W. (2010). Glucose and lactate supply to the synapse. *Brain Research Reviews*, *63*(1–2), 149–159. https://doi.org/10.1016/J.BRAINRESREV.2009.10.002

Barthelme, D., Jauregui, R., & Sauer, R. T. (2015). An ALS disease mutation in Cdc48/p97 impairs 20S proteasome binding and proteolytic communication. *Protein Science : A Publication of the Protein Society*, *24*(9), 1521–1527. https://doi.org/10.1002/PRO.2740

Bartolome, F., Wu, H. C., Burchell, V. S., Preza, E., Wray, S., Mahoney, C. J., Fox, N. C., Calvo, A., Canosa, A., Moglia, C., Mandrioli, J., Chiò, A., Orrell, R. W., Houlden, H., Hardy, J., Abramov, A. Y., & Plun-Favreau, H. (2013). Pathogenic VCP mutations induce mitochondrial uncoupling and reduced ATP levels. *Neuron*, *78*(1), 57–64. https://doi.org/10.1016/J.NEURON.2013.02.028

Beal, M. F. (2005). Mitochondria take center stage in aging and neurodegeneration. *Annals of Neurology*, *58*(4), 495–505. https://doi.org/10.1002/ANA.20624

Beard, J. D., & Kamel, F. (2015). Military service, deployments, and exposures in relation to amyotrophic lateral sclerosis etiology and survival. *Epidemiologic Reviews*, *37*(1), 55–70. https://doi.org/10.1093/EPIREV/MXU001

Bélanger, M., Allaman, I., & Magistretti, P. J. (2011a). Brain energy metabolism: focus on astrocyte-neuron metabolic cooperation. *Cell Metabolism*, *14*(6), 724–738. https://doi.org/10.1016/J.CMET.2011.08.016

Bélanger, M., Allaman, I., & Magistretti, P. J. (2011b). Brain energy metabolism: focus on astrocyte-neuron metabolic cooperation. *Cell Metabolism*, *14*(6), 724–738. https://doi.org/10.1016/J.CMET.2011.08.016

Bélanger, M., Allaman, I., & Magistretti, P. J. (2011c). Brain energy metabolism: focus on astrocyte-neuron metabolic cooperation. *Cell Metabolism*, *14*(6), 724–738. https://doi.org/10.1016/J.CMET.2011.08.016

Bell, S. M., Burgess, T., Lee, J., Blackburn, D. J., Allen, S. P., & Mortiboys, H. (2020). Peripheral Glycolysis in Neurodegenerative Diseases. *International Journal of Molecular Sciences*, *21*(23), 1–19. https://doi.org/10.3390/IJMS21238924

Bendotti, C., Marino, M., Cheroni, C., Fontana, E., Crippa, V., Poletti, A., & de Biasi, S. (2012). Dysfunction of constitutive and inducible ubiquitin-proteasome system in amyotrophic lateral sclerosis: implication for protein aggregation and immune response. *Progress in Neurobiology*, *97*(2), 101–126. https://doi.org/10.1016/J.PNEUROBIO.2011.10.001

Bentmann, E., Neumann, M., Tahirovic, S., Rodde, R., Dormann, D., & Haass, C. (2012). Requirements for stress granule recruitment of fused in sarcoma (FUS) and TAR DNA-binding protein of 43 kDa (TDP-43). *Journal of Biological Chemistry*, *287*(27), 23079–23094. https://doi.org/10.1074/jbc.M111.328757

Berning, B. A., & Walker, A. K. (2019). The pathobiology of TDP-43 C-terminal fragments in ALS and FTLD. In *Frontiers in Neuroscience* (Vol. 13, Issue APR). Frontiers Media S.A. https://doi.org/10.3389/fnins.2019.00335

Bhinge, A., Namboori, S. C., Zhang, X., VanDongen, A. M. J., & Stanton, L. W. (2017). Genetic Correction of SOD1 Mutant iPSCs Reveals ERK and JNK Activated AP1 as a Driver of Neurodegeneration in Amyotrophic Lateral Sclerosis. *Stem Cell Reports*, *8*(4), 856–869. https://doi.org/10.1016/J.STEMCR.2017.02.019/ATTACHMENT/EC94530E-CCB8-4469-8EA9-5260F1EA3A06/MMC1.PDF

Blackburn, R. v., Spitz, D. R., Liu, X., Galoforo, S. S., Sim, J. E., Ridnour, L. A., Chen, J. C., Davis, B. H., Corry, P. M., & Lee, Y. J. (1999). Metabolic oxidative stress activates signal transduction and gene expression during glucose deprivation in human tumor cells. *Free Radical Biology & Medicine*, *26*(3–4), 419–430. https://doi.org/10.1016/S0891-5849(98)00217-2

Bleazard, W., McCaffery, J. M., King, E. J., Bale, S., Mozdy, A., Tieu, Q., Nunnari, J., & Shaw, J. M. (1999). The dynamin-related GTPase Dnm1 regulates mitochondrial fission in yeast. *Nature Cell Biology*, *1*(5), 298–304. https://doi.org/10.1038/13014

Blobel, G., & Potter, V. R. (1966). Nuclei from rat liver: isolation method that combines purity with high yield. *Science (New York, N.Y.)*, *154*(3757), 1662–1665. https://doi.org/10.1126/SCIENCE.154.3757.1662

Blokhuis, A. M., Groen, E. J. N., Koppers, M., van den Berg, L. H., & Pasterkamp, R. J. (2013). Protein aggregation in amyotrophic lateral sclerosis. *Acta Neuropathologica*, *125*(6), 777. https://doi.org/10.1007/S00401-013-1125-6

Blumberg, A., Sailaja, B. S., Kundaje, A., Levin, L., Dadon, S., Shmorak, S., Shaulian, E., Meshorer, E., & Mishmar, D. (2014). Transcription Factors Bind Negatively Selected Sites within Human mtDNA Genes. *Genome Biology and Evolution*, *6*(10), 2634. https://doi.org/10.1093/GBE/EVU210

Borroni, B., Archetti, S., del Bo, R., Papetti, A., Buratti, E., Bonvicini, C., Agosti, C., Cosseddu, M., Turla, M., di Lorenzo, D., pietro Comi, G., Gennarelli, M., & Padovani, A. (2010). TARDBP mutations in frontotemporal lobar degeneration: frequency, clinical features, and disease course. *Rejuvenation Research*, *13*(5), 509–517. https://doi.org/10.1089/REJ.2010.1017

Bos, P. H., Lowry, E. R., Costa, J., Thams, S., Garcia-Diaz, A., Zask, A., Wichterle, H., & Stockwell, B. R. (2019). Development of MAP4 Kinase Inhibitors as Motor Neuron-Protecting Agents. *Cell Chemical Biology*, *26*(12), 1703-1715.e37. https://doi.org/10.1016/J.CHEMBIOL.2019.10.005

Boumil, E. F., Vohnoutka, R. B., Liu, Y., Lee, S., & Shea, T. B. (2017). Omega-3 Hastens and Omega-6 Delays the Progression of Neuropathology in a Murine Model of Familial ALS. *The Open Neurology Journal*, *11*(1), 84. https://doi.org/10.2174/1874205X01711010084

Boylan, K. (2015). Familial Amyotrophic Lateral Sclerosis. *Neurologic Clinics*, *33*(4), 807–830. https://doi.org/10.1016/J.NCL.2015.07.001

Bozza, P. T., Bakker-Abreu, I., Navarro-Xavier, R. A., & Bandeira-Melo, C. (2011). Lipid body function in eicosanoid synthesis: an update. *Prostaglandins, Leukotrienes, and Essential Fatty Acids*, *85*(5), 205–213. https://doi.org/10.1016/J.PLEFA.2011.04.020

Bozza, P. T., & Viola, J. P. B. (2010). Lipid droplets in inflammation and cancer. *Prostaglandins, Leukotrienes, and Essential Fatty Acids*, *82*(4–6), 243–250. https://doi.org/10.1016/J.PLEFA.2010.02.005

Branchu, J., Boutry, M., Sourd, L., Depp, M., Leone, C., Corriger, A., Vallucci, M., Esteves, T., Matusiak, R., Dumont, M., Muriel, M. P., Santorelli, F. M., Brice, A., el Hachimi, K. H., Stevanin, G., & Darios, F. (2017a). Loss of spatacsin function alters lysosomal lipid clearance leading to upper and lower motor neuron degeneration. *Neurobiology of Disease*, *102*, 21–37. https://doi.org/10.1016/J.NBD.2017.02.007

Branchu, J., Boutry, M., Sourd, L., Depp, M., Leone, C., Corriger, A., Vallucci, M., Esteves, T., Matusiak, R., Dumont, M., Muriel, M. P., Santorelli, F. M., Brice, A., el Hachimi, K. H., Stevanin, G., & Darios, F. (2017b). Loss of spatacsin function alters lysosomal lipid clearance leading to upper and lower motor neuron degeneration. *Neurobiology of Disease*, *102*, 21–37. https://doi.org/10.1016/J.NBD.2017.02.007

Brandt, U. (2006). Energy Converting NADH: Quinone Oxidoreductase (Complex I). *Http://Dx.Doi.Org/10.1146/Annurev.Biochem.75.103004.142539*, *75*, 69–92. https://doi.org/10.1146/ANNUREV.BIOCHEM.75.103004.142539

Browne, S. E., Yang, L., DiMauro, J. P., Fuller, S. W., Licata, S. C., & Beal, M. F. (2006). Bioenergetic abnormalities in discrete cerebral motor pathways presage spinal cord pathology in the G93A SOD1 mouse model of ALS. *Neurobiology of Disease*, *22*(3), 599–610. https://doi.org/10.1016/J.NBD.2006.01.001

Bruce, A. W., Donaldson, I. J., Wood, I. C., Yerbury, S. A., Sadowski, M. I., Chapman, M., Göttgens, B., & Buckley, N. J. (2004). Genome-wide analysis of repressor element 1 silencing transcription factor/neuron-restrictive silencing factor (REST/NRSF) target genes. *Proceedings of the National Academy of Sciences*, *101*(28), 10458–10463. https://doi.org/10.1073/PNAS.0401827101

Bruce, K. D., Zsombok, A., & Eckel, R. H. (2017). Lipid Processing in the Brain: A Key Regulator of Systemic Metabolism. *Frontiers in Endocrinology*, *8*(APR). https://doi.org/10.3389/FENDO.2017.00060

Buratti, E. (2015). Functional Significance of TDP-43 Mutations in Disease. *Advances in Genetics*, *91*, 1–53. https://doi.org/10.1016/BS.ADGEN.2015.07.001

Butti, Z., Pan, Y. E., Giacomotto, J., & Patten, S. A. (2021). Reduced C9orf72 function leads to defective synaptic vesicle release and neuromuscular dysfunction in zebrafish. *Communications Biology*, *4*(1), 792. https://doi.org/10.1038/s42003-021-02302-y

Cabodevilla, A. G., Sánchez-Caballero, L., Nintou, E., Boiadjieva, V. G., Picatoste, F., Gubern, A., & Claro, E. (2013). Cell survival during complete nutrient deprivation depends on lipid droplet-fueled β-oxidation of fatty acids. *The Journal of Biological Chemistry*, *288*(39), 27777–27788. https://doi.org/10.1074/JBC.M113.466656

Cacabelos, D., Ramírez-Núñez, O., Granado-Serrano, A. B., Torres, P., Ayala, V., Moiseeva, V., Povedano, M., Ferrer, I., Pamplona, R., Portero-Otin, M., & Boada, J. (2016). Early and gender-specific differences in spinal cord mitochondrial function and oxidative stress markers in a mouse model of ALS. *Acta Neuropathologica Communications*, *4*, 3. https://doi.org/10.1186/S40478-015-0271-6

Calderone, A., Jover, T., Noh, K. M., Tanaka, H., Yokota, H., Lin, Y., Grooms, S. Y., Regis, R., Bennett, M. V. L., & Zukin, R. S. (2003). Ischemic Insults Derepress the Gene Silencer REST in Neurons Destined to Die. *Journal of Neuroscience*, *23*(6), 2112–2121. https://doi.org/10.1523/JNEUROSCI.23-06-02112.2003

Campbell, K. M., Xu, Y., Patel, C., Rayl, J. M., Zomer, H. D., Osuru, H. P., Pratt, M., Pramoonjago, P., Timken, M., Miller, L. M., Ralph, A., Storey, K. M., Peng, Y., Drnevich, J., Lagier-Tourenne, C., Wong, P. C., Qiao, H., & Reddi, P. P. (2021). Loss of TDP-43 in male germ cells causes meiotic failure and impairs fertility in mice. *The Journal of Biological Chemistry*, *297*(5), 101231–101231. https://doi.org/10.1016/J.JBC.2021.101231

Cantwell, H., & Dey, G. (2021). Nuclear size and shape control. *Seminars in Cell & Developmental Biology*. https://doi.org/10.1016/J.SEMCDB.2021.10.013

Carrì, M. T., Valle, C., Bozzo, F., & Cozzolino, M. (2015). Oxidative stress and mitochondrial damage: importance in non-SOD1 ALS. *Frontiers in Cellular Neuroscience*, *9*(FEB). https://doi.org/10.3389/FNCEL.2015.00041

Cascella, R., Fani, G., Bigi, A., Chiti, F., & Cecchi, C. (2019). Partial failure of proteostasis systems counteracting TDP-43 aggregates in neurodegenerative diseases. *International Journal of Molecular Sciences*, *20*(15). https://doi.org/10.3390/ijms20153685

Celik, A., He, F., & Jacobson, A. (2017). NMD monitors translational fidelity 24/7. *Current Genetics*, *63*(6), 1007–1010. https://doi.org/10.1007/S00294-017-0709-4

Chadt, A., Leicht, K., Deshmukh, A., Jiang, L. Q., Scherneck, S., Bernhardt, U., Dreja, T., Vogel, H., Schmolz, K., Kluge, R., Zierath, J. R., Hultschig, C., Hoeben, R. C., Schürmann, A., Joost, H. G., & Al-Hasani, H. (2008). Tbc1d1 mutation in lean mouse strain confers leanness and protects from diet-induced obesity. *Nature Genetics*, *40*(11), 1354–1359. https://doi.org/10.1038/NG.244

Chalupníková, K., Lattmann, S., Selak, N., Iwamoto, F., Fujiki, Y., & Nagamine, Y. (2008). Recruitment of the RNA helicase RHAU to stress granules via a unique RNA-binding domain. *Journal of Biological Chemistry*, *283*(50), 35186–35198. https://doi.org/10.1074/JBC.M804857200/ATTACHMENT/DE443B25-E94A-4049-8B81-C25E3B5109F2/MMC1.PDF

Chan, D. C. (2006). Mitochondria: dynamic organelles in disease, aging, and development. *Cell*, *125*(7), 1241–1252. https://doi.org/10.1016/J.CELL.2006.06.010

Chaves-Filho, A. B., Pinto, I. F. D., Dantas, L. S., Xavier, A. M., Inague, A., Faria, R. L., Medeiros, M. H. G., Glezer, I., Yoshinaga, M. Y., & Miyamoto, S. (2019). Alterations in lipid metabolism of spinal cord linked to amyotrophic lateral sclerosis. *Scientific Reports*, *9*(1). https://doi.org/10.1038/S41598-019-48059-7

Cheah, B. C., Vucic, S., Krishnan, A., & Kiernan, M. C. (2010). Riluzole, neuroprotection and amyotrophic lateral sclerosis. *Current Medicinal Chemistry*, *17*(18), 1942–1959. https://doi.org/10.2174/092986710791163939

Cheignon, C., Tomas, M., Bonnefont-Rousselot, D., Faller, P., Hureau, C., & Collin, F. (2018). Oxidative stress and the amyloid beta peptide in Alzheimer's disease. *Redox Biology*, *14*, 450–464. https://doi.org/10.1016/J.REDOX.2017.10.014

Chen, D., Yu, J., & Zhang, L. (2016). Necroptosis: an alternative cell death program defending against cancer. *Biochimica et Biophysica Acta*, *1865*(2), 228. https://doi.org/10.1016/J.BBCAN.2016.03.003

Chen, S., Sayana, P., Zhang, X., & Le, W. (2013). Genetics of amyotrophic lateral sclerosis: An update. *Molecular Neurodegeneration*, *8*(1), 1–15. https://doi.org/10.1186/1750-1326-8-28/TABLES/2

Chen, T., Turner, B. J., Beart, P. M., Sheehan-Hennessy, L., Elekwachi, C., & Muyderman, H. (2018). Glutathione monoethyl ester prevents TDP-43 pathology in motor neuronal NSC-34 cells. *Neurochemistry International*, *112*, 278–287. https://doi.org/10.1016/J.NEUINT.2017.08.009

Chen, Z. F., Paquette, A. J., & Anderson, D. J. (1998). NRSF/REST is required in vivo for repression of multiple neuronal target genes during embryogenesis. *Nature Genetics 1998 20:2*, *20*(2), 136–142. https://doi.org/10.1038/2431

Chernivec, E., Cooper, J., & Naylor, K. (2018). Exploring the Effect of Rotenone-A Known Inducer of Parkinson's Disease-On Mitochondrial Dynamics in Dictyostelium discoideum. *Cells*, *7*(11). https://doi.org/10.3390/CELLS7110201

Chiang, P. M., Ling, J., Jeong, Y. H., Price, D. L., Aja, S. M., & Wong, P. C. (2010). Deletion of TDP-43 down-regulates Tbc1d1, a gene linked to obesity, and alters body fat metabolism. *Proceedings of the National Academy of Sciences of the United States of America*, *107*(37), 16320–16324. https://doi.org/10.1073/PNAS.1002176107

Chiò, A., Borghero, G., Pugliatti, M., Ticca, A., Calvo, A., Moglia, C., Mutani, R., Brunetti, M., Ossola, I., Marrosu, M. G., Murru, M. R., Floris, G., Cannas, A., Parish, L. D., Cossu, P., Abramzon, Y., Johnson, J. O., Nalls, M. A., Arepalli, S., … Volanti, P. (2011). Large proportion of amyotrophic lateral sclerosis cases in Sardinia due to a single founder mutation of the TARDBP gene. *Archives of Neurology*, *68*(5), 594–598. https://doi.org/10.1001/ARCHNEUROL.2010.352

Choi, S. Y., Lee, J. H., Chung, A. Y., Jo, Y., Shin, J. ho, Park, H. C., Kim, H., Lopez-Gonzalez, R., Ryu, J. R., & Sun, W. (2020). Prevention of mitochondrial impairment by inhibition of protein phosphatase 1 activity in amyotrophic lateral sclerosis. *Cell Death & Disease*, *11*(10). https://doi.org/10.1038/S41419-020-03102-8

Chong, J. A., Tapia-Ramirez, J., Kim, S., Toledo-Aral, J. J., Zheng, Y., Boutros, M. C., Altshuller, Y. M., Frohman, M. A., Kraner, S. D., & Mandel, G. (1995). REST: A mammalian silencer protein that restricts sodium channel gene expression to neurons. *Cell*, *80*(6), 949–957. https://doi.org/10.1016/0092-8674(95)90298-8

Ciechanover, A., & Kwon, Y. T. ae. (2015). Degradation of misfolded proteins in neurodegenerative diseases: therapeutic targets and strategies. In *Experimental & molecular medicine* (Vol. 47, p. e147). https://doi.org/10.1038/emm.2014.117

Ciechanover, A., Orian, A., & Schwartz, A. L. (2000). Ubiquitin-mediated proteolysis: biological regulation via destruction. In *BioEssays* (Vol. 22). John Wiley & Sons, Inc.

Cingolani, F., & Czaja, M. J. (2016). Regulation and Functions of Autophagic Lipolysis. *Trends in Endocrinology and Metabolism: TEM*, *27*(10), 696–705. https://doi.org/10.1016/J.TEM.2016.06.003

Clayton, E. L., Mizielinska, S., Edgar, J. R., Nielsen, T. T., Marshall, S., Norona, F. E., Robbins, M., Damirji, H., Holm, I. E., Johannsen, P., Nielsen, J. E., Asante, E. A., Collinge, J., & Isaacs, A. M. (2015). Frontotemporal dementia caused by CHMP2B mutation is characterised by neuronal lysosomal storage pathology. *Acta Neuropathologica*, *130*(4), 511–523. https://doi.org/10.1007/S00401-015-1475-3/FIGURES/7

Cohen, T. J., Hwang, A. W., Restrepo, C. R., Yuan, C. X., Trojanowski, J. Q., & Lee, V. M. Y. (2015). An acetylation switch controls TDP-43 function and aggregation propensity. *Nature Communications 2015 6:1*, *6*(1), 1–13. https://doi.org/10.1038/ncomms6845

Cohen, T. J., Hwang, A. W., Unger, T., Trojanowski, J. Q., & Lee, V. M. Y. (2012). Redox signalling directly regulates TDP-43 via cysteine oxidation and disulphide cross-linking. *The EMBO Journal*, *31*(5), 1241–1252. https://doi.org/10.1038/EMBOJ.2011.471

Colebc, N. B., Murphy, D. D., Grider, T., Rueter, S., Brasaemle, D., & Nussbaum, R. L. (2002). Lipid droplet binding and oligomerization properties of the Parkinson's disease protein alpha-synuclein. *The Journal of Biological Chemistry*, *277*(8), 6344–6352. https://doi.org/10.1074/JBC.M108414200

Colombrita, C., Zennaro, E., Fallini, C., Weber, M., Sommacal, A., Buratti, E., Silani, V., & Ratti, A. (2009). TDP-43 is recruited to stress granules in conditions of oxidative insult. *Journal of Neurochemistry*, *111*(4), 1051–1061. https://doi.org/10.1111/J.1471-4159.2009.06383.X

Corona, J. C., Tovar-y-Romo, L. B., & Tapia, R. (2007). Glutamate excitotoxicity and therapeutic targets for amyotrophic lateral sclerosis. *Http://Dx.Doi.Org/10.1517/14728222.11.11.1415*, *11*(11), 1415–1428. https://doi.org/10.1517/14728222.11.11.1415

Cox, P. A., Davis, D. A., Mash, D. C., Metcalf, J. S., & Banack, S. A. (2016). Dietary exposure to an environmental toxin triggers neurofibrillary tangles and amyloid deposits in the brain. *Proceedings of the Royal Society B: Biological Sciences*, *283*(1823). https://doi.org/10.1098/RSPB.2015.2397

Cozzolino, M., & Carrì, M. T. (2012). Mitochondrial dysfunction in ALS. *Progress in Neurobiology*, *97*(2), 54–66. https://doi.org/10.1016/J.PNEUROBIO.2011.06.003

Criollo, A., Galluzzi, L., Chiara Maiuri, M., Tasdemir, E., Lavandero, S., & Kroemer, G. (2007). Mitochondrial control of cell death induced by hyperosmotic stress. *Apoptosis : An International Journal on Programmed Cell Death*, *12*(1), 3–18. https://doi.org/10.1007/S10495-006-0328-X

Cruz, M. P. (2018). Edaravone (Radicava): A Novel Neuroprotective Agent for the Treatment of Amyotrophic Lateral Sclerosis. *Pharmacy and Therapeutics*, *43*(1), 25. /pmc/articles/PMC5737249/

Cucovici, A., Ivashynka, A., Fontana, A., Russo, S., Mazzini, L., Mandrioli, J., Lisnic, V., Muresanu, D. F., & Leone, M. A. (2021). Coffee and Tea Consumption Impact on Amyotrophic Lateral Sclerosis Progression: A Multicenter Cross-Sectional Study. *Frontiers in Neurology*, *12*, 1257. https://doi.org/10.3389/FNEUR.2021.637939/BIBTEX

Cuevas, B. D., Abell, A. N., & Johnson, G. L. (2007). Role of mitogen-activated protein kinase kinase kinases in signal integration. *Oncogene*, *26*(22), 3159–3171. https://doi.org/10.1038/SJ.ONC.1210409

Cui, L., & Liu, P. (2020). Two Types of Contact Between Lipid Droplets and Mitochondria. *Frontiers in Cell and Developmental Biology*, *8*. https://doi.org/10.3389/FCELL.2020.618322

Cui, X., Wang, L., Zuo, P., Han, Z., Fang, Z., Li, W., & Liu, J. (2004). D-galactose-caused life shortening in Drosophila melanogaster and Musca domestica is associated with oxidative stress. *Biogerontology*, *5*(5), 317–325. https://doi.org/10.1007/S10522-004-2570-3

Cunha-Oliveira, T., Montezinho, L., Mendes, C., Firuzi, O., Saso, L., Oliveira, P. J., & Silva, F. S. G. (2020). Oxidative Stress in Amyotrophic Lateral Sclerosis: Pathophysiology and Opportunities for Pharmacological Intervention. In *Oxidative Medicine and Cellular Longevity* (Vol. 2020). Hindawi Limited. https://doi.org/10.1155/2020/5021694

Cutrona, M. B., Beznoussenko, G. v., Fusella, A., Martella, O., Moral, P., & Mironov, A. A. (2013). Silencing of Mammalian Sar1 Isoforms Reveals COPII-Independent Protein Sorting and Transport. *Traffic*, *14*(6), 691–708. https://doi.org/10.1111/TRA.12060

Danbolt, N. C. (2001). Glutamate uptake. *Progress in Neurobiology*, *65*(1), 1–105. https://doi.org/10.1016/S0301-0082(00)00067-8

Dangond, F., Hwang, D., Camelo, S., Pasinelli, P., Frosch, M. P., Stephanopoulos, G., Stephanopoulos, G., Brown, R. H., & Gullans, S. R. (2004). Molecular signature of late-stage human ALS revealed by expression profiling of postmortem spinal cord gray matter. *Physiological Genomics*, *16*, 229–239. https://doi.org/10.1152/PHYSIOLGENOMICS.00087.2001/ASSET/IMAGES/LARGE/ZH701804048800 02.JPEG

Darling, N. J., & Cook, S. J. (2014). The role of MAPK signalling pathways in the response to endoplasmic reticulum stress. *Biochimica et Biophysica Acta (BBA) - Molecular Cell Research*, *1843*(10), 2150–2163. https://doi.org/10.1016/J.BBAMCR.2014.01.009

de Aguilar, J. L. G., Dupuis, L., Oudart, H., & Loeffler, J. P. (2005). The metabolic hypothesis in amyotrophic lateral sclerosis: insights from mutant Cu/Zn-superoxide dismutase mice. *Biomedicine & Pharmacotherapy*, *59*(4), 190–196. https://doi.org/10.1016/J.BIOPHA.2005.03.003

de Boer, E. M. J., Orie, V. K., Williams, T., Baker, M. R., de Oliveira, H. M., Polvikoski, T., Silsby, M., Menon, P., van den Bos, M., Halliday, G. M., van den Berg, L. H., van den Bosch, L., van Damme, P., Kiernan, M., van Es, M. A., & Vucic, S. (2021). Review: TDP-43 proteinopathies: a

new wave of neurodegenerative diseases. *Journal of Neurology, Neurosurgery, and Psychiatry*, *92*(1), 86. https://doi.org/10.1136/JNNP-2020-322983

de Giorgio, F., Maduro, C., Fisher, E. M. C., & Acevedo-Arozena, A. (2019). Transgenic and physiological mouse models give insights into different aspects of amyotrophic lateral sclerosis. *Disease Models & Mechanisms*, *12*(1). https://doi.org/10.1242/DMM.037424

de Mena, L., Lopez-Scarim, J., & Rincon-Limas, D. E. (2021). TDP-43 and ER Stress in Neurodegeneration: Friends or Foes? *Frontiers in Molecular Neuroscience*, *14*, 25. https://doi.org/10.3389/FNMOL.2021.772226

Dean, J. M., & Lodhi, I. J. (2018). Structural and functional roles of ether lipids. *Protein & Cell*, *9*(2), 196–206. https://doi.org/10.1007/S13238-017-0423-5

del Boca, M., Caputto, B. L., Maggio, B., & Borioli, G. A. (2005). c-Jun interacts with phospholipids and c-Fos at the interface. *Journal of Colloid and Interface Science*, *287*(1), 80–84. https://doi.org/10.1016/J.JCIS.2005.01.069

Delic, V., Kurien, C., Cruz, J., Zivkovic, S., Barretta, J., Thomson, A., Hennessey, D., Joseph, J., Ehrhart, J., Willing, A. E., Bradshaw, P., & Garbuzova-Davis, S. (2018). Discrete mitochondrial aberrations in the spinal cord of sporadic ALS patients. *Journal of Neuroscience Research*, *96*(8), 1353–1366. https://doi.org/10.1002/JNR.24249

Deng, H. X., Chen, W., Hong, S. T., Boycott, K. M., Gorrie, G. H., Siddique, N., Yang, Y., Fecto, F., Shi, Y., Zhai, H., Jiang, H., Hirano, M., Rampersaud, E., Jansen, G. H., Donkervoort, S., Bigio, E. H., Brooks, B. R., Ajroud, K., Sufit, R. L., … Siddique, T. (2011). Mutations in UBQLN2 cause dominant X-linked juvenile and adult-onset ALS and ALS/dementia. *Nature*, *477*(7363), 211–215. https://doi.org/10.1038/NATURE10353

Deng, J., Yang, M., Chen, Y., Chen, X., Liu, J., Sun, S., Cheng, H., Li, Y., Bigio, E. H., Mesulam, M., Xu, Q., Du, S., Fushimi, K., Zhu, L., & Wu, J. Y. (2015). FUS Interacts with HSP60 to Promote Mitochondrial Damage. *PLOS Genetics*, *11*(9), e1005357. https://doi.org/10.1371/JOURNAL.PGEN.1005357

D'Erchia, A. M., Gallo, A., Manzari, C., Raho, S., Horner, D. S., Chiara, M., Valletti, A., Aiello, I., Mastropasqua, F., Ciaccia, L., Locatelli, F., Pisani, F., Nicchia, G. P., Svelto, M., Pesole, G., & Picardi, E. (2017). Massive transcriptome sequencing of human spinal cord tissues provides new insights into motor neuron degeneration in ALS. *Scientific Reports*, *7*(1). https://doi.org/10.1038/S41598-017-10488-7

Derk, J., Hernandez, K. B., Rodriguez, M., He, M., Koh, H., Abedini, A., Li, H., Fenyö, D., & Schmidt, A. M. (2018). Diaphanous 1 (DIAPH1) is Highly Expressed in the Aged Human Medial Temporal Cortex and Upregulated in Myeloid Cells During Alzheimer's Disease. *Journal of Alzheimer's Disease : JAD*, *64*(3), 995–1007. https://doi.org/10.3233/JAD-180088

Devi, L., Prabhu, B. M., Galati, D. F., Avadhani, N. G., & Anandatheerthavarada, H. K. (2006). Accumulation of Amyloid Precursor Protein in the Mitochondrial Import Channels of Human

Alzheimer's Disease Brain Is Associated with Mitochondrial Dysfunction. *Journal of Neuroscience*, *26*(35), 9057–9068. https://doi.org/10.1523/JNEUROSCI.1469-06.2006

Dewey, C. M., Cenik, B., Sephton, C. F., Dries, D. R., Mayer, P., Good, S. K., Johnson, B. A., Herz, J., & Yu, G. (2011a). TDP-43 Is Directed to Stress Granules by Sorbitol, a Novel Physiological Osmotic and Oxidative Stressor. *Molecular and Cellular Biology*, *31*(5), 1098–1108. https://doi.org/10.1128/mcb.01279-10

Dewey, C. M., Cenik, B., Sephton, C. F., Dries, D. R., Mayer, P., Good, S. K., Johnson, B. A., Herz, J., & Yu, G. (2011b). TDP-43 Is Directed to Stress Granules by Sorbitol, a Novel Physiological Osmotic and Oxidative Stressor. *Molecular and Cellular Biology*, *31*(5), 1098–1108. https://doi.org/10.1128/MCB.01279-10/ASSET/7A1FE03F-F008-4AFF-90B5-A4996D7DA6CF/ASSETS/GRAPHIC/ZMB9991089620008.JPEG

Dewil, M., dela Cruz, V. F., van den Bosch, L., & Robberecht, W. (2007). Inhibition of p38 mitogen activated protein kinase activation and mutant SOD1G93A-induced motor neuron death. *Neurobiology of Disease*, *26*(2), 332–341. https://doi.org/10.1016/J.NBD.2006.12.023

di Domenico, F., Barone, E., Perluigi, M., & Butterfield, D. A. (2017). The Triangle of Death in Alzheimer's Disease Brain: The Aberrant Cross-Talk Among Energy Metabolism, Mammalian Target of Rapamycin Signaling, and Protein Homeostasis Revealed by Redox Proteomics. *Https://Home.Liebertpub.Com/Ars*, *26*(8), 364–387. https://doi.org/10.1089/ARS.2016.6759

Diaz, B., Shani, G., Pass, I., Anderson, D., Quintavalle, M., & Courtneidge, S. A. (2009). Tks5-dependent, nox-mediated generation of reactive oxygen species is necessary for invadopodia formation. *Science Signaling*, *2*(88). https://doi.org/10.1126/SCISIGNAL.2000368

Dichlberger, A., Schlager, S., Kovanen, P. T., & Schneider, W. J. (2016). Lipid droplets in activated mast cells - a significant source of triglyceride-derived arachidonic acid for eicosanoid production. *European Journal of Pharmacology*, *785*, 59–69. https://doi.org/10.1016/J.EJPHAR.2015.07.020

Dienel, G. A. (2012). Brain lactate metabolism: the discoveries and the controversies. *Journal of Cerebral Blood Flow and Metabolism : Official Journal of the International Society of Cerebral Blood Flow and Metabolism*, *32*(7), 1107–1138. https://doi.org/10.1038/JCBFM.2011.175

Dienel, G. A., & Cruz, N. F. (2016). Aerobic glycolysis during brain activation: adrenergic regulation and influence of norepinephrine on astrocytic metabolism. *Journal of Neurochemistry*, *138*(1), 14–52. https://doi.org/10.1111/JNC.13630

Dienel, G. A., & Rothman, D. L. (2020a). Reevaluation of Astrocyte-Neuron Energy Metabolism with Astrocyte Volume Fraction Correction: Impact on Cellular Glucose Oxidation Rates, Glutamate-Glutamine Cycle Energetics, Glycogen Levels and Utilization Rates vs. Exercising Muscle, and Na +/K + Pumping Rates. *Neurochemical Research*, *45*(11), 2607–2630. https://doi.org/10.1007/S11064-020-03125-9

Dienel, G. A., & Rothman, D. L. (2020b). Reevaluation of Astrocyte-Neuron Energy Metabolism with Astrocyte Volume Fraction Correction: Impact on Cellular Glucose Oxidation Rates, Glutamate-Glutamine Cycle Energetics, Glycogen Levels and Utilization Rates vs. Exercising Muscle, and Na +/K + Pumping Rates. *Neurochemical Research*, *45*(11), 2607–2630. https://doi.org/10.1007/S11064-020-03125-9

Ding, Q., & Keller, J. N. (2001). Proteasome inhibition in oxidative stress neurotoxicity: implications for heat shock proteins. *Journal of Neurochemistry*, *77*(4), 1010–1017. https://doi.org/10.1046/J.1471-4159.2001.00302.X

Ding, W. X., & Yin, X. M. (2012). Mitophagy: mechanisms, pathophysiological roles, and analysis. *Biological Chemistry*, *393*(7), 547–564. https://doi.org/10.1515/HSZ-2012-0119

Dinuzzo, M., Mangia, S., Maraviglia, B., & Giove, F. (2010). Glycogenolysis in astrocytes supports blood-borne glucose channeling not glycogen-derived lactate shuttling to neurons: evidence from mathematical modeling. *Journal of Cerebral Blood Flow and Metabolism : Official Journal of the International Society of Cerebral Blood Flow and Metabolism*, *30*(12), 1895–1904. https://doi.org/10.1038/JCBFM.2010.151

DiNuzzo, M., Mangia, S., Maraviglia, B., & Giove, F. (2012). The role of astrocytic glycogen in supporting the energetics of neuronal activity. *Neurochemical Research*, *37*(11), 2432–2438. https://doi.org/10.1007/S11064-012-0802-5

Docherty, P. A., & Snider, M. D. (1991). Effects of hypertonic and sodium-free medium on transport of a membrane glycoprotein along the secretory pathway in cultured mammalian cells. *Journal of Cellular Physiology*, *146*(1), 34–42. https://doi.org/10.1002/JCP.1041460106

Dodge, J. C., Treleaven, C. M., Pacheco, J., Cooper, S., Bao, C., Abraham, M., Cromwell, M., Sardi, S. P., Chuang, W. L., Sidman, R. L., Cheng, S. H., & Shihabuddin, L. S. (2015). Glycosphingolipids are modulators of disease pathogenesis in amyotrophic lateral sclerosis. *Proceedings of the National Academy of Sciences of the United States of America*, *112*(26), 8100–8105. https://doi.org/10.1073/PNAS.1508767112/-/DCSUPPLEMENTAL

Du, Z. W., Chen, H., Liu, H., Lu, J., Qian, K., Huang, C. T. L., Zhong, X., Fan, F., & Zhang, S. C. (2015). Generation and expansion of highly pure motor neuron progenitors from human pluripotent stem cells. *Nature Communications*, *6*. https://doi.org/10.1038/NCOMMS7626

Durkee, C. A., & Araque, A. (2019). Diversity and Specificity of Astrocyte-neuron Communication. *Neuroscience*, *396*, 73–78. https://doi.org/10.1016/J.NEUROSCIENCE.2018.11.010

Ederle, H., & Dormann, D. (2017). TDP-43 and FUS en route from the nucleus to the cytoplasm. In *FEBS Letters* (Vol. 591, Issue 11, pp. 1489–1507). Wiley Blackwell. https://doi.org/10.1002/1873-3468.12646

Elkalaf, M., Anděl, M., & Trnka, J. (2013). Low glucose but not galactose enhances oxidative mitochondrial metabolism in C2C12 myoblasts and myotubes. *PloS One*, *8*(8). https://doi.org/10.1371/JOURNAL.PONE.0070772

Erickson, G. R., Alexopoulos, L. G., & Guilak, F. (2001). Hyper-osmotic stress induces volume change and calcium transients in chondrocytes by transmembrane, phospholipid, and G-protein pathways. *Journal of Biomechanics*, *34*(12), 1527–1535. https://doi.org/10.1016/S0021-9290(01)00156-7

Espinosa-Diez, C., Miguel, V., Mennerich, D., Kietzmann, T., Sánchez-Pérez, P., Cadenas, S., & Lamas, S. (2015). Antioxidant responses and cellular adjustments to oxidative stress. *Redox Biology*, *6*, 183–197. https://doi.org/10.1016/J.REDOX.2015.07.008

Etschmaier, K., Becker, T., Eichmann, T. O., Schweinzer, C., Scholler, M., Tam-Amersdorfer, C., Poeckl, M., Schuligoi, R., Kober, A., Chirackal Manavalan, A. P., Rechberger, G. N., Streith, I. E., Zechner, R., Zimmermann, R., & Panzenboeck, U. (2011). Adipose triglyceride lipase affects triacylglycerol metabolism at brain barriers. *Journal of Neurochemistry*, *119*(5), 1016–1028. https://doi.org/10.1111/J.1471-4159.2011.07498.X

Evers, B. M., Rodriguez-Navas, C., Tesla, R. J., Prange-Kiel, J., Wasser, C. R., Yoo, K. S., McDonald, J., Cenik, B., Ravenscroft, T. A., Plattner, F., Rademakers, R., Yu, G., White, C. L., & Herz, J. (2017). Lipidomic and Transcriptomic Basis of Lysosomal Dysfunction in Progranulin Deficiency. *Cell Reports*, *20*(11), 2565–2574. https://doi.org/10.1016/J.CELREP.2017.08.056

Fang, F., Hållmarker, U., James, S., Ingre, C., Michaëlsson, K., Ahlbom, A., & Feychting, M. (2016). Amyotrophic lateral sclerosis among cross-country skiers in Sweden. *European Journal of Epidemiology*, *31*(3), 247–253. https://doi.org/10.1007/S10654-015-0077-7

Farese, R. v., & Walther, T. C. (2009). Lipid Droplets Finally Get a Little R-E-S-P-E-C-T. *Cell*, *139*(5), 855–860. https://doi.org/10.1016/J.CELL.2009.11.005

Farg, M. A., Soo, K. Y., Warraich, S. T., Sundaramoorthy, V., Blair, I. P., & Atkin, J. D. (2013). Ataxin-2 interacts with FUS and intermediate-length polyglutamine expansions enhance FUS-related pathology in amyotrophic lateral sclerosis. *Human Molecular Genetics*, *22*(4), 717–728. https://doi.org/10.1093/HMG/DDS479

Farmer, B. C., Walsh, A. E., Kluemper, J. C., & Johnson, L. A. (2020). Lipid Droplets in Neurodegenerative Disorders. *Frontiers in Neuroscience*, *14*, 742. https://doi.org/10.3389/FNINS.2020.00742/BIBTEX

Farmer, B., Kluemper, J., & Johnson, L. (2019). Apolipoprotein E4 Alters Astrocyte Fatty Acid Metabolism and Lipid Droplet Formation. *Cells*, *8*(2), 182. https://doi.org/10.3390/CELLS8020182

Ferraiuolo, L., Heath, P. R., Holden, H., Kasher, P., Kirby, J., & Shaw, P. J. (2007). Microarray Analysis of the Cellular Pathways Involved in the Adaptation to and Progression of Motor Neuron Injury in the SOD1 G93A Mouse Model of Familial ALS. *Journal of Neuroscience*, *27*(34), 9201–9219. https://doi.org/10.1523/JNEUROSCI.1470-07.2007

Ferrari, R., Kapogiannis, D., Huey, E. D., & Momeni, P. (2011). FTD and ALS: a tale of two diseases. In *Curr Alzheimer Res* (Vol. 8, Issue 3).

Ferri, A., Cozzolino, M., Crosio, C., Nencini, M., Casciati, A., Gralla, E. B., Rotilio, G., Valentine, J. S., & Carri, M. T. (2006). Familial ALS-superoxide dismutases associate with mitochondria and shift their redox potentials. *Proceedings of the National Academy of Sciences*, *103*(37), 13860–13865. https://doi.org/10.1073/PNAS.0605814103

Formisano, L., Noh, K. M., Miyawaki, T., Mashiko, T., Bennett, M. V. L., & Zukin, R. S. (2007). Ischemic insults promote epigenetic reprogramming of μ opioid receptor expression in hippocampal neurons. *Proceedings of the National Academy of Sciences*, *104*(10), 4170–4175. https://doi.org/10.1073/PNAS.0611704104

Foster, L. J., Weir, M. L., Lim, D. Y., Liu, Z., Trimble, W. S., & Klip, A. (2000). A functional role for VAP-33 in insulin-stimulated GLUT4 traffic. *Traffic (Copenhagen, Denmark)*, *1*(6), 512–521. https://doi.org/10.1034/J.1600-0854.2000.010609.X

Fowler, P. C., Garcia-Pardo, M. E., Simpson, J. C., & O'Sullivan, N. C. (2019). NeurodegenERation: The Central Role for ER Contacts in Neuronal Function and Axonopathy, Lessons From Hereditary Spastic Paraplegias and Related Diseases. *Frontiers in Neuroscience*, *13*. https://doi.org/10.3389/FNINS.2019.01051

Franzini-Armstrong, C. (2007). ER-mitochondria communication. How privileged? *Physiology*, *22*(4), 261–268. https://doi.org/10.1152/PHYSIOL.00017.2007/ASSET/IMAGES/LARGE/Y0017-7-04.JPEG

Fratta, P., Sivakumar, P., Humphrey, J., Lo, K., Ricketts, T., Oliveira, H., Brito-Armas, J. M., Kalmar, B., Ule, A., Yu, Y., Birsa, N., Bodo, C., Collins, T., Conicella, A. E., Maza, A. M., Marrero-Gagliardi, A., Stewart, M., Mianne, J., Corrochano, S., … Acevedo-Arozena, A. (2018). Mice with endogenous TDP-43 mutations exhibit gain of splicing function and characteristics of amyotrophic lateral sclerosis. *The EMBO Journal*, *37*(11). https://doi.org/10.15252/EMBJ.201798684

Fratta, P., Sivakumar, P., Humphrey, J., Lo, K., Ricketts, T., Oliveira, H., Brito-Armas, J. M., Kalmar, B., Ule, A., Yu, Y., Birsa, N., Bodo, C., Collins, T., Conicella, A. E., Mejia Maza, A., Marrero-Gagliardi, A., Stewart, M., Mianne, J., Corrochano, S., … Acevedo-Arozena, A. (2018a). Mice with endogenous TDP -43 mutations exhibit gain of splicing function and characteristics of amyotrophic lateral sclerosis . *The EMBO Journal*, *37*(11). https://doi.org/10.15252/embj.201798684

Fratta, P., Sivakumar, P., Humphrey, J., Lo, K., Ricketts, T., Oliveira, H., Brito-Armas, J. M., Kalmar, B., Ule, A., Yu, Y., Birsa, N., Bodo, C., Collins, T., Conicella, A. E., Mejia Maza, A., Marrero-Gagliardi, A., Stewart, M., Mianne, J., Corrochano, S., … Acevedo-Arozena, A. (2018b). Mice with endogenous TDP -43 mutations exhibit gain of splicing function and characteristics of amyotrophic lateral sclerosis . *The EMBO Journal*, *37*(11). https://doi.org/10.15252/embj.201798684

Fridavich, I. (2003). SUPEROXIDE RADICAL AND SUPEROXIDE DISMUTASES. *Https://Doi.Org/10.1146/Annurev.Bi.64.070195.000525*, *64*, 97–112. https://doi.org/10.1146/ANNUREV.BI.64.070195.000525

Fujita, Y., Mizuno, Y., Takatama, M., & Okamoto, K. (2008a). Anterior horn cells with abnormal TDP-43 immunoreactivities show fragmentation of the Golgi apparatus in ALS. *Journal of the Neurological Sciences*, *269*(1–2), 30–34. https://doi.org/10.1016/J.JNS.2007.12.016

Fujita, Y., Mizuno, Y., Takatama, M., & Okamoto, K. (2008b). Anterior horn cells with abnormal TDP-43 immunoreactivities show fragmentation of the Golgi apparatus in ALS. *Journal of the Neurological Sciences*, *269*(1–2), 30–34. https://doi.org/10.1016/J.JNS.2007.12.016

Fujita, Y., Okamoto, K., Sakurai, A., Amari, M., Nakazato, Y., & Gonatas, N. K. (1999). Fragmentation of the Golgi apparatus of Betz cells in patients with amyotrophic lateral sclerosis. *Journal of the Neurological Sciences*, *163*(1), 81–85. https://doi.org/10.1016/S0022-510X(99)00014-3

Fujita, Y., Okamoto, K., Sakurai, A., Gonatas, N. K., & Hirano, A. (2000). Fragmentation of the Golgi apparatus of the anterior horn cells in patients with familial amyotrophic lateral sclerosis with SOD1 mutations and posterior column involvement. *Journal of the Neurological Sciences*, *174*(2), 137–140. https://doi.org/10.1016/S0022-510X(00)00265-3

Gallo, V., Vanacore, N., Bueno-de-Mesquita, H. B., Vermeulen, R., Brayne, C., Pearce, N., Wark, P. A., Ward, H. A., Ferrari, P., Jenab, M., Andersen, P. M., Wennberg, P., Wareham, N., Katzke, V., Kaaks, R., Weiderpass, E., Peeters, P. H., Mattiello, A., Pala, V., … Vineis, P. (2016). Physical activity and risk of Amyotrophic Lateral Sclerosis in a prospective cohort study. *European Journal of Epidemiology*, *31*(3), 255. https://doi.org/10.1007/S10654-016-0119-9

Gao, G., Chen, F. J., Zhou, L., Su, L., Xu, D., Xu, L., & Li, P. (2017). Control of lipid droplet fusion and growth by CIDE family proteins. *Biochimica et Biophysica Acta. Molecular and Cell Biology of Lipids*, *1862*(10 Pt B), 1197–1204. https://doi.org/10.1016/J.BBALIP.2017.06.009

Garriga-Canut, M., Schoenike, B., Qazi, R., Bergendahl, K., Daley, T. J., Pfender, R. M., Morrison, J. F., Ockuly, J., Stafstrom, C., Sutula, T., & Roopra, A. (2006). 2-Deoxy-D-glucose reduces epilepsy progression by NRSF-CtBP–dependent metabolic regulation of chromatin structure. *Nature Neuroscience 2006 9:11*, *9*(11), 1382–1387. https://doi.org/10.1038/nn1791

Gautam, M., Jara, J. H., Kocak, N., Rylaarsdam, L. E., Kim, K. D., Bigio, E. H., & Hande Özdinler, P. (2019). Mitochondria, ER, and nuclear membrane defects reveal early mechanisms for upper motor neuron vulnerability with respect to TDP-43 pathology. *Acta Neuropathologica*, *137*(1), 47–69. https://doi.org/10.1007/S00401-018-1934-8

Gemmink, A., Goodpaster, B. H., Schrauwen, P., & Hesselink, M. K. C. (2017). Intramyocellular lipid droplets and insulin sensitivity, the human perspective. *Biochimica et Biophysica Acta. Molecular and Cell Biology of Lipids*, *1862*(10 Pt B), 1242–1249. https://doi.org/10.1016/J.BBALIP.2017.07.010

Getty, A., Kovács, A. D., Lengyel-Nelson, T., Cardillo, A., Hof, C., Chan, C. H., & Pearce, D. A. (2013). Osmotic Stress Changes the Expression and Subcellular Localization of the Batten Disease Protein CLN3. *PLOS ONE*, *8*(6), e66203. https://doi.org/10.1371/JOURNAL.PONE.0066203

Geuens, T., Bouhy, D., & Timmerman, V. (2016). The hnRNP family: insights into their role in health and disease. In *Human Genetics* (Vol. 135, Issue 8, pp. 851–867). Springer Verlag. https://doi.org/10.1007/s00439-016-1683-5

Ghiasi, P., Hosseinkhani, S., Noori, A., Nafissi, S., & Khajeh, K. (2013). Mitochondrial complex I deficiency and ATP/ADP ratio in lymphocytes of amyotrophic lateral sclerosis patients. *Http://Dx.Doi.Org/10.1179/1743132812Y.0000000012*, *34*(3), 297–303. https://doi.org/10.1179/1743132812Y.0000000012

Giacomello, M., & Pellegrini, L. (2016). The coming of age of the mitochondria–ER contact: a matter of thickness. *Cell Death & Differentiation 2016 23:9*, *23*(9), 1417–1427. https://doi.org/10.1038/cdd.2016.52

Glancy, B., Kim, Y., Katti, P., & Willingham, T. B. (2020). The Functional Impact of Mitochondrial Structure Across Subcellular Scales. *Frontiers in Physiology*, *11*, 1462. https://doi.org/10.3389/FPHYS.2020.541040/BIBTEX

Glickman, M. H., & Ciechanover, A. (2002). The ubiquitin-proteasome proteolytic pathway: destruction for the sake of construction. *Physiological Reviews*, *82*(2), 373–428. https://doi.org/10.1152/PHYSREV.00027.2001

Gogia, N., Sarkar, A., Mehta, A. S., Ramesh, N., Deshpande, P., Kango-Singh, M., Pandey, U. B., & Singh, A. (2020). Inactivation of Hippo and cJun-N-terminal Kinase (JNK) signaling mitigate FUS mediated neurodegeneration in vivo. *Neurobiology of Disease*, *140*. https://doi.org/10.1016/J.NBD.2020.104837

Gómez-Ramos, P., & Morán, M. A. (2007). Ultrastructural localization of intraneuronal Abeta-peptide in Alzheimer disease brains. *Journal of Alzheimer's Disease : JAD*, *11*(1), 53–59. https://doi.org/10.3233/JAD-2007-11109

Gonatas, N. K., Stieber, A., & Gonatas, J. O. (2006). Fragmentation of the Golgi apparatus in neurodegenerative diseases and cell death. *Journal of the Neurological Sciences*, *246*(1–2), 21–30. https://doi.org/10.1016/J.JNS.2006.01.019

Goodier, J. L., Zhang, L., Vetter, M. R., & Kazazian, H. H. (2007). LINE-1 ORF1 Protein Localizes in Stress Granules with Other RNA-Binding Proteins, Including Components of RNA Interference RNA-Induced Silencing Complex. *Molecular and Cellular Biology*, *27*(18), 6469–6483. https://doi.org/10.1128/mcb.00332-07

Gordaliza-Alaguero, I., Cantó, C., & Zorzano, A. (2019). Metabolic implications of organelle-mitochondria communication. *EMBO Reports*, *20*(9). https://doi.org/10.15252/EMBR.201947928

Goyal, N. A., & Mozaffar, T. (2014). Experimental trials in amyotrophic lateral sclerosis: a review of recently completed, ongoing and planned trials using existing and novel drugs. *Https://Doi.Org/10.1517/13543784.2014.933807*, *23*(11), 1541–1551. https://doi.org/10.1517/13543784.2014.933807

Graham, N. A., Tahmasian, M., Kohli, B., Komisopoulou, E., Zhu, M., Vivanco, I., Teitell, M. A., Wu, H., Ribas, A., Lo, R. S., Mellinghoff, I. K., Mischel, P. S., & Graeber, T. G. (2012). Glucose deprivation activates a metabolic and signaling amplification loop leading to cell death. *Molecular Systems Biology*, *8*, 589. https://doi.org/10.1038/MSB.2012.20

Grajchen, E., Hendriks, J. J. A., & Bogie, J. F. J. (2018). The physiology of foamy phagocytes in multiple sclerosis. *Acta Neuropathologica Communications*, *6*(1), 124. https://doi.org/10.1186/S40478-018-0628-8

Grassi, D., Howard, S., Zhou, M., Diaz-Perez, N., Urban, N. T., Guerrero-Given, D., Kamasawa, N., Volpicelli-Daley, L. A., LoGrasso, P., & Lasmézas, C. I. (2018). Identification of a highly neurotoxic α-synuclein species inducing mitochondrial damage and mitophagy in Parkinson's disease. *Proceedings of the National Academy of Sciences of the United States of America*, *115*(11), E2634–E2643. https://doi.org/10.1073/PNAS.1713849115/VIDEO-1

Grimm, M. O. W., Kuchenbecker, J., Rothhaar, T. L., Grösgen, S., Hundsdörfer, B., Burg, V. K., Friess, P., Müller, U., Grimm, H. S., Riemenschneider, M., & Hartmann, T. (2011). Plasmalogen synthesis is regulated via alkyl-dihydroxyacetonephosphate-synthase by amyloid precursor protein processing and is affected in Alzheimer's disease. *Journal of Neurochemistry*, *116*(5), 916–925. https://doi.org/10.1111/J.1471-4159.2010.07070.X

Grosskreutz, J., van den Bosch, L., & Keller, B. U. (2010). Calcium dysregulation in amyotrophic lateral sclerosis. *Cell Calcium*, *47*(2), 165–174. https://doi.org/10.1016/J.CECA.2009.12.002

Gruber, J., Schaffer, S., & Halliwell, B. (2008). The mitochondrial free radical theory of ageing - Where do we stand? *Frontiers in Bioscience*, *13*(17), 6554–6579. https://doi.org/10.2741/3174

Guerrero, E. N., Mitra, J., Wang, H., Rangaswamy, S., Hegde, P. M., Basu, P., Rao, K. S., & Hegde, M. L. (2019). Amyotrophic lateral sclerosis-associated TDP-43 mutation Q331K prevents nuclear translocation of XRCC4-DNA ligase 4 complex and is linked to genome damage-mediated neuronal apoptosis. *Human Molecular Genetics*, *28*(15), 2459. https://doi.org/10.1093/HMG/DDZ062

Guo, L., & Shorter, J. (2017). Biology and pathobiology of TDP-43 and emergent therapeutic strategies. *Cold Spring Harbor Perspectives in Medicine*, *7*(9). https://doi.org/10.1101/cshperspect.a024554

Haase, M., Koslowski, R., Lengnick, A., Hahn, R., Wenzel, K. W., Schuh, D., Kasper, M., & Müller, M. (1997). Cellular distribution of c-Jun and c-Fos in rat lung before and after bleomycin induced injury. *Virchows Archiv*, *431*(6), 441–448. https://doi.org/10.1007/S004280050121

Haidet-Phillips, A. M., Hester, M. E., Miranda, C. J., Meyer, K., Braun, L., Frakes, A., Song, S., Likhite, S., Murtha, M. J., Foust, K. D., Rao, M., Eagle, A., Kammesheidt, A., Christensen, A., Mendell, J. R., Burghes, A. H. M., & Kaspar, B. K. (2011). Astrocytes from familial and sporadic ALS patients are toxic to motor neurons. *Nature Biotechnology*, *29*(9), 824–828. https://doi.org/10.1038/nbt.1957

Halpern, M., Brennand, K. J., & Gregory, J. (2019). Examining the relationship between astrocyte dysfunction and neurodegeneration in ALS using hiPSCs. In *Neurobiology of Disease* (Vol. 132). Academic Press Inc. https://doi.org/10.1016/j.nbd.2019.104562

Hamilton, J. A., Hillard, C. J., Spector, A. A., & Watkins, P. A. (2007). Brain Uptake and Utilization of Fatty Acids, Lipids and Lipoproteins: Application to Neurological Disorders. *Journal of Molecular Neuroscience 2007 33:1*, *33*(1), 2–11. https://doi.org/10.1007/S12031-007-0060-1

Hamilton, L. K., Dufresne, M., Joppé, S. E., Petryszyn, S., Aumont, A., Calon, F., Barnabé-Heider, F., Furtos, A., Parent, M., Chaurand, P., & Fernandes, K. J. L. (2015). Aberrant Lipid Metabolism in the Forebrain Niche Suppresses Adult Neural Stem Cell Proliferation in an Animal Model of Alzheimer's Disease. *Cell Stem Cell*, *17*(4), 397–411. https://doi.org/10.1016/J.STEM.2015.08.001

Hamilton, L. K., & Fernandes, K. J. L. (2018). Neural stem cells and adult brain fatty acid metabolism: Lessons from the 3xTg model of Alzheimer's disease. *Biology of the Cell*, *110*(1), 6–25. https://doi.org/10.1111/BOC.201700037

Han, S. M., el Oussini, H., Scekic-Zahirovic, J., Vibbert, J., Cottee, P., Prasain, J. K., Bellen, H. J., Dupuis, L., & Miller, M. A. (2013). VAPB/ALS8 MSP ligands regulate striated muscle energy metabolism critical for adult survival in caenorhabditis elegans. *PLoS Genetics*, *9*(9). https://doi.org/10.1371/JOURNAL.PGEN.1003738

Hans, F., Glasebach, H., & Kahle, P. J. (2020). Multiple distinct pathways lead to hyperubiquitylated insoluble TDP-43 protein independent of its translocation into stress granules. *The Journal of Biological Chemistry*, *295*(3), 673–689. https://doi.org/10.1074/JBC.RA119.010617

Harding, H. P., Zhang, Y., & Ron, D. (1999). Protein translation and folding are coupled by an endoplasmic-reticulum-resident kinase. *Nature 1999 397:6716*, *397*(6716), 271–274. https://doi.org/10.1038/16729

Hargreaves, I., Mody, N., Land, J., & Heales, S. (2018). Blood Mononuclear Cell Mitochondrial Respiratory Chain Complex IV Activity is Decreased in Multiple Sclerosis Patients: Effects of β-Interferon Treatment. *Journal of Clinical Medicine*, *7*(2). https://doi.org/10.3390/JCM7020036

Harley, J., & Patani, R. (2020). Stress-Specific Spatiotemporal Responses of RNA-Binding Proteins in Human Stem Cell-Derived Motor Neurons. *International Journal of Molecular Sciences*, *21*(21), 1–17. https://doi.org/10.3390/IJMS21218346

Harris, C. A., Haas, J. T., Streeper, R. S., Stone, S. J., Kumari, M., Yang, K., Han, X., Brownell, N., Gross, R. W., Zechner, R., & Farese, R. v. (2011). DGAT enzymes are required for triacylglycerol synthesis and lipid droplets in adipocytes. *Journal of Lipid Research*, *52*(4), 657–667. https://doi.org/10.1194/JLR.M013003

Hartl, F. U., Bracher, A., & Hayer-Hartl, M. (2011). Molecular chaperones in protein folding and proteostasis. *Nature 2011 475:7356*, *475*(7356), 324–332. https://doi.org/10.1038/nature10317

Haze, K., Yoshida, H., Yanagi, H., Yura, T., and Mori, K. (1999). Mammalian transcription factor ATF6 is synthesized as a transmembrane protein and ac. (n.d.). Retrieved December 29, 2021, from https://www.google.com/search?channel=crow5&client=firefox-b-d&q=Haze%2C+K.%2C+Yoshida%2C+H.%2C+Yanagi%2C+H.%2C+Yura%2C+T.%2C+and+Mori%2C+K.+%281999%29.+Mammalian+transcription+factor+ATF6+is+synthesized+as+a+transmembrane+protein+and+ac

Heath, P. R., Kirby, J., & Shaw, P. J. (2013). Investigating cell death mechanisms in amyotrophic lateral sclerosis using transcriptomics. *Frontiers in Cellular Neuroscience*, *7*(DEC). https://doi.org/10.3389/FNCEL.2013.00259

Heidari, M. M., Houshmand, M., Hosseinkhani, S., Nafissi, S., & Khatami, M. (2009). Complex I and ATP content deficiency in lymphocytes from Friedreich's ataxia. *The Canadian Journal of Neurological Sciences. Le Journal Canadien Des Sciences Neurologiques*, *36*(1), 26–31. https://doi.org/10.1017/S0317167100006260

Hergesheimer, R. C., Chami, A. A., de Assis, D. R., Vourc'h, P., Andres, C. R., Corcia, P., Lanznaster, D., & Blasco, H. (2019). The debated toxic role of aggregated TDP-43 in amyotrophic lateral sclerosis: a resolution in sight? *Brain : A Journal of Neurology*, *142*(5), 1176–1194. https://doi.org/10.1093/BRAIN/AWZ078

Hernandez-Resendiz, S., Prunier, F., Girao, H., Dorn, G., & Hausenloy, D. J. (2020). Targeting mitochondrial fusion and fission proteins for cardioprotection. *Journal of Cellular and Molecular Medicine*, *24*(12), 6571–6585. https://doi.org/10.1111/JCMM.15384

Hervias, I., Beal, M. F., & Manfredi, G. (2006). Mitochondrial dysfunction and amyotrophic lateral sclerosis. *Muscle & Nerve*, *33*(5), 598–608. https://doi.org/10.1002/MUS.20489

Heslop, K. A., Rovini, A., Hunt, E. G., Fang, D., Morris, M. E., Christie, C. F., Gooz, M. B., DeHart, D. N., Dang, Y., Lemasters, J. J., & Maldonado, E. N. (2020). JNK activation and translocation to mitochondria mediates mitochondrial dysfunction and cell death induced by VDAC opening and sorafenib in hepatocarcinoma cells. *Biochemical Pharmacology*, *171*, 113728. https://doi.org/10.1016/J.BCP.2019.113728

Hetz, C. (2012). The unfolded protein response: controlling cell fate decisions under ER stress and beyond. *Nature Reviews. Molecular Cell Biology*, *13*(2), 89–102. https://doi.org/10.1038/NRM3270

Hetz, C., Chevet, E., & Oakes, S. A. (2015). Proteostasis control by the unfolded protein response. *Nature Cell Biology*, *17*(7), 829–838. https://doi.org/10.1038/NCB3184

Hill, S., Sataranatarajan, K., & van Remmen, H. (2018). Role of signaling molecules in mitochondrial stress response. *Frontiers in Genetics*, *9*(JUL), 225. https://doi.org/10.3389/FGENE.2018.00225/BIBTEX

Hirano, A., Donnenfeld, H., Sasaki, S., & Nakano, I. (1984). Fine structural observations of neurofilamentous changes in amyotrophic lateral sclerosis. *Journal of Neuropathology and Experimental Neurology*, *43*(5), 461–470. https://doi.org/10.1097/00005072-198409000-00001

Ho, S. N. (2006). Intracellular water homeostasis and the mammalian cellular osmotic stress response. *Journal of Cellular Physiology*, *206*(1), 9–15. https://doi.org/10.1002/JCP.20445

Hock, E.-M., Maniecka, Z., Hruska-Plochan, M., Ruepp, M.-D., Dormann, D., & Correspondence, M. P. (2018). Hypertonic Stress Causes Cytoplasmic Translocation of Neuronal, but Not Astrocytic, FUS due to Impaired Transportin Function. *CellReports*, *24*, 987-1000.e7. https://doi.org/10.1016/j.celrep.2018.06.094

Höhn, A., Tramutola, A., & Cascella, R. (2020a). Proteostasis Failure in Neurodegenerative Diseases: Focus on Oxidative Stress. *Oxidative Medicine and Cellular Longevity*, *2020*. https://doi.org/10.1155/2020/5497046

Höhn, A., Tramutola, A., & Cascella, R. (2020b). Proteostasis Failure in Neurodegenerative Diseases: Focus on Oxidative Stress. In *Oxidative Medicine and Cellular Longevity* (Vol. 2020). Hindawi Limited. https://doi.org/10.1155/2020/5497046

Holasek, S. S., Wengenack, T. M., Kandimalla, K. K., Montano, C., Gregor, D. M., Curran, G. L., & Poduslo, J. F. (2005). Activation of the stress-activated MAP kinase, p38, but not JNK in cortical motor neurons during early presymptomatic stages of amyotrophic lateral sclerosis in transgenic mice. *Brain Research*, *1045*(1–2), 185–198. https://doi.org/10.1016/J.BRAINRES.2005.03.037

Hollien, J., & Weissman, J. S. (2006). Decay of endoplasmic reticulum-localized mRNAs during the unfolded protein response. *Science*, *313*(5783), 104–107. https://doi.org/10.1126/SCIENCE.1129631/SUPPL_FILE/HOLLIEN.SOM.PDF

Hor, J. H., Santosa, M. M., Lim, V. J. W., Ho, B. X., Taylor, A., Khong, Z. J., Ravits, J., Fan, Y., Liou, Y. C., Soh, B. S., & Ng, S. Y. (2020). ALS motor neurons exhibit hallmark metabolic defects that are rescued by SIRT3 activation. *Cell Death & Differentiation 2020 28:4*, *28*(4), 1379–1397. https://doi.org/10.1038/s41418-020-00664-0

Hosaka, T., Tsuji, H., & Tamaoka, A. (2021). Biomolecular modifications linked to oxidative stress in amyotrophic lateral sclerosis: Determining promising biomarkers related to oxidative stress. In *Processes* (Vol. 9, Issue 9). MDPI. https://doi.org/10.3390/pr9091667

Hu, M., & Np, R. (2020). Physical activity as a risk factor for amyotrophic lateral sclerosis-findings from three large European cohorts. *Journal of Neurology 2020 267:7*, *267*(7), 2173–2175. https://doi.org/10.1007/S00415-020-09995-X

Huang, X., Wu, B. P., Nguyen, D., Liu, Y. T., Marani, M., Hench, J., Bénit, P., Kozjak-Pavlovic, V., Rustin, P., Frank, S., & Narendra, D. P. (2018). CHCHD2 accumulates in distressed mitochondria and facilitates oligomerization of CHCHD10. *Human Molecular Genetics*, *27*(22), 3881–3900. https://doi.org/10.1093/HMG/DDY270

Huntley, M. L., Gao, J., Termsarasab, P., Wang, L., Zeng, S., Thammongkolchai, T., Liu, Y., Cohen, M. L., & Wang, X. (2019). Association between TDP-43 and mitochondria in inclusion body myositis. *Laboratory Investigation; a Journal of Technical Methods and Pathology*, *99*(7), 1041–1048. https://doi.org/10.1038/S41374-019-0233-X

Hwang, J., & Qi, L. (2018). Quality Control in the Endoplasmic Reticulum: Crosstalk between ERAD and UPR pathways. *Trends in Biochemical Sciences*, *43*(8), 593. https://doi.org/10.1016/J.TIBS.2018.06.005

Hwang, J. Y., & Zukin, R. S. (2018). REST, a master transcriptional regulator in neurodegenerative disease. *Current Opinion in Neurobiology*, *48*, 193–200. https://doi.org/10.1016/J.CONB.2017.12.008

Igaz, L. M., Kwong, L. K., Chen-Plotkin, A., Winton, M. J., Unger, T. L., Xu, Y., Neumann, M., Trojanowski, J. Q., & Lee, V. M. Y. (2009). Expression of TDP-43 C-terminal fragments in vitro recapitulates pathological features of TDP-43 proteinopathies. *Journal of Biological Chemistry*, *284*(13), 8516–8524. https://doi.org/10.1074/jbc.M809462200

Ighodaro, O. M., & Akinloye, O. A. (2019). First line defence antioxidants-superoxide dismutase (SOD), catalase (CAT) and glutathione peroxidase (GPX): Their fundamental role in the entire antioxidant defence grid. *Https://Doi.Org/10.1016/j.Ajme.2017.09.001*, *54*(4), 287–293. https://doi.org/10.1016/J.AJME.2017.09.001

Ilieva, E. v., Ayala, V., Jové, M., Dalfó, E., Cacabelos, D., Povedano, M., Bellmunt, M. J., Ferrer, I., Pamplona, R., & Portero-Otín, M. (2007). Oxidative and endoplasmic reticulum stress interplay in sporadic amyotrophic lateral sclerosis. *Brain*, *130*(12), 3111–3123. https://doi.org/10.1093/BRAIN/AWM190

Ingre, C., Roos, P. M., Piehl, F., Kamel, F., & Fang, F. (2015). Risk factors for amyotrophic lateral sclerosis. *Clinical Epidemiology*, *7*, 181–193. https://doi.org/10.2147/CLEP.S37505

Ioannou, M. S., Jackson, J., Sheu, S. H., Chang, C. L., Weigel, A. v., Liu, H., Pasolli, H. A., Xu, C. S., Pang, S., Matthies, D., Hess, H. F., Lippincott-Schwartz, J., & Liu, Z. (2019). Neuron-Astrocyte Metabolic Coupling Protects against Activity-Induced Fatty Acid Toxicity. *Cell*, *177*(6), 1522-1535.e14. https://doi.org/10.1016/J.CELL.2019.04.001

Israelson, A., Arbel, N., da Cruz, S., Ilieva, H., Yamanaka, K., Shoshan-Barmatz, V., & Cleveland, D. W. (2010). Misfolded mutant SOD1 directly inhibits VDAC1 conductance in a mouse model of inherited ALS. *Neuron*, *67*(4), 575–587. https://doi.org/10.1016/J.NEURON.2010.07.019

Ito, H., Nakamura, M., Komure, O., Ayaki, T., Wate, R., Maruyama, H., Nakamura, Y., Fujita, K., Kaneko, S., Okamoto, Y., Ihara, M., Konishi, T., Ogasawara, K., Hirano, A., Kusaka, H., Kaji, R., Takahashi, R., & Kawakami, H. (2011). Clinicopathologic study on an ALS family with a heterozygous E478G optineurin mutation. *Acta Neuropathologica*, *122*(2), 223–229. https://doi.org/10.1007/S00401-011-0842-Y

Jain, A., & Shivanna, K. R. (1989). Loss of viability during storage is associated with changes in membrane phospholipid. *Phytochemistry*, *28*(4), 999–1002. https://doi.org/10.1016/0031-9422(89)80171-2

Jansen, M., Ohsaki, Y., Rita Rega, L., Bittman, R., Olkkonen, V. M., & Ikonen, E. (2011). Role of ORPs in sterol transport from plasma membrane to ER and lipid droplets in mammalian cells. *Traffic (Copenhagen, Denmark)*, *12*(2), 218–231. https://doi.org/10.1111/J.1600-0854.2010.01142.X

Jarc, E., & Petan, T. (2019). Focus: Organelles: Lipid Droplets and the Management of Cellular Stress. *The Yale Journal of Biology and Medicine*, *92*(3), 435. /pmc/articles/PMC6747940/

Jena, N. R. (2012). DNA damage by reactive species: Mechanisms, mutation and repair. *Journal of Biosciences*, *37*(3), 503–517. https://doi.org/10.1007/S12038-012-9218-2/SCHEMES/10

Jiang, Z., Wang, W., Perry, G., Zhu, X., & Wang, X. (2015). Mitochondrial dynamic abnormalities in amyotrophic lateral sclerosis. *Translational Neurodegeneration*, *4*(1). https://doi.org/10.1186/S40035-015-0037-X

Jin, G., Xu, C., Zhang, X., Long, J., Rezaeian, A. H., Liu, C., Furth, M. E., Kridel, S., Pasche, B., Bian, X. W., & Lin, H. K. (2018). Atad3a suppresses Pink1-dependent mitophagy to maintain homeostasis of hematopoietic progenitor cells. *Nature Immunology*, *19*(1), 29–40. https://doi.org/10.1038/S41590-017-0002-1

Jin, Y., Tan, Y., Chen, L., Liu, Y., & Ren, Z. (2018). Reactive Oxygen Species Induces Lipid Droplet Accumulation in HepG2 Cells by Increasing Perilipin 2 Expression. *International Journal of Molecular Sciences*, *19*(11). https://doi.org/10.3390/IJMS19113445

Jo, M., Lee, S., Jeon, Y. M., Kim, S., Kwon, Y., & Kim, H. J. (2020a). The role of TDP-43 propagation in neurodegenerative diseases: integrating insights from clinical and experimental studies. In *Experimental and Molecular Medicine* (Vol. 52, Issue 10, pp. 1652–1662). Springer Nature. https://doi.org/10.1038/s12276-020-00513-7

Jo, M., Lee, S., Jeon, Y. M., Kim, S., Kwon, Y., & Kim, H. J. (2020b). The role of TDP-43 propagation in neurodegenerative diseases: integrating insights from clinical and experimental studies. *Experimental & Molecular Medicine 2020 52:10*, *52*(10), 1652–1662. https://doi.org/10.1038/s12276-020-00513-7

Johnsen, B., Pugdahl, K., Fuglsang-Frederiksen, A., Kollewe, K., Paracka, L., Dengler, R., Camdessanché, J. P., Nix, W., Liguori, R., Schofield, I., Maderna, L., Czell, D., Neuwirth, C., Weber, M., Drory, V. E., Abraham, A., Swash, M., & de Carvalho, M. (2019). Diagnostic criteria for amyotrophic lateral sclerosis: A multicentre study of inter-rater variation and sensitivity. *Clinical Neurophysiology : Official Journal of the International Federation of Clinical Neurophysiology*, *130*(2), 307–314. https://doi.org/10.1016/J.CLINPH.2018.11.021

Johnson, J. O., Glynn, S. M., Raphael Gibbs, J., Nalls, M. A., Sabatelli, M., Restagno, G., Drory, V. E., Chiò, A., Rogaeva, E., & Traynor, B. J. (2014). Mutations in the CHCHD10 gene are a common

cause of familial amyotrophic lateral sclerosis. *Brain : A Journal of Neurology*, *137*(Pt 12), e311. https://doi.org/10.1093/BRAIN/AWU265

Jung, C., Higgins, C. M. J., & Xu, Z. (2002). Mitochondrial electron transport chain complex dysfunction in a transgenic mouse model for amyotrophic lateral sclerosis. *Journal of Neurochemistry*, *83*(3), 535–545. https://doi.org/10.1046/J.1471-4159.2002.01112.X

Kabashi, E., Agar, J. N., Strong, M. J., & Durham, H. D. (2012). Impaired proteasome function in sporadic amyotrophic lateral sclerosis. *Amyotrophic Lateral Sclerosis : Official Publication of the World Federation of Neurology Research Group on Motor Neuron Diseases*, *13*(4), 367–371. https://doi.org/10.3109/17482968.2012.686511

Kabashi, E., Agar, J. N., Taylor, D. M., Minotti, S., & Durham, H. D. (2004a). Focal dysfunction of the proteasome: a pathogenic factor in a mouse model of amyotrophic lateral sclerosis. *Journal of Neurochemistry*, *89*(6), 1325–1335. https://doi.org/10.1111/J.1471-4159.2004.02453.X

Kabashi, E., Agar, J. N., Taylor, D. M., Minotti, S., & Durham, H. D. (2004b). Focal dysfunction of the proteasome: a pathogenic factor in a mouse model of amyotrophic lateral sclerosis. *Journal of Neurochemistry*, *89*(6), 1325–1335. https://doi.org/10.1111/J.1471-4159.2004.02453.X

Kamalian, L., Douglas, O., Jolly, C. E., Snoeys, J., Simic, D., Monshouwer, M., Williams, D. P., Park, B. K., & Chadwick, A. E. (2019). Acute Metabolic Switch Assay Using Glucose/Galactose Medium in HepaRG Cells to Detect Mitochondrial Toxicity. *Current Protocols in Toxicology*, *80*(1). https://doi.org/10.1002/CPTX.76

Kamelgarn, M., Chen, J., Kuang, L., Jin, H., Kasarskis, E. J., & Zhu, H. (2018). ALS mutations of FUS suppress protein translation and disrupt the regulation of nonsense-mediated decay. *Proceedings of the National Academy of Sciences of the United States of America*, *115*(51), E11904–E11913. https://doi.org/10.1073/PNAS.1810413115/-/DCSUPPLEMENTAL

Kamentsky, L., Jones, T. R., Fraser, A., Bray, M. A., Logan, D. J., Madden, K. L., Ljosa, V., Rueden, C., Eliceiri, K. W., & Carpenter, A. E. (2011). Improved structure, function and compatibility for CellProfiler: modular high-throughput image analysis software. *Bioinformatics (Oxford, England)*, *27*(8), 1179–1180. https://doi.org/10.1093/BIOINFORMATICS/BTR095

Karam, R., Wengrod, J., Gardner, L. B., & Wilkinson, M. F. (2013). Regulation of nonsense-mediated mRNA decay: implications for physiology and disease. *Biochimica et Biophysica Acta*, *1829*(6–7), 624–633. https://doi.org/10.1016/J.BBAGRM.2013.03.002

Karnati, S., Lüers, G., Pfreimer, S., & Baumgart-Vogt, E. (2013). Mammalian SOD2 is exclusively located in mitochondria and not present in peroxisomes. *Histochemistry and Cell Biology*, *140*(2), 105–117. https://doi.org/10.1007/S00418-013-1099-4/TABLES/3

Kassan, A., Herms, A., Fernández-Vidal, A., Bosch, M., Schieber, N. L., Reddy, B. J. N., Fajardo, A., Gelabert-Baldrich, M., Tebar, F., Enrich, C., Gross, S. P., Parton, R. G., & Pol, A. (2013). Acyl-

CoA synthetase 3 promotes lipid droplet biogenesis in ER microdomains. *The Journal of Cell Biology*, *203*(6), 985–1001. https://doi.org/10.1083/JCB.201305142

Kaur, J., & Debnath, J. (2015). Autophagy at the crossroads of catabolism and anabolism. *Nature Reviews Molecular Cell Biology 2015 16:8*, *16*(8), 461–472. https://doi.org/10.1038/nrm4024

Kawahara, Y., & Mieda-Sato, A. (2012). TDP-43 promotes microRNA biogenesis as a component of the Drosha and Dicer complexes. *Proceedings of the National Academy of Sciences of the United States of America*, *109*(9), 3347–3352. https://doi.org/10.1073/pnas.1112427109

Kawamura, M., Sato, S., Matsumoto, G., Fukuda, T., Shiba-Fukushima, K., Noda, S., Takanashi, M., Mori, N., & Hattori, N. (2019). Loss of nuclear REST/NRSF in aged-dopaminergic neurons in Parkinson's disease patients. *Neuroscience Letters*, *699*, 59–63. https://doi.org/10.1016/J.NEULET.2019.01.042

Keon, M., Musrie, B., Dinger, M., Brennan, S. E., Santos, J., & Saksena, N. K. (2021). Destination Amyotrophic Lateral Sclerosis. *Frontiers in Neurology*, *12*, 392. https://doi.org/10.3389/FNEUR.2021.596006/BIBTEX

Keyes, J., Ganesan, A., Molinar-Inglis, O., Hamidzadeh, A., Zhang, J., Ling, M., Trejo, J., Levchenko, A., & Zhang, J. (2020). Signaling diversity enabled by rap1-regulated plasma membrane ERK with distinct temporal dynamics. *ELife*, *9*. https://doi.org/10.7554/ELIFE.57410

Khan, N. A., Nikkanen, J., Yatsuga, S., Jackson, C., Wang, L., Pradhan, S., Kivelä, R., Pessia, A., Velagapudi, V., & Suomalainen, A. (2017). mTORC1 Regulates Mitochondrial Integrated Stress Response and Mitochondrial Myopathy Progression. *Cell Metabolism*, *26*(2), 419-428.e5. https://doi.org/10.1016/J.CMET.2017.07.007

Khatchadourian, A., Bourque, S. D., Richard, V. R., Titorenko, V. I., & Maysinger, D. (2012). Dynamics and regulation of lipid droplet formation in lipopolysaccharide (LPS)-stimulated microglia. *Biochimica et Biophysica Acta*, *1821*(4), 607–617. https://doi.org/10.1016/J.BBALIP.2012.01.007

Khosravi, B., Hartmann, H., May, S., Möhl, C., Ederle, H., Michaelsen, M., Schludi, M. H., Dormann, D., & Edbauer, D. (2017). Cytoplasmic poly-GA aggregates impair nuclear import of TDP-43 in C9orf72 ALS/FTLD. *Human Molecular Genetics*, *26*(4), 790–800. https://doi.org/10.1093/HMG/DDW432

Kikuchi, H., Almer, G., Yamashita, S., Guégan, C., Nagai, M., Xu, Z., Sosunov, A. A., McKhann, G. M., & Przedborski, S. (2006). Spinal cord endoplasmic reticulum stress associated with a microsomal accumulation of mutant superoxide dismutase-1 in an ALS model. *Proceedings of the National Academy of Sciences*, *103*(15), 6025–6030. https://doi.org/10.1073/PNAS.0509227103

Kim, B. W., Jeong, Y. E., Wong, M., & Martin, L. J. (2020). DNA damage accumulates and responses are engaged in human ALS brain and spinal motor neurons and DNA repair is activatable in iPSC-derived motor neurons with SOD1 mutations. *Acta Neuropathologica Communications*, *8*(1). https://doi.org/10.1186/S40478-019-0874-4

Kim, E. K., & Choi, E. J. (2010). Pathological roles of MAPK signaling pathways in human diseases. *Biochimica et Biophysica Acta (BBA) - Molecular Basis of Disease*, *1802*(4), 396–405. https://doi.org/10.1016/J.BBADIS.2009.12.009

King, M. C., & Lusk, C. P. (2016). A model for coordinating nuclear mechanics and membrane remodeling to support nuclear integrity. *Current Opinion in Cell Biology*, *41*, 9–17. https://doi.org/10.1016/J.CEB.2016.03.009

Kirby, J., al Sultan, A., Waller, R., & Heath, P. (2016). The genetics of amyotrophic lateral sclerosis: current insights. *Degenerative Neurological and Neuromuscular Disease*, *6*, 49. https://doi.org/10.2147/DNND.S84956

Kirby, J., Halligan, E., Baptista, M. J., Allen, S., Heath, P. R., Holden, H., Barber, S. C., Loynes, C. A., Wood-Allum, C. A., Lunec, J., & Shaw, P. J. (2005). Mutant SOD1 alters the motor neuronal transcriptome: implications for familial ALS. *Brain : A Journal of Neurology*, *128*(Pt 7), 1686–1706. https://doi.org/10.1093/BRAIN/AWH503

Kish, S. J., Bergeron, C., Rajput, A., Dozic, S., Mastrogiacomo, F., Chang, L. -J, Wilson, J. M., DiStefano, L. M., & Nobrega, J. N. (1992). Brain cytochrome oxidase in Alzheimer's disease. *Journal of Neurochemistry*, *59*(2), 776–779. https://doi.org/10.1111/J.1471-4159.1992.TB09439.X

Klecker, T., Braun, R. J., & Westermann, B. (2017). Lipid Droplets Guard Mitochondria during Autophagy. *Developmental Cell*, *42*(1), 1–2. https://doi.org/10.1016/J.DEVCEL.2017.06.018

Kodavati, M., Wang, H., & Hegde, M. L. (2020). Altered Mitochondrial Dynamics in Motor Neuron Disease: An Emerging Perspective. *Cells*, *9*(4). https://doi.org/10.3390/CELLS9041065

Kovalevich, J., & Langford, D. (2013). Considerations for the use of SH-SY5Y neuroblastoma cells in neurobiology. *Methods in Molecular Biology (Clifton, N.J.)*, *1078*, 9–21. https://doi.org/10.1007/978-1-62703-640-5_2

Kraemer, B. C., Schuck, T., Wheeler, J. M., Robinson, L. C., Trojanowski, J. Q., Lee, V. M. Y., & Schellenberg, G. D. (2010). Loss of murine TDP-43 disrupts motor function and plays an essential role in embryogenesis. *Acta Neuropathologica*, *119*(4), 409–419. https://doi.org/10.1007/S00401-010-0659-0

Kültz, D. (2007). Osmotic stress sensing and signaling in animals. *The FEBS Journal*, *274*(22), 5781–5781. https://doi.org/10.1111/J.1742-4658.2007.06097.X

Kültz, D., & Burg, M. (1998). Evolution of osmotic stress signaling via MAP kinase cascades. *Journal of Experimental Biology*, *201*(22), 3015–3021. https://doi.org/10.1242/JEB.201.22.3015

Kumar, D. R., Aslinia, F., Yale, S. H., & Mazza, J. J. (2011). Jean-martin charcot: The father of neurology. *Clinical Medicine and Research*, *9*(1), 46–49. https://doi.org/10.3121/CMR.2009.883

Kumar, V., & Maity, S. (2021). ER Stress-Sensor Proteins and ER-Mitochondrial Crosstalk—Signaling Beyond (ER) Stress Response. *Biomolecules*, *11*(2), 1–31. https://doi.org/10.3390/BIOM11020173

Kundu, M., & Thompson, C. B. (2008). Autophagy: Basic principles and relevance to disease. In *Annual Review of Pathology: Mechanisms of Disease* (Vol. 3, pp. 427–455). https://doi.org/10.1146/annurev.pathmechdis.2.010506.091842

Kwon, Y. H., Kim, J., Kim, C. S., Tu, T. H., Kim, M. S., Suk, K., Kim, D. H., Lee, B. J., Choi, H. S., Park, T., Choi, M. S., Goto, T., Kawada, T., Ha, T. Y., & Yu, R. (2017). Hypothalamic lipid-laden astrocytes induce microglia migration and activation. *FEBS Letters*, *591*(12), 1742–1751. https://doi.org/10.1002/1873-3468.12691

Laake, J. H., Takumi, Y., Eidet, J., Torgner, I. A., Roberg, B., Kvamme, E., & Ottersen, O. P. (1999). Postembedding immunogold labelling reveals subcellular localization and pathway-specific enrichment of phosphate activated glutaminase in rat cerebellum. *Neuroscience*, *88*(4), 1137–1151. https://doi.org/10.1016/S0306-4522(98)00298-X

Lagier-Tourenne, C., Polymenidou, M., & Cleveland, D. W. (2010). TDP-43 and FUS/TLS: Emerging roles in RNA processing and neurodegeneration. *Human Molecular Genetics*, *19*(R1). https://doi.org/10.1093/hmg/ddq137

Lakhani, S. A., Masud, A., Kuida, K., Porter, G. A., Booth, C. J., Mehal, W. Z., Inayat, I., & Flavell, R. A. (2006). Caspases 3 and 7: Key Mediators of Mitochondrial Events of Apoptosis. *Science (New York, N.Y.)*, *311*(5762), 847. https://doi.org/10.1126/SCIENCE.1115035

Lang, K. S., Lang, P. A., Bauer, C., Duranton, C., Wieder, T., Huber, S. M., & Lang, F. (2005). Mechanisms of Suicidal Erythrocyte Death. *Cellular Physiology and Biochemistry*, *15*(5), 195–202. https://doi.org/10.1159/000086406

Lazar, M. A., & McIntyre, R. S. (2019). Novel therapeutic targets for major depressive disorder. *Neurobiology of Depression: Road to Novel Therapeutics*, 383–400. https://doi.org/10.1016/B978-0-12-813333-0.00034-2

Le, N. T. T., Chang, L., Kovlyagina, I., Georgiou, P., Safren, N., Braunstein, K. E., Kvarta, M. D., Dyke, A. M. V., Legates, T. A., Philips, T., Morrison, B. M., Thompson, S. M., Puche, A. C., Gould, T. D., Rothstein, J. D., Wong, P. C., & Monteiro, M. J. (2016). Motor neuron disease, TDP-43 pathology, and memory deficits in mice expressing ALS-FTD-linked UBQLN2 mutations. *Proceedings of the National Academy of Sciences of the United States of America*, *113*(47), E7580–E7589. https://doi.org/10.1073/PNAS.1608432113

Lederer, C. W., Torrisi, A., Pantelidou, M., Santama, N., & Cavallaro, S. (2007). Pathways and genes differentially expressed in the motor cortex of patients with sporadic amyotrophic lateral sclerosis. *BMC Genomics*, *8*(1), 1–26. https://doi.org/10.1186/1471-2164-8-26/FIGURES/7

Lee, J. A., Hall, B., Allsop, J., Alqarni, R., & Allen, S. P. (2021). Lipid metabolism in astrocytic structure and function. *Seminars in Cell & Developmental Biology*, *112*, 123–136. https://doi.org/10.1016/J.SEMCDB.2020.07.017

Lee, S. C., & Raine, C. S. (1989). Multiple sclerosis: Oligodendrocytes in active lesions do not express class II major histocompatibility complex molecules. *Journal of Neuroimmunology*, *25*(2–3), 261–266. https://doi.org/10.1016/0165-5728(89)90145-8

Lee, S. J., Zhang, J., Choi, A. M. K., & Kim, H. P. (2013). Mitochondrial dysfunction induces formation of lipid droplets as a generalized response to stress. *Oxidative Medicine and Cellular Longevity*, *2013*. https://doi.org/10.1155/2013/327167

Lee, S. R., Kwont, K. S., Kim, S. R., & Rhee, S. G. (1998). Reversible inactivation of protein-tyrosine phosphatase 1B in A431 cells stimulated with epidermal growth factor. *The Journal of Biological Chemistry*, *273*(25), 15366–15372. https://doi.org/10.1074/JBC.273.25.15366

Lee, S., Shang, Y., Redmond, S. A., Urisman, A., Tang, A. A., Li, K. H., Burlingame, A. L., Pak, R. A., Jovičić, A., Gitler, A. D., Wang, J., Gray, N. S., Seeley, W. W., Siddique, T., Bigio, E. H., Lee, V. M. Y., Trojanowski, J. Q., Chan, J. R., & Huang, E. J. (2016). Activation of HIPK2 Promotes ER Stress-Mediated Neurodegeneration in Amyotrophic Lateral Sclerosis. *Neuron*, *91*(1), 41–55. https://doi.org/10.1016/J.NEURON.2016.05.021

Lee, T. H., & Linstedt, A. D. (1999). Osmotically induced cell volume changes alter anterograde and retrograde transport, Golgi structure, and COPI dissociation. *Molecular Biology of the Cell*, *10*(5), 1445–1462. https://doi.org/10.1091/MBC.10.5.1445/ASSET/IMAGES/LARGE/MK0590869010.JPEG

Lee, Y. B., Scotter, E. L., Lee, D. Y., Troakes, C., Mitchell, J., Rogelj, B., Gallo, J. M., & Shaw, C. E. (2021). Cytoplasmic TDP-43 is involved in cell fate during stress recovery. *Human Molecular Genetics*, *31*(2), 166–175. https://doi.org/10.1093/HMG/DDAB227

Lee, Y. J., Galoforo, S. S., Berns, C. M., Chen, J. C., Davis, B. H., Sim, J. E., Corry, P. M., & Spitz, D. R. (1998). Glucose deprivation-induced cytotoxicity and alterations in mitogen-activated protein kinase activation are mediated by oxidative stress in multidrug-resistant human breast carcinoma cells. *The Journal of Biological Chemistry*, *273*(9), 5294–5299. https://doi.org/10.1074/JBC.273.9.5294

Lee, Y.-B., Scotter, E. L., Lee, D.-Y., Troakes, C., Mitchell, J., Rogelj, B., Gallo, J.-M., & Shaw, C. E. (2021). Cytoplasmic TDP-43 is involved in cell fate during stress recovery. *Human Molecular Genetics*, *00*. https://doi.org/10.1093/HMG/DDAB227

Lei, Y., Zhang, Z. F., Lei, R. X., Wang, S., Zhuang, Y., Liu, A. C., Wu, Y., Chen, J., Tang, J. C., Pan, M. X., Liu, R., Liao, W. J., Feng, Y. G., Wan, Q., & Zheng, M. (2018). DJ-1 Suppresses Cytoplasmic TDP-43 Aggregation in Oxidative Stress-Induced Cell Injury. *Journal of Alzheimer's Disease : JAD*, *66*(3), 1001–1014. https://doi.org/10.3233/JAD-180460

Lévy, E., el Banna, N., Baïlle, D., Heneman-Masurel, A., Truchet, S., Rezaei, H., Huang, M. E., Béringue, V., Martin, D., & Vernis, L. (2019). Causative Links between Protein Aggregation and Oxidative Stress: A Review. *International Journal of Molecular Sciences*, *20*(16). https://doi.org/10.3390/IJMS20163896

Lim, L., Wei, Y., Lu, Y., & Song, J. (2016). ALS-Causing Mutations Significantly Perturb the Self-Assembly and Interaction with Nucleic Acid of the Intrinsically Disordered Prion-Like Domain of TDP-43. *PLoS Biology*, *14*(1). https://doi.org/10.1371/JOURNAL.PBIO.1002338

Ling, J. P., Pletnikova, O., Troncoso, J. C., & Wong, P. C. (2015). TDP-43 repression of nonconserved cryptic exons is compromised in ALS-FTD. *Science (New York, N.Y.)*, *349*(6248), 650. https://doi.org/10.1126/SCIENCE.AAB0983

Ling, Y. H., Liebes, L., Zou, Y., & Perez-Soler, R. (2003). Reactive Oxygen Species Generation and Mitochondrial Dysfunction in the Apoptotic Response to Bortezomib, a Novel Proteasome Inhibitor, in Human H460 Non-small Cell Lung Cancer Cells *. *Journal of Biological Chemistry*, *278*(36), 33714–33723. https://doi.org/10.1074/JBC.M302559200

Liu, H., Deng, X., Shyu, Y. J., Jian, J. L., Taparowsky, E. J., & Hu, C. D. (2006). Mutual regulation of c-Jun and ATF2 by transcriptional activation and subcellular localization. *The EMBO Journal*, *25*(5), 1058–1069. https://doi.org/10.1038/SJ.EMBOJ.7601020

Liu, L., MacKenzie, K. R., Putluri, N., Maletić-Savatić, M., & Bellen, H. J. (2017). The Glia-Neuron Lactate Shuttle and Elevated ROS Promote Lipid Synthesis in Neurons and Lipid Droplet Accumulation in Glia via APOE/D. *Cell Metabolism*, *26*(5), 719-737.e6. https://doi.org/10.1016/J.CMET.2017.08.024

Longinetti, E., & Fang, F. (2019). Epidemiology of amyotrophic lateral sclerosis: an update of recent literature. *Current Opinion in Neurology*, *32*(5), 771. https://doi.org/10.1097/WCO.0000000000000730

López-Hernández, T., Puchkov, D., Krause, E., Maritzen, T., & Haucke, V. (2020). Endocytic regulation of cellular ion homeostasis controls lysosome biogenesis. *Nature Cell Biology*, *22*(7), 815–827. https://doi.org/10.1038/S41556-020-0535-7

Lu, T., Aron, L., Zullo, J., Pan, Y., Kim, H., Chen, Y., Yang, T. H., Kim, H. M., Drake, D., Liu, X. S., Bennett, D. A., Colaiácovo, M. P., & Yankner, B. A. (2014a). REST and stress resistance in ageing and Alzheimer's disease. *Nature 2014 507:7493*, *507*(7493), 448–454. https://doi.org/10.1038/nature13163

Lu, T., Aron, L., Zullo, J., Pan, Y., Kim, H., Chen, Y., Yang, T. H., Kim, H. M., Drake, D., Liu, X. S., Bennett, D. A., Colaiácovo, M. P., & Yankner, B. A. (2014b). REST and stress resistance in ageing and Alzheimer's disease. *Nature 2014 507:7493*, *507*(7493), 448–454. https://doi.org/10.1038/nature13163

Lu, T., Aron, L., Zullo, J., Pan, Y., Kim, H., Chen, Y., Yang, T. H., Kim, H. M., Drake, D., Liu, X. S., Bennett, D. A., Colaiácovo, M. P., & Yankner, B. A. (2014c). REST and stress resistance in ageing and Alzheimer's disease. *Nature 2014 507:7493*, *507*(7493), 448–454. https://doi.org/10.1038/nature13163

Madeira, J. B., Masuda, C. A., Maya-Monteiro, C. M., Matos, G. S., Montero-Lomelí, M., & Bozaquel-Morais, B. L. (2015). TORC1 inhibition induces lipid droplet replenishment in yeast. *Molecular and Cellular Biology*, *35*(4), 737–746. https://doi.org/10.1128/MCB.01314-14

Magistretti, P. J., & Chatton, J. Y. (2004). Relationship between L-glutamate-regulated intracellular Na+ dynamics and ATP hydrolysis in astrocytes. *Journal of Neural Transmission 2004 112:1*, *112*(1), 77–85. https://doi.org/10.1007/S00702-004-0171-6

Magrané, J., Cortez, C., Gan, W. B., & Manfredi, G. (2014). Abnormal mitochondrial transport and morphology are common pathological denominators in SOD1 and TDP43 ALS mouse models. *Human Molecular Genetics*, *23*(6), 1413–1424. https://doi.org/10.1093/HMG/DDT528

Mahadev, K., Zilbering, A., Zhu, L., & Goldstein, B. J. (2001). Insulin-stimulated hydrogen peroxide reversibly inhibits protein-tyrosine phosphatase 1b in vivo and enhances the early insulin action cascade. *The Journal of Biological Chemistry*, *276*(24), 21938–21942. https://doi.org/10.1074/JBC.C100109200

Mahul-Mellier, A. L., Burtscher, J., Maharjan, N., Weerens, L., Croisier, M., Kuttler, F., Leleu, M., Knott, G. W., & Lashuel, H. A. (2020). The process of Lewy body formation, rather than simply α-synuclein fibrillization, is one of the major drivers of neurodegeneration. *Proceedings of the National Academy of Sciences of the United States of America*, *117*(9), 4971–4982. https://doi.org/10.1073/PNAS.1913904117/-/DCSUPPLEMENTAL

Malhotra, J. D., & Kaufman, R. J. (2011). ER Stress and Its Functional Link to Mitochondria: Role in Cell Survival and Death. *Cold Spring Harbor Perspectives in Biology*, *3*(9), 1–13. https://doi.org/10.1101/CSHPERSPECT.A004424

Marcus, C., Mena, E., & Subramaniam, R. M. (2014). Brain PET in the diagnosis of Alzheimer's disease. *Clinical Nuclear Medicine*, *39*(10), e413–e426. https://doi.org/10.1097/RLU.0000000000000547

Marfè, G., Morgante, E., di Stefano, C., di Renzo, L., de Martino, L., Iovane, G., Russo, M. A., & Sinibaldi-Salimei, P. (2008). Sorbitol-induced apoptosis of human leukemia is mediated by caspase activation and cytochrome c release. *Archives of Toxicology*, *82*(6), 371–377. https://doi.org/10.1007/S00204-007-0261-Y

Marroquin, L. D., Hynes, J., Dykens, J. A., Jamieson, J. D., & Will, Y. (2007). Circumventing the Crabtree effect: replacing media glucose with galactose increases susceptibility of HepG2 cells to mitochondrial toxicants. *Toxicological Sciences : An Official Journal of the Society of Toxicology*, *97*(2), 539–547. https://doi.org/10.1093/TOXSCI/KFM052

Marschallinger, J., Iram, T., Zardeneta, M., Lee, S. E., Lehallier, B., Haney, M. S., Pluvinage, J. v., Mathur, V., Hahn, O., Morgens, D. W., Kim, J., Tevini, J., Felder, T. K., Wolinski, H., Bertozzi, C. R., Bassik, M. C., Aigner, L., & Wyss-Coray, T. (2020). Lipid-droplet-accumulating microglia represent a dysfunctional and proinflammatory state in the aging brain. *Nature Neuroscience*, *23*(2), 194–208. https://doi.org/10.1038/S41593-019-0566-1

Martinez-Hernandez, A., Bell, K. P., & Norenberg, M. D. (1977). Glutamine Synthetase: Glial Localization in Brain. *Science*, *195*(4284), 1356–1358. https://doi.org/10.1126/SCIENCE.14400

Masgras, I., Ciscato, F., Brunati, A. M., Tibaldi, E., Indraccolo, S., Curtarello, M., Chiara, F., Cannino, G., Papaleo, E., Lambrughi, M., Guzzo, G., Gambalunga, A., Pizzi, M., Guzzardo, V., Rugge, M., Vuljan, S. E., Calabrese, F., Bernardi, P., & Rasola, A. (2017). Absence of Neurofibromin Induces an Oncogenic Metabolic Switch via Mitochondrial ERK-Mediated Phosphorylation of the Chaperone TRAP1. *Cell Reports*, *18*(3), 659–672. https://doi.org/10.1016/J.CELREP.2016.12.056

Masrori, P., & van Damme, P. (2020). Amyotrophic lateral sclerosis: a clinical review. *European Journal of Neurology*, *27*(10), 1918. https://doi.org/10.1111/ENE.14393

Matus, S., Lopez, E., Valenzuela, V., Nassif, M., & Hetz, C. (2013). Functional contribution of the transcription factor ATF4 to the pathogenesis of amyotrophic lateral sclerosis. *PloS One*, *8*(7). https://doi.org/10.1371/JOURNAL.PONE.0066672

McAlary, L., Chew, Y. L., Lum, J. S., Geraghty, N. J., Yerbury, J. J., & Cashman, N. R. (2020). Amyotrophic Lateral Sclerosis: Proteins, Proteostasis, Prions, and Promises. *Frontiers in Cellular Neuroscience*, *14*. https://doi.org/10.3389/FNCEL.2020.581907

McClelland, S., Flynn, C., Dubé, C., Richichi, C., Zha, Q., Ghestem, A., Esclapez, M., Bernard, C., & Baram, T. Z. (2011). Neuron-restrictive silencer factor-mediated hyperpolarization-activated cyclic nucleotide gated channelopathy in experimental temporal lobe epilepsy. *Annals of Neurology*, *70*(3), 454–465. https://doi.org/10.1002/ANA.22479

McDonald, K. K., Aulas, A., Destroismaisons, L., Pickles, S., Beleac, E., Camu, W., Rouleau, G. A., & Velde, C. vande. (2011). TAR DNA-binding protein 43 (TDP-43) regulates stress granule dynamics via differential regulation of G3BP and TIA-1. *Human Molecular Genetics*, *20*(7), 1400–1410. https://doi.org/10.1093/HMG/DDR021

McKenna, M. C., Dienel, G. A., Sonnewald, U., Waagepetersen, H. S., & Schousboe, A. (2012a). Energy Metabolism of the Brain. *Basic Neurochemistry*, 200–231. https://doi.org/10.1016/B978-0-12-374947-5.00011-0

McKenna, M. C., Dienel, G. A., Sonnewald, U., Waagepetersen, H. S., & Schousboe, A. (2012b). Energy Metabolism of the Brain. *Basic Neurochemistry*, 200–231. https://doi.org/10.1016/B978-0-12-374947-5.00011-0

Medinas, D. B., Valenzuela, V., & Hetz, C. (2017). Proteostasis disturbance in amyotrophic lateral sclerosis. *Human Molecular Genetics*, *26*(R2), R91–R104. https://doi.org/10.1093/HMG/DDX274

Mehta, P., Kaye, W., Raymond, J., Punjani, R., Larson, T., Cohen, J., Muravov, O., & Horton, K. (2018). Prevalence of Amyotrophic Lateral Sclerosis - United States, 2015. *MMWR. Morbidity and Mortality Weekly Report*, *67*(46), 1285–1289. https://doi.org/10.15585/MMWR.MM6746A1

Mejzini, R., Flynn, L. L., Pitout, I. L., Fletcher, S., Wilton, S. D., & Akkari, P. A. (2019). ALS Genetics, Mechanisms, and Therapeutics: Where Are We Now? *Frontiers in Neuroscience*, *13*. https://doi.org/10.3389/FNINS.2019.01310/FULL

Meng, T. C., Fukada, T., & Tonks, N. K. (2002). Reversible oxidation and inactivation of protein tyrosine phosphatases in vivo. *Molecular Cell*, *9*(2), 387–399. https://doi.org/10.1016/S1097-2765(02)00445-8

Menzies, F. M., Ince, P. G., & Shaw, P. J. (2002). Mitochondrial involvement in amyotrophic lateral sclerosis. *Neurochemistry International*, *40*(6), 543–551. https://doi.org/10.1016/S0197-0186(01)00125-5

Mergenthaler, P., Lindauer, U., Dienel, G. A., & Meisel, A. (2013). Sugar for the brain: the role of glucose in physiological and pathological brain function. *Trends in Neurosciences*, *36*(10), 587–597. https://doi.org/10.1016/J.TINS.2013.07.001

Meyer, H., & Weihl, C. C. (2014). The VCP/p97 system at a glance: connecting cellular function to disease pathogenesis. *Journal of Cell Science*, *127*(Pt 18), 3877–3883. https://doi.org/10.1242/JCS.093831

Meyerowitz, J., Parker, S. J., Vella, L. J., Ng, D. C., Price, K. A., Liddell, J. R., Caragounis, A., Li, Q. X., Masters, C. L., Nonaka, T., Hasegawa, M., Bogoyevitch, M. A., Kanninen, K. M., Crouch, P. J., & White, A. R. (2011). C-Jun N-terminal kinase controls TDP-43 accumulation in stress granules induced by oxidative stress. *Molecular Neurodegeneration*, *6*(1), 1–22. https://doi.org/10.1186/1750-1326-6-57/FIGURES/11

Meyers, A., Chourey, K., Weiskittel, T. M., Pfiffner, S., Dunlap, J. R., Hettich, R. L., & Dalhaimer, P. (2017). The protein and neutral lipid composition of lipid droplets isolated from the fission yeast, Schizosaccharomyces pombe. *Journal of Microbiology (Seoul, Korea)*, *55*(2), 112–122. https://doi.org/10.1007/S12275-017-6205-1

Michael Y. Sherman Alfred, & L. Goldberg. (2001). Review Cellular Defenses against Unfolded Proteins: A Cell Biologist Thinks about Neurodegenerative Diseases. *Neuron*, *29*, 15–32.

Misrani, A., Tabassum, S., & Yang, L. (2021). Mitochondrial Dysfunction and Oxidative Stress in Alzheimer's Disease. *Frontiers in Aging Neuroscience*, *13*, 57. https://doi.org/10.3389/FNAGI.2021.617588/BIBTEX

Missaglia, S., Coleman, R., Mordente, A., & Tavian, D. (2019). Neutral Lipid Storage Diseases as Cellular Model to Study Lipid Droplet Function. *Cells*, *8*(2), 187. https://doi.org/10.3390/CELLS8020187

Mitra, J., & Hegde, M. L. (2019). A Commentary on TDP-43 and DNA Damage Response in Amyotrophic Lateral Sclerosis. *Journal of Experimental Neuroscience*, *13*, 1179069519880166. https://doi.org/10.1177/1179069519880166

Miyazaki, K., Masamoto, K., Morimoto, N., Kurata, T., Mimoto, T., Obata, T., Kanno, I., & Abe, K. (2012). Early and progressive impairment of spinal blood flow-glucose metabolism coupling in motor neuron degeneration of ALS model mice. *Journal of Cerebral Blood Flow and Metabolism : Official Journal of the International Society of Cerebral Blood Flow and Metabolism*, *32*(3), 456–467. https://doi.org/10.1038/JCBFM.2011.155

Momtaz, S., Memariani, Z., El-Senduny, F. F., Sanadgol, N., Golab, F., Katebi, M., Abdolghaffari, A. H., Farzaei, M. H., & Abdollahi, M. (2020). Targeting ubiquitin-proteasome pathway by natural products: Novel therapeutic strategy for treatment of neurodegenerative diseases. *Frontiers in Physiology*, *11*, 361. https://doi.org/10.3389/FPHYS.2020.00361/BIBTEX

Montesinos, J., Guardia-Laguarta, C., & Area-Gomez, E. (2020). The fat brain. *Current Opinion in Clinical Nutrition and Metabolic Care*, *23*(2), 68–75. https://doi.org/10.1097/MCO.0000000000000634

Montibeller, L., & de Belleroche, J. (2018). Amyotrophic lateral sclerosis (ALS) and Alzheimer's disease (AD) are characterised by differential activation of ER stress pathways: focus on UPR target genes. *Cell Stress & Chaperones*, *23*(5), 897–912. https://doi.org/10.1007/S12192-018-0897-Y

Moreno-García, A., Kun, A., Calero, O., Medina, M., & Calero, M. (2018). An overview of the role of lipofuscin in age-related neurodegeneration. *Frontiers in Neuroscience*, *12*(JUL), 464. https://doi.org/10.3389/FNINS.2018.00464/BIBTEX

Morita, M., Ikeshima-Kataoka, H., Kreft, M., Vardjan, N., Zorec, R., & Noda, M. (2019). Metabolic Plasticity of Astrocytes and Aging of the Brain. *International Journal of Molecular Sciences*, *20*(4). https://doi.org/10.3390/IJMS20040941

Morrice, J. R., Gregory-Evans, C. Y., & Shaw, C. A. (2017). Necroptosis in amyotrophic lateral sclerosis and other neurological disorders. *Biochimica et Biophysica Acta (BBA) - Molecular Basis of Disease*, *1863*(2), 347–353. https://doi.org/10.1016/J.BBADIS.2016.11.025

Mosienko, V., Teschemacher, A. G., & Kasparov, S. (2015). Is L-lactate a novel signaling molecule in the brain? *Journal of Cerebral Blood Flow and Metabolism : Official Journal of the International Society of Cerebral Blood Flow and Metabolism*, *35*(7), 1069–1075. https://doi.org/10.1038/JCBFM.2015.77

Mourelatos, Z., Gonatas, N. K., Stieber, A., Gurney, M. E., & Dal Canto, M. C. (1996). The Golgi apparatus of spinal cord motor neurons in transgenic mice expressing mutant Cu,Zn superoxide dismutase becomes fragmented in early, preclinical stages of the disease. *Proceedings of the National Academy of Sciences of the United States of America*, *93*(11), 5472–5477. https://doi.org/10.1073/PNAS.93.11.5472

Mourelatos, Z., Yachnis, A., Rorke, L., Mikol, J., & Gonatas, N. K. (1993). The Golgi apparatus of moptor neurons in amyotrophic lateral sclerosis. *Annals of Neurology*, *33*(6), 608–615. https://doi.org/10.1002/ana.410330609

Müller, K., Andersen, P. M., Hübers, A., Marroquin, N., Volk, A. E., Danzer, K. M., Meitinger, T., Ludolph, A. C., Strom, T. M., & Weishaupt, J. H. (2014). Two novel mutations in conserved codons indicate that CHCHD10 is a gene associated with motor neuron disease. *Brain : A Journal of Neurology*, *137*(Pt 12), e309. https://doi.org/10.1093/BRAIN/AWU227

Müller, K., Oh, K.-W., Nordin, A., Panthi, S., Kim, S. H., Nordin, F., Freischmidt, A., Ludolph, A. C., Ki, C. S., Forsberg, K., Weishaupt, J., Kim, Y.-E., & Andersen, P. M. (2021). De novo mutations

in SOD1 are a cause of ALS. *J Neurol Neurosurg Psychiatry*, *0*, 1–6. https://doi.org/10.1136/jnnp-2021-327520

Nakajima, S., Gotoh, M., Fukasawa, K., Murakami-Murofushi, K., & Kunugi, H. (2019). Oleic acid is a potent inducer for lipid droplet accumulation through its esterification to glycerol by diacylglycerol acyltransferase in primary cortical astrocytes. *Brain Research*, *1725*, 146484. https://doi.org/10.1016/J.BRAINRES.2019.146484

Nehls, J., Koppensteiner, H., Brack-Werner, R., Floss, T., & Schindler, M. (2014). HIV-1 replication in human immune cells is independent of TAR DNA binding protein 43 (TDP-43) expression. *PLoS ONE*, *9*(8). https://doi.org/10.1371/journal.pone.0105478

Neumann, M., Sampathu, D. M., Kwong, L. K., Truax, A. C., Micsenyi, M. C., Chou, T. T., Bruce, J., Schuck, T., Grossman, M., Clark, C. M., McCluskey, L. F., Miller, B. L., Masliah, E., Mackenzie, I. R., Feldman, H., Feiden, W., Kretzschmar, H. A., Trojanowski, J. Q., & Lee, V. M. Y. (2006). Ubiquitinated TDP-43 in frontotemporal lobar degeneration and amyotrophic lateral sclerosis. *Science (New York, N.Y.)*, *314*(5796), 130–133. https://doi.org/10.1126/SCIENCE.1134108

Nguyen, T. B., Louie, S. M., Daniele, J. R., Tran, Q., Dillin, A., Zoncu, R., Nomura, D. K., & Olzmann, J. A. (2017). DGAT1-Dependent Lipid Droplet Biogenesis Protects Mitochondrial Function during Starvation-Induced Autophagy. *Developmental Cell*, *42*(1), 9-21.e5. https://doi.org/10.1016/J.DEVCEL.2017.06.003

Nishitoh, H., Matsuzawa, A., Tobiume, K., Saegusa, K., Takeda, K., Inoue, K., Hori, S., Kakizuka, A., & Ichijo, H. (2002). ASK1 is essential for endoplasmic reticulum stress-induced neuronal cell death triggered by expanded polyglutamine repeats. *Genes & Development*, *16*(11), 1345–1355. https://doi.org/10.1101/GAD.992302

Niwa, J. I., Ishigaki, S., Hishikawa, N., Yamamoto, M., Doyu, M., Murata, S., Tanaka, K., Taniguchi, N., & Sobue, G. (2002). Dorfin ubiquitylates mutant SOD1 and prevents mutant SOD1-mediated neurotoxicity. *The Journal of Biological Chemistry*, *277*(39), 36793–36798. https://doi.org/10.1074/JBC.M206559200

Obrador, E., Salvador, R., Estrela, J. M., López-Blanch, R., Jihad-Jebbar, A., & Vallés, S. L. (2020). Oxidative stress, neuroinflammation and mitochondria in the pathophysiology of amyotrophic lateral sclerosis. In *Antioxidants* (Vol. 9, Issue 9, pp. 1–16). MDPI. https://doi.org/10.3390/antiox9090901

Ohta, Y., Yamashita, T., Nomura, E., Hishikawa, N., Ikegami, K., Osakada, Y., Matsumoto, N., Kawahara, Y., Yunoki, T., Takahashi, Y., Takamiya, M., Tadokoro, K., Sasaki, R., Nakano, Y., Tsunoda, K., Sato, K., Omote, Y., Takemoto, M., & Abe, K. (2020). Improvement of a decreased anti-oxidative activity by edaravone in amyotrophic lateral sclerosis patients. *Journal of the Neurological Sciences*, *415*. https://doi.org/10.1016/J.JNS.2020.116906

Okada, A. K., Teranishi, K., Lobo, F., Isas, J. M., Xiao, J., Yen, K., Cohen, P., & Langen, R. (2017). The Mitochondrial-Derived Peptides, HumaninS14G and Small Humanin-like Peptide 2, Exhibit

Chaperone-like Activity. *Scientific Reports 2017 7:1*, *7*(1), 1–10. https://doi.org/10.1038/s41598-017-08372-5

Okamoto, K., Kihira, T., Kobashi, G., Washio, M., Sasaki, S., Yokoyama, T., Miyake, Y., Sakamoto, N., Inaba, Y., & Nagai, M. (2009). Fruit and vegetable intake and risk of amyotrophic lateral sclerosis in Japan. *Neuroepidemiology*, *32*(4), 251–256. https://doi.org/10.1159/000201563

Olzmann, J. A., & Carvalho, P. (2019). Dynamics and functions of lipid droplets. *Nature Reviews. Molecular Cell Biology*, *20*(3), 137–155. https://doi.org/10.1038/S41580-018-0085-Z

O'Malley, H. A., & Isom, L. L. (2015). Sodium channel β subunits: Emerging targets in channelopathies. *Annual Review of Physiology*, *77*, 481–504. https://doi.org/10.1146/annurev-physiol-021014-071846

Ooi, L., & Wood, I. C. (2007). Chromatin crosstalk in development and disease: lessons from REST. *Nature Reviews Genetics 2007 8:7*, *8*(7), 544–554. https://doi.org/10.1038/nrg2100

Orlicka-Płocka, M., Gurda-Wozna, D., Fedoruk-Wyszomirska, A., & Wyszko, E. (2020). Circumventing the Crabtree effect: forcing oxidative phosphorylation (OXPHOS) via galactose medium increases sensitivity of HepG2 cells to the purine derivative kinetin riboside. *Apoptosis*, *25*(11–12), 835–852. https://doi.org/10.1007/S10495-020-01637-X/FIGURES/5

Öst, A., Örtegren, U., Gustavsson, J., Nystrom, F. H., & Strålfors, P. (2005). Triacylglycerol is synthesized in a specific subclass of caveolae in primary adipocytes. *The Journal of Biological Chemistry*, *280*(1), 5–8. https://doi.org/10.1074/JBC.C400429200

Pajares, M., Jiménez-Moreno, N., Dias, I. H. K., Debelec, B., Vucetic, M., Fladmark, K. E., Basaga, H., Ribaric, S., Milisav, I., & Cuadrado, A. (2015). Redox control of protein degradation. *Redox Biology*, *6*, 409–420. https://doi.org/10.1016/J.REDOX.2015.07.003

Palamiuc, L., Schlagowski, A., Ngo, S. T., Vernay, A., Dirrig-Grosch, S., Henriques, A., Boutillier, A., Zoll, J., Echaniz-Laguna, A., Loeffler, J., & René, F. (2015). A metabolic switch toward lipid use in glycolytic muscle is an early pathologic event in a mouse model of amyotrophic lateral sclerosis. *EMBO Molecular Medicine*, *7*(5), 526–546. https://doi.org/10.15252/EMMM.201404433

Pang, W., & Hu, F. (2021). Cellular and physiological functions of C9ORF72 and implications for ALS/FTD. *Journal of Neurochemistry*, *157*(3), 334–350. https://doi.org/10.1111/JNC.15255

Papadopoulos, C., Orso, G., Mancuso, G., Herholz, M., Gumeni, S., Tadepalle, N., Jüngst, C., Tzschichholz, A., Schauss, A., Höning, S., Trifunovic, A., Daga, A., & Rugarli, E. I. (2015). Spastin binds to lipid droplets and affects lipid metabolism. *PLoS Genetics*, *11*(4). https://doi.org/10.1371/JOURNAL.PGEN.1005149

Park, C., & Cuervo, A. M. (2013). Selective Autophagy: Talking with the UPS. *Cell Biochemistry and Biophysics 2013 67:1*, *67*(1), 3–13. https://doi.org/10.1007/S12013-013-9623-7

Pastor, M. M., Proft, M., & Pascual-Ahuir, A. (2009). Mitochondrial function is an inducible determinant of osmotic stress adaptation in yeast. *The Journal of Biological Chemistry*, *284*(44), 30307–30317. https://doi.org/10.1074/JBC.M109.050682

Pellerin, L., Bouzier-Sore, A. K., Aubert, A., Serres, S., Merle, M., Costalat, R., & Magistretti, P. J. (2007). Activity-dependent regulation of energy metabolism by astrocytes: an update. *Glia*, *55*(12), 1251–1262. https://doi.org/10.1002/GLIA.20528

Pellerin, L., & Magistretti, P. J. (1994). Glutamate uptake into astrocytes stimulates aerobic glycolysis: a mechanism coupling neuronal activity to glucose utilization. *Proceedings of the National Academy of Sciences of the United States of America*, *91*(22), 10625–10629. https://doi.org/10.1073/PNAS.91.22.10625

Peng, K., Yang, L., Wang, J., Ye, F., Dan, G., Zhao, Y., Cai, Y., Cui, Z., Ao, L., Liu, J., Zou, Z., Sai, Y., & Cao, J. (2017). The Interaction of Mitochondrial Biogenesis and Fission/Fusion Mediated by PGC-1α Regulates Rotenone-Induced Dopaminergic Neurotoxicity. *Molecular Neurobiology*, *54*(5), 3783–3797. https://doi.org/10.1007/S12035-016-9944-9

Pennetta, G., & Welte, M. A. (2018a). Developmental Cell Essay Emerging Links between Lipid Droplets and Motor Neuron Diseases. *Developmental Cell*, *45*, 427–432. https://doi.org/10.1016/j.devcel.2018.05.002

Pennetta, G., & Welte, M. A. (2018b). Emerging Links between Lipid Droplets and Motor Neuron Diseases. *Developmental Cell*, *45*(4), 427–432. https://doi.org/10.1016/J.DEVCEL.2018.05.002

Pham, Q. D., Wolde-Kidan, A., Gupta, A., Schlaich, A., Schneck, E., Netz, R. R., & Sparr, E. (2018). Effects of Urea and TMAO on Lipid Self-Assembly under Osmotic Stress Conditions. *Journal of Physical Chemistry B*, *122*(25), 6471–6482. https://doi.org/10.1021/acs.jpcb.8b02159

Philips, T., & Rothstein, J. D. (2015). Rodent Models of Amyotrophic Lateral Sclerosis. *Current Protocols in Pharmacology*, *69*, 5.67.1-5.67.21. https://doi.org/10.1002/0471141755.PH0567S69

Picard, M., Wallace, D. C., & Burelle, Y. (2016). The rise of mitochondria in medicine. *Mitochondrion*, *30*, 105–116. https://doi.org/10.1016/J.MITO.2016.07.003

Pierre, K., & Pellerin, L. (2005). Monocarboxylate transporters in the central nervous system: distribution, regulation and function. *Journal of Neurochemistry*, *94*(1), 1–14. https://doi.org/10.1111/J.1471-4159.2005.03168.X

Plotnikov, A., Zehorai, E., Procaccia, S., & Seger, R. (2011). The MAPK cascades: Signaling components, nuclear roles and mechanisms of nuclear translocation. *Biochimica et Biophysica Acta (BBA) - Molecular Cell Research*, *1813*(9), 1619–1633. https://doi.org/10.1016/J.BBAMCR.2010.12.012

Pol, A., Gross, S. P., & Parton, R. G. (2014). Biogenesis of the multifunctional lipid droplet: Lipids, proteins, and sites. *Journal of Cell Biology*, *204*(5), 635–646. https://doi.org/10.1083/JCB.201311051

Polymenidou, M., & Cleveland, D. W. (2017). Biological Spectrum of Amyotrophic Lateral Sclerosis Prions. *Cold Spring Harbor Perspectives in Medicine*, *7*(11). https://doi.org/10.1101/CSHPERSPECT.A024133

Ponath, G., Ramanan, S., Mubarak, M., Housley, W., Lee, S., Sahinkaya, F. R., Vortmeyer, A., Raine, C. S., & Pitt, D. (2017). Myelin phagocytosis by astrocytes after myelin damage promotes lesion pathology. *Brain : A Journal of Neurology*, *140*(2), 399–413. https://doi.org/10.1093/BRAIN/AWW298

Purandare, N., Somayajulu, M., Hüttemann, M., Grossman, L. I., & Aras, S. (2018). The cellular stress proteins CHCHD10 and MNRR1 (CHCHD2): Partners in mitochondrial and nuclear function and dysfunction. *The Journal of Biological Chemistry*, *293*(17), 6517. https://doi.org/10.1074/JBC.RA117.001073

Puri, V., Konda, S., Ranjit, S., Aouadi, M., Chawla, A., Chouinard, M., Chakladar, A., & Czech, M. P. (2007). Fat-specific protein 27, a novel lipid droplet protein that enhances triglyceride storage. *Journal of Biological Chemistry*, *282*(47), 34213–34218. https://doi.org/10.1074/JBC.M707404200/ATTACHMENT/48235075-B267-429C-A5FB-6C246C6BF609/MMC1.PDF

Puri, V., Ranjit, S., Konda, S., Nicoloro, S. M. C., Straubhaar, J., Chawla, A., Chouinard, M., Lin, C., Burkart, A., Corvera, S., Perugini, R. A., & Czech, M. P. (2008). Cidea is associated with lipid droplets and insulin sensitivity in humans. *Proceedings of the National Academy of Sciences of the United States of America*, *105*(22), 7833–7838. https://doi.org/10.1073/PNAS.0802063105

Radford, R. A., Morsch, M., Rayner, S. L., Cole, N. J., Pountney, D. L., & Chung, R. S. (2015). The established and emerging roles of astrocytes and microglia in amyotrophic lateral sclerosis and frontotemporal dementia. In *Frontiers in Cellular Neuroscience* (Vol. 9, Issue OCTOBER). Frontiers Research Foundation. https://doi.org/10.3389/fncel.2015.00414

Rambold, A. S., Cohen, S., & Lippincott-Schwartz, J. (2015). Fatty acid trafficking in starved cells: regulation by lipid droplet lipolysis, autophagy, and mitochondrial fusion dynamics. *Developmental Cell*, *32*(6), 678–692. https://doi.org/10.1016/J.DEVCEL.2015.01.029

Ramesh, N., & Pandey, U. B. (2017). Autophagy Dysregulation in ALS: When Protein Aggregates Get Out of Hand. *Frontiers in Molecular Neuroscience*, *10*. https://doi.org/10.3389/FNMOL.2017.00263

Ramírez-Nuñez, O., Jové, M., Torres, P., Sol, J., Fontdevila, L., Romero-Guevara, R., Andrés-Benito, P., Ayala, V., Rossi, C., Boada, J., Povedano, M., Ferrer, I., Pamplona, R., & Portero-Otin, M. (2021). Nuclear lipidome is altered in amyotrophic lateral sclerosis: A pilot study. *Journal of Neurochemistry*, *158*(2), 482–499. https://doi.org/10.1111/JNC.15373

Rao, M. v., Campbell, J., Palaniappan, A., Kumar, A., & Nixon, R. A. (2016). Calpastatin inhibits motor neuron death and increases survival of hSOD1(G93A) mice. *Journal of Neurochemistry*, *137*(2), 253–265. https://doi.org/10.1111/JNC.13536

Rasola, A., Sciacovelli, M., Chiara, F., Pantic, B., Brusilow, W. S., & Bernardi, P. (2010). Activation of mitochondrial ERK protects cancer cells from death through inhibition of the permeability transition. *Proceedings of the National Academy of Sciences of the United States of America*, *107*(2), 726–731. https://doi.org/10.1073/PNAS.0912742107

Rawat, S., Ghosh, S., Mondal, D., Anusha, V., & Raychaudhuri, S. (2021). Increased supraorganization of respiratory complexes is a dynamic multistep remodelling in response to proteostasis stress. *Journal of Cell Science*, *133*(18). https://doi.org/10.1242/JCS.248492/266609/AM/INCREASED-SUPRA-ORGANIZATION-IS-A-DYNAMIC

Reitzer, L. J., Wice, B. M., & Kennel1, D. (1979). *Evidence That Glutamine, Not Sugar, Is the Major Energy Source for Cultured HeLa Cells** (Vol. 254, Issue 8).

Rémy, C., Fouilhé, N., Barba, I., Sam-Laï, E., Lahrech, H., Cucurella, M.-G., Izquierdo, M., Moreno, A., Ziegler, A., Massarelli, R., Décorps, M., & Arús, C. (1997). Evidence That Mobile Lipids Detected in Rat Brain Glioma by 1H Nuclear Magnetic Resonance Correspond to Lipid Droplets. *Cancer Research*, *57*(3).

Renvoisé, B., Malone, B., Falgairolle, M., Munasinghe, J., Stadler, J., Sibilla, C., Park, S. H., & Blackstone, C. (2016). Reep1 null mice reveal a converging role for hereditary spastic paraplegia proteins in lipid droplet regulation. *Human Molecular Genetics*, *25*(23), 5111–5125. https://doi.org/10.1093/HMG/DDW315

Richards, D., Morren, J. A., & Pioro, E. P. (2020). Time to diagnosis and factors affecting diagnostic delay in amyotrophic lateral sclerosis. *Journal of the Neurological Sciences*, *417*, 117054. https://doi.org/10.1016/J.JNS.2020.117054

Robberecht, W., & Philips, T. (2013). The changing scene of amyotrophic lateral sclerosis. *Nature Reviews. Neuroscience*, *14*(4), 248–264. https://doi.org/10.1038/NRN3430

Robciuc, A., Hyötyläinen, T., Jauhiainen, M., & Holopainen, J. M. (2012). Hyperosmolarity-induced lipid droplet formation depends on ceramide production by neutral sphingomyelinase 2. *Journal of Lipid Research*, *53*(11), 2286. https://doi.org/10.1194/JLR.M026732

Rodenas-Ruano, A., Chávez, A. E., Cossio, M. J., Castillo, P. E., & Zukin, R. S. (2012). REST-dependent epigenetic remodeling promotes the developmental switch in synaptic NMDA receptors. *Nature Neuroscience 2012 15:10*, *15*(10), 1382–1390. https://doi.org/10.1038/nn.3214

Roos, P. M., Vesterberg, O., Syversen, T., Flaten, T. P., & Nordberg, M. (2013). Metal concentrations in cerebrospinal fluid and blood plasma from patients with amyotrophic lateral sclerosis. *Biological Trace Element Research*, *151*(2), 159–170. https://doi.org/10.1007/S12011-012-9547-X

Rossignol, R., Gilkerson, R., Aggeler, R., Yamagata, K., Remington, S. J., & Capaldi, R. A. (2004). Energy substrate modulates mitochondrial structure and oxidative capacity in cancer cells. *Cancer Research*, *64*(3), 985–993. https://doi.org/10.1158/0008-5472.CAN-03-1101

Rothstein, J. D., Martin, L., Levey, A. I., Dykes-Hoberg, M., Jin, L., Wu, D., Nash, N., & Kuncl, R. W. (1994). Localization of neuronal and glial glutamate transporters. *Neuron*, *13*(3), 713–725. https://doi.org/10.1016/0896-6273(94)90038-8

Rotunno, M. S., & Bosco, D. A. (2013). An emerging role for misfolded wild-type SOD1 in sporadic ALS pathogenesis. *Frontiers in Cellular Neuroscience*, *7*(DEC). https://doi.org/10.3389/FNCEL.2013.00253

Rouaux, C., Gonzalez, J.-L., Aguilar, D., & Dupuis, L. (2018). Unmasking the skiptic task of TDP-43. *The EMBO Journal*, *37*(11), e99645. https://doi.org/10.15252/EMBJ.201899645

Rowland, L. P. (2001). How amyotrophic lateral sclerosis got its name: the clinical-pathologic genius of Jean-Martin Charcot. *Archives of Neurology*, *58*(3), 512–515. https://doi.org/10.1001/ARCHNEUR.58.3.512

Roy, J., Galano, J. M., Durand, T., le Guennec, J. Y., & Lee, J. C. Y. (2017). Physiological role of reactive oxygen species as promoters of natural defenses. In *FASEB Journal* (Vol. 31, Issue 9, pp. 3729–3745). FASEB. https://doi.org/10.1096/fj.201700170R

Ruegsegger, C., & Saxena, S. (2016). Proteostasis impairment in ALS. *Brain Research*, *1648*(Pt B), 571–579. https://doi.org/10.1016/J.BRAINRES.2016.03.032

Ryan, B. J., Bengoa-Vergniory, N., Williamson, M., Kirkiz, E., Roberts, R., Corda, G., Sloan, M., Saqlain, S., Cherubini, M., Poppinga, J., Bogtofte, H., Cioroch, M., Hester, S., & Wade-Martins, R. (2021). REST Protects Dopaminergic Neurons from Mitochondrial and α-Synuclein Oligomer Pathology in an Alpha Synuclein Overexpressing BAC-Transgenic Mouse Model. *The Journal of Neuroscience : The Official Journal of the Society for Neuroscience*, *41*(16), 3731–3746. https://doi.org/10.1523/JNEUROSCI.1478-20.2021

Ryu, H. H., Kim, T. H., Kim, J. W., Kang, M., Park, P., Kim, Y. G., Kim, H., Ha, J., Choi, J. E., Lee, J., Lim, C. S., Kim, C. H., Kim, S. J., Silva, A. J., Kaang, B. K., & Lee, Y. S. (2019). Excitatory neuron–specific SHP2-ERK signaling network regulates synaptic plasticity and memory. *Science Signaling*, *12*(571). https://doi.org/10.1126/SCISIGNAL.AAU5755/SUPPL_FILE/AAU5755_TABLE_S4.XLSX

Saad, S., Cereghetti, G., Feng, Y., Picotti, P., Peter, M., & Dechant, R. (2017). Reversible protein aggregation is a protective mechanism to ensure cell cycle restart after stress. *Nature Cell Biology*, *19*(10), 1202–1213. https://doi.org/10.1038/NCB3600

Sábado, J., Casanovas, A., Tarabal, O., Hereu, M., Piedrafita, L., Calderó, J., & Esquerda, J. E. (2014). Accumulation of misfolded SOD1 in dorsal root ganglion degenerating proprioceptive sensory neurons of transgenic mice with amyotrophic lateral sclerosis. *BioMed Research International*, *2014*. https://doi.org/10.1155/2014/852163

Sadigh-Eteghad, S., Majdi, A., McCann, S. K., Mahmoudi, J., Vafaee, M. S., & Macleod, M. R. (2017). D-galactose-induced brain ageing model: A systematic review and meta-analysis on cognitive outcomes and oxidative stress indices. *PLOS ONE*, *12*(8), e0184122. https://doi.org/10.1371/JOURNAL.PONE.0184122

Sahana, T. G., & Zhang, K. (2021). Mitogen-Activated Protein Kinase Pathway in Amyotrophic Lateral Sclerosis. *Biomedicines 2021, Vol. 9, Page 969*, *9*(8), 969. https://doi.org/10.3390/BIOMEDICINES9080969

Saka, H. A., & Valdivia, R. (2012). Emerging roles for lipid droplets in immunity and host-pathogen interactions. *Annual Review of Cell and Developmental Biology*, *28*, 411–437. https://doi.org/10.1146/ANNUREV-CELLBIO-092910-153958

Salim, S. (2017). Oxidative stress and the central nervous system. In *Journal of Pharmacology and Experimental Therapeutics* (Vol. 360, Issue 1, pp. 201–205). American Society for Pharmacology and Experimental Therapy. https://doi.org/10.1124/jpet.116.237503

Sanhueza, M., Chai, A., Smith, C., McCray, B. A., Simpson, T. I., Taylor, J. P., & Pennetta, G. (2015). Network analyses reveal novel aspects of ALS pathogenesis. *PLoS Genetics*, *11*(3). https://doi.org/10.1371/JOURNAL.PGEN.1005107

Sasaki, S. (2011). Autophagy in Spinal Cord Motor Neurons in Sporadic Amyotrophic Lateral Sclerosis. *Journal of Neuropathology & Experimental Neurology*, *70*(5), 349–359. https://doi.org/10.1097/NEN.0B013E3182160690

Sasaki, S., & Iwata, M. (1996). Ultrastructural study of synapses in the anterior horn neurons of patients with amyotrophic lateral sclerosis. *Neuroscience Letters*, *204*(1–2), 53–56. https://doi.org/10.1016/0304-3940(96)12314-4

Schapira, A. H. V., Cooper, J. M., Dexter, D., Clark, J. B., Jenner, P., & Marsden, C. D. (1990). Mitochondrial complex I deficiency in Parkinson's disease. *Journal of Neurochemistry*, *54*(3), 823–827. https://doi.org/10.1111/J.1471-4159.1990.TB02325.X

Schmitt, F., Hussain, G., Dupuis, L., Loeffler, J. P., & Henriques, A. (2014). A plural role for lipids in motor neuron diseases: energy, signaling and structure. *Frontiers in Cellular Neuroscience*, *8*(FEB). https://doi.org/10.3389/FNCEL.2014.00025

Schneider, C. A., Rasband, W. S., & Eliceiri, K. W. (2012). NIH Image to ImageJ: 25 years of image analysis. *Nature Methods 2012 9:7*, *9*(7), 671–675. https://doi.org/10.1038/nmeth.2089

Schoenherr, C. J., & Anderson, D. J. (1995). The Neuron-Restrictive Silencer Factor (NRSF): A Coordinate Repressor of Multiple Neuron-Specific Genes. *Science*, *267*(5202), 1360–1363. https://doi.org/10.1126/SCIENCE.7871435

Schousboe, A., Westergaard, N., Sonnewald, U., Petersen, S. B., Huang, R., Peng, L., & Hertz, L. (1993). Glutamate and Glutamine Metabolism and Compartmentation in Astrocytes. *Developmental Neuroscience*, *15*(3–5), 359–366. https://doi.org/10.1159/000111356

Scotter, E. L., Vance, C., Nishimura, A. L., Lee, Y. B., Chen, H. J., Urwin, H., Sardone, V., Mitchell, J. C., Rogelj, B., Rubinsztein, D. C., & Shaw, C. E. (2014). Differential roles of the ubiquitin proteasome system and autophagy in the clearance of soluble and aggregated TDP-43 species. *Journal of Cell Science*, *127*(Pt 6), 1263–1278. https://doi.org/10.1242/JCS.140087

Sephton, C. F., Good, S. K., Atkin, S., Dewey, C. M., Mayer, P., Herz, J., & Yu, G. (2010). TDP-43 is a developmentally regulated protein essential for early embryonic development. *Journal of Biological Chemistry*, *285*(9), 6826–6834. https://doi.org/10.1074/jbc.M109.061846

Shahmoradian, S. H., Lewis, A. J., Genoud, C., Hench, J., Moors, T. E., Navarro, P. P., Castaño-Díez, D., Schweighauser, G., Graff-Meyer, A., Goldie, K. N., Sütterlin, R., Huisman, E., Ingrassia, A., Gier, Y. de, Rozemuller, A. J. M., Wang, J., Paepe, A. de, Erny, J., Staempfli, A., … Lauer, M. E. (2019). Lewy pathology in Parkinson's disease consists of crowded organelles and lipid membranes. *Nature Neuroscience 2019 22:7*, *22*(7), 1099–1109. https://doi.org/10.1038/s41593-019-0423-2

Shan, X., Chiang, P. M., Price, D. L., & Wong, P. C. (2010). Altered distributions of Gemini of coiled bodies and mitochondria in motor neurons of TDP-43 transgenic mice. *Proceedings of the National Academy of Sciences of the United States of America*, *107*(37), 16325–16330. https://doi.org/10.1073/PNAS.1003459107/-/DCSUPPLEMENTAL

Sharifi, S., Barar, J., Hejazi, M. S., & Samadi, N. (2015). Doxorubicin Changes Bax /Bcl-xL Ratio, Caspase-8 and 9 in Breast Cancer Cells. *Advanced Pharmaceutical Bulletin*, *5*(3), 351. https://doi.org/10.15171/APB.2015.049

Shelkovnikova, T. A., Kukharsky, M. S., An, H., Dimasi, P., Alexeeva, S., Shabir, O., Heath, P. R., & Buchman, V. L. (2018). Protective paraspeckle hyper-assembly downstream of TDP-43 loss of function in amyotrophic lateral sclerosis. *Molecular Neurodegeneration*, *13*(1). https://doi.org/10.1186/s13024-018-0263-7

Shen, J., Chen, X., Hendershot, L., & Prywes, R. (2002). ER Stress Regulation of ATF6 Localization by Dissociation of BiP/GRP78 Binding and Unmasking of Golgi Localization Signals. *Developmental Cell*, *3*(1), 99–111. https://doi.org/10.1016/S1534-5807(02)00203-4

Shi, Y., Lin, S., Staats, K. A., Li, Y., Chang, W. H., Hung, S. T., Hendricks, E., Linares, G. R., Wang, Y., Son, E. Y., Wen, X., Kisler, K., Wilkinson, B., Menendez, L., Sugawara, T., Woolwine, P., Huang, M., Cowan, M. J., Ge, B., … Ichida, J. K. (2018). Haploinsufficiency leads to neurodegeneration in C9ORF72 ALS/FTD human induced motor neurons. *Nature Medicine 2018 24:3*, *24*(3), 313–325. https://doi.org/10.1038/nm.4490

Shimabukuro, M. K., Langhi, L. G. P., Cordeiro, I., Brito, J. M., Batista, C. M. D. C., Mattson, M. P., & de Mello Coelho, V. (2016). Lipid-laden cells differentially distributed in the aging brain are functionally active and correspond to distinct phenotypes. *Scientific Reports 2016 6:1*, *6*(1), 1–12. https://doi.org/10.1038/srep23795

Sies, H., & Cadenas, E. (1985). Oxidative stress: damage to intact cells and organs. *Philosophical Transactions of the Royal Society of London. B, Biological Sciences*, *311*(1152), 617–631. https://doi.org/10.1098/RSTB.1985.0168

Silingardi, D., Angelucci, A., de Pasquale, R., Borsotti, M., Squitieri, G., Brambilla, R., Putignano, E., Pizzorusso, T., & Berardi, N. (2011). ERK pathway activation bidirectionally affects visual recognition memory and synaptic plasticity in the perirhinal cortex. *Frontiers in Behavioral Neuroscience*, *0*(DECEMBER), 84. https://doi.org/10.3389/FNBEH.2011.00084/BIBTEX

Simpson, E. P., Henry, Y. K., Henkel, J. S., Smith, R. G., & Appel, S. H. (2004). Increased lipid peroxidation in sera of ALS patients: a potential biomarker of disease burden. *Neurology*, *62*(10), 1758–1765. https://doi.org/10.1212/WNL.62.10.1758

Singh, T., Jiao, Y., Ferrando, L. M., Yablonska, S., Li, F., Horoszko, E. C., Lacomis, D., Friedlander, R. M., & Carlisle, D. L. (2021a). Neuronal mitochondrial dysfunction in sporadic amyotrophic lateral sclerosis is developmentally regulated. *Scientific Reports 2021 11:1*, *11*(1), 1–16. https://doi.org/10.1038/s41598-021-97928-7

Singh, T., Jiao, Y., Ferrando, L. M., Yablonska, S., Li, F., Horoszko, E. C., Lacomis, D., Friedlander, R. M., & Carlisle, D. L. (2021b). Neuronal mitochondrial dysfunction in sporadic amyotrophic lateral sclerosis is developmentally regulated. *Scientific Reports 2021 11:1*, *11*(1), 1–16. https://doi.org/10.1038/s41598-021-97928-7

Sladowska, M., Turek, M., Kim, M. J., Drabikowski, K., Mussulini, B. H. M., Mohanraj, K., Serwa, R. A., Topf, U., & Chacinska, A. (2021). Proteasome activity contributes to pro-survival response upon mild mitochondrial stress in Caenorhabditis elegans. *PLoS Biology*, *19*(7). https://doi.org/10.1371/JOURNAL.PBIO.3001302

Smeyers, J., Banchi, E. G., & Latouche, M. (2021). C9ORF72: What It Is, What It Does, and Why It Matters. In *Frontiers in Cellular Neuroscience* (Vol. 15). Frontiers Media S.A. https://doi.org/10.3389/fncel.2021.661447

Smith, R. G., Henry, Y. K., Mattson, M. P., & Appel, S. H. (1998). Presence of 4-hydroxynonenal in cerebrospinal fluid of patients with sporadic amyotrophic lateral sclerosis. *Annals of Neurology*, *44*(4), 696–699. https://doi.org/10.1002/ANA.410440419

Smolič, T., Tavčar, P., Horvat, A., Černe, U., Halužan Vasle, A., Tratnjek, L., Kreft, M. E., Scholz, N., Matis, M., Petan, T., Zorec, R., & Vardjan, N. (2021). Astrocytes in stress accumulate lipid droplets. *Glia*, *69*(6), 1540. https://doi.org/10.1002/GLIA.23978

Snowden, J. S., Adams, J., Harris, J., Thompson, J. C., Rollinson, S., Richardson, A., Jones, M., Neary, D., Mann, D. M., & Pickering-Brown, S. (2015). Distinct clinical and pathological phenotypes in frontotemporal dementia associated with MAPT, PGRN and C9orf72 mutations. *Amyotrophic Lateral Sclerosis & Frontotemporal Degeneration*, *16*(7–8), 497–505. https://doi.org/10.3109/21678421.2015.1074700

Sola, A., Rogido, M. R., & Deulofeut, R. (2007). Oxygen as a neonatal health hazard: Call for détente in clinical practice. In *Acta Paediatrica, International Journal of Paediatrics* (Vol. 96, Issue 6, pp. 801–812). https://doi.org/10.1111/j.1651-2227.2007.00287.x

Song, W. (2012). Defective Dynamics Of Mitochondria In Amyotrophic Lateral Sclerosis And Huntington's Disease. *Electronic Theses and Dissertations*. https://stars.library.ucf.edu/etd/2370

Song, W., Song, Y., Kincaid, B., Bossy, B., & Bossy-Wetzel, E. (2013). Mutant SOD1G93A triggers mitochondrial fragmentation in spinal cord motor neurons: neuroprotection by SIRT3 and PGC-1α. *Neurobiology of Disease*, *51*, 72–81. https://doi.org/10.1016/J.NBD.2012.07.004

Spires-Jones, T. L., Attems, J., & Thal, D. R. (2017). Interactions of pathological proteins in neurodegenerative diseases. *Acta Neuropathologica*, *134*(2), 187. https://doi.org/10.1007/S00401-017-1709-7

Spitz, D. R., Sim, J. E., Ridnour, L. A., Galoforo, S. S., & Lee, Y. J. (2000). Glucose deprivation-induced oxidative stress in human tumor cells. A fundamental defect in metabolism? *Annals of the New York Academy of Sciences*, *899*, 349–362. https://doi.org/10.1111/J.1749-6632.2000.TB06199.X

Stab, B. R., Martinez, L., Grismaldo, A., Lerma, A., Gutiérrez, M. L., Barrera, L. A., Sutachan, J. J., & Albarracín, S. L. (2016). Mitochondrial functional changes characterization in young and senescent human adipose derived MSCs. *Frontiers in Aging Neuroscience*, *8*(DEC), 299. https://doi.org/10.3389/FNAGI.2016.00299/BIBTEX

Stallings, N. R., Puttaparthi, K., Dowling, K. J., Luther, C. M., Burns, D. K., Davis, K., & Elliott, J. L. (2013). TDP-43, an ALS linked protein, regulates fat deposition and glucose homeostasis. *PloS One*, *8*(8). https://doi.org/10.1371/JOURNAL.PONE.0071793

Stieber, A., Gonatas, J. O., Moore, J. S., Bantly, A., Yim, H. S., Yim, M. B., & Gonatas, N. K. (2004). Disruption of the structure of the Golgi apparatus and the function of the secretory pathway by mutants G93A and G85R of Cu, Zn superoxide dismutase (SOD1) of familial amyotrophic lateral sclerosis. *Journal of the Neurological Sciences*, *219*(1–2), 45–53. https://doi.org/10.1016/J.JNS.2003.12.004

Straub, I. R., Janer, A., Weraarpachai, W., Zinman, L., Robertson, J., Rogaeva, E., & Shoubridge, E. A. (2018). Loss of CHCHD10-CHCHD2 complexes required for respiration underlies the pathogenicity of a CHCHD10 mutation in ALS. *Human Molecular Genetics*, *27*(1), 178–189. https://doi.org/10.1093/HMG/DDX393

Sturtz, L. A., Diekert, K., Jensen, L. T., Lill, R., & Culotta, V. C. (2001). A fraction of yeast Cu,Zn-superoxide dismutase and its metallochaperone, CCS, localize to the intermembrane space of mitochondria. A physiological role for SOD1 in guarding against mitochondrial oxidative damage. *The Journal of Biological Chemistry*, *276*(41), 38084–38089. https://doi.org/10.1074/JBC.M105296200

Sulkshane, P., Ram, J., & Glickman, M. H. (2020). *Ubiquitination of Intramitochondrial Proteins: Implications for Metabolic Adaptability*. https://doi.org/10.20944/PREPRINTS202010.0512.V1

Sundaramoorthy, V., Walker, A. K., Tan, V., Fifita, J. A., McCann, E. P., Williams, K. L., Blair, I. P., Guillemin, G. J., Farg, M. A., & Atkin, J. D. (2015). Defects in optineurin- and myosin VI-mediated cellular trafficking in amyotrophic lateral sclerosis. *Human Molecular Genetics*, *24*(13), 3830–3846. https://doi.org/10.1093/HMG/DDV126

Svetoni, F., Frisone, P., & Paronetto, M. P. (2016). Role of FET proteins in neurodegenerative disorders. *Http://Dx.Doi.Org/10.1080/15476286.2016.1211225*, *13*(11), 1089–1102. https://doi.org/10.1080/15476286.2016.1211225

Sztalryd, C., & Brasaemle, D. L. (2017). The perilipin family of lipid droplet proteins: Gatekeepers of intracellular lipolysis. *Biochimica et Biophysica Acta. Molecular and Cell Biology of Lipids*, *1862*(10 Pt B), 1221–1232. https://doi.org/10.1016/J.BBALIP.2017.07.009

Tabas, I., & Ron, D. (2011). Integrating the mechanisms of apoptosis induced by endoplasmic reticulum stress. *Nature Cell Biology*, *13*(3), 184–190. https://doi.org/10.1038/NCB0311-184

Takalo, M., Salminen, A., Soininen, H., Hiltunen, M., & Haapasalo, A. (2013). Protein aggregation and degradation mechanisms in neurodegenerative diseases. In *Am J Neurodegener Dis* (Vol. 2, Issue 1). www.AJND.us/

Tan, W., Pasinelli, P., & Trotti, D. (2014). Role of mitochondria in mutant SOD1 linked amyotrophic lateral sclerosis. *Biochimica et Biophysica Acta*, *1842*(8), 1295. https://doi.org/10.1016/J.BBADIS.2014.02.009

Tang, F., Lane, S., Korsak, A., Paton, J. F. R., Gourine, A. v., Kasparov, S., & Teschemacher, A. G. (2014). Lactate-mediated glia-neuronal signalling in the mammalian brain. *Nature Communications*, *5*. https://doi.org/10.1038/NCOMMS4284

Taylor, J. P., Brown, R. H., & Cleveland, D. W. (2016). Decoding ALS: from genes to mechanism. *Nature 2016 539:7628*, *539*(7628), 197–206. https://doi.org/10.1038/nature20413

Tefera, T. W., Steyn, F. J., Ngo, S. T., & Borges, K. (2021). CNS glucose metabolism in Amyotrophic Lateral Sclerosis: a therapeutic target? *Cell & Bioscience*, *11*(1), 14. https://doi.org/10.1186/S13578-020-00511-2

Teuling, E., Ahmed, S., Haasdijk, E., Demmers, J., Steinmetz, M. O., Akhmanova, A., Jaarsma, D., & Hoogenraad, C. C. (2007). Motor neuron disease-associated mutant vesicle-associated membrane protein-associated protein (VAP) B recruits wild-type VAPs into endoplasmic reticulum-derived tubular aggregates. *The Journal of Neuroscience : The Official Journal of the Society for Neuroscience*, *27*(36), 9801–9815. https://doi.org/10.1523/JNEUROSCI.2661-07.2007

Thiel, G., Ekici, M., & Rössler, O. G. (2015). RE-1 silencing transcription factor (REST): A regulator of neuronal development and neuronal/endocrine function. *Cell and Tissue Research*, *359*(1), 99–109. https://doi.org/10.1007/S00441-014-1963-0/TABLES/1

Tomer, D., Chippalkatti, R., Mitra, K., & Rikhy, R. (2018). ERK regulates mitochondrial membrane potential in fission deficient Drosophila follicle cells during differentiation. *Developmental Biology*, *434*(1), 48–62. https://doi.org/10.1016/J.YDBIO.2017.11.009

Tong, J., Huang, C., Bi, F., Wu, Q., Huang, B., & Zhou, H. (2012). XBP1 depletion precedes ubiquitin aggregation and Golgi fragmentation in TDP-43 transgenic rats. *Journal of Neurochemistry*, *123*(3), 406–416. https://doi.org/10.1111/JNC.12014

Torres, P., Cacabelos, D., Pairada, J., Bauer, K. C., Boada, J., Fontdevila, L., Rossi, C., Povedano, M., Ferrer, I., Pamplona, R., Finlay, B. B., Portero-Otín, M., & Ayala, V. (2020). Gender-Specific Beneficial Effects of Docosahexaenoic Acid Dietary Supplementation in G93A-SOD1 Amyotrophic Lateral Sclerosis Mice. *Neurotherapeutics : The Journal of the American Society for Experimental NeuroTherapeutics*, *17*(1), 269–281. https://doi.org/10.1007/S13311-019-00808-2

Torres, P., Ramírez-Núñez, O., Romero-Guevara, R., Barés, G., Granado-Serrano, A. B., Ayala, V., Boada, J., Fontdevila, L., Povedano, M., Sanchís, D., Pamplona, R., Ferrer, I., & Portero-Otín, M. (2018). Cryptic exon splicing function of TARDBP interacts with autophagy in nervous tissue. *Autophagy*, *14*(8), 1398–1403. https://doi.org/10.1080/15548627.2018.1474311

Toth, K., & Wold, W. S. M. (2002). HEK? No! *MOLECULAR THERAPY*, *5*(6). https://doi.org/10.1006/mthe.2002.0618

Tremblay, R. G., Sikorska, M., Sandhu, J. K., Lanthier, P., Ribecco-Lutkiewicz, M., & Bani-Yaghoub, M. (2010). Differentiation of mouse Neuro 2A cells into dopamine neurons. *Journal of Neuroscience Methods*, *186*(1), 60–67. https://doi.org/10.1016/J.JNEUMETH.2009.11.004

Tresse, E., Salomons, F. A., Vesa, J., Bott, L. C., Kimonis, V., Yao, T. P., Dantuma, N. P., & Taylor, J. P. (2010). VCP/p97 is essential for maturation of ubiquitin-containing autophagosomes and this function is impaired by mutations that cause IBMPFD. *Https://Doi.Org/10.4161/Auto.6.2.11014*, *6*(2), 217–227. https://doi.org/10.4161/AUTO.6.2.11014

Tsacopoulos, M., & Magistretti, P. J. (1996). Metabolic coupling between glia and neurons. *The Journal of Neuroscience : The Official Journal of the Society for Neuroscience*, *16*(3), 877–885. https://doi.org/10.1523/JNEUROSCI.16-03-00877.1996

Tsang, C. K. wan, Liu, Y., Thomas, J., Zhang, Y., & Zheng, X. F. S. (2014). Superoxide dismutase 1 acts as a nuclear transcription factor to regulate oxidative stress resistance. *Nature Communications 2014 5:1*, *5*(1), 1–11. https://doi.org/10.1038/ncomms4446

Turner, B., & Atkin, J. (2006). ER Stress and UPR in Familial Amyotrophic Lateral Sclerosis. *Current Molecular Medicine*, *6*(1), 79–86. https://doi.org/10.2174/156652406775574550

Urwin, H., Authier, A., Nielsen, J. E., Metcalf, D., Powell, C., Froud, K., Malcolm, D. S., Holm, I., Johannsen, P., Brown, J., Fisher, E. M. C., van der Zee, J., Bruyland, M., van Broeckhoven, C., Collinge, J., Brandner, S., Futter, C., & Isaacs, A. M. (2010). Disruption of endocytic trafficking in frontotemporal dementia with CHMP2B mutations. *Human Molecular Genetics*, *19*(11), 2228–2238. https://doi.org/10.1093/HMG/DDQ100

Valente, A. J., Maddalena, L. A., Robb, E. L., Moradi, F., & Stuart, J. A. (2017). A simple ImageJ macro tool for analyzing mitochondrial network morphology in mammalian cell culture. *Acta Histochemica*, *119*(3), 315–326. https://doi.org/10.1016/J.ACTHIS.2017.03.001

Valera-Alberni, M., & Canto, C. (2018). Mitochondrial stress management: a dynamic journey. *Cell Stress*, *2*(10), 253. https://doi.org/10.15698/CST2018.10.158

van Acker, Z. P., Declerck, K., Luyckx, E., vanden Berghe, W., & Dewilde, S. (2019). Non-Methylation-Linked Mechanism of REST-Induced Neuroglobin Expression Impacts Mitochondrial Phenotypes in a Mouse Model of Amyotrophic Lateral Sclerosis. *Neuroscience*, *412*, 233–247. https://doi.org/10.1016/J.NEUROSCIENCE.2019.05.039

van den Bosch, L., van Damme, P., Bogaert, E., & Robberecht, W. (2006). The role of excitotoxicity in the pathogenesis of amyotrophic lateral sclerosis. *Biochimica et Biophysica Acta (BBA) - Molecular Basis of Disease*, *1762*(11–12), 1068–1082. https://doi.org/10.1016/J.BBADIS.2006.05.002

van Dis, V., Kuijpers, M., Haasdijk, E. D., Teuling, E., Oakes, S. A., Hoogenraad, C. C., & Jaarsma, D. (2014). Golgi fragmentation precedes neuromuscular denervation and is associated with endosome abnormalities in SOD1-ALS mouse motor neurons. *Acta Neuropathologica Communications*, *2*(1). https://doi.org/10.1186/2051-5960-2-38

vande Velde, C., McDonald, K. K., Boukhedimi, Y., McAlonis-Downes, M., Lobsiger, C. S., Hadj, S. B., Zandona, A., Julien, J. P., Shah, S. B., & Cleveland, D. W. (2011). Misfolded SOD1 associated with motor neuron mitochondria alters mitochondrial shape and distribution prior to clinical onset. *PloS One*, *6*(7). https://doi.org/10.1371/JOURNAL.PONE.0022031

Vardjan, N., Chowdhury, H. H., Horvat, A., Velebit, J., Malnar, M., Muhič, M., Kreft, M., Krivec, Š. G., Bobnar, S. T., Miš, K., Pirkmajer, S., Offermanns, S., Henriksen, G., Storm-Mathisen, J., Bergersen, L. H., & Zorec, R. (2018). Enhancement of Astroglial Aerobic Glycolysis by Extracellular Lactate-Mediated Increase in cAMP. *Frontiers in Molecular Neuroscience*, *11*. https://doi.org/10.3389/FNMOL.2018.00148

Vargas, M. R., & Johnson, J. A. (n.d.). *Astrogliosis in Amyotrophic Lateral Sclerosis: Role and Therapeutic Potential of Astrocytes*.

Veglianese, P., lo Coco, D., Bao Cutrona, M., Magnoni, R., Pennacchini, D., Pozzi, B., Gowing, G., Julien, J. P., Tortarolo, M., & Bendotti, C. (2006). Activation of the p38MAPK cascade is associated with upregulation of TNF alpha receptors in the spinal motor neurons of mouse models of familial ALS. *Molecular and Cellular Neurosciences*, *31*(2), 218–231. https://doi.org/10.1016/J.MCN.2005.09.009

Velebit, J., Horvat, A., Smolič, T., Prpar Mihevc, S., Rogelj, B., Zorec, R., & Vardjan, N. (2020). Astrocytes with TDP-43 inclusions exhibit reduced noradrenergic cAMP and Ca 2+ signaling and dysregulated cell metabolism. *Scientific Reports*, *10*(1). https://doi.org/10.1038/S41598-020-62864-5

Venturini, V., Pezzano, F., Castro, F. C., Häkkinen, H. M., Jiménez-Delgado, S., Colomer-Rosell, M., Marro, M., Tolosa-Ramon, Q., Paz-López, S., Valverde, M. A., Weghuber, J., Loza-Alvarez, P., Krieg, M., Wieser, S., & Ruprecht, V. (2020). The nucleus measures shape changes for cellular proprioception to control dynamic cell behavior. *Science (New York, N.Y.)*, *370*(6514). https://doi.org/10.1126/SCIENCE.ABA2644

Verber, N. S., Shepheard, S. R., Sassani, M., McDonough, H. E., Moore, S. A., Alix, J. J. P., Wilkinson, I. D., Jenkins, T. M., & Shaw, P. J. (2019). Biomarkers in Motor Neuron Disease: A State of the Art Review. *Frontiers in Neurology*, *10*(APR). https://doi.org/10.3389/FNEUR.2019.00291

Vidal, R. L., Matus, S., Bargsted, L., & Hetz, C. (2014). Targeting autophagy in neurodegenerative diseases. *Trends in Pharmacological Sciences*, *35*(11), 583–591. https://doi.org/10.1016/J.TIPS.2014.09.002

Vijayvergiya, C., Beal, M. F., Buck, J., & Manfredi, G. (2005). Mutant Superoxide Dismutase 1 Forms Aggregates in the Brain Mitochondrial Matrix of Amyotrophic Lateral Sclerosis Mice. *Journal of Neuroscience*, *25*(10), 2463–2470. https://doi.org/10.1523/JNEUROSCI.4385-04.2005

Visser, A. E., Rooney, J. P. K., D'ovidio, F., Westeneng, H. J., Vermeulen, R. C. H., Beghi, E., Chiò, A., Logroscino, G., Bru-No, A., Fanti, C., Fascendini, S., Tomasoni, A., Arnaboldi, M., Valsecchi, M., Moleri, M., Poloni, M., Alimonti, D., Tagliavini, F., Redaelli, V., … Riva, N. (2018). Multicentre, cross-cultural, population-based, case–control study of physical activity as risk factor for amyotrophic lateral sclerosis. *Journal of Neurology, Neurosurgery & Psychiatry*, *89*(8), 797–803. https://doi.org/10.1136/JNNP-2017-317724

Vlassenko, A. G., Gordon, B. A., Goyal, M. S., Su, Y., Blazey, T. M., Durbin, T. J., Couture, L. E., Christensen, J. J., Jafri, H., Morris, J. C., Raichle, M. E., & Benzinger, T. L. S. (2018). Aerobic glycolysis and tau deposition in preclinical Alzheimer's disease. *Neurobiology of Aging*, *67*, 95–98. https://doi.org/10.1016/J.NEUROBIOLAGING.2018.03.014

Walker, A. K., Soo, K. Y., Sundaramoorthy, V., Parakh, S., Ma, Y., Farg, M. A., Wallace, R. H., Crouch, P. J., Turner, B. J., Horne, M. K., & Atkin, J. D. (2013). ALS-associated TDP-43 induces endoplasmic reticulum stress, which drives cytoplasmic TDP-43 accumulation and stress granule formation. *PloS One*, *8*(11). https://doi.org/10.1371/JOURNAL.PONE.0081170

Walter, P., & Ron, D. (2011). The unfolded protein response: from stress pathway to homeostatic regulation. *Science (New York, N.Y.)*, *334*(6059), 1081–1086. https://doi.org/10.1126/SCIENCE.1209038

Walther, T. C., Chung, J., & Farese, R. v. (2017). Lipid droplet biogenesis. *Annual Review of Cell and Developmental Biology*, *33*, 491–510. https://doi.org/10.1146/ANNUREV-CELLBIO-100616-060608

Walther, T. C., & Farese, R. v. (2012a). Lipid Droplets and Cellular Lipid Metabolism. *Http://Dx.Doi.Org/10.1146/Annurev-Biochem-061009-102430*, *81*, 687–714. https://doi.org/10.1146/ANNUREV-BIOCHEM-061009-102430

Walther, T. C., & Farese, R. v. (2012b). Lipid Droplets and Cellular Lipid Metabolism. *Http://Dx.Doi.Org/10.1146/Annurev-Biochem-061009-102430*, *81*, 687–714. https://doi.org/10.1146/ANNUREV-BIOCHEM-061009-102430

Wang, H., O'Reilly, É. J., Weisskopf, M. G., Logroscino, G., McCullough, M. L., Thun, M. J., Schatzkin, A., Kolonel, L. N., & Ascherio, A. (2011). Smoking and risk of amyotrophic lateral sclerosis: a pooled analysis of five prospective cohorts. *Archives of Neurology*, *68*(2), 207. https://doi.org/10.1001/ARCHNEUROL.2010.367

Wang, H., Wang, R., Xu, S., & Lakshmana, M. K. (2016). *Transcription Factor EB Is Selectively Reduced in the Nuclear Fractions of Alzheimer's and Amyotrophic Lateral Sclerosis Brains*. https://doi.org/10.1155/2016/4732837

Wang, P., Deng, J., Dong, J., Liu, J., Bigio, E. H., Mesulam, M., Wang, T., Sun, L., Wang, L., Lee, A. Y. L., McGee, W. A., Chen, X., Fushimi, K., Zhu, L., & Wu, J. Y. (2019). TDP-43 induces mitochondrial damage and activates the mitochondrial unfolded protein response. *PLOS Genetics*, *15*(5), e1007947. https://doi.org/10.1371/JOURNAL.PGEN.1007947

Ward, M. E., Chen, R., Huang, H. Y., Ludwig, C., Telpoukhovskaia, M., Taubes, A., Boudin, H., Minami, S. S., Reichert, M., Albrecht, P., Gelfand, J. M., Cruz-Herranz, A., Cordano, C., Alavi, M. v., Leslie, S., Seeley, W. W., Miller, B. L., Bigio, E., Mesulam, M. M., … Green, A. J. (2017). Individuals with progranulin haploinsufficiency exhibit features of neuronal ceroid lipofuscinosis. *Science Translational Medicine*, *9*(385). https://doi.org/10.1126/SCITRANSLMED.AAH5642/SUPPL_FILE/AAH5642_TABLE_S3.ZIP

Watkins, J. A., Alix, J. J. P., Shaw, P. J., & Mead, R. J. (2021). Extensive phenotypic characterisation of a human TDP-43Q331K transgenic mouse model of amyotrophic lateral sclerosis (ALS). *Scientific Reports*, *11*(1). https://doi.org/10.1038/s41598-021-96122-z

Wei, Z., & Liu, H. T. (2002). MAPK signal pathways in the regulation of cell proliferation in mammalian cells. *Cell Research*, *12*(1), 9–18. https://doi.org/10.1038/SJ.CR.7290105

Weidberg, H., & Amon, A. (n.d.). *MitoCPR-A surveillance pathway that protects mitochondria in response to protein import stress*. https://doi.org/10.1126/science.aan4146

Weids, A. J., Ibstedt, S., Tamás, M. J., & Grant, C. M. (2016). Distinct stress conditions result in aggregation of proteins with similar properties. *Scientific Reports*, *6*. https://doi.org/10.1038/SREP24554

Weiduschat, N., Mao, X., Hupf, J., Armstrong, N., Kang, G., Lange, D. J., Mitsumoto, H., & Shungu, D. C. (2014). Motor cortex glutathione deficit in ALS measured in vivo with the J-editing technique. *Neuroscience Letters*, *570*, 102–107. https://doi.org/10.1016/j.neulet.2014.04.020

Welte, M. A. (2015). Expanding roles for lipid droplets. *Current Biology : CB*, *25*(11), R470–R481. https://doi.org/10.1016/J.CUB.2015.04.004

White, M. A., Kim, E., Duffy, A., Adalbert, R., Phillips, B. U., Peters, O. M., Stephenson, J., Yang, S., Massenzio, F., Lin, Z., Andrews, S., Segonds-Pichon, A., Metterville, J., Saksida, L. M., Mead, R., Ribchester, R. R., Barhomi, Y., Serre, T., Coleman, M. P., … Sreedharan, J. (2018). TDP-43 gains function due to perturbed autoregulation in a Tardbp knock-in mouse model of ALS-FTD. *Nature Neuroscience*, *21*(4), 552–563. https://doi.org/10.1038/s41593-018-0113-5

Wiedemann, F. R., Manfredi, G., Mawrin, C., Flint Beal, M., & Schon, E. A. (2002). Mitochondrial DNA and respiratory chain function in spinal cords of ALS patients. *Journal of Neurochemistry*, *80*(4), 616–625. https://doi.org/10.1046/J.0022-3042.2001.00731.X

Wiedemann, F. R., Winkler, K., Kuznetsov, A. v., Bartels, C., Vielhaber, S., Feistner, H., & Kunz, W. S. (1998). Impairment of mitochondrial function in skeletal muscle of patients with amyotrophic lateral sclerosis. *Journal of the Neurological Sciences*, *156*(1), 65–72. https://doi.org/10.1016/S0022-510X(98)00008-2

Wijesekera, L. C., & Leigh, P. N. (2009). Amyotrophic lateral sclerosis. *Orphanet Journal of Rare Diseases*, *4*(1), 3. https://doi.org/10.1186/1750-1172-4-3

Wilfling, F., Wang, H., Haas, J., Krahmer, N., cell, T. G.-D., & 2013, undefined. (n.d.). Triacylglycerol synthesis enzymes mediate lipid droplet growth by relocalizing from the ER to lipid droplets. *Elsevier*. Retrieved January 9, 2022, from https://www.sciencedirect.com/science/article/pii/S1534580713000415

Williams, K. L., Topp, S., Yang, S., Smith, B., Fifita, J. A., Warraich, S. T., Zhang, K. Y., Farrawell, N., Vance, C., Hu, X., Chesi, A., Leblond, C. S., Lee, A., Rayner, S. L., Sundaramoorthy, V., Dobson-Stone, C., Molloy, M. P., van Blitterswijk, M., Dickson, D. W., … Blair, I. P. (2016). CCNF mutations in amyotrophic lateral sclerosis and frontotemporal dementia. *Nature Communications*, *7*. https://doi.org/10.1038/NCOMMS11253

Win, S., Than, T. A., & Kaplowitz, N. (2018). The Regulation of JNK Signaling Pathways in Cell Death through the Interplay with Mitochondrial SAB and Upstream Post-Translational Effects. *International Journal of Molecular Sciences 2018, Vol. 19, Page 3657*, *19*(11), 3657. https://doi.org/10.3390/IJMS19113657

Woehlbier, U., Colombo, A., Saaranen, M. J., Pérez, V., Ojeda, J., Bustos, F. J., Andreu, C. I., Torres, M., Valenzuela, V., Medinas, D. B., Rozas, P., Vidal, R. L., Lopez-Gonzalez, R., Salameh, J., Fernandez-Collemann, S., Muñoz, N., Matus, S., Armisen, R., Sagredo, A., … Hetz, C. (2016). ALS-linked protein disulfide isomerase variants cause motor dysfunction. *The EMBO Journal*, *35*(8), 845. https://doi.org/10.15252/EMBJ.201592224

Wong, P. C., Pardo, C. A., Borchelt, D. R., Lee, M. K., Copeland, N. G., Jenkins, N. A., Sisodia, S. S., Cleveland, D. W., & Price, D. L. (1995). An adverse property of a familial ALS-linked SOD1 mutation causes motor neuron disease characterized by vacuolar degeneration of mitochondria. *Neuron*, *14*(6), 1105–1116. https://doi.org/10.1016/0896-6273(95)90259-7

Woods, L. C., Berbusse, G. W., & Naylor, K. (2016). Microtubules Are Essential for Mitochondrial Dynamics-Fission, Fusion, and Motility-in Dictyostelium discoideum. *Frontiers in Cell and Developmental Biology*, *4*(MAR). https://doi.org/10.3389/FCELL.2016.00019

Wrobel, L., Topf, U., Bragoszewski, P., Wiese, S., Sztolsztener, M. E., Oeljeklaus, S., Varabyova, A., Lirski, M., Chroscicki, P., Mroczek, S., Januszewicz, E., Dziembowski, A., Koblowska, M., Warscheid, B., & Chacinska, A. (2015). Mistargeted mitochondrial proteins activate a proteostatic response in the cytosol. *Nature*, *524*(7566), 485–488. https://doi.org/10.1038/NATURE14951

Wu, C., Watts, M. E., & Rubin, L. L. (2019). MAP4K4 Activation Mediates Motor Neuron Degeneration in Amyotrophic Lateral Sclerosis. *Cell Reports*, *26*(5), 1143-1156.e5. https://doi.org/10.1016/J.CELREP.2019.01.019

Wu, L., Xu, D., Zhou, L., Xie, B., Yu, L., Yang, H., Huang, L., Ye, J., Deng, H., Yuan, Y. A., Chen, S., & Li, P. (2014). Rab8a-AS160-MSS4 regulatory circuit controls lipid droplet fusion and growth. *Developmental Cell*, *30*(4), 378–393. https://doi.org/10.1016/J.DEVCEL.2014.07.005

Wu, R. F., Xu, Y. C., Ma, Z., Nwariaku, F. E., Sarosi, G. A., & Terada, L. S. (2005). Subcellular targeting of oxidants during endothelial cell migration. *The Journal of Cell Biology*, *171*(5), 893–904. https://doi.org/10.1083/JCB.200507004

Wu, W., Li, W., Chen, H., Jiang, L., Zhu, R., & Feng, D. (2016). FUNDC1 is a novel mitochondrial-associated-membrane (MAM) protein required for hypoxia-induced mitochondrial fission and mitophagy. *Autophagy*, *12*(9), 1675–1676. https://doi.org/10.1080/15548627.2016.1193656

Xu, J., Qin, X., Cai, X., Yang, L., Xing, Y., Li, J., Zhang, L., Tang, Y., Liu, J., Zhang, X., & Gao, F. (2015). Mitochondrial JNK activation triggers autophagy and apoptosis and aggravates myocardial injury following ischemia/reperfusion. *Biochimica et Biophysica Acta (BBA) - Molecular Basis of Disease*, *1852*(2), 262–270. https://doi.org/10.1016/J.BBADIS.2014.05.012

Xu, Y. F., Gendron, T. F., Zhang, Y. J., Lin, W. L., D'Alton, S., Sheng, H., Casey, M. C., Tong, J., Knight, J., Yu, X., Rademakers, R., Boylan, K., Hutton, M., McGowan, E., Dickson, D. W., Lewis, J., & Petrucelli, L. (2010). Wild-Type Human TDP-43 Expression Causes TDP-43 Phosphorylation, Mitochondrial Aggregation, Motor Deficits, and Early Mortality in Transgenic Mice. *The Journal of Neuroscience*, *30*(32), 10851. https://doi.org/10.1523/JNEUROSCI.1630-10.2010

Yagi, T., Ito, D., Nihei, Y., Ishihara, T., & Suzuki, N. (2011). N88S seipin mutant transgenic mice develop features of seipinopathy/BSCL2-related motor neuron disease via endoplasmic reticulum stress. *Human Molecular Genetics*, *20*(19), 3831–3840. https://doi.org/10.1093/HMG/DDR304

Yanar, K., Aydin, S., Çakatay, U., Mengi, M., Buyukpinarbaşili, N., Atukeren, P., Sitar, M. E., Sönmez, A., & Uslu, E. (2011). Protein and DNA oxidation in different anatomic regions of rat brain in a mimetic ageing model. *Basic & Clinical Pharmacology & Toxicology*, *109*(6), 423–433. https://doi.org/10.1111/J.1742-7843.2011.00756.X

Yang, L., Liang, J., Lam, S. M., Yavuz, A., Shui, G., Ding, M., & Huang, X. (2020). Neuronal lipolysis participates in PUFA-mediated neural function and neurodegeneration. *EMBO Reports*, *21*(11), e50214. https://doi.org/10.15252/EMBR.202050214

Yang, Q., Jiao, B., & Shen, L. (2020a). The Development of C9orf72-Related Amyotrophic Lateral Sclerosis and Frontotemporal Dementia Disorders. In *Frontiers in Genetics* (Vol. 11). Frontiers Media S.A. https://doi.org/10.3389/fgene.2020.562758

Yang, Q., Jiao, B., & Shen, L. (2020b). The Development of C9orf72-Related Amyotrophic Lateral Sclerosis and Frontotemporal Dementia Disorders. *Frontiers in Genetics*, *11*. https://doi.org/10.3389/FGENE.2020.562758

Yin, F., Sancheti, H., Patil, I., & Cadenas, E. (2016). Energy metabolism and inflammation in brain aging and Alzheimer's disease. *Free Radical Biology & Medicine*, *100*, 108–122. https://doi.org/10.1016/J.FREERADBIOMED.2016.04.200

Yoon, H. C., Kyeung, M. J., Heon, C. L., Mi, H. C., Kim, D., Won, B. L., & Choong, I. C. (2005). Immunohistochemical study on the distribution of phosphorylated extracellular signal-regulated kinase (ERK) in the central nervous system of SOD1G93A transgenic mice. *Brain Research*, *1050*(1–2), 203–209. https://doi.org/10.1016/J.BRAINRES.2005.05.060

Yu, A. C. H., Drejer, J., Hertz, L., & Schousboe, A. (1983). Pyruvate Carboxylase Activity in Primary Cultures of Astrocytes and Neurons. *Journal of Neurochemistry*, *41*(5), 1484–1487. https://doi.org/10.1111/J.1471-4159.1983.TB00849.X

Yu, C. H., Davidson, S., Harapas, C. R., Hilton, J. B., Mlodzianoski, M. J., Laohamonthonkul, P., Louis, C., Low, R. R. J., Moecking, J., de Nardo, D., Balka, K. R., Calleja, D. J., Moghaddas, F., Ni, E., McLean, C. A., Samson, A. L., Tyebji, S., Tonkin, C. J., Bye, C. R., … Masters, S. L. (2020a). TDP-43 Triggers Mitochondrial DNA Release via mPTP to Activate cGAS/STING in ALS. *Cell*, *183*(3), 636-649.e18. https://doi.org/10.1016/J.CELL.2020.09.020

Yu, C. H., Davidson, S., Harapas, C. R., Hilton, J. B., Mlodzianoski, M. J., Laohamonthonkul, P., Louis, C., Low, R. R. J., Moecking, J., de Nardo, D., Balka, K. R., Calleja, D. J., Moghaddas, F., Ni, E., McLean, C. A., Samson, A. L., Tyebji, S., Tonkin, C. J., Bye, C. R., … Masters, S. L. (2020b). TDP-43 Triggers Mitochondrial DNA Release via mPTP to Activate cGAS/STING in ALS. *Cell*, *183*(3), 636-649.e18. https://doi.org/10.1016/J.CELL.2020.09.020

Yuan, Z., Becker, E. B. E., Merlo, P., Yamada, T., DiBacco, S., Konishi, Y., Schaefer, E. M., & Bonni, A. (2008). Activation of FOXO1 by Cdk1 in cycling cells and postmitotic neurons. *Science (New York, N.Y.)*, *319*(5870), 1665–1668. https://doi.org/10.1126/SCIENCE.1152337

Zechner, R., Zimmermann, R., metabolism, T. E.-C., & 2012, undefined. (n.d.). FAT SIGNALS-lipases and lipolysis in lipid metabolism and signaling. *Elsevier*. Retrieved January 9, 2022, from https://www.sciencedirect.com/science/article/pii/S1550413112000186

Zehmer, J. K., Huang, Y., Peng, G., Pu, J., Anderson, R. G. W., & Liu, P. (2009). A role for lipid droplets in inter-membrane lipid traffic. *PROTEOMICS*, *9*(4), 914–921. https://doi.org/10.1002/PMIC.200800584

Zhang, J., cell, Q. L.-P. &, & 2015, undefined. (n.d.). Cholesterol metabolism and homeostasis in the brain. *Springer*. https://doi.org/10.1007/s13238-014-0131-3

Zhang, J., Chai, W., Xiang, Z., Zhou, X., & Zhang, P. (2021). MZF1 alleviates oxidative stress and apoptosis induced by rotenone in SH-SY5Y cells by promoting RBM3 transcription. *The Journal of Toxicological Sciences*, *46*(10), 477–486. https://doi.org/10.2131/JTS.46.477

Zhang, J., Wang, X., Vikash, V., Ye, Q., Wu, D., Liu, Y., & Dong, W. (2016). ROS and ROS-Mediated Cellular Signaling. *Oxidative Medicine and Cellular Longevity*, *2016*. https://doi.org/10.1155/2016/4350965

Zhang, M., Xi, Z., Zinman, L., Bruni, A. C., Maletta, R. G., Curcio, S. A. M., Rainero, I., Rubino, E., Pinessi, L., Nacmias, B., Sorbi, S., Galimberti, D., Lang, A. E., Fox, S., Surace, E. I., Ghani, M., Guo, J., Sato, C., Moreno, D., … Rogaeva, E. (2015). Mutation analysis of CHCHD10 in different neurodegenerative diseases. *Brain : A Journal of Neurology*, *138*(Pt 9), e380. https://doi.org/10.1093/BRAIN/AWV082

Zhang, Y. J., Jansen-West, K., Xu, Y. F., Gendron, T. F., Bieniek, K. F., Lin, W. L., Sasaguri, H., Caulfield, T., Hubbard, J., Daughrity, L., Chew, J., Belzil, V. v., Prudencio, M., Stankowski, J. N., Castanedes-Casey, M., Whitelaw, E., Ash, P. E. A., DeTure, M., Rademakers, R., … Petrucelli, L. (2014). Aggregation-prone c9FTD/ALS poly(GA) RAN-translated proteins cause neurotoxicity by inducing ER stress. *Acta Neuropathologica*, *128*(4), 505–524. https://doi.org/10.1007/S00401-014-1336-5

Zhou, Y. Y., Li, Y., Jiang, W. Q., & Zhou, L. F. (2015). MAPK/JNK signalling: a potential autophagy regulation pathway. *Bioscience Reports*, *35*(3), 1–10. https://doi.org/10.1042/BSR20140141

Zhu, J. H., Guo, F., Shelburne, J., Watkins, S., & Chu, C. T. (2003). Localization of Phosphorylated ERK/MAP Kinases to Mitochondria and Autophagosomes in Lewy Body Diseases. *Brain Pathology*, *13*(4), 473. https://doi.org/10.1111/J.1750-3639.2003.TB00478.X

Zhu, Y., Chen, C., Li, J., Cheng, J., Jang, M., research, K. K.-J. of lipid, & 2018, undefined. (n.d.). In vitro exploration of ACAT contributions to lipid droplet formation during adipogenesis. *ASBMB*. Retrieved January 9, 2022, from https://www.jlr.org/article/S0022-2275(20)33117-5/abstract

Zorova, L. D., Popkov, V. A., Plotnikov, E. Y., Silachev, D. N., Pevzner, I. B., Jankauskas, S. S., Babenko, V. A., Zorov, S. D., Balakireva, A. v., Juhaszova, M., Sollott, S. J., & Zorov, D. B. (2018). Mitochondrial membrane potential. *Analytical Biochemistry*, *552*, 50–59. https://doi.org/10.1016/J.AB.2017.07.009

Zou, Z. Y., Liu, M. S., Li, X. G., & Cui, L. Y. (2015). Mutations in SOD1 and FUS caused juvenile-onset sporadic amyotrophic lateral sclerosis with aggressive progression. *Annals of Translational Medicine*, *3*(15). https://doi.org/10.3978/j.issn.2305-5839.2015.09.04

Zou, Z. Y., Zhou, Z. R., Che, C. H., Liu, C. Y., He, R. L., & Huang, H. P. (2017). Genetic epidemiology of amyotrophic lateral sclerosis: a systematic review and meta-analysis. *Journal of Neurology, Neurosurgery, and Psychiatry*, *88*(7), 540–549. https://doi.org/10.1136/JNNP-2016-315018

Zoula, S., Rijken, P. F. J. W., Peters, J. P. W., Farion, R., van der Sanden, B. P. J., van der Kogel, A. J., Décorps, M., & Rémy, C. (2003). Pimonidazole binding in C6 rat brain glioma: relation with lipid droplet detection. *British Journal of Cancer*, *88*(9), 1439–1444. https://doi.org/10.1038/SJ.BJC.6600837

Zu, T., Gibbens, B., Doty, N. S., Gomes-Pereira, M., Huguet, A., Stone, M. D., Margolis, J., Peterson, M., Markowski, T. W., Ingram, M. A. C., Nan, Z., Forster, C., Low, W. C., Schoser, B., Somia, N. v., Clark, H. B., Schmechel, S., Bitterman, P. B., Gourdon, G., … Ranum, L. P. W. (2011). Non-ATG-initiated translation directed by microsatellite expansions. *Proceedings of the National Academy of Sciences of the United States of America*, *108*(1), 260–265. https://doi.org/10.1073/pnas.1013343108

Zuccato, C., Tartari, M., Crotti, A., Goffredo, D., Valenza, M., Conti, L., Cataudella, T., Leavitt, B. R., Hayden, M. R., Timmusk, T., Rigamonti, D., & Cattaneo, E. (2003). Huntingtin interacts with REST/NRSF to modulate the transcription of NRSE-controlled neuronal genes. *Nature Genetics 2003 35:1*, *35*(1), 76–83. https://doi.org/10.1038/ng1219

Zuo, X., Zhou, J., Li, Y., Wu, K., Chen, Z., Luo, Z., Zhang, X., Liang, Y., Esteban, M. A., Zhou, Y., & Fu, X. D. (2021). TDP-43 aggregation induced by oxidative stress causes global mitochondrial imbalance in ALS. *Nature Structural & Molecular Biology*, *28*(2), 132–142. https://doi.org/10.1038/S41594-020-00537-7

ANNEX I

Supplemental table ST1. List of the sequences of the primers used to explore the effects of REST target genes in SHSY-5Y cells, as reported in Figure 33.

Gene	Accession No.	Application	Sequence (5' → 3')
BID	NM_197967	RT-PCR	(F) agtgggagggctacgatgag
			(R) gatgctacggtccatgctgt
PUMA	NM_014417	RT-PCR	(F) cccgtgaagagcaaatgag
			(R) acccccctgatgaaggtgag
BAX	NM_138761	RT-PCR	(F) tctgacggcaacttcaactg
			(R) cgtcccaaagtaggagagga
FADD	NM_003824	RT-PCR	(F) ctggggaagaagacctgtg
			(R) gcacacgctctgtcaggtt
DAXX	NM_001350	RT-PCR	(F) aagcctccttggattctggt
			(R) atcatcctcctgaccctcct
FAS	NM_000043	RT-PCR	(F) agttggggaagctctttcactt
			(R) cagtcttcctcaattccaatcc
PSEN2	NM_000447	RT-PCR	(F) cctcggggacttcatcttc
			(R) tgaacacagcaagcagcag
PESENEN	NM_172341	RT-PCR	(F) tgaacctggagcgagtgtc
			(R) taggctgggacaaggaagg
P35	NM_003885	RT-PCR	(F) caaaccaggagcattttgtgt
			(R) attcctgtggcttgttctgtg
P39	NM_003936	RT-PCR	(F) ccttcattacgcctgcaaa
			(R) tctcgttgcccatgtagga
KCNQ2	NM_172106	RT-PCR	(F) gcgcaacgccttctacc
			(R) gacagcacgaggcagga
KV2.1	NM_004975	RT-PCR	(F) ggaaggcgaggagttcg
			(R) gggcaatggtggagagg
KCNJ6	NM_002240	RT-PCR	(F) ctctcggtgctgatgtgaaa
			(R) tgaaacggagcaagactgaa
CAT	NM_001752	RT-PCR	(F) atccagaagaaagcggtcaa
			(R) cagatttgccttctcccttg
FOXO1	NM_002015	RT-PCR	(F) tggggcaacctgtcctac
			(R) ggcacgctcttgaccatc
SOD1	NM_000454	RT-PCR	(F) ggcaaaggtggaaatgaaga
			(R) gggcctcagactacatccaa
1433ζ	NM_145690	RT-PCR	(F) agcccgtaggtcatcttgg
			(R) tgaagcattggggatcaag
ARC	NM_015193	RT-PCR	(F) cgcctggagaagaatcagag
			(R) gggaaccttgagacctgttg
BCL2	NM_000633	RT-PCR	(F) ggaggattgtggccttcttt
			(R) gccgtacagttccacaaagg
CASP2	NM_032982	RT-PCR	(F) ttgccgaagatgagactgc

Gene	Accession No.	Application	Sequence (5' → 3')
			(R) gcgttcaccttaaccagca
ANT1	NM_001151	RT-PCR	(F) gggctctaccagggtttca
			(R) cgtcacactctgggcaatc
PDCD7	NM_005707	RT-PCR	(F) gcaggaggtggaggagaag
			(R) tggaggacagacccctttc
MAPK11	NM_002751	RT-PCR	(F) taccggcaggagctgaac
			(R) ttcttcaccgccaccttc
MAPK12	NM_002969	RT-PCR	(F) ccaccttcaccttccacct
			(R) gcgtctgctctgatggatg
GAP43	NM_001130064	RT-PCR	(F) gggaggcttgaggaaaaatc
			(R) gcagcttggacatcatcctt
EGR1	NM_001964	RT-PCR	(F) gttaccccagccaaaccac
			(R) tgggttggtcatgctcact
NRXN3	NM_004796	RT-PCR	(F) gggaacaacacagacgacct
			(R) ctcggctcacattcaacaaa
GRIA4	NM_000829	RT-PCR	(F) gcagcgccttacatatctcc
			(R) ccaaccattttgtcctgctt
MEF2C	NM_001193350	RT-PCR	(F) ggggactatggggagaaaaa
			(R) gcttgttggtgctgttgaag
SANP25	NM_003081	RT-PCR	(F) tcatccgcagggtaacaaa
			(R) ttggcctcatcaattctgg
SST	NM_001048	RT-PCR	(F) gaccccagactccgtcagt
			(R) gctcaagcctcatttcatcc
ATP2B2	NM_001683	RT-PCR	(F) ggctcacacagaaggaggag
			(R) ggatggaggttcgagattca
GAD1	NM_000817	RT-PCR	(F) ttgcaccagtgtttgtcctc
			(R) aggaccagtttaggcacagc
GAD2	NM_000818	RT-PCR	(F) gacctgctccagtctccaaa
			(R) agggcgcacagtttgtttc
CYCS	NM_018947	RT-PCR	(F) tgaaaagggaggcaagca
			(R) ccccagatgatgcctttg
mCYCS	NM_007808	RT-PCR	(F) ccaaatctccacggtctgtt
			(R) gtctgccctttctcccttct
mMAPK11	NM_011161	RT-PCR	(F) ccagaaggtggctgtaaagaag
			(R) gcctgacacttgacgatgttatt
mCASP3	NM_00981	RT-PCR	(F) tgtcatctcgctctggtacg
			(R) aaatgacccttcatcacca
mβ-actin	NM_007393	RT-PCR	(F) tgggacgacatggagaaga
			(R) tggggtgttgaaggtctca
mCIDEA	NM_007702	RT-PCR	(F) agggacaacacgcatttca
			(R)cattgagacagccgaggaa

Gene	Accession No.	Application	Sequence (5' → 3')
CALB1	NM_004929	RT-PCR	(F) gaactctggaggaacgctga
			(R) aggctgtgatgagggatgac
SCN3B	NM_018400	RT-PCR	(F) attgtttcccctggcttctc
			(R) gcctccacctcctctctctt
GABRB3	NM_021912	RT-PCR	(F) gcttcttggcttctctggtg
			(R) aacgagatgccattcactcc
JIP1	NM_005456	RT-PCR	(F) caccacgctcaacctctttc
			(R) gtgtctgctcccctgtcttc

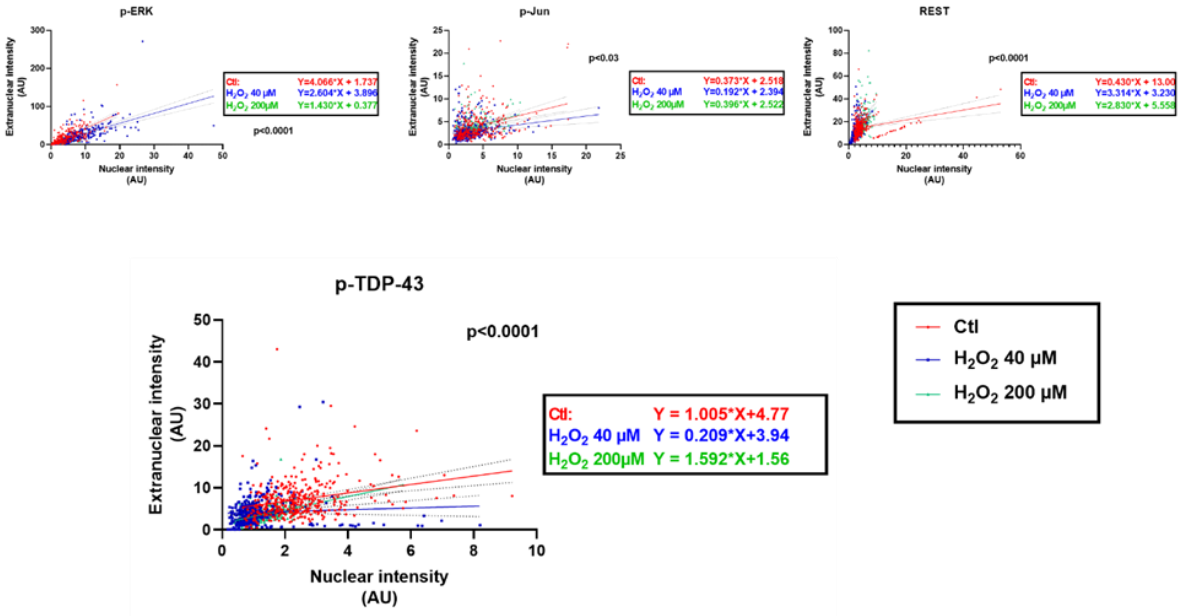

Supplemental Figure SF1. Oxidative stress induces changes between the nucleocytosolic relationships of proteins implicated in neurodegeneration. In all cases, total immunoreactivities found in nuclear and cytosolic compartments are related linearly significantly (in all cases p<0.001), though the slope is significantly affected by oxidative stress (shown p values for comparison of slopes). Shown are the linear relationships between nuclear and cytosolic content, with 95% confidence intervals indicated with discontinuous lines (n=200 to 296 cells for p-TDP-43; n=191-255 for p-ERK; n=234-326 for p-Jun and n=217-415 for REST, obtained in at least 4 independent replicates). Inset of graphs show the equations of the linear relationships, separated by colors.

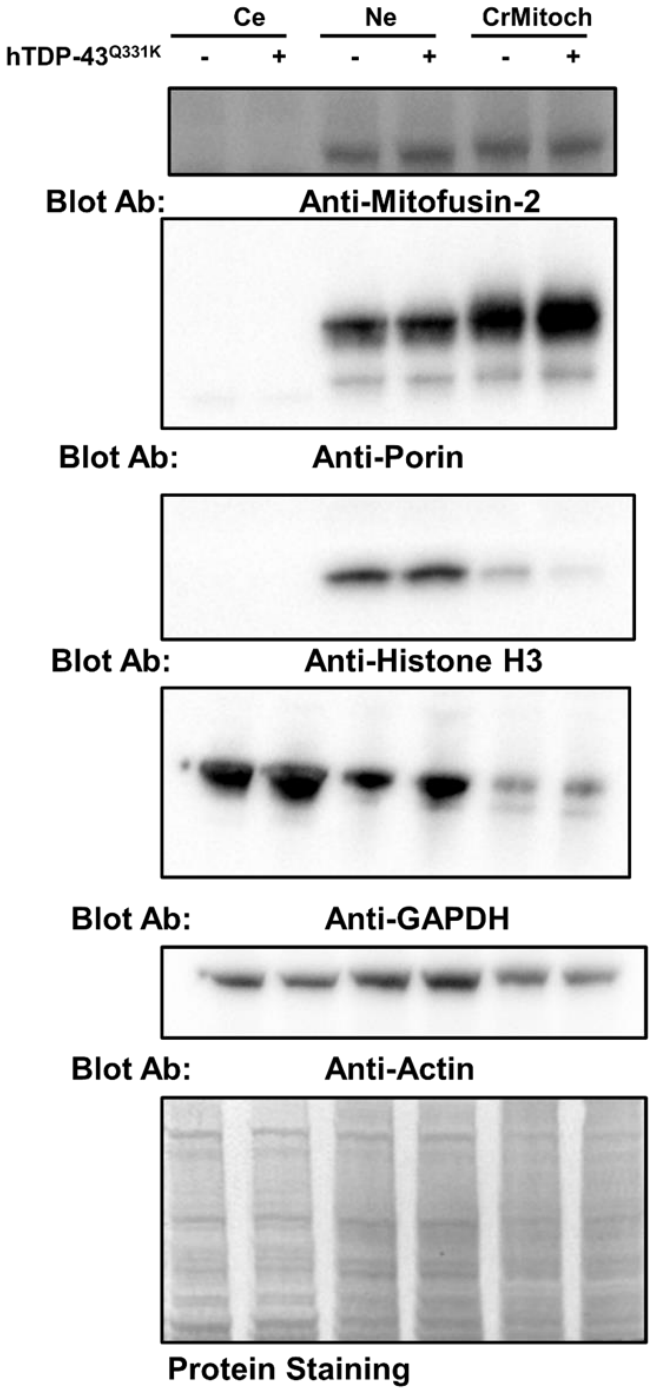

Supplemental Figure SF2. **Enrichment of protein markers in subcellular fractionation**. As shown by western-blot analyses of brain lysates after subcellular fractionation, in addition to nuclear enriched (Ne) and cytosolic enriched (Ce) compartments, crude mitochondrial fractions (CrMitoch) both non transgenic and transgenic hTDP-43 mice show the relative enrichment of Mitofusin-2 and porin in crude mitochondria, with almost the absence of histone H3 in non-nuclear fractions, and the high abundance of GAPDH in cytosolic extracts. Actin was distributed equally among the three fractions.

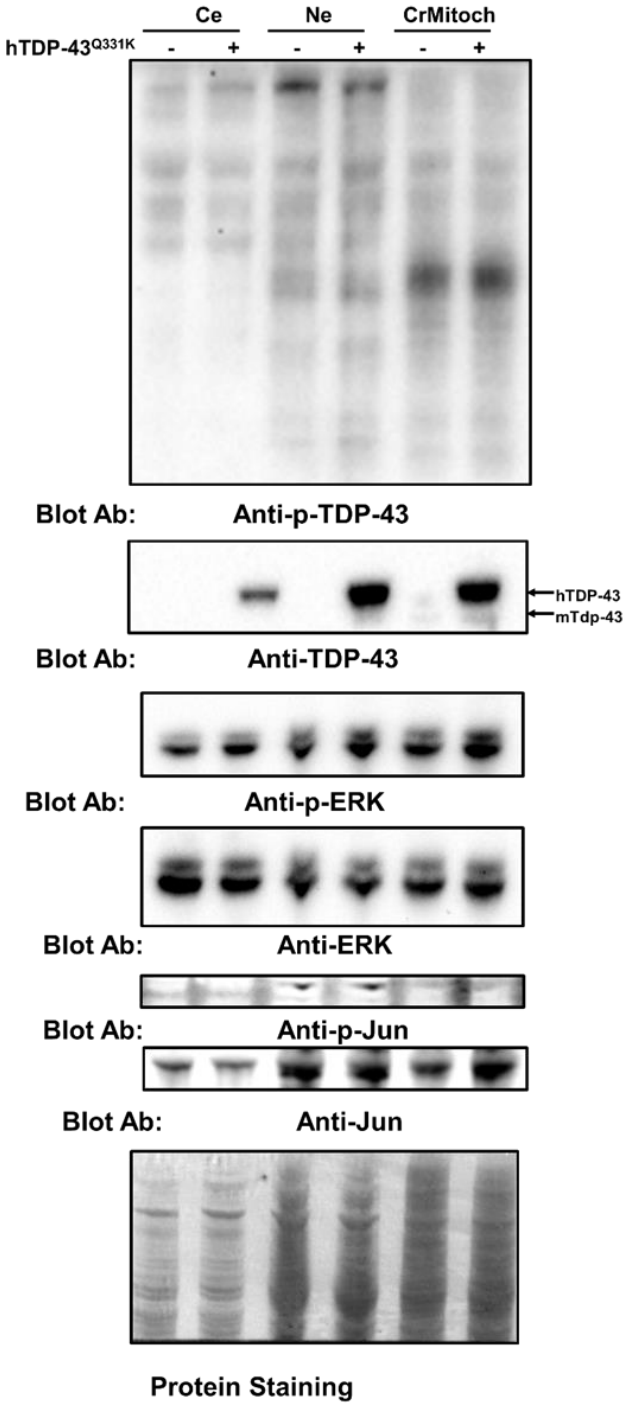

Supplemental Figure SF3. Cellular subfractionation evidence for in vivo colocalization of proteins implicated in neurodegeneration with mitochondrial components. As shown by western-blot analyses of brain lysates after subcellular fractionation, in addition to nuclear enriched (Ne) and cytosolic enriched (Ce) compartments, crude mitochondrial fractions (CrMitoch) both non transgenic and transgenic hTDP-43 mice show the presence of p-TDP-43, p-ERK and Jun. Levels were quantified by densitometry in brains from 90 days old mice. Western-blot shown are for male specimens.

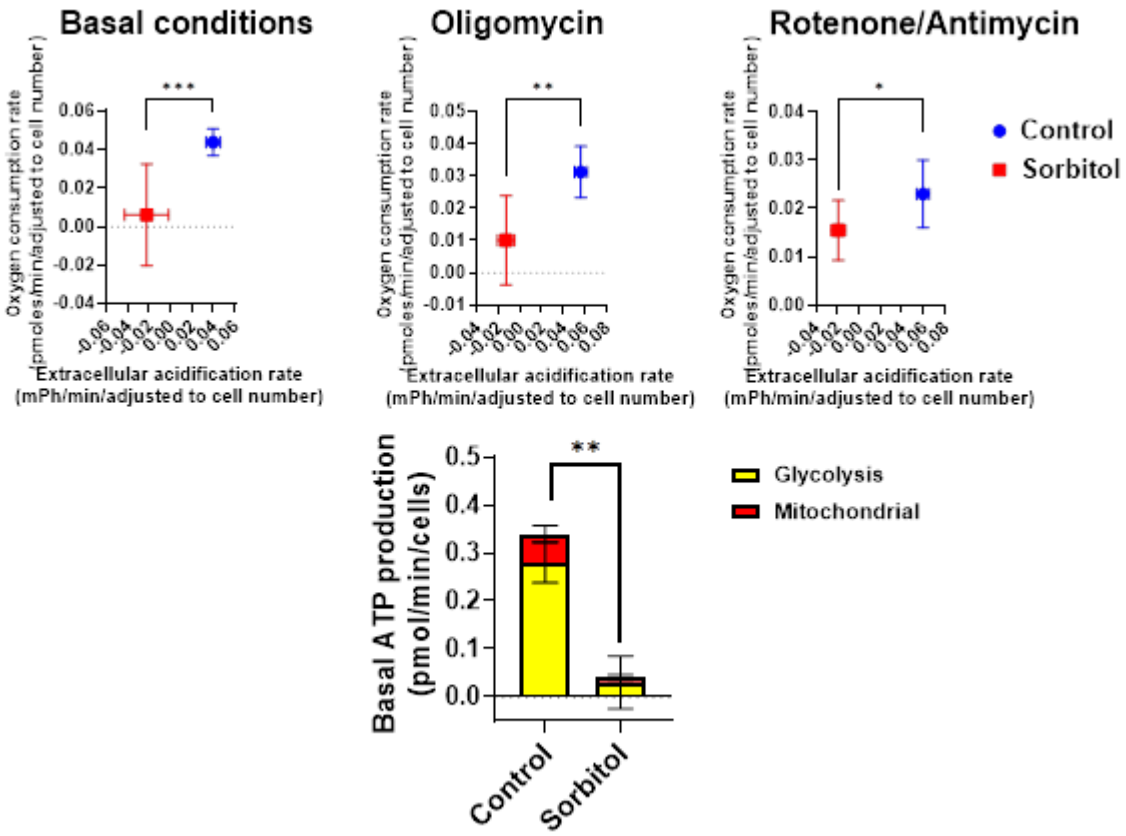

Supplemental figure SF4. TDP-43 aggregation is linked to mitochondrial dysfunction. Sorbitol incubation in SHSY-5Y stress induces changes in oxygen consumption and extracellular acidification rates, measured by using Seahorse respirometry. Data shown is for 6 independent cell plates for each condition. *** indicates p<0.001, ** p<0.01 and * p<0.05 by Uncorrected Fisher's LSD post-hoc test after one-way ANOVA

Open Access Article

Cell Stress Induces Mislocalization of Transcription Factors with Mitochondrial Enrichment

by Chiara Rossi [1], Anna Fernàndez [1], Pascual Torres [1], Omar Ramírez-Nuñez [1], Ana Belén Granado-Serrano [1], Laia Fontdevila [1], Mònica Povedano [2], Reinald Pamplona [1], Isidro Ferrer [3,4,5,6,7] and Manuel Portero-Otín [1,8,*]

[1] Metabolic Physiopathology Research Group, Experimental Medicine Department, Lleida University-Lleida Biochemical Research Institute (UdL-IRBLleida), E25198 Lleida, Spain

[2] Functional Unit of Amyotrophic Lateral Sclerosis (UFELA), Service of Neurology, Bellvitge University Hospital, L'Hospitalet de Llobregat, E08907 Barcelona, Spain

[3] Department of Pathology and Experimental Therapeutics, University of Barcelona, E08900 Barcelona, Spain

[4] CIBERNED (Network Centre of Biomedical Research of Neurodegenerative Diseases), Institute of Health Carlos III, Ministry of Economy and Competitiveness, E08900 Barcelona, Spain

[5] Bellvitge Biomedical Research Institute (IDIBELL), Hospitalet de Llobregat, E08907 Barcelona, Spain

[6] Senior Consultant, Bellvitge University Hospital, E08900 Barcelona, Spain

[7] Institute of Neurosciences, University of Barcelona, E08000 Barcelona, Spain

[8] Edifici Biomedicina I, Avda Rovira Roure, E25196 Lleida, Spain

* Author to whom correspondence should be addressed.